Gauge Models of Topological Phases and Applications to Quantum Gravity

by

Clément Martin Lucas Hugo Delcamp

A thesis
presented to the University Of Waterloo
in fulfillment of the
thesis requirement for the degree of
Doctor of Philosophy
in
Physics

Waterloo, Ontario, Canada, 2018

Examining Committee Membership

The following served on the Examining Committee for this thesis. The decision of the Examining Committee is by majority vote.

External Examiner	JOHN BARRETT Professor University of Nottingham
Supervisors	BIANCA DITTRICH Faculty Perimeter Institute for Theoretical Physics
	LEE SMOLIN Faculty Perimeter Institute for Theoretical Physics
Internal member	NIAYESH AFSHORDI Associate Professor University of Waterloo
Internal/external member	FLORIAN GIRELLI Associate Professor University of Waterloo
Examiner	GUIFRE VIDAL Faculty Perimeter Institute for Theoretical Physics

Author's declaration

This thesis consists of material all of which I authored or co-authored: see *Statement of Contributions* included in the thesis. This is a true copy of the thesis, including any required final revisions, as accepted by my examiners.

I understand that my thesis may be made electronically available to the public.

Statement of contributions

Chap. 2 of this thesis consists of material from the paper [1], co-authored with Laurent Freidel and Florian Girelli.

Chap. 3 of this thesis mainly consists of material from the paper [2] I solely wrote, as well as a few paragraphs from the paper [3] co-authored with Apoorv Tiwari.

Chap. 4 and chap. 5 of this thesis consist of material from the papers [4, 5] co-authored with Bianca Dittrich and Aldo Riello.

Chap. 6 of this thesis consists of material from the paper [2] of which I am the sole author.

Chap. 7 of this thesis consists of material from the paper [6] co-authored with Bianca Dittrich as well as some unpublished notes co-authored with Bianca Dittrich.

Abstract

In 2+1 dimensions, gravity is an SU(2) topological gauge theory that can be written as BF theory. In the condensed matter literature, the Hamiltonian realization of BF theory for finite groups is known as the Kitaev model. The corresponding Hamiltonian yields magnetic and electric point-like excitations, both supported by punctures. In this context, the cylinder plays a special role since the gluing of two cylinders results in another cylinder, hence defining an algebra on the Hilbert space of states, referred to as Ocneanu's tube algebra. By choosing specific graph-states on the cylinder, we can confirm explicitly that this algebra is equivalent to the Drinfel'd double of the gauge group. The representation theory of the Drinfel'd double can then be used to define a basis of excited states associated with any punctured Riemann surface. This result can be adapted so as to define a new basis for the gauge invariant Hilbert space of lattice gauge theories, and a fortiori loop quantum gravity, replacing the well-known spin network basis. In doing so, we naturally shift the focus from the underlying lattice to the excitations themselves, this notion of excitations being understood with respect to a given vacuum state, namely the so-called BF vacuum. This basis diagonalizes so-called ribbon operators that provide Dirac observables. Furthermore, it has an inherent hierarchical organization allowing to design states with a multi-scale structure. This turns out to be extremely precious for studying the large scale structure of the theory. It also provides a new notion of subsystems for gauge theories. Being solely based on excitations, this leads to a completely relational way of defining regions. This can be used to define a new notion of entanglement entropy for lattice gauge theories and (2+1)d gravity coupled to point particles. These techniques can also be generalized so as to define excitation bases for (3+1)d gauge models of topological phases. Two approaches are considered in this thesis. The first one consists in generalizing Ocneanu's tube algebra by replacing the cylinder with the manifold obtained by cutting open a three-torus along one direction. This defines an algebraic structure extending the Drinfel'd double that can be used in a similar fashion as in (2+1)d. The other approach relies on Heegaard splittings of three-manifolds which perform a decomposition into handle-bodies along so-called Heegaard surfaces. We use this technique to encode the Hilbert space of flat connections with curvature excitations of a three-manifold into the Hilbert space of flat connections on a 2d Heegaard surface, hence making the results derived in (2+1)d available to the study of the (3+1)d case.

Acknowledgments

First and foremost, I would like to thank my advisor, Bianca Dittrich, for giving me the opportunity to study alongside brilliant people in an inspiring place like the Perimeter Institute. Through our countless discussions, I learned how to carry out research in a bold but rigorous way. She has given me invaluable support and continuous guidance throughout the past three years. I am also grateful to all my committee members: Niayesh Afshordi, Florian Girelli, Lee Smolin and Guifré Vidal, for their valuable advices and encouragement. A special gratitude goes to Guifré for introducing me to a different field and for his precious support when I was applying for postdocs.

During the first years of my PhD, I had the pleasure to collaborate with Aldo Riello with whom I had numerous fruitful conversations regarding the topics covered in this thesis. I would also like to thank Marc Geiller for patiently answering all my questions about quantum gravity. I feel indebted to Markus Hauru and Sebastian Mizera for our enriching collaboration on the renormalization of tensor networks: It was long and frustrating, but, definitely worth it. I am thankul to Florian Girelli and Laurent Freidel for our inspiring collaboration that motivated me to study new mathematical subjects. Finally, I am indebted to my most recent colloborator, Apoorv Tiwari: Together, we have been exploring many topics outside of our scientific comfort zone.

My stay at Perimeter Institute would not have been the same without the good company of the friends I made there. I am particularly grateful to Andres, Gabriel, Lauren, Lucía, Markus, Naty and Peter for all our fun times together, away from our worrisome academic life. A special thank goes to Pablito for everything.

Last but not least, I am deeply indebted to my family for their continuous support over the years. Most special thanks go to The Minou and Bonaparte for making me feel like home.

Table of Contents

List of Figures

Chapter 1

Introduction

Gauge theory plays a crucial role in modern physics. It is a basic building block that appears in the description of elementary particles, general relativity, but also as the low-energy limit of numerous condensed matter systems. But it enjoys a bipolar status. On the one hand, its perturbative framework, in the case of weak interactions, is highly successful as exemplified by the very accurate experimental predictions of the standard model. On the other hand, strongly coupled regimes, which require non-perturbative techniques, are still poorly understood. The most famous strategy to make progress in this direction is *lattice gauge theory*.

Yang-Mills theory and general relativity are prime examples of theories with gauge symmetries, which have become indispensable in modern physics. The Ashtekar formulation of canonical general relativity [7, 8] brought the two theories even closer. Roughly speaking, this was achieved by including the group of local rotations, as an extra gauge symmetry beside space-time diffeomorphisms. This allowed to incorporate lattice gauge theory techniques in the realm of *background independent field theories* and led to the development of *loop quantum gravity* [9, 10].

Lattice gauge theories allow for *non-perturbative quantization schemes*, which are needed in particular for the understanding of quantum chromodynamics as well as quantum gravity. The success of such schemes relies on a clever choice of discrete observables [11, 12] transforming nicely under the gauge symmetries.[1] These observables are based on holonomies, built out of the gauge connection, and on fluxes, built out of the electric field and—in non-abelian gauge theories—out of the connection, too.

The major drawback of gauge formulations is, however, that it still needs the identification of a complete set of mutually independent gauge invariant degrees of freedom and observables. This is particularly important when it comes to the quantum theory. A gauge invariant basis for lattice field theory, allowing a convenient description of the gauge invariant Hilbert space, is the so-called *spin network basis* [16]. Such a basis has found wide applications in both lattice gauge theories and loop quantum gravity. In particular, it solved the problem of over-completeness of the Wilson loop observables, as encoded by the Mandelstam identities, which plagued the early developments of loop quantum gravity, see e.g. [17].

One purpose of this thesis is to introduce another basis for the Hilbert space of gauge invariant functionals, namely the so-called *fusion basis*. Among its desirable properties, one of the most important ones is that in this basis coarse-graining of states simplifies considerably with respect to an

[1] The issue is, however, much more involved for the space-time diffeomorphism group [13–15].

approach based on the spin network basis [18, 19]. This feature makes it the natural candidate to study the large scale dynamics of loop quantum gravity, in terms of coarse-graining and renormalization [15].

The fusion basis relies upon a shift of focus from the original lattice, underlying the construction of the spin network basis, directly to that of the *magnetic* (curvature) and *electric* (torsion) excitations themselves [4]. This is a setup very familiar to people studying topological phases of matter. As a matter of fact, the definition of this new basis relies on a reformulation of lattice gauge theories and loop quantum gravity in terms of extended topological field theories. Adapting well-known arguments from algebraic topology and condensed matter theory, we can show how the excitations are classified by the irreducible representations of the *Drinfel'd double* of the gauge group [20, 21]. The recoupling theory of the Drinfel'd double then provides all the necessary ingredients for the definition of the fusion basis.

The amenability of the fusion basis to coarse-graining is due to the fact that in non-abelian gauge theories, effective electric excitations (or torsion excitations, in a gravity context) emerge at large scales even if they are not present at the lattice scale [22]. Since these excitations are not present from the onset in the spin network basis, one needs to devise extension of the 'standard' framework (see [23] for proposals). In contrast, the fusion basis improves this state of things in a twofold way: On the one hand, it allows from the onset for both magnetic (curvature) and electric (torsion) excitations, and on the other hand it can be designed to have a notion of coarse-graining directly built in its combinatorial structure. This inherent notion of coarse-graining is due to the fact that the fusion basis diagonalizes a hierarchical set of so-called ribbon operators which create and measure the local excitations. Another way to employ this hierarchical structure is to encode a notion of subsystems for lattice gauge theories and (2+1)d gravity coupled to point particles. In particular, this can be exploited to provide a notion of entanglement entropy.

Entanglement entropy has become an important tool for characterizing the correlation structure of quantum field theories [24–26], in particular with regard to correlations in space. In the latter case, one presupposes that field degrees of freedom can be localized. Gauge theories, however, feature a form of non-locality that prevents the strict localization of the so-called physical, as opposed to gauge-variant, degrees of freedom. For instance, in Yang Mills theories, including electromagnetism, the presence of Gauß constraints implies that one can compute the total electric charge contained in a region solely in terms of the electric flux across the region's boundary: No information about the bulk fields is needed.

Quantum mechanically, this non-locality is reflected in the fact that the Hilbert space of gauge-invariant states does not factorize into the tensor product of Hilbert spaces associated to a spacetime region A and its complement B. More precisely, the algebra of gauge invariant observables does not factorize into the product of two commuting subalgebras each containing only operators supported in either A or B. Consequently, the definition of the entanglement entropy between one region and its complement requires further discussion, especially in the light of the privileged role gauge theories play in nature.

In quantum gravity this problem appears even more cogent, see for instance the recent discussions [27]. This happens not so much because a complete quantum theory of gravity is yet to be defined and agreed upon (in three dimensions one can actually argue for the opposite), but rather because of the very defining property of gravity, namely background independence. Indeed, because of background independence, which implies diffeomorphism invariance, the localization of regions and their separation into distinguished subsystems, when performed from *within* the theory itself, is already a thorny subject. To address the definition of entanglement entropy in a background-independent fashion, we

will advance in this thesis an approach that sheds light onto some of the issues encountered already within the standard gauge-theoretical framework.

In this context, essentially two approaches have been proposed for how to define entanglement entropy between two regions, namely the *extended Hilbert space* approach and the *observables algebra* approach. The first one [28–31], in particular put forward by Donnelly, is based on the embedding of the Hilbert space of gauge invariant states—which displays the non-local features discussed above—into an extended Hilbert space where gauge-invariance violations are allowed at the interface. This extended Hilbert space does factorize, allowing to define the entanglement entropy of a gauge invariant state as the entropy of its embedding. This proposal works for abelian as well as non-abelian gauge theories and is typically applied to the spin network basis. It turns out that there are different possible extension procedures. In fact, the procedure chosen in [28–31] relates to a choice of vacuum state describing the strong coupling limit of lattice gauge theory. In this thesis, we will present an alternative extension procedure—this time related to the weak coupling limit—leading to an alternative definition of the entanglement entropy. In practice, it boils down to applying the known procedure for the spin network basis but this time to the newly introduced fusion basis. Therefore, this new definition is based on the notion of excitations hence providing a completely relational way of defining a regions. As such, it naturally applies to background independent theories such as gravity by circumventing the difficulty of specifying the position of the *entangling surface*. Furthermore, it turns out that this definition provides the non-abelian analogue of the *magnetic centre choice* in the context of the observable algebra approach.

We alluded earlier how the crucial ingredient leading to the definition of the fusion basis is the algebraic structure of the excitations. In the context of gauge models of topological phases with defects, the relevant model is the so-called *Kitaev double model* which is nothing else than a lattice Hamiltonian realization of BF theory in (2+1)d. This lattice Hamiltonian yields magnetic and electric point-like excitations, both supported by punctures, where punctures are obtained by removing solid disks from the surface. In this context, the twice-punctured two-sphere (or cylinder) plays a special role for two reasons. Firstly, this is the simplest topology supporting excitations. Secondly, the gluing of two cylinders results in another cylinder, hence defining an algebraic structure on the Hilbert space of states, referred to as Ocneanu's tube algebra [21, 32]. By defining specific excited states on the cylinder, we can confirm explicitly that this algebra is equivalent to the Drinfel'd double $\mathcal{D}(G)$ of the gauge group [4, 33–35]. The representation theory of $\mathcal{D}(G)$ can then be used to define the *fusion basis* [4, 34, 36, 37] for any punctured Riemann surface.

More generally, in recent years considerable effort has been focused on understanding topological quantum field theories (TQFTs) with defect excitations. Much progress has been made in understanding topological quantum field theories and their associated defects in (2+1)d dimensions, e.g. [33, 37–43]. In particular (Levin-Wen) string nets [39] provide a huge class of models whose input data are unitary fusion categories. The structure of the excitations of these models is well-understood [33, 37, 40]: Given a fusion category $\mathcal{C}$, the excitations correspond to the objects of the Drinfel'd center $\mathcal{Z}(\mathcal{C})$. This is essentially a generalization of the previous statement. In contrast, TQFTs in (3+1) dimensions with defect excitations are less developed. As part of an ongoing attempt to make progress in this direction [44–56], we propose in this thesis two possible higher-dimensional extensions of the fusion basis.

The first approach follows closely the (2+1)d one and the model under consideration is a straightforward 3d generalization of Kitaev's model. The excitations are now supported by torus-boundaries which arise from removing solid tori from a three-manifold. The equivalent of the cylinder is obtained

by cutting open along one direction the three-torus. The resulting manifold, which is bounded by two tori, is the support of states which satisfy a 3d generalization of Ocneanu's tube algebra. It turns out that the corresponding gluing operation yields an extension of the Drinfel'd double referred to as the *quantum triple* $\mathcal{T}(G)$. The representation theory of $\mathcal{T}(G)$ can then be used, as in the (2+1)d case, to define a basis of excited states. While the (2+1)d fusion basis can be constructed for any punctured surface Σ, the extension we propose in this paper for (3+1)d models is defined on manifolds of the form $\Sigma \times \mathbb{S}_1$. In other words, we can think of this basis as a lifting of the (2+1)d fusion basis via a direct product with the circle $\mathbb{S}_1$. Therefore, this construction follows the strategy known *dimensional reduction*, which is a technique widely used for the study of three-dimensional topological phases [44, 46, 47, 54, 57]. This technique relies upon the compactification of one of the spatial directions into a small circle $\mathbb{S}_1$. The study of a (3+1)d topological order $\mathcal{C}^{3\mathrm{d}}$ then boils down to studying several (2+1)d topological orders $\mathcal{C}^{2\mathrm{d}}$. More precisely, in the case of a topological order $\mathcal{C}^{3\mathrm{d}}_G$ described by a gauge theory with finite group G, we can symbolically write the dimensional reduction as $\mathcal{C}^{3\mathrm{d}}_G = \bigoplus_C \mathcal{C}^{2\mathrm{d}}_{Z_C}$, where C is a conjugacy class of the full group G and Z_C the centralizer of a representative element of C.

The second approach consists in making many of the techniques developed in (2+1)d available for the (3+1)d case. The main ingredient of this program are *Heegaard splittings* which perform handle decompositions of three-dimensional surfaces. Given a three-dimensional surface representing a spatial slice of the (3+1)d space-time manifold, the result of a Heegaard splitting is two 3d handlebodies which, when glued along their common boundary, recover the original 3d surface. On this 2d boundary, the usual topological lattice models can be defined. By imposing additional flatness constraints associated with cycles which are non-contractible on this 2d boundary but contractible in the corresponding 3d manifold, we can systematically induce 3d models with magnetic excitations. An interesting question is then whether it is possible to parametrize the corresponding excited states in a way similar to the fusion basis in terms of irreducible representations of the Drinfel'd double. We offer in this thesis a preliminary answer to this question.

In spite of gravity not being a topological theory in (3+1)d, the study of (3+1)d topological phases with defects is very relevant for quantum gravity. In particular, spin foam models [9, 58, 59] are one approach to quantum gravity that rely on a constrained BF theory. A main open problem for spin foam models is the exploration of the large scale limit [15, 19, 60–66]. Generically the large scale limit, constructed via coarse-graining, is given by some (possibly trivial) topological field theory [19, 63], whereas interacting theories, such as gravity, are expected to arise at phase transitions between these topological field theories [15, 61, 66]. To understand the dynamics of spin foam models it is therefore important to understand better 4d topological field theories, which could arise via coarse-graining from spin foam models, and their possible (defect) excitations. This would then help to study possible phase transitions.

Organization of the thesis

In chap. 2 of this thesis, we recall basic facts about the first order formalism of 3d gravity, its discretization, and a general overview of its quantization procedure. We emphasize in particular the construction of the spin network basis for the Hilbert space of gauge invariant functionals which diagonalize Casimir operators. In chap. 3, we present the Hamiltonian realization of 3d BF theory for finite groups in the context of the study of topological phases of matter. We then carry out a study of the excitations yielded by this Hamiltonian by revisiting Ocneanu's tube algebra and explain how the Drinfel'd double structure naturally emerges. After presenting the main properties of this algebraic structure, we construct the fusion basis for gauge models of (2+1)d topological phases.

By adapting results from the previous chapter, we present in chap. 4 the construction of the fusion basis for lattice gauge theories and 3d gravity. This requires formulating the so-called (2+1)d BF representation, which provides an interpretation of lattice gauge theories as topological field theories with defects, then making the results from the topological order literature available for these cases. We reproduce the tube algebra in this context and redefine the fusion basis. Furthermore, the open ribbon operators that generate the fusion basis by acting on the BF vacuum are defined, as well as the correspondifng closed ribbon operators that project onto the fusion basis states. We finally discuss applications of the fusion basis to the design of multi-scale states and coarse-graining.

In chap. 5, we explain how the gluing procedure underlying the tube algebra can be dualized to define a splitting procedure. This splitting can be used in order to define the notion of extended Hilbert space. We then present in detail the extended Hilbert space method of computing entanglement entropy and emphasize the relation with the observable algebra approach. A new notion of entanglement entropy for lattice gauge theories is introduced which is adapted to the previously defined fusion basis. Several explicit calculations are presented. Finally, we discuss the implications of this new definition for the case of 3d quantum gravity.

Chap. 6 & 7 deal with generalizations and extensions of the fusion basis to the study of (3+1)d topological phases with defects. In chap. 6, we propose a generalization of Ocneanu's tube algebra in order to reveal the algebraic structure of the (3+1)d torus-excitations, namely the quantum triple. The representation theory of the quantum triple is presented and then used to define a basis of excitations for gauge theory model of (3+1)d topological phases. In chap. 7, the Heegaard splitting approach is exposed. We first describe how to encode the space of flat connections on a 3d manifold with defects into the space of flat connections on a 2d surface. This 2d surface is the so-called Heegaard surface defined by the structure of the defects. We furthermore discuss how the 2d fusion basis yields bases of excited states with magnetic excitations in 3d. Accordingly, we discuss which class of 2d operators are lifted to (excitations generating) operators in 3d. Specific examples are discussed in detail.

We will sometimes review some material discussed in the previous chapters in order to adapt it to the application at hand. The reader should therefore expect some overlap between the chapters.

Chapter 2

Canonical quantization of 3d BF theory

In (2+1)d, general relativity is a topological field theory where by 'topological' it is meant that physically distinct topological solutions can be parametrized using a finite set of global parameters. More precisely, in three dimensions, the first order action for gravity is provided by the BF action which provides in any dimension a topological field theory. In this first chapter, we briefly review the canonical quantization *à la loop* of 3d BF theory. In particular, we present the construction of the spin network basis for the Hilbert space of gauge invariant functionals, which has proven very useful both in the context of quantum gravity and more generally in the context of lattice gauge theories. In this introductory chapter, we do not explicitly make use of the topological nature of BF theory but merely follow *Dirac's quantization program*. Making explicit use of the topological nature of BF theory will be the subject of the following chapters. This will lead to a different formulation of 3d quantum gravity and will allow us to define an alternative gauge invariant basis which will be compared to the spin network basis. This basis will be relevant for lattice gauge theories in general and in particular for 3d quantum gravity.

2.1 Continuous formulation and discretization

Let us briefly review the canonical analysis of the theory in the case where the gauge group is a Lie group $\mathcal{G}$ whose Lie algebra is denoted by $\mathfrak{g}$. In d dimensions, the action reads

$$S[e,\omega] = \int_{\mathcal{M}} \mathrm{tr}(e \wedge F(\omega)) \tag{2.1}$$

where $\mathcal{M} = \Sigma \times \mathbb{R}$, e denotes a $\mathfrak{g}$-valued $(d-2)$-form, ω a connection on a trivial $\mathcal{G}$-bundle and $F = \mathrm{d}\omega + \omega \wedge \omega$ its curvature. The BF action displays two kinds of gauge symmetries. First, there is a local $\mathcal{G}$–rotation symmetry

$$\delta_\Lambda e = [e, \Lambda] \quad , \quad \delta_\Lambda \omega = \mathrm{d}_\omega \Lambda \tag{2.2}$$

with Λ a $\mathfrak{g}$-valued $(d-3)$-form. Secondly, there is a translational symmetry parametrized by a $\mathfrak{g}$-valued 0–form N

$$\delta_N e = \mathrm{d}_\omega N \quad , \quad \delta_N \omega = 0 \tag{2.3}$$

which follows from the Bianchi identity $\mathrm{d}_\omega F = 0$. The phase space of this theory is parametrized by the pull-back of both the field e and the connection ω to Σ, denoted by A_a^i and E_j^b in local coordinates, respectively, whose Poisson brackets read

$$\{\, A_a^i(x)\,,\, E_j^b(y)\,\} = \delta_j^i \delta_a^b \delta(x,y) \quad , \quad \{\, A_a^i(x)\,,\, A_b^j(y)\,\} = 0 \quad , \quad \{\, E_i^a(x)\,,\, E_j^b(y)\,\} = 0\,. \tag{2.4}$$

Canonical analysis of the action reveals the first class constraints

$$D_b E_j^b = 0 \quad , \quad F_{ab}^i(A) = 0\,, \tag{2.5}$$

which generate the local symmetries of the action. We shall refer to these two constraints as the Gauß constraint and the flatness constraint (or zero-flux condition), respectively. The $\mathfrak{g}$–valued connection transforms under gauge transformation as

$$g \triangleright A_a = g A_a g^{-1} + g \partial_a g^{-1}\,. \tag{2.6}$$

Upon canonical quantization, we need to choose a basic set of phase space functions that are then promoted to operators [67–69]. However, in order to make such quantization feasible, we require two conditions on the basis: (i) Poisson brackets between canonical variables which form an algebra and (ii) that they possess simple expressions under gauge transformations. Let us now focus on the case of 3d BF theory with an SU(2) connection. So far, we have a phase space parametrized by A_a^i and E_j^b whose Poisson brackets are distributional.

A simple way to achieve both (i) and (ii) is to consider holonomies of the connection A along paths in Σ. More precisely, let γ be a piecewise analytic curve, the holonomy $h_\gamma(A) \in \mathrm{SU}(2)$ along γ in Σ is given by the path ordered exponential

$$h_\gamma(A) = \mathcal{P}\mathrm{exp}\Big(\int_\gamma A\Big)\,, \tag{2.7}$$

which transforms as

$$g \triangleright h_\gamma = g_{t(\gamma)} h_\gamma g_{s(\gamma)}^{-1}\,, \tag{2.8}$$

where $s(\gamma)$ and $t(\gamma)$ denote the source and target nodes of γ, respectively. Similarly, the frame field is smeared over a one dimensional submanifold so as to define the flux variables

$$X_\gamma = \int_e h_{\gamma,x}^{-1} \mathbf{e}(x) h_{\gamma,x} \mathrm{d}x \tag{2.9}$$

where e intersects transversally γ in one point, $h_{\gamma,x}$ is the holonomy going from the point $s(\gamma)$ to $x \in e$, and $\mathbf{e}$ is the *dyad*. The flux variables transform as

$$g \triangleright X_\gamma = g_{s(\gamma)} X_\gamma g_{s(\gamma)}^{-1} \tag{2.10}$$

and the holonomy-flux algebra finally reads

$$\{h_\gamma, h_\gamma\} = 0 \quad , \quad \{X_\gamma^a, h_\gamma\} = h_\gamma \tau^a \quad , \quad \{X_\gamma^a, X_\gamma^b\} = \epsilon^{ab}{}_c X_\gamma^c\,, \tag{2.11}$$

with τ^a being the generators of $\mathfrak{su}(2)$ satisfying the algebra $[\tau^a, \tau^b] = \epsilon^{ab}{}_c \tau^c$.

2.2 Canonical quantization

In this section, we briefly review well-known aspects of the derivation of loop quantum gravity (LQG) in (2+1)d [9, 70, 71]. Roughly speaking, Dirac's quantization program consists in: (*i*) Choosing a representation of the phase space variables as operators in a so-called *kinematical* Hilbert space $\mathcal{H}^{\rm kin}$, (*ii*) promote the constraints to operators in this Hilbert space, (*iii*) finally find the states which solve these quantum constraints. The space of solutions equipped with a physical inner product define the physical Hilbert space $\mathcal{H}^{\rm phys}$. In the context of 3d gravity, the two constraints are the Gauß constraint and the flatness constraint. The Gauß constraint is typically implemented first and as such it is referred to as the *kinematical constraint* while the flatness constraint encodes the dynamics of the theory and is referred to as the *dynamical constraint*. We can summarize this quantization scheme as follows

$$\mathcal{H}^{\rm kin} \longrightarrow \mathcal{H}^{\rm G\cdot} \longrightarrow \mathcal{H}^{\rm phys} \tag{2.12}$$

where $\mathcal{H}^{\rm G\cdot}$ denotes the Hilbert space of functionals satisfying the Gauß constraint

In the following, we restrict our attention to the definition of the kinematical Hilbert space on a fixed graph Γ. We could choose this graph Γ to be either the one-skeleton of a discretization or its dual graph. We choose it to be the graph dual to a triangulation and refer to the 0-simplices, 1-simplices and 2-simplices as nodes, links and plaquettes, respectively. It is also possible to consider all the graphs at once by constructing the so-called *inductive limit* of the family of Hilbert spaces $\{\mathcal{H}_\Gamma\}$ that requires a choice of vacuum state. However, for our purpose, it is enough to work with a fixed graph for now. The inductive limit will be discussed in detail in chap. 4.

2.2.1 Kinematical space and representation of the holonomy-flux algebra

In the standard picture of LQG, the Hilbert space $\mathcal{H}^{\rm G\cdot}_\Gamma$ of gauge invariant functionals defined on the graph Γ is built from spin network states, which naturally solve the Gauß constraint. We will now recall the main steps which lead to the definition of such basis states.

First, the Poisson brackets (2.11) are turned into commutators so as to obtain the *holonomy-flux* algebra $\mathcal{A}_\Gamma$ associated with the graph Γ. This algebra is a direct sum of *link algebras* $\mathcal{A}_l$ associated with each link $l \subset \Gamma$ and generated by the pair $(\widehat{X}^j_l, \widehat{h}_l)$ satisfying the commutation relations

$$[\widehat{h}_l, \widehat{h}_l] = 0 \quad , \quad [\widehat{X}^a_l, \widehat{h}_l] = i\widehat{h}_l\tau^a \quad , \quad [\widehat{X}^a_l, \widehat{X}^b_l] = i\epsilon^{ab}{}_c\widehat{X}^c_l \ . \tag{2.13}$$

At this stage, several important facts should be noticed. Firstly, we note that this algebra contains two sub-algebras: a non-commutative algebra, which is generated by $\widehat{X}^a_l$, and a commutative one, which is generated by the matrix element operators $\widehat{h}_l$. Secondly, we remark that the combination $\widehat{X}_{l^{-1}} := -h_l\widehat{X}_l h_l^{-1}$ commutes with $\widehat{X}_l$ while satisfying the same commutation relations $[\widehat{X}^a_{l^{-1}}, \widehat{X}^b_{l^{-1}}] = i\epsilon^{ab}{}_c\widehat{X}^c_{l^{-1}}$. The fact that $\widehat{X}_l$ and $\widehat{X}_{l^{-1}}$ commute follows from the property that $\widehat{X}_l$ acts as the left invariant derivative on functions of the holonomy while $\widehat{X}_{l^{-1}}$ acts as a right invariant derivative: $[\widehat{X}^a_{l^{-1}}, \widehat{h}_l] = -i\tau^a\widehat{h}_l$. Under reversal of the orientation we also assume that $\widehat{h}_{l^{-1}} = \widehat{h}_l^{-1}$. This implies in particular that the algebra $\mathcal{A}_l$ is independent on the choice of orientation of the edge.

The choice of a representation of the algebra $\mathcal{A}_l$ is characterized by a choice of maximally commuting sub-algebra. Any maximally commuting algebra is three-dimensional and there are two natural choices for this sub-algebra. The first choice amounts to diagonalizing the set of fluxes

$$(\widehat{X}_l)^2 = (\widehat{X}_{l^{-1}})^2 \quad , \quad \widehat{X}^3_l \quad , \quad \widehat{X}^3_{l^{-1}} \ . \tag{2.14}$$

This is the choice made in the construction of the usual LQG basis since it is well-adapted to the case where we solve first the Gauß constraint specified in terms of the fluxes $\widehat{X}_l$ meeting at a node n. We therefore focus on the non-commutative sub-algebra generated by the fluxes.

The representation that diagonalizes the flux operators (2.14) is labeled by $\mathfrak{su}(2)$-irreducible representations V_j. Due to the nature of the commuting operators, we expect the link Hilbert space $\mathcal{H}_l$ to be characterized by the representations j_l, $j_{l^{-1}}$ together with the corresponding magnetic numbers. By construction, we have the constraint $|\widehat{X}_l| = |\widehat{X}_{l^{-1}}|$ which in turn imposes $j_l = j_{l^{-1}} \equiv j$. This suggests that the natural Hilbert space for a link l is

$$\mathcal{H}_l^{\text{kin}} \equiv \bigoplus_j V_j \otimes V_{j^*} \ni |j,m,n\rangle \equiv |j,n\rangle\langle j,m| \tag{2.15}$$

where we use the dual representation V_{j^*} for the right-hand side in order to keep track of the orientation of the link. It is understood from the notation that the links are oriented such that the magnetic numbers m and n are associated with the target and source nodes, respectively. We will refer to the condition $|\widehat{X}_l| = |\widehat{X}_{l^{-1}}|$ as the *matching condition*. The implementation of such condition can be made more explicit by defining the projector $\mathfrak{P} : |j,n\rangle\langle j',m| \mapsto \delta_{jj'}|j,n\rangle\langle j,m|$. We will make use of such a projector later on. Furthermore, we remark that the Hilbert space $\mathcal{H}_l^{\text{kin}}$ is actually an $\mathfrak{su}(2)$-bimodule since the fluxes $\widehat{X}_l$ acts as left invariant derivatives while the fluxes $\widehat{X}_{l^{-1}}$ act as right invariant derivatives. These correspond to infinitesimal generators of right and left translations, respectively, i.e.

$$\widehat{X}_l^a|j,m,n\rangle = i\sum_p |j,m,p\rangle D^j_{pn}(\tau^a) \quad , \quad \widehat{X}_{l^{-1}}^a|j,m,n\rangle = i\sum_q |j,q,n\rangle D^j_{mq}(-\tau^a) \tag{2.16}$$

so that the spaces spanned by $\{\,|j,m,p\rangle \mid p = -j,\dots,+j\}$ and $\{\,|j,q,n\rangle \mid q = -j,\dots,+j\}$ are sub-representation spaces carrying a representation D^j and a contragradient representation D^{j^*}, respectively.

In order to have a complete picture, we also need to identify the action of the holonomy operator, or more exactly of the matrix element operators $\widehat{h}_{BA}$. For simplicity, we choose to express it in the spinor representation. Defining the Clebsch-Gordan coefficients $C^{j_1\ j_2\ j_3}_{m_1 m_2 m_3}$ via

$$\sum_{m_1,m_2} C^{j_1\ j_2\ j_3}_{m_1 m_2 m_3}|j_1,m_1\rangle \otimes |j_2,m_2\rangle = |j_3,m_3\rangle \ , \tag{2.17}$$

and similarly its conjugate $\overline{C}^{j_1\ j_2\ j_3}_{m_1 m_2 m_3}$ via

$$|j_1,m_1\rangle \otimes |j_2,m_2\rangle = \sum_{j_3,m_3} \overline{C}^{j_1\ j_2\ j_3}_{m_1 m_2 m_3}|j_3,m_3\rangle \ , \tag{2.18}$$

the action of the holonomy matrix element operators reads

$$\widehat{h}_{BA}\ |j,m,n\rangle = \sum_{J=j\pm\frac{1}{2}} \sum_{\substack{-J\leq M\leq J \\ -J\leq N\leq J}} \overline{C}^{\frac{1}{2}\ j\ J}_{A\,nN}\, C^{\frac{1}{2}\ j\ J}_{BmM}|J,M,N\rangle \tag{2.19}$$

where $\widehat{h}_{BA} = \langle B|\widehat{h}|A\rangle$ and $|A\rangle = |1/2,A\rangle$ simply denotes the state A in the spinorial representation.

The definition (2.19) shows that the holonomy operator acts on both side of the link, unlike the flux operator. As a consistency check, we can show how it is possible to recover a representation of the

link algebra (2.13). To do so, we first rewrite the action (2.19) using the definition (2.15) together with the projector $\mathfrak{P}$:

$$\widehat{h}_{BA}\ |j,m,n\rangle = \sum_{J=j\pm\frac{1}{2}} \sum_{\substack{-J\leq M\leq J\\ -J\leq N\leq J}} \overline{C}^{\frac{1}{2}\,j\,J}_{A\,n\,N}\, |J,N\rangle\langle J,M|\, C^{\frac{1}{2}\,j\,J}_{B\,m\,M} = \mathfrak{P}\big(\,|A\rangle\otimes|j,n\rangle\langle j,m|\otimes\langle B|\,\big) \tag{2.20}$$

where $\langle j,m|\otimes\langle B| := (|B\rangle\otimes|j,m\rangle)^\dagger$. Using the fact that $\widehat{X}^a|j,n\rangle\langle j,m| = D^j(\tau^a)|j,n\rangle\langle j,m|$ together with the group action so that

$$\widehat{X}^a\widehat{h}_{BA}|j,n\rangle\langle j,m| = \mathfrak{P}\big([\tau^a\otimes 1 + 1\otimes D^j(\tau^a)]\,|A\rangle\otimes|j,n\rangle\langle j,m|\otimes\langle B|\,\big) \tag{2.21}$$

$$\widehat{h}_{BA}\widehat{X}^a|j,n\rangle\langle j,m| = \mathfrak{P}\big([1\otimes D^j(\tau^a)]\,|A\rangle\otimes|j,n\rangle\langle j,m|\otimes\langle B|\,\big)\ , \tag{2.22}$$

we can now evaluate the following quantity

$$[\widehat{X}^a,\widehat{h}_{BA}]\ |j,m,n\rangle = \mathfrak{P}\big(\tau^a\,|A\rangle\otimes|j,n\rangle\langle j,m|\otimes\langle B|\,\big) = \Big(\sum_{A'}\tau^a_{A'A}\widehat{h}_{BA'}\Big)|j,m,n\rangle \tag{2.23}$$

and we recover the expected commutation relation between $\widehat{h}$ and $\widehat{X}$. We can also express the action of h^{-1}_{AB} as

$$(\widehat{h}^{-1})_{AB}\ |j,m,n\rangle = \mathfrak{P}\big(|A^*\rangle\otimes|j,n\rangle\langle j,m|\otimes\langle B^*|\,\big) \tag{2.24}$$

where $|A^*\rangle = (-1)^{1/2-A}|-A\rangle$ is the conjugate state. The identity $\sum_A \widehat{h}_{BA}(\widehat{h}^{-1})_{AC} = \delta_{BC}$ finally follows from the fact that $\sum_A |A\rangle\otimes|A^*\rangle$ is the singlet state.

The next step is to specify what is the Hilbert space structure associate with a link l. From the fact that the states $|j,m,n\rangle$ diagonalizes $X^3_l, X^3_{l^{-1}}$ and $(X_l)^2$, we already know that they form an orthogonal basis. Demanding that $(\widehat{h}_{BA})^\dagger = (\widehat{h}^{-1})_{AB}$ then forces the normalization condition

$$\langle j',m',n'|j,m,n\rangle = \frac{1}{d_j}\delta_{jj'}\delta_{mm'}\delta_{nn'} \tag{2.25}$$

where $d_j = 2j+1$. Moreover, thinking of the states $|\phi\rangle = \sum_j \phi_j$, with $\phi_j = \sum_{mn}\phi_{jmn}|j,m,n\rangle$, as endomorphisms $\widehat{\phi} = \sum_{jmn}\phi_{jmn}|j,n\rangle\langle j,m|$, we can express the previous scalar product as a weighted trace:

$$\langle\phi|\psi\rangle = \mathrm{tr}(\widehat{\phi}^\dagger\widehat{\psi}) := \sum_j \frac{1}{d_j}\mathrm{tr}_{V_j}(\widehat{\phi}^\dagger_j\widehat{\psi}_j)\ . \tag{2.26}$$

Furthermore, it follows from the symmetry property[1] of the Clebsh-Gordan coefficients that

$$\begin{aligned}\langle J,M,N|\widehat{h}_{BA}|j,m,n\rangle &= \frac{1}{d_J}\overline{C}^{\frac{1}{2}\,j\,J}_{A\,n\,N}\, C^{\frac{1}{2}\,j\,J}_{B\,m\,M} = \frac{(-1)^{1-A-B}}{d_j}\overline{C}^{\ \frac{1}{2}\,J\,j}_{-A\,N\,n}\, C^{\ \frac{1}{2}\,J\,j}_{-B\,M\,m}\\ &= \langle j,m,n|(\widehat{h}^{-1})_{AB}|J,M,N\rangle\ .\end{aligned} \tag{2.28}$$

Now that we have the holonomy action on the spin states we can construct the holonomy state $|g)$ which diagonalizes $\hat{h}$. This is the state that enters in the wave functional $\psi(g)\equiv(g|\psi\rangle$ and its explicit expression in terms of the states $|j,m,n\rangle$ is provided by the generalized Fourier transform

$$|g) = \sum_{j,m,n} d_j\overline{D^j_{mn}(g)}|jmn\rangle = \sum_{jmn} d_j|j,n\rangle\overline{D^j_{mn}(g)}\langle j,m|\ . \tag{2.29}$$

[1] Explicitely given by

$$\frac{1}{\sqrt{\mathrm{d}_{j_3}}}C^{j_1\ j_2\ j_3}_{m_1 m_2 m_3} = \frac{(-1)^{j_1-m_1}}{\sqrt{\mathrm{d}_{j_2}}}C^{j_3\ j_1\ j_2}_{m_3 m_1^* m_2}\quad,\quad C^{j_1\ j_2\ j_3}_{m_1 m_2 m_3} = (-1)^{j_1+j_2-j_3}C^{j_2\ j_1\ j_3}_{m_2 m_1 m_3}\ . \tag{2.27}$$

We can check that the action of the holonomy on such state is diagonal, i.e. $\widehat{h}_{BA}|g) = g_{BA}|g)$ as follows:

$$\begin{aligned}\sum_A \widehat{h}_{BA}|g) &= \sum_{j,m,n}\sum_{J,M,N} d_j \overline{D^j_{mn}(g)}\,\overline{C}^{\frac{1}{2}\,j\,J}_{A\,n\,N}\,|J,N\rangle\langle J,M|\,C^{\frac{1}{2}\,j\,J}_{B\,m\,M}\\ &= \sum_{j,m,n}\sum_{J,M,N}\sum_{B',n',N'} d_j D^j_{nm}(g^{-1})\,\overline{C}^{\frac{1}{2}\,j\,J}_{A\,n\,N}\,|J,N\rangle\langle J,M|\,D^{\frac{1}{2}}_{BB'}(g) D^j_{mm'}(g)\overline{D^J_{MM'}(g)}\,C^{\frac{1}{2}\,j\,J}_{B'\,m'\,M'}\\ &= \sum_{j,n}\sum_{J,M,N}\sum_{A',M'} d_j D^{\frac{1}{2}}_{BB'}(g)\overline{D^J_{MM'}(g)}\,\overline{C}^{\frac{1}{2}\,j\,J}_{A\,n\,N}\,|J,N\rangle\langle J,M|\,C^{\frac{1}{2}\,j\,J}_{B'\,n\,M'}\\ &= \sum_{J,M,N} d_J D^{\frac{1}{2}}_{BA}(g)\overline{D^J_{MN}(g)}\,|J,N\rangle\langle J,M| = g_{BA}|g)\ . \end{aligned} \tag{2.30}$$

In the first line we used the formula (2.19) for the action of the holonomy operator. In the second line we made use of the property $\overline{D^j_{mn}(g)} = D^j_{nm}(g^{-1})$ together with the invariance property

$$\sum_{n_1,n_2,n_3} D^{j_1}_{m_1n_1}(g) D^{j_2}_{m_2n_2}(g)\overline{D^{j_3}_{m_3n_3}(g)}\,C^{j_1\,j_2\,j_3}_{n_1n_2n_3} = C^{j_1\,j_2\,j_3}_{m_1m_2m_3}\ .$$

Finally we used a symmetry property similar to (2.28) in order to make us of the orthogonality of the Clebsch-Gordan coefficients

$$\sum_{j_3,m_3} C^{j_1\,j_2\,j_3}_{m_1m_2m_3}\,\overline{C}^{j_1\,j_2\,j_3}_{n_1n_2m_3} = \delta_{m_1n_1}\delta_{m_2n_2}\ .$$

It turns out that we could have defined directly the Hilbert space $\mathcal{H}_l^{\text{kin}}$ from the space of functions on SU(2) after decomposition via the Peter-Weyl theorem. However, thanks to this approach, we can now explain how this representation of the Hilbert space $\mathcal{H}_l^{\text{kin}}$ arises from a general gluing procedure of half-links. This gluing procedure naturally encodes the Gauß constraint.

2.2.2 Fusion tensor product

Each node of Γ has incoming and outgoing half-links that are associated with a given state. These half-links need to be *glued* together so as to form full links. Furthermore, half-links meeting at a node also need to be glued together. In both cases, the gluing conditions are obtained by imposing some constraints on the corresponding states, which in turn give rise to the notion of *fusion tensor product* denoted by $\boxtimes$, i.e., a modified tensor product taking into account the constraints.

Roughly speaking, the kinematical Hilbert space associated with a full link $\mathcal{H}_l^{\text{kin}}$ can be defined as the fusion product of Hilbert spaces $\mathcal{H}_{l_L,l_R}$ associated with the corresponding left and right half-links, i.e. $\mathcal{H}_l^{\text{kin}} \simeq \mathcal{H}_{l_L} \boxtimes_{\text{SU}(2)} \mathcal{H}_{l_R}$. Remark that the Hilbert spaces under consideration should be bimodules themselves since we require to have a group action at each one of the extremities of the half-links. Starting from the bimodule $\mathcal{H}_{l_L} \otimes \mathcal{H}_{l_R}$ which does posses a left and a right action of the symmetry group SU(2) associated with each half-link, we define the corresponding fusion tensor product as

$$\mathcal{H}_{l_L} \boxtimes_{\text{SU}(2)} \mathcal{H}_{l_R} \ni v \boxtimes w \quad \text{ such that } \quad v \boxtimes (w \triangleleft g) \sim (g \triangleright v) \boxtimes w\,,\ g \in \text{SU}(2) \tag{2.31}$$

where g acts at the node connecting the half-links. In this sense, we are gluing the half-links via a 2-leg intertwiner (between bimodules). Since equivalence classes are defined with respect to a given symmetry, which in turn is associated with a given constraint, this gluing step encodes the implementation of some constraint, which in our context is the Gauß constraint.

Let us now make these statements more precise. We start with two half-links referred to as left l_L and right l_R so that the corresponding half-link algebras are denoted by $\mathcal{A}_{l_{L,R}}$ and the corresponding half-link Hilbert spaces by $\mathcal{H}_{l_L,l_R}$, respectively. States living in such Hilbert spaces are denoted by

$$|j_L, m_L, n_L\rangle \equiv \overset{j_L}{\underset{n_L}{\bullet}\!\!-\!\!\!\dashv\underset{m_L}{}} \in \mathcal{H}_{l_L}$$
$$|j_R, m_R, n_R\rangle \equiv \overset{j_R}{\underset{n_R}{\vdash\!\!-\!\!\bullet\underset{m_R}{}}} \in \mathcal{H}_{l_R} \ .$$

As mentioned above, our goal is to implement the fusion product so as to recover the Hilbert space $\mathcal{H}_l^{\rm kin}$ for the full link, i.e.

$$\mathcal{H}_l^{\rm kin} \simeq \mathcal{H}_{l_L} \boxtimes_{\rm SU(2)} \mathcal{H}_{l_R} \ . \tag{2.32}$$

To do so we need to look at the equivalence classes of states such that the action of the flux operator on the right of the left half-link and the one on the left of the right half-link are the same. We refer to this requirement as the *matching constraint* which is directly related to the implementation of the Gauß constraint. We know that the action of the flux operator at one end of the half-link and its action at the other end are related via parallel transport. We denote by $\widehat{X}_L$ the flux operator acting on the left of l_L and $\widehat{X}_R$ the flux operator acting on the right of l_R. The operators acting on the right of l_L and on the left of l_R are obtained via parallel transport as $\widehat{g}_L \triangleright \widehat{X}_L$ and $\widehat{g}_R \triangleright \widehat{X}_R$, respectively, so that the matching constraint explicitly reads

$$\widehat{g}_L \triangleright \widehat{X}_L = \widehat{g}_R \triangleright \widehat{X}_R \tag{2.33}$$

which can be rewritten

$$(\widehat{g}_R^{-1}\widehat{g}_L) \triangleright \widehat{X}_L = \widehat{X}_R \ . \tag{2.34}$$

By identifying $\widehat{X}_l$ with $\widehat{X}_L$ and $\widehat{g}_l$ with $(\widehat{g}_R^{-1}\widehat{g}_L)$, we finally obtain

$$\widehat{g}_l \triangleright \widehat{X}_L = \widehat{X}_R \iff -\widehat{X}_{l^{-1}} = \widehat{g}_l \triangleright \widehat{X}_l \ . \tag{2.35}$$

This finally implies that the basis states for the Hilbert space $\mathcal{H}_l^{\rm kin}$ are obtained from the gluing of half-links states as the following fusion tensor product

$$|j_L, m_L, n_L\rangle \boxtimes_{\rm SU(2)} |j_R, m_R, n_R\rangle \tag{2.36}$$

which satisfies

$$\big(|j_L, m_L, n_L\rangle \triangleleft g\big) \boxtimes_{\rm SU(2)} |j_R, m_R, n_R\rangle \sim |j_L, m_L, n_L\rangle \boxtimes_{\rm SU(2)} \big(g \triangleright |j_R, m_R, n_R\rangle\big) \ , \tag{2.37}$$

where the right and left group actions read

$$g \triangleright |j_R, m_R, n_R\rangle \equiv \sum_q D^{j_R}_{m_R q}(g^{-1}) \, |j_R, n_R\rangle\langle j_R, q| \tag{2.38}$$

$$|j_L, m_L, n_L\rangle \triangleleft g \equiv \sum_p |j_L, p\rangle\langle j_L, m_L| \, D^{j_L}_{p n_L}(g) \ . \tag{2.39}$$

Equivalence (2.37) implies that the fusion tensor product projects down to states that have matching j_L and j_R, as well as matching m_R and n_L, and on zero otherwise. This is nothing else than the definition of a bivalent intertwiner which implements the Gauß constraint at the bivalent node along which the gluing of the half-links is performed. Indeed, states of the form

$$\sum_p |j, m_L, p\rangle \otimes |j, p, n_R\rangle \tag{2.40}$$

satisfy explicitly the equivalence relation as the l.h.s and the r.h.s of (2.37) are in that case equal. We therefore recover the fact that the full link state should be identified with

$$|j, n_R\rangle\langle j, m_L| \equiv \quad (2.41)$$

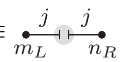

where the gray dot reminds us of the presence of the matching constraint. The reason why we introduced this notion of fusion tensor product is because the idea of a gluing procedure encoding some constraints will be central in the following chapters. Furthermore, in chap. 5, we will explain how such gluing procedure can be dualized so as to define the splitting of a link.

So far, we have defined the kinematical Hilbert space associated to a single link. The next step consists in defining the kinematical Hilbert space for a general graph $\Gamma = (l_1, \dots, l_L)$. As mentioned before, we choose this graph to be the dual of some triangulation $\triangle$ so that it only contains three-valent nodes. By assigning a state $|j, n\rangle\langle j, m|$ to every link $l \subset \Gamma$, we obain a basis for the Hilbert space $\mathcal{H}_\Gamma^{\text{kin}}$. The next step consists in gluing the link states together along nodes $n \subset \Gamma$ so as to obtain the *spin network basis*.

2.2.3 Spin network basis

Since we are dealing with a graph Γ that only contains three-valent nodes, it is sufficient to define the state associated with a single three-valent node. Such state can be obtained as the gluing of three half-link states. As before, this gluing is performed so as to implement the Gauß constraint at the corresponding node. Let n be a three-valent node, we denote three outgoing states meeting at this node by $|j_i, m_i\rangle$, $i = 1, \dots, 3$. The vector space associated with the node is therefore given by the tensor product $V_{j_1} \otimes \cdots \otimes V_{j_3}$ which is well-defined because the group SU(2) is also a Hopf algebra which comes equipped with a comultiplication map allowing to compute tensor product of representations. In order to enforce the gauge invariance, we are looking for an invariant linear map $\iota_n^{j_1 j_2 j_3} : V_{j_1} \otimes V_{j_2} \otimes V_{j_3} \to \mathbb{C}$. Its explicit expression is provided by the so-called Wigner-3jm symbols[2] which satisfy

$$\sum_{m_1, m_2, m_3} \begin{pmatrix} j_1 & j_2 & j_3 \\ m_1 & m_2 & m_3 \end{pmatrix} |j_1, m_1\rangle \otimes |j_2, m_2\rangle \otimes |j_3, m_3\rangle = |0, 0\rangle \ . \quad (2.43)$$

It turns out that the equation above can be interpreted as a higher-valent version of the fusion tensor product $\boxtimes_{\text{SU}(2)}$ discussed above. In the case of a higher than three-valent node, the intertwiner is not unique and can be obtained as a contraction of several Wigner-3jm symbols. We can now define spin network states which form a basis for the Hilbert space of functionals satisfying the Gauß constraint at every node. A spin network is a triplet $(\Gamma, \{j_l\}, \{\iota_n\})$ where

- Γ is a oriented graph embedded on Σ .
- $\{j_l\}$ is a set of group representations labeling the links l of Γ .
- $\{\iota_n\}$ is a set of intertwiners labeling the nodes n of Γ living in the invariant subspace of the tensor product of the representations spaces associated with the incoming and outgoing edges attached to n *i.e.*

$$\iota_n : \bigotimes_{l: n = t(l)} V_{j_l} \longrightarrow \bigotimes_{l: n = s(l)} V_{j_l} \ . \quad (2.44)$$

[2]These are related to the Clebsh-Gordan coefficients via

$$\begin{pmatrix} j_1 & j_2 & J \\ m_1 & m_2 & M \end{pmatrix} = (-1)^{j_2 - j_1 - J} \frac{1}{\sqrt{d_J}} C^{j_1 j_2 J}_{m_1 m_2 M^*} \quad (2.42)$$

where $|J, M^*\rangle = (-1)^{J-M}|J, -M\rangle$ is the conjugate state.

A spin network state is finally obtained by contracting the spin-j states living on the links with the chosen intertwiners, the contraction pattern being dictated by the choice of graph:

$$\Psi[\Gamma, \{j_l\}, \{\iota_n\}] \equiv \mathrm{tr}_{\{V_j\}}\Big[\bigotimes_l |j_l\rangle\langle j_l| \otimes \bigotimes_n \iota_n\Big] \,. \tag{2.45}$$

States satisfying the Gauß constraint can then be obtained as a superposition of spin network states and the corresponding Hilbert space is denoted by $\mathcal{H}^{\mathrm{G}\cdot}_{\Gamma}$.

2.2.4 Dynamics

Let us now very briefly turn to the implementation of the dynamics in the case of 3d gravity. This means characterizing the space of states solving the flatness constraint and defining the physical inner product. This can be done by turning the constraint into a projector. This is particularly easy when dealing with wave functionals $\psi(g) \equiv (g|\psi\rangle$ as it suffices to set all the plaquette holonomies to the identity. More precisely, for a state $|\psi_\Gamma\rangle \in \mathcal{H}^{\mathrm{G}\cdot}_{\Gamma}$, we have

$$\begin{aligned} \mathbb{B} \;:\; \mathcal{H}^{\mathrm{G}\cdot}_{\Gamma} &\longrightarrow \mathcal{H}^{\mathrm{phys}}_{\Gamma} \\ |\psi_\Gamma\rangle &\longmapsto \prod_{p\subset\Gamma} \mathbb{B}_p |\psi_\Gamma\rangle \end{aligned} \tag{2.46}$$

with $\mathbb{B}_p|\psi_p\rangle = |\delta(g_p, \mathbb{1})\psi_p\rangle$ and the inner product is formally provided via

$$\big\langle\, \mathbb{B}\psi_2 \mid \mathbb{B}\psi_1 \,\big\rangle_{\mathrm{phys}} := \big\langle\, \psi_2 \mid \mathbb{B}\psi_1 \,\big\rangle_{\mathrm{kin}} \,. \tag{2.47}$$

Note, however, that this does not define a proper projection since $\delta(\mathbb{1})$ diverges. For instance, in the case of a tetrahedral spin network, whose underlying graph is dual to a triangulation of the two-sphere, the physical wave functions which satisfy the Gauß constraint and the flatness constraint are proportional to the evaluation of the spin network, which in that case is given by a Wigner $6j$–symbol.

Furthermore, it turns out that such a projection onto the space of flat connections can be performed directly in the spin network basis by defining a new projector, whose action is expressed in terms of the Ponzano-Regge state-sum model [72, 73] via so-called *tent moves*. The fact that the projector onto the space of flat connections is not proper is then reminiscent of the divergences appearing in the Ponzano-Regge model. The corresponding lattice Hamiltonian model is the so-called *Levin-Wen* model [39] for the Rep[SU(2)] fusion category of finite dimensional representations. We will not describe precisely this model here, however, in the next chapter we will present a Hamiltonian model, namely the Kitaev double model, which is effectively a Levin-Wen model for the category of $\mathcal{G}$-graded vector spaces.

Chapter 3

Gauge models of topological phases

Over the past few years, there has been a lot of progress in our understanding of *quantum phases of matter* [74, 75]. A quantum phase may be defined as a path connected component in the space of *models*. Since the language that currently most accurately describes quantum many body phases of matter is *quantum field theory*, one may say that a quantum phase of matter is a path connected component in the space of quantum field theories.

Such a space is very difficult to study in its full generality but one may make some progress by restricting to smaller and perhaps more manageable subspaces. This is often done by introducing some adjectives that specify what kind of models or phases we are interested in. These adjectives may refer to the spacetime dimension, the kind of matter involved such as fermionic or bosonic, the symmetry structures the theory is endowed with, broad descriptions of entanglement patterns such as *short-range* or *long-range entanglement*, and broad properties about the spectrum of the theory such as *gapped* or *gapless*.

In this chapter, we focus on gapped phases of matter. Gapped phases are those that have a spectral gap, above the groundstate of the many-body Hamiltonian, that persists in the thermodynamics limit. Focusing on gapped phases greatly simplifies the tasks of classification and characterization due to the expectation that these phases are described by *topological quantum field theories* (TQFTs) in the thermodynamic limit. In other words, all geometric or non-topological correlation functions are exponentially suppressed in some characteristic correlation length scale that depends on the microscopics of the model. Therefore, if we consider a setup where the system size is much larger than any microscopic length scale of the system, we would expect that the only correlation functions that survive are topological in nature and can be captured by a topological theory. Describing a gapped phase is thus easier because TQFTs are much simpler than interacting QFTs in many ways, e.g. their configuration space usually reduces to a finite sum from an integral over an (often divergent) infinite dimensional space. This being said, it is not completely clear that there is a bijection between TQFTs and physically realizable phases of matter, i.e whether all such theories can be realized by physically sensible Hamiltonian lattice models for example. In a recent beautiful work [76] the relation between TQFTs and gapped phases of matter was carefully studied for theories with global symmetries.

There is a particularly tractable class of TQFTs which have a topological gauge theory interpretation. Given a $(d{+}1)$-manifold, the data that goes into defining them is simply a pair $(G, [\omega])$ where G is a finite group and $[\omega] \in H^{d+1}(G, U(1))$ a cohomology class [77, 78]. Such cohomological models are typically defined as space-time state-sum models as in the original paper by Dijkgraaf and Witten [77]. Considering a triangulation $\triangle$ with a G-coloring of the 1-simplices, the path integral

is just a sum over the moduli space of principal G-bundles and the topological action is provided by a cocycle $\omega \in [\omega]$ evaluated on each $(d+1)$-simplex. Because of their gauge theory interpretation, it is particularly easy to define the corresponding Hamiltonian models [48, 79–82]. In this chapter, we focus on the simple setting where the cohomology class is trivial so that the model we consider boils down to an Hamiltonian realization of BF theory which is nothing else than Kitaev quantum double model. So we are effectively studying the same theory as in the previous chapter but this time from a topological phases point of view.

The main point of this chapter is to display in a succinct way how the quasi-excitations are labeled by the Drinfel'd double irreducible representations and explain how this can be used to construct a general basis of excited states. We derive these results from a condensed matter point of view using the language of topological order. In the following chapter, we will adapt, reformulate and make more precise these results in the more general context of lattice gauge theories. Therefore, the reader should expect some overlap between this chapter and the following one. Note finally that we will make use of the conventions introduced here in chap. 6 where we generalize the construction to (3+1)d.

3.1 Gauge model of topological phases

Gapped quantum phases of matter can be defined in terms of equivalences classes of states (or many-body wave functions) under *local unitary transformations*. These equivalence classes are associated with a given pattern of long-range entanglement, which is the defining feature of intrinsic topological orders. Thinking of these local transformations as implementing a wave function renormalization group flow, the task to find equivalence classes of states boils down to defining fixed-point wave functions. The fixed-point wave functions are expected to capture all the universal long-range features of the corresponding phase.

3.1.1 Moduli space and Hilbert space

String net models, or Levin-Wen models [80], were introduced as a systematic way to construct ground states exhibiting the phenomenon of string net condensation. These models are expressed in terms of graphs embedded in Cauchy hypersurfaces. Each graph, together with a given labeling, defines a state. The Hilbert space of the model is then defined as the linear superposition of spatial configurations of string nets. In particular, the fixed-point wave functions we are interested in are obtained as superpositions of such graph-based states. These wave functions are specified uniquely by the local transformations defined on the graph and in turn define ground states of given Hamiltonians. Below, we follow the opposite approach as we first introduce the lattice Hamiltonian and then define the corresponding local transformations.

We are interested in a model which is an Hamiltonian realization of BF theory. As recalled briefly in the previous chapter, the BF action has two equations of motion which impose the connection to be flat and torsionless, respectively. For a Lie group, a connection is fully described by holonomies of a 1-form field $A \in \Omega^1(\Sigma, \mathfrak{g})$. In case the group is discrete, it is convenient to work with a more local description wherein the analog of a 1-connection is a 1-cochain valued in the group. *In the following and for the rest of this thesis, we will work with finite groups. A lot of these results can be generalized easily to the case of Lie groups and we will discuss these generalizations when deemed interesting.*

By definition, flat connections have non-trivial holonomies along non-contractible cycles only and therefore we can label the gauge field configurations by homeomorphisms of the fundamental group

$\pi_1(\Sigma)$ to the finite group $\mathcal{G}$. The configuration space is then given [83] by the moduli space $\mathcal{V}^{\text{flat}}$ of flat $\mathcal{G}$-bundles over Σ

$$\mathcal{V}^{\text{flat}} = \text{Hom}(\pi_1(\Sigma), \mathcal{G})/\mathcal{G} \tag{3.1}$$

where the group acts by conjugation.

From now on and for the rest of this section, we will of focus on the (2+1)d case, however the construction will generalize straightforwardly to the (3+1)d case. Let $\Sigma^{\mathtt{g}}$ be a Riemann surface of genus $\mathtt{g}$ such that $\mathcal{M} = \Sigma^{\mathtt{g}} \times \mathbb{R}$. A presentation of the fundamental group is provided by the group elements $(g_i, h_i)_{i=1}^{\mathtt{g}}$ satisfying $\prod_{i=1}^{\mathtt{g}}[g_i, h_i] = \mathbb{1}_{\mathcal{G}}$. A flat $\mathcal{G}$-bundle is then obtained by such a presentation up to conjugation. Note that taking the quotient by the action of $\mathcal{G}$ is to enforce gauge invariance at a root node which acts as source and target node of all the cycles of $\pi_1(\Sigma^{\mathtt{g}})$. Upon quantization of BF theory on the space-time $\Sigma^{\mathtt{g}} \times \mathbb{R}$, the Hilbert space $\mathcal{H}_{\Sigma^{\mathtt{g}}}$ of gauge-invariant functionals on the space of flat connections on $\Sigma^{\mathtt{g}}$ is introduced. It is well-known [83] that in the case of BF theory, every point of the finite set $\mathcal{V}^{\text{flat}}$ gives rise to one independent quantum state and therefore

$$\dim \mathcal{H}_{\Sigma^{\mathtt{g}}} = |\mathcal{V}^{\text{flat}}| \,. \tag{3.2}$$

This means in particular that the Hilbert space is spanned by states $|g_1, h_1, \cdots, g_{\mathtt{g}}, h_{\mathtt{g}}\rangle$, with the group elements defined up to simultaneous conjugation, such that $\prod_{i=1}^{\mathtt{g}}[g_i, h_i] = \mathbb{1}$, which are in one-to-one correspondence with the flat $\mathcal{G}$-bundles described above. Note that this equality is not true anymore in the case of the Dijkgraaf-Witten model which can be thought as a deformed version of BF theory where the gauge invariance is twisted by a cohomology class.

More generally, let us consider a genus-$\mathtt{g}$ surface $\Sigma_p^{\mathtt{g}}$ which contains p punctures. The surface $\Sigma_p^{\mathtt{g}}$ is a genus-$\mathtt{g}$ surface with one disk removed around each puncture. Additionally, we require the presence of one *marked point* located at the boundary of every such disk. Naturally, punctures introduce additional non-contractible cycles along which the corresponding holonomies can be non-trivial. Let Γ be a graph embedded in $\Sigma_p^{\mathtt{g}}$ which captures at least the loops of the fundamental group $\pi_1(\Sigma_p^{\mathtt{g}})$ and such that for each puncture there is a vertex of Γ coinciding with the marked point.

Furthermore, for every puncture, we decide to relax the gauge invariance at every vertex coinciding with a marked point. Note that we could allow for more vertices at punctures (or more generally at the boundary) at which the gauge invariance would also be relaxed. This would require introducing an equal number of additional marked points [4]. However, in this chapter, there will always be a single marked point at each puncture (or more generally at each piece of boundary) and therefore only a single vertex per puncture at which the gauge invariance is relaxed. The Hilbert space $\mathcal{H}_\Gamma$ is then given by the set of functionals $\psi : \mathcal{G}^E \to \mathbb{C}$ on the space of flat connections, with E the number of edges on Γ, which are everywhere gauge invariant but at the *boundary* vertices.

The group action is therefore reduced to *bulk vertices* only and punctures are the support of both *magnetic* and *electric* point-like excitations. The purpose of the next section will be to compute the non-abelian statistics of these topological excitations supported by punctures.

3.1.2 Lattice Hamiltonian

The physical states of the theory are given by everywhere-gauge-invariant functionals on the space of flat connections. Given a surface $\Sigma^{\mathtt{g}}$, the physical states span a Hilbert space which can be represented by $\mathcal{H}_\Gamma$, such that Γ captures at least the non-contractible cycles. These states define the fixed point wave funtions we are interested in and they appear as ground states of a given lattice Hamiltonian. We will now introduce this lattice Hamiltonian. To each bulk vertex v of Γ, we associate a projector

$\mathbb{A}_v$ which realizes the projection onto gauge invariant states. To every face f of Γ, we associate a projector $\mathbb{B}_f$ which enforces the zero-flux condition (or flatness constraint).

Let us consider a three-valent vertex with all the edges outgoing. According to (2.8), the action of $\mathbb{A}_v$ must read

$\mathbb{A}_v \triangleright$ 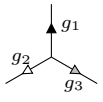 $= \frac{1}{|\mathcal{G}|} \sum_{h\in\mathcal{G}}$ 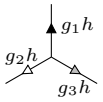 . (3.3)

More generally, it can be expressed as follows

$$\mathbb{A}_v = \frac{1}{|\mathcal{G}|} \sum_{h\in\mathcal{G}} \Big(\bigotimes_{e:s(e)=v} R_h^e \Big) \otimes \Big(\bigotimes_{e:t(e)=v} L_h^e \Big) \tag{3.4}$$

where R_h and L_h correspond to the right and the left group action, respectively, such that $R_h \triangleright \psi(g) = \psi(gh)$ and $L_h \triangleright \psi(g) = \psi(h^{-1}g)$. The operator $\mathbb{B}_f$ simply acts by multiplying the wave function with a delta function

$$\mathbb{B}_f \ \triangleright \psi(\{g\}) = \delta_{h_f,\mathbb{1}_\mathcal{G}}\, \psi(\{g\}) \tag{3.5}$$

where $h_f = \prod^{\leftarrow}_{e\subset f} g_e$ is the oriented product of the holonomies along the boundary of the face f. For instance, in the case of a triangular face, the action simply reads

$\mathbb{B}_f \triangleright$ 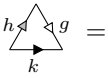 $= \delta_{ghk^{-1},\mathbb{1}_\mathcal{G}}$ 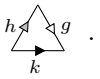 . (3.6)

The operators $\mathbb{A}_v$ and $\mathbb{B}_f$ commute [84, 85] and the lattice Hamiltonian is finally given by

$$\boxed{\mathbb{H} = -\sum_v \mathbb{A}_v - \sum_f \mathbb{B}_f} \tag{3.7}$$

which describes nothing else than Kitaev's quantum double model [84]. Excited states with respect to the ground state wave functions are then obtained as eigenstates for which at least one constraint as imposed by the operators $\mathbb{A}_v$ and $\mathbb{B}_f$ is not satisfied. Within our framework, the introduction of a puncture induces a violation of both the constraints $\mathbb{A}_v \triangleright |\psi\rangle = |\psi\rangle$ and $\mathbb{B}_f \triangleright |\psi\rangle = |\psi\rangle$.

Let us now look at a specific example, namely the two-torus $\mathbb{T}_2$. By definition, we know that the Hilbert space $\mathcal{H}_{\mathbb{T}_2}$ of gauge invariant functionals on the space of flat connections is spanned by states

$$\mathcal{H}_{\mathbb{T}_2} = \Big\{ \frac{1}{|\mathcal{G}|} \sum_{x\in\mathcal{G}} |xgx^{-1}, xhx^{-1}\rangle_{\mathbb{T}_2} \mid gh = hg \Big\} =: \Big\{$ 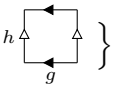 $\Big\}$ (3.8)

where $|g, h\rangle$ is a state defined on a graph capturing the two non-contractible cycles of $\mathbb{T}_2 = \mathbb{S}_1 \times \mathbb{S}_1$. We just introduced (3.8) a graphical representation that we will now justify. Graph states can be chosen to be defined on the one-skeleton of a minimal discretization of the surface. The simplest discretization of the two-torus is provided by one parallelogram whose opposite edges are identified. This discretization is made of one face on which $\mathbb{B}_f$ acts, two oriented edges, and one bulk vertex on which $\mathbb{A}_v$ acts. The two edges correspond to the non-contractible cycles. Furthermore, we decide to label with identical arrows (same shape and same color) edges which are identified. Making the

identification of the edges explicit, we have the correspondence:

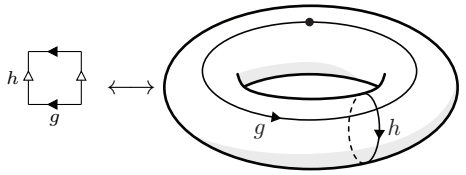

(3.9)

In the following, every time we will make use of the graphical representation as in (3.8), it will be understood that the state is already projected so that gauge invariance is satisfied at every bulk vertex, and every magnetic flux going through a face associated with a contractible cycle is zero. In particular, when the labeling can be deduced from the identification of the edges or the zero-flux condition, it will often be left implicit. Let us examine carefully the case of the basis states on the torus (3.8). First, the torus topology is encoded in the arrows decorating the edges. We can then deduce that there is a single bulk vertex, not located at a puncture, at which a group averaging is performed. Moreover, the zero-flux condition on the square face provides the delta function which enforces the commutation of the two holonomies. Thus, we have the equality

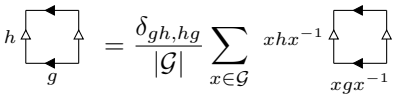

(3.10)

where both the delta function and the group averaging are redundant with the graphical representation, as such, it illustrates the projector property of both $\mathbb{A}_v$ and $\mathbb{B}_f$.

In the following, we will focus on states defined on the twice-punctured two-sphere $\Sigma_2^2 \equiv \mathbb{I}$ which is obtained by cutting open the two-torus along one direction. Every flat bundle is trivial on the two-sphere. There is no non-contractible cycle. However, we introduce punctures which support both electric and magnetic excitations. Anywhere else, both constraints are satisfied. The twice-punctured two-sphere (which is topologically equivalent to a cylinder) $\mathbb{I}$ has a single non-contractible cycle. The discretization is now made of one face on which $\mathbb{B}_f$ acts, three edges, such that two of them define the boundary, and two vertices. Since the vertices, which are required to coincide with the marked points associated with the punctures, are now located at the boundary, we decide to relax the Gauß contraint which leads to electric excitations. As before, we have a graphical representation for the states spanning the Hilbert space $\mathcal{H}_\mathbb{I}$:

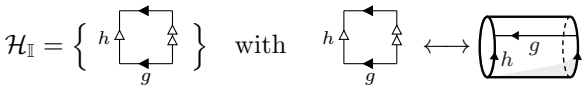

(3.11)

Recall that the states as represented above are already projected. Therefore, the zero-flux condition is enforced on the square face so that we can deduce the labeling for the edge decorated with a double white arrow, namely $g^{-1}hg$. However, it is clear from the graphical representation that, unlike the two-torus, there is no bulk vertex (not located at a puncture) on which $\mathbb{A}_v$ would act, and therefore there is no group averaging in the definition of the states (3.11). Following the same strategy, we could define, for any surface $\Sigma_p^\mathbf{g}$, basis states in terms of holonomies labeling a graph capturing $\pi_1(\Sigma_p^\mathbf{g})$. For instance, we will cover later the case of the thrice-punctured two-sphere.

3.1.3 Equivalence relations

Starting from a graph Hilbert spaces $\mathcal{H}_\Gamma$ such that Γ is embedded in $\Sigma_p^\mathbf{g}$ and captures ar least the non-contractible cycles, we obtain the Hilbert space $\mathcal{H}_{\Sigma_p^\mathbf{g}}$ by identifying graph states equivalent under

deformation maps [4, 34, 86]. More precisely, we identify states defined on different graphs if they are related by the following deformation maps:

- *Changing orientation*—Two graph-states with opposite orientations and inverse group configurations are equivalent:

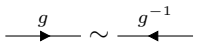

(3.12)

- *Edge deformation*—Every edge can be freely deformed as long as the initial path and the resulting one are homotopy equivalent:

(3.13)

- *Adding/removing vertices*—After subdivision of an edge, the Gauß constraint is enforced at the new vertex and the resulting graph-state equivalent to the original one is given by

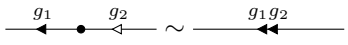

(3.14)

  or conversely, we can remove a bivalent vertex at which the Gauß constraint is imposed and the resulting group-labeling is the oriented product of the original ones.

- *Adding/removing edges*—After addition of an edge, a new closed face is created on which the operator $\mathbb{B}_f$ acts, hence enforcing the zero-flux condition. In the case of a triangular face, the resulting graph-state equivalent to the original one is given by

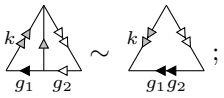

(3.15)

  or conversely, we can remove an edge which is shared by closed faces on which the zero-flux condition is enforced.

These are the local transformations which are required to be satisfied by the fixed-point wave functions, or more precisely, by any graph states such that the constraints imposed by the operators $\mathbb{A}$ and $\mathbb{B}$ are satisfied. They fully define the fixed point wave functions as well as the corresponding lattice Hamiltonian. In the following, we will consider the gluing of graph-states and use these equivalence relations in order to simplify the resulting states.

3.2 Ocneanu's tube algebra and Drinfel'd double

In the previous section, we introduced basis states for the Hilbert space $\mathcal{H}_{\mathbb{I}}$ defined on the twice-punctured two-sphere. These cylinder states play a very important role in the characterization of elementary anyonic excitations. The fundamental reason is that the gluing of two cylinders gives another cylinder. Therefore, states defined on cylinders define an algebra called Ocneanu's tube algebra [21, 32]. In this section, we will define precisely the gluing procedure, show that this algebra actually corresponds to the Drinfel'd double $\mathcal{D}(\mathcal{G})$ of the finite gauge group and present the main features of this rich algebraic structure. To do so, we will follow the steps of [4] where, to the best of our knowledge, the explicit definition of Ocneanu's tube algebra in the holonomy picture was first introduced. The representation theory of $\mathcal{D}(\mathcal{G})$ will provide a natural way of constructing the so-called fusion basis for excited states.

3.2.1 Gluing of cylinders

Starting from the simple observation that gluing two cylinders along a common boundary component leads to another cylinder, we will see that the gluing operation hides a well-known algebraic structure [4, 21, 32, 33, 35]. First, let us define more precisely this gluing operation [5]. Let $\mathcal{M}$ and $\mathcal{N}$ be two manifolds, $\partial\mathcal{M}$ and $\partial\mathcal{N}$ their boundary, which is a disjoint union of submanifolds, and $\mathcal{W}$ such a submanifold of both $\partial\mathcal{M}$ and $\partial\mathcal{N}$. We furthermore require $\mathcal{W}$ to be equipped with a marked point. This last requirement is only true in (2+1)d as in (3+1)d it is also necessary to specify marked edges. The gluing of the manifold $\mathcal{M}$ and $\mathcal{N}$ along $\mathcal{W}$ is defined by identifying the boundary component $\mathcal{W}$ of both $\partial\mathcal{M}$ and $\partial\mathcal{N}$ as well as the corresponding marked points. In the case of the cylinder, the boundary has two components, namely the two punctures, and the gluing of two cylinders consists in stacking them on top of each other.

At the level of the graph-states, the gluing is performed by first identifying the edges and the vertices (associated to the marked points) located at the common boundary along which the gluing is performed. This identification procedure is denoted by $\mathfrak{G}$. After identification, the vertices which once were located at boundaries are now bulk vertices at which the Gauß constraint must therefore be enforced using the operator $\mathbb{A}$. Similarly, in case the identification step $\mathfrak{G}$ produces new faces associated to contractible cycles, the zero-flux condition is enforced using the operator $\mathbb{B}$. Let Γ_1 and Γ_2 be two graphs embedded in the surfaces Σ_1 and Σ_2. The gluing operation of graph-states living in $\mathcal{H}_{\Gamma_1}$ and $\mathcal{H}_{\Gamma_2}$ is denoted by $\star$ and is defined as

$$\begin{array}{rccccc} \star: & \mathcal{H}_{\Gamma_1}\otimes\mathcal{H}_{\Gamma_2} & \xrightarrow{\mathfrak{G}} & \mathcal{H}_{\text{aux}} & \xrightarrow{\mathbb{A}\circ\mathbb{B}} & \mathcal{H}_{\Gamma_1\cup\Gamma_2/\sim} \\ & (\psi_1,\psi_2) & \longmapsto & \mathfrak{G}(\psi_1,\psi_2) & \longmapsto & \mathbb{A}\circ\mathbb{B}\triangleright\mathfrak{G}(\psi_1,\psi_2) \end{array} \tag{3.16}$$

where $\mathcal{H}_{\text{aux}}$ is the Hilbert space of functionals before enforcement of the constraints at the newly created bulk vertices and closed faces, and $\Gamma_1\cup\Gamma_2/\sim$ is the graph obtained after gluing of Γ_1 and Γ_2 up to equivalence relations. In the case of graph-states (3.11) defined on the cylinder, the computation goes as follows

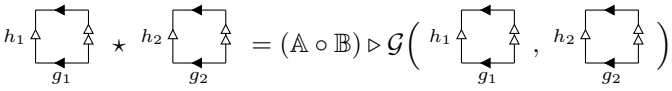

(3.17)

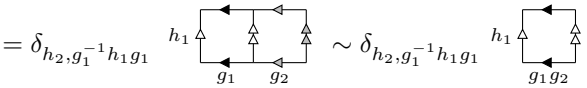

(3.18)

First, the two boundary components are identified which imposes a delta function between two holonomies, then the Gauß constraint is imposed at the four-valent vertex resulting from the gluing. The equivalence relations (3.14) and (3.15) can then be used to first remove the edge labeled by h_2 which leaves a two-valent vertex which can in turn be removed. We summarize this operation as follows, where it is understood that the result is up to equivalence relations:

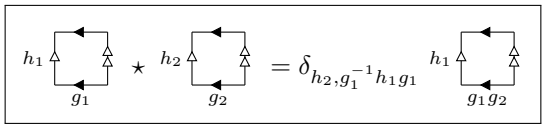

(3.19)

which we recognize as the multiplication rule of the Drinfel'd double.

3.2.2 Drinfel'd double $\mathcal{D}(\mathcal{G})$

For a finite group $\mathcal{G}$, the Drinfel'd double $\mathcal{D}(\mathcal{G})$ is an example of quasi-triangular Hopf algebra. We will not provide here a detailed description of this algebraic structure, only some of its main features. In particular, we will focus on the Hopf algebra structure and leave aside the quasi-triangularity property which describes the braiding of the corresponding anyonic excitations. A detailed construction can be found in [20, 87], see also [4] for many useful identities.

As a Hopf algebra, the Drinfel'd double is a bialgebra obtained as a tensor product of an algebra and its dual coalgebra with opposite comultiplication, together with an antipode map S. A bialgebra A over a field k is a tuple $(A, \star, \mathbb{1}, \Delta, \epsilon)$, such that $(A, \star, \mathbb{1})$ is an algebra over k with multiplication $\star : A \otimes A \to A$ and unit $\mathbb{1} : k \to A$, and (A, Δ, ϵ) is a coalgebra over k with comultiplication $\Delta : A \to A \otimes A$ and a counit $\epsilon : A \to k$, such that Δ and ϵ are algebra homomorphisms. The antipode S is an antihomomorphism such that

$$\star \circ (\mathrm{id} \otimes \mathrm{S}) \circ \Delta = \star \circ (\mathrm{S} \otimes \mathrm{id}) \circ \Delta = \mathbb{1} \circ \epsilon \, . \tag{3.20}$$

Let us now make all these definitions explicit in the case of the Drinfel'd double. As a vector space, the Drinfel'd double is isomorphic to

$$\mathcal{D}(\mathcal{G}) \simeq \mathbb{C}[\mathcal{G}] \otimes \mathcal{F}(\mathcal{G}) \tag{3.21}$$

where $\mathbb{C}[\mathcal{G}]$ is the group ring and $\mathcal{F}(\mathcal{G})$ is the abelian algebra of linear functions on $\mathcal{G}$. A basis for $\mathcal{D}(\mathcal{G})$ is therefore provided by $\{g \otimes \delta_h\}_{g,h \in \mathcal{G}}$ where $\delta_h(\bullet) \equiv \delta(h, \bullet) \equiv \delta_{h,\bullet}$ is the Kronecker delta function supported on h.

As a Hopf algebra, the Drinfel'd double comes equipped with the maps:

- *Multiplication:*
$$(g_1 \otimes \delta_{h_1}) \star (g_2 \otimes \delta_{h_2}) := \delta_{h_1, g_1 h_2 g_1^{-1}} (g_1 g_2 \otimes \delta_{h_1}) \tag{3.22}$$
with corresponding unit element $\mathbb{1}_{\mathcal{D}(\mathcal{G})} = \sum_{h \in \mathcal{G}} \mathbb{1}_{\mathcal{G}} \otimes \delta_h$.

- *Comultiplication:*
$$\Delta(g \otimes \delta_h) := \sum_{\substack{x,y \in \mathcal{G} \\ xy = h}} (g \otimes \delta_x) \otimes (g \otimes \delta_y) \tag{3.23}$$
with corresponding counit map $\epsilon(g \otimes \delta_h) = \delta_{h, \mathbb{1}_{\mathcal{G}}}$.

- *Antipode:*
$$S(g \otimes \delta_h) := g^{-1} \otimes \delta_{g^{-1} h^{-1} g} \, . \tag{3.24}$$

From the identification between the multiplication rule (3.22) of $\mathcal{D}(\mathcal{G})$ and the gluing map (3.19) of cylinder states, we deduce the correspondence

$\mathcal{H}_{\mathbb{I}} \ni$  $\longleftrightarrow \; (g \otimes \delta_h) \in \mathcal{D}(\mathcal{G})$ (3.25)

between cylinder (basis) states and Drinfel'd double (basis) elements. It follows that the elementary excitations or quasiparticles are labeled by the irreducible representations of $\mathcal{D}(\mathcal{G})$ which provide the idempotents of the tube algebra [4, 21, 32]. Indeed the physical excitations are expected to be stable under the operation of gluing cylinders. Since the Drinfel'd double is semisimple, such idempotent states are naturally provided by the irreducible representations.

3.2.3 Representation theory of $\mathcal{D}(\mathcal{G})$

The irreducible representations $\{\rho\}$ of $\mathcal{D}(\mathcal{G})$ are labeled [88, 89] by a conjugacy class C and an irreducible representation R of the centralizer Z_C of C so that $\rho = (C, R)$. The elements of the conjugacy class C are denoted c_a and c_1 is chosen as representative. The centralizer Z_C is then defined as the subgroup of elements commuting with the representative c_1 of C, *i.e.*

$$Z_C = \{g \in \mathcal{G} \,|\, gc_1 = c_1 g\} \,. \tag{3.26}$$

The elements of the quotient $Q_C \simeq \mathcal{G}/Z_C$ are denoted q_a and they satisfy the relation $c_a = q_a c_1 q_a^{-1}$. Finally, the matrix elements of the Drinfel'd double element $g \otimes \delta_h$ in the representation $\rho = (C, R)$ are given by

$$\boxed{D^{C,R}_{am,bn}(g \otimes \delta_h) = \delta(h, c_a)\delta(c_a, gc_b g^{-1}) D^R_{mn}(q_a^{-1} g q_b)} \tag{3.27}$$

where m and n are the matrix indices of the representation R of Z_C, and the delta function $\delta(c_a, gc_b g^{-1})$ ensures that $q_a^{-1} g q_b$ belongs to Z_C. Thereafter, the more compact notation $D^\rho_{MN} \equiv D^{C,R}_{am,bn}$ is used, such that $M \equiv am$, $N \equiv bn$ and $\rho \equiv (C, R)$.

The set $\{\rho\}$ of irreducible representations is complete and orthogonal. The completeness relation reads

$$\sum_\rho \sum_{M,N} d_\rho D^\rho_{MN}(g_1 \otimes \delta_{h_1}) \overline{D^\rho_{MN}(g_2 \otimes \delta_{h_2})} = |\mathcal{G}| \delta_{g_1, g_2} \delta_{h_1, h_2} \tag{3.28}$$

while the orthogonality is provided by

$$\frac{1}{|\mathcal{G}|} \sum_{g,h \in \mathcal{G}} D^{\rho_1}_{M_1 N_1}(g \otimes \delta_h) \overline{D^{\rho_2}_{M_2 N_2}(g \otimes \delta_h)} = \frac{\delta_{\rho_1, \rho_2}}{d_{\rho_1}} \delta_{M_1, M_2} \delta_{N_1, N_2} \,, \tag{3.29}$$

where $d_\rho = d_{C,R} = d_R \cdot |C|$ is the dimension of the representation ρ. Furthermore, thanks to the antipode map S, we can define the representation ρ^* dual to the representation ρ and the expression for the matrix elements is provided by

$$D^{\rho^*}_{MN}(g \otimes \delta_h) = D^\rho_{NM}(S(g \otimes \delta_h)) = D^\rho_{NM}(g^{-1} \otimes \delta_{g^{-1} h^{-1} g}) \,. \tag{3.30}$$

Thanks to the comultiplication, tensor product of representations can be defined such that

$$(D^{\rho_1} \otimes D^{\rho_2})(\Delta(g \otimes \delta_h)) = \sum_{\substack{x,y \in \mathcal{G} \\ xy = h}} (D^{\rho_1} \otimes D^{\rho_2})((g \otimes \delta_x) \otimes (g \otimes \delta_y)) \,. \tag{3.31}$$

Tensor products of representations can then be decomposed into irreducible representations according to the fusion rules $N^{\rho_3}_{\rho_1 \rho_2}$ *i.e.*

$$\rho_1 \otimes \rho_2 = \bigoplus_{\rho_3} N^{\rho_3}_{\rho_1 \rho_2} \, \rho_3 \,. \tag{3.32}$$

For notational convenience, we assume in the following that the fusion category $\mathrm{Rep}[\mathcal{D}(\mathcal{G})]$ of the finite dimensional representations is multiplicity free, *i.e.* $N^{\rho_3}_{\rho_1 \rho_2} \in \{0, 1\}$. Moreover, (3.32) implies the existence of a unitary map $\mathcal{C}^{\rho_1 \rho_2} : \bigoplus_{\rho_3 \in \rho_1 \otimes \rho_2} V_{\rho_3} \to V_{\rho_1} \otimes V_{\rho_2}$ which satisfies

$$D^{\rho_1}_{M_1 N_1} \otimes D^{\rho_2}_{M_2 N_2}(\Delta(g \otimes \delta_h)) = \sum_{\rho_3} \sum_{M_3 N_3} \mathcal{C}^{\rho_1 \rho_2 \rho_3}_{M_1 M_2 M_3} \, D^{\rho_3}_{M_3 N_3}(g \otimes \delta_h) \, \overline{\mathcal{C}^{\rho_1 \rho_2 \rho_3}_{N_1 N_2 N_3}} \,. \tag{3.33}$$

where $(M_1 M_2)$ and $(\rho_3 M_3)$ have to be understood as the indices of the matrix $\mathcal{C}^{\rho_1 \rho_2}$. By analogy with the group case, these maps will be referred to as Clebsch-Gordan coefficients. In the following, it will

be more convenient to work with the analogue of the Wigner $3jm$-symbols, obtained by symmetrizing the Clebsch-Gordan coefficients

$$\begin{pmatrix} \rho_1 & \rho_2 & \rho_3 \\ M_1 & M_2 & M_3 \end{pmatrix} := \frac{1}{\sqrt{d_{\rho_3}}} \mathcal{C}^{\rho_1 \rho_2 \rho_3^*}_{M_1 M_2 M_3} \ , \tag{3.34}$$

which we will refer to as the $3\rho M$-symbols. The interwining map whose coefficients are given by the $3\rho M$-symbols is denoted $\mathcal{I}^{\rho_1 \rho_2 \rho_3}$. The unitarity of $\mathcal{C}^{\rho_1 \rho_2}$ yields the orthogonality relation

$$\sum_{M_1, M_2} \begin{pmatrix} \rho_1 & \rho_2 & \rho \\ M_1 & M_2 & M \end{pmatrix} \overline{\begin{pmatrix} \rho_1 & \rho_2 & \rho' \\ M_1 & M_2 & M' \end{pmatrix}} = \frac{1}{d_\rho} \delta_{\rho, \rho'} \delta_{M, M'}, \tag{3.35}$$

as well as the completeness relation

$$\sum_{\rho} \sum_{M} d_\rho \begin{pmatrix} \rho_1 & \rho_2 & \rho \\ M_1 & M_2 & M \end{pmatrix} \overline{\begin{pmatrix} \rho_1 & \rho_2 & \rho \\ N_1 & N_2 & M \end{pmatrix}} = \delta_{M_1, N_1} \delta_{M_2, N_2} \ . \tag{3.36}$$

Finally, it follows directly from the definition that the $3\rho M$-symbols satisfy the invariance property [4]:

$$\sum_{h_1, h_2} D^{\rho_1}_{M_1 N_1}(g \otimes \delta_{h_1}) D^{\rho_2}_{M_2 N_2}(g \otimes \delta_{h_2}) D^{\rho_3}_{M_3 N_3}(g \otimes \delta_{h_2^{-1} h_1^{-1}}) \begin{pmatrix} \rho_1 & \rho_2 & \rho_3 \\ N_1 & N_2 & N_3 \end{pmatrix} = \begin{pmatrix} \rho_1 & \rho_2 & \rho_3 \\ M_1 & M_2 & M_3 \end{pmatrix} . \tag{3.37}$$

3.2.4 Excitation basis for (2+1)d topological phases

We now have all the necessary ingredients to define our excitation basis for (2+1)d topological phases in terms of irreducible representations of the Drinfel'd double. This basis will be referred to as the *fusion basis* [4, 34, 36, 90]. So far, we have defined basis states for the cylinder $\mathbb{I}$ and the two-torus $\mathbb{T}$ in terms of group holonomies. The correspondence (3.25) provides the fusion basis states for the cylinder as the 'Fourier transform' of the basis states (3.11):

$$|\rho, MN\rangle_{\mathbb{I}} = \frac{1}{|\mathcal{G}|} \sum_{g,h \in \mathcal{G}} \sqrt{d_\rho} D^{\rho}_{MN}(g \otimes \delta_h) \ \ h \ \ g \ . \tag{3.38}$$

Such fusion basis states diagonalize the $\star$-multiplication:

$$|\rho_1, M_1 N_1\rangle_{\mathbb{I}} \star |\rho_2, M_2 N_2\rangle_{\mathbb{I}} = \frac{\delta_{\rho_1, \rho_2}}{\sqrt{d_{\rho_1}}} \delta_{N_1, M_2} |\rho_1, M_1 N_2\rangle_{\mathbb{I}} \tag{3.39}$$

which confirms that the fusion basis states (3.38) on the cylinder are the states of elementary quasi-excitations such that the conjugacy class C labels fluxes while the representation R labels charges. This means in particular that the irreducible representations trivialize the gluing operation presented in (3.16). Indeed, with the fusion basis, the gluing boils down to a contraction of the states by summing over the corresponding magnetic indices. For instance, since the torus is nothing else than a cylinder with the pieces of its boundary identified, we deduce immediately that the fusion basis states for the torus read

$$\boxed{|\rho\rangle_{\mathbb{T}} = \frac{1}{|\mathcal{G}|} \sum_{g,h \in \mathcal{G}} \chi^{\rho}(g \otimes \delta_h) \ \ h \ \ g \ = \frac{1}{|\mathcal{G}|} \sum_{\substack{h \in C \\ g \in Z_h}} \chi^{R_h}(g) \ \ h \ \ g}} \tag{3.40}$$

where χ^ρ denotes the character of the representation ρ and $Z_h = \{g \in \mathcal{G} \,|\, gh = hg\}$ the centralizer of the group element h and χ^{R_h} the character of the representation R_h of Z_h isomorphic to R. The vertices which once were at the boundary of the cylinder are identified to become a bulk vertex at which $\mathbb{A}_v$ acts. The group averaging induces the contraction of the magnetic indices which turns the representation matrix D^ρ into the character χ^ρ defined as

$$\chi^\rho(g \otimes \delta_h) = \Theta_C(h)\delta_{gh,hg}\chi^R(q^{-1}_{\iota_C(h)}\, g\, q_{\iota_C(h)}) \tag{3.41}$$

where $\Theta_C(\bullet)$ is the characteristic function of C and $\iota_C(\bullet)$ is a labeling function defined such that $\iota_C(c_a) = a$. Recall that the holonomy basis states, as represented in (3.40), are already projected so that both the Gauß constraint and the zero-flux condition are imposed. However, these constraints are already encoded in the Fourier transform so that the fusion basis states for the two-torus can equivalently be rewritten $|\rho\rangle_{\mathbb{T}} = \frac{1}{|\mathcal{G}|}\sum_{\substack{h\in C\\ g\in Z_h}} \chi^{R_h}(g)|g,h\rangle_{\mathbb{T}}$. Furthermore, we recover with (3.40) the well-known result that the number of irreducible representations of $\mathcal{D}(\mathcal{G})$ is equal to the ground state degeneracy on the torus, which counts quasi-excitation types [91].

In order to construct the fusion basis for arbitrary surfaces $\Sigma^p_{\mathbf{g}}$, we use the fact that any punctured Riemann surface can be obtained by gluing together several copies of the thrice-punctured two-sphere $\mathbb{Y}$. A 'minimal' thrice-punctured two-sphere can be discretized by a triangular face, on which $\mathbb{B}_f$ acts, with its three vertices identified. The corresponding basis states are labeled by two group holonomies associated to two independent non-contractible cycles and are represented by

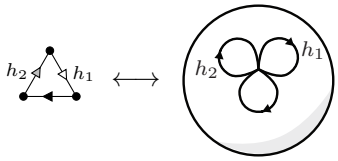

(3.42)

where the dotted vertices are identified. In this example, the holonomies h_1 and h_2 only account for magnetic degrees of freedom. The thrice-punctured sphere as discretized by (3.42) is somewhat degenerate. In order to allow for point-like electric excitations associated to each one of the punctures, we need to choose a slightly more complicated discretization. This will support holonomies accounting for electric degrees of freedom, in addition to the ones accounting for magnetic degrees of freedom. Such discretization is obtained by gluing three outgoing cylinders to the minimal thrice-punctured sphere. The corresponding basis states span the Hilbert space $\mathcal{H}_{\mathbb{Y}}$ and can be represented as

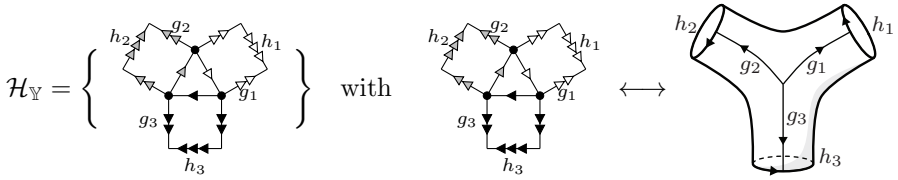

(3.43)

where the black-dotted vertex is now a bulk vertex at which the Gauß constraint is enforced. It now remains to find the corresponding fusion basis. As suggested by the group representation, the basis states of $\mathcal{H}_{\mathbb{Y}}$ can be obtained by gluing three outgoing cylinder basis states (3.11) to the thrice-punctured two-sphere state (3.42). The same happens for the fusion basis. The fusion basis states for the thrice-punctured sphere are defined as the gluing of three cylinder states $|\rho, MN\rangle_{\mathbb{I}}$ via an

intertwining map $\mathcal{I}^{\rho_1\rho_2\rho_3}$, *i.e.*

$$
\begin{aligned}
|\{\rho_i, M_i\}_{i=1}^3\rangle_{\mathbb{Y}} &= \mathrm{tr}_{\{V^\rho\}}\big[|\rho_1, M_1\rangle_{\mathbb{I}} \otimes |\rho_2, M_2\rangle_{\mathbb{I}} \otimes |\rho_3, M_3\rangle_{\mathbb{I}} \otimes \mathcal{I}^{\rho_1\rho_2\rho_3}\big] \\
&= \sum_{\{N_i\}_{i=1}^3} |\rho_1, M_1N_1\rangle_{\mathbb{I}} \otimes |\rho_2, M_2N_2\rangle_{\mathbb{I}} \otimes |\rho_3, M_3N_3\rangle_{\mathbb{I}} \begin{pmatrix} \rho_1 & \rho_2 & \rho_3 \\ N_1 & N_2 & N_3 \end{pmatrix} \\
&= \frac{1}{|\mathcal{G}|^3} \sum_{\{N_i\}_{i=1}^3} \sum_{\{g_i, h_i\}_{i=1}^3} \prod_{i=1}^3 \bigg(\sqrt{d_{\rho_i}} D^{\rho_i}_{M_iN_i}(g_i \otimes \delta_{h_i}) \; h_i \; [\text{diagram}]_{g_i} \bigg) \begin{pmatrix} \rho_1 & \rho_2 & \rho_3 \\ N_1 & N_2 & N_3 \end{pmatrix} .
\end{aligned}
\tag{3.44}
$$

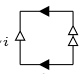

Thanks to the invariance property (3.37), the intertwining map $\mathcal{I}^{\rho_1\rho_2\rho_3}$ ensures that the zero-flux condition on the closed surface of the thrice-punctured sphere is satisfied as well as the gauge invariance at the single bulk vertex. In (3.43), the closed surface in question is the one represented by a triangle with its three vertices identified. Using the zero-flux conditions on the surface of each cylinder, we compute that imposing the zero-flux condition at the triangle boils down to the factor $\delta(g_1^{-1}h_1g_1g_2^{-1}h_2g_2g_3^{-1}h_3g_3, \mathbb{1}_{\mathcal{G}})$. Let us work out how this zero-flux condition and the gauge invariance at the identified vertices are implicitly encoded in the $3\rho M$-symbols in (3.44). Using the invariance property (3.37), one has

$$
\begin{aligned}
&\sum_{\{N_i\}_{i=1}^3} \bigg(\prod_{i=1}^3 D^{\rho_i}_{M_iN_i}(g_i \otimes \delta_{h_i}) \bigg) \begin{pmatrix} \rho_1 & \rho_2 & \rho_3 \\ N_1 & N_2 & N_3 \end{pmatrix} \\
&\quad = \sum_{k_1,k_2 \in \mathcal{G}} \sum_{\{N_i\}_{i=1}^3} \sum_{\{O_i\}_{i=1}^3} \bigg(\prod_{i=1}^3 D^{\rho_i}_{M_iN_i}(g_i \otimes \delta_{h_i}) \bigg) \\
&\qquad\qquad \times D^{\rho_1}_{N_1O_1}(g \otimes \delta_{k_1}) D^{\rho_2}_{N_2O_2}(g \otimes \delta_{k_2}) D^{\rho_3}_{N_3O_3}(g \otimes \delta_{k_2^{-1}k_1^{-1}}) \begin{pmatrix} \rho_1 & \rho_2 & \rho_3 \\ O_1 & O_2 & O_3 \end{pmatrix} \\
&\quad = \sum_{k_1,k_2 \in \mathcal{G}} \sum_{\{O_i\}_{i=1}^3} \bigg(\prod_{i=1}^3 D^{\rho_i}_{M_iO_i}(g_ig \otimes \delta_{h_i}) \bigg) \delta_{k_1, g_1^{-1}h_1g_1} \delta_{k_2, g_2^{-1}h_2g_2} \delta_{k_2^{-1}k_1^{-1}, g_3^{-1}h_3g_3} \begin{pmatrix} \rho_1 & \rho_2 & \rho_3 \\ O_1 & O_2 & O_3 \end{pmatrix} \\
&\quad = \sum_{\{O_i\}_{i=1}^3} \bigg(\prod_{i=1}^3 D^{\rho_i}_{M_iO_i}(g_ig \otimes \delta_{h_i}) \bigg) \delta(g_1^{-1}h_1g_1g_2^{-1}h_2g_2g_3^{-1}h_3g_3, \mathbb{1}_{\mathcal{G}}) \begin{pmatrix} \rho_1 & \rho_2 & \rho_3 \\ O_1 & O_2 & O_3 \end{pmatrix}
\end{aligned}
\tag{3.45}
$$

where we used the defining property of the representations of the Drinfel'd double. By comparing the first and the last line of (3.45), we conclude that the $3\rho M$-symbols implicitly encode the zero-flux condition as well as the gauge invariance. Note that we first introduced the comultiplication rule of the Drinfel'd double together with the corresponding tensor product and then use it to define states on the thrice-punctured two-sphere. Conversely, we could have first considered the gluing of three cylinder basis states as in (3.44) and derived which constraints needed to be imposed for this gluing to be consistent, from which we could have derived the comultiplication rule.

Using the states (3.44), we can construct a fusion basis for any Riemann surface Σ_p^{g}. It suffices to decompose the surface Σ_p^{g} as a sewing of several copies of $\mathbb{Y}$, associate a state $|\{\rho_i, M_i\}_{i=1}^3\rangle_{\mathbb{Y}}$ to each copy of $\mathbb{Y}$ and contract them to each other following the decomposition pattern. Equivalently, we can associate an intertwining map $\mathcal{I}^{\rho_1\rho_2\rho_3}$ to each copy of $\mathbb{Y}$ and contract them via cylinder states $|\rho, MN\rangle_{\mathbb{I}}$. For a given surface Σ_p^{g}, and for a given pant decomposition $\{\mathbb{Y}\}$, a formal expression for the corresponding fusion basis states therefore reads

$$
\boxed{\big|\{\rho_i\}_{i=1}^L\big\rangle_{\Sigma_p^{\mathsf{g}}} = \mathrm{tr}_{\{V^\rho\}}\Big[\bigotimes_{\mathbb{I}} |\rho\rangle_{\mathbb{I}} \otimes \bigotimes_{\mathbb{Y}} \mathcal{I}^{\{\rho\}}\Big]}
\tag{3.46}
$$

where L is the number of 'connections' between the thrice-punctured spheres. The fusion basis is *orthogonal* and *complete* [4]. This follows directly from the orthogonality (3.29) and completeness (3.28) of the representation matrices as well as the orthogonality (3.35) and completeness (3.36) of the $3\rho M$-symbols.

Chapter 4

Fusion basis for LGT and 3d gravity

In this chapter, we adapt and expand on the results of the previous chapter in order to derive a new basis, namely the so-called *fusion basis*, for lattice gauge theories (LTGs) and in particular for 3d quantum gravity. This basis turns out to be a very interesting alternative to the usual spin network basis whose definition was recalled in chap. 2. In doing so, we shift the focus from the original lattice structure directly to that of the magnetic (curvature) and electric (torsion) excitations themselves. Since the fusion basis allows for both magnetic and electric excitations from the onset, it turns out to be a precious tool for studying the large scale structure and coarse-graining flow of lattice gauge theories and loop quantum gravity. This is in neat contrast with the spin network basis, in which it is much more complicated to account for electric excitations, i.e. for Gauß constraint violations, emerging at larger scales. Moreover, since the fusion basis comes equipped with a hierarchical structure, it readily provides the language to design states with sophisticated multiscale structures.

4.1 Motivation

The fusion basis we introduce here is adapted from the theory of topological phases in (2+1)d. We therefore restrict here to (2+1)d lattice gauge theories and loop quantum gravity. Furthermore, another simplification we introduce in order to focus on the main ideas without bothering about technical details, is that we consider only a finite gauge or structure group $\mathcal{G}$. We will comment on the application to Lie groups.

Let us briefly describe and compare the main features of the spin network and fusion basis. The spin network basis diagonalizes at each link of the lattice the quadratic Casimir operator built from the electric fluxes. These operators are gauge invariant and coincide with the electric contribution to the Yang-Mills Hamiltonian. For a non-abelian structure group, additional, gauge-invariant, information on the electric fluxes is encoded at the nodes, in so-called intertwiners. Therefore, the spin network basis provides a polarization of the state space based on the flux observables.[1] The fusion basis, on the other hand, diagonalizes Wilson loop operators, i.e. traces of holonomies associated to closed paths.

[1] Flux observables do actually *not* commute in non-abelian gauge theories. In [92], this is made explicit and a polarization is constructed, in which fluxes compose by non-commutative multiplication.

In this sense, the fusion basis provides a polarization dual to the spin network one. To avoid over-parametrization, one does, however, not include all possible Wilson loops supported on the lattice, but only a certain hierarchically ordered set.

A crucial feature of non-abelian gauge theories is that this set of Wilson loops does *not* define a maximal set of commuting observables. In fact, it is necessary to also consider certain flux observables, based again on closed loops, that capture the electric (or torsion) degrees of freedom arising at scales larger than the lattice one. Maybe surprisingly, these large scale data are not already encoded in the multilevel Wilson loop observables. The fusion basis is designed to encode both Wilson loop and large scale flux observables in a unified framework.

In fact, it turns out that the fusion basis diagonalizes closed *ribbon* operators, which directly classify the magnetic (curvature) and electric (torsion) excitations. This notion of excitation has to be understood with respect to some vacuum state. Here, the relevant one is the so-called BF vacuum. Taking its name from the BF topological field theory, of which it is a physical state, this vacuum state is a gauge invariant state peaked sharply on vanishing curvature, i.e. on a flat connection. It is then not surprising, that the fusion basis framework bares a close relationship with the theory of extended topological quantum field theories on the mathematical side, and with topological phases and their defect excitations on the condensed matter side [39, 93, 94].

After introducing the fusion basis and the ribbon operators characterizing it, we will give an overview of various applications. Firstly, we will discuss how to use the fusion basis to easily design multi-scale states. It is interesting to compare the tools developed here to the closely related philosophy underlying the introduction of tensor network states, which provide an Ansatz for the ground state of Yang-Mills theories [95].[2] Secondly, using the muli-scale states, we describe a coarse-graining scheme based on the fusion basis. At this point of the discussion, the advantage in using the fusion basis should be obvious: Coarse-graining is directly given by the fusion of excitations, which are in turn naturally encoded in the fusion basis itself.

4.2 BF representation in 2+1 dimensions

In lattice gauge theories, observables can be given in terms of holonomies (or Wilson lines), encoding the magnetic degrees of freedom, and fluxes, encoding the electric degrees of freedom. In 2+1 dimensions, both holonomy and flux observables test the continuum field along a one-dimensional path embedded in the spatial manifold. On a fixed graph (or lattice) one has only access to a restricted set of such holonomies and fluxes, that is those that can be composed from the elementary holonomies and fluxes associated to the links of the graph itself. In this way different graphs Γ lead to different Hilbert spaces $\mathcal{H}_\Gamma$, hence providing a representation of the holonomies and fluxes based on Γ.

One can however consider also all possible graphs at once (or at least a suitable set of graphs allowing for infinite refinement) by constructing a so-called inductive limit of the family of Hilbert spaces $\{\mathcal{H}_\Gamma\}_\Gamma$. This allows for the representation of holonomies and fluxes based on arbitrary paths (or again based on a suitable set of paths). Such an inductive limit construction led to the Ashtekar-Lewandowski-Isham (ALI) representation [67–69, 71] of the kinematical[3] observable algebra in loop quantum gravity. Here the selection of a (kinematical) vacuum state is essential, which in the case of the ALI representation is given by a state for which the expectation values vanishes for all operators

[2] In the context of (2+1)d gravity, on the other hand, the BF vacuum already provides the physical state of the theory, i.e. the state invariant under full diffeomorphism symmetry. Fusion basis states, then, encode multi-particle states coupled to gravity. Therefore, this basis could be a useful tool to understand their coupled dynamics.

[3] That is the observables are not completely space-time diffeomorphism invariant.

composed from fluxes. This implies that the resulting Hilbert space supports states which have vanishing flux expectation values almost everywhere. Since the fluxes encode the spatial metric, the states describe therefore an almost everywhere degenerate geometry.

This was one of the motivations for the construction of an alternative representation based on a different—actually dual—vacuum, sharply peaked on vanishing curvature [22, 86, 96]. This vacuum is a solution of the BF theory and describes in lattice gauge theory the weak coupling limit. BF theory plays also an important role in the gravity context: It is itself a formulation of (2+1)d gravity as recalled in chap. 2, and moreover, in 3+1 dimensions, it is the starting point for the construction of spin-foam models, a covariant version of loop quantum gravity [59]. A quantum deformed version [34], based on the Turaev-Viro topological theory[4] [97], describing (2+1)d Euclidean gravity with positive cosmological constant, is more directly formulated as an extended topological field theory. Here the notion of defect excitations, supported in 2+1 dimensions on punctures, is essential.

In this section, we shortly explain the BF representation for loop quantum gravity and a related understanding of lattice gauge theory as an extended topological field theory. The BF representation in [22, 86, 96] is based on an inductive limit involving triangulations and their dual lattices. We will review this notion and then lay out an alternative construction, similar to [34], which is nearer to the spirit of extended topological field theory. In the latter case, the graphs or lattices have a less fundamental role. Instead, one uses punctures (or 'defects') which carry the excitations. These defect excitations are to be understood as deviations from a vacuum or alternatively violations of constraints, which characterize the vacuum. This vacuum is here given as the BF vacuum, i.e. a state without curvature (magnetic excitation) or torsion (electric excitation). These considerations will also allow to understand lattice gauge theory as an extended topological field theory, that is a topological field theory with a (fixed) number of defects allowed.

4.2.1 Triangulation-based BF representation: review and limitations

The BF representation is based on a so-called inductive limit of Hilbert spaces. The inductive limit is defined via a family of Hilbert spaces labelled by elements of a partially ordered (and directed) set. Each Hilbert space of this family can be understood to capture a certain subset of the degrees of freedom of the continuum, given by the inductive limit. In this sense, a given Hilbert space of this family defines also a discretization.

In [22, 86, 96], such an inductive limit was based on the refinement of triangulations of a given 2d hypersurface Σ. Specifically, given Σ and a triangulation $\triangle$ thereof, the configuration space underlying the Hilbert space $\mathcal{H}_\triangle$ is given by the moduli space of flat connection on $\Sigma \setminus \triangle_0$, that is $\mathcal{V}^{\text{flat}}(\Sigma \setminus \triangle_0)$. Here $\triangle_0$ is the set of 0-simplices, i.e. vertices, of the triangulation. As is well known, $\mathcal{V}^{\text{flat}}(\Sigma \setminus \triangle_0)$ can be fully described by considering the set of holonomies[5] along the links of a graph Γ dual to the triangulation. Clearly, the flatness conditions ensures that the specific choice of dual graph is irrelevant. Then, $\mathcal{H}_\triangle$ is given by the gauge invariant functions of such holonomies, equipped with a specific inner product. For a well-defined inductive limit, the measure on the underlying gauge group $\mathcal{G}$ has to be discrete, even if $\mathcal{G}$ is a Lie group [22, 86].

It is often convenient to choose a marked point on the manifold, the 'root', at which gauge invariance is relaxed. Fully gauge-invariant functions can be re-obtained via a gauge averaging procedure.

[4] This representation is so far only applicable to 2+1 dimensions, for a strategy to generalize to 3+1 dimensions, see [6].

[5] We use the word 'holonomy' for the group-valued path-ordered exponential of a connection along a path between two points on the manifold. It transforms covariantly upon gauge transformations at its starting and ending points, and it is invariant upon any other gauge transformation.

The advantage of having a root is clear if $\mathcal{G}$ is a Lie group: The gauge averaging procedure over $\mathcal{G}$ equipped with a discrete measure would in general lead to many subtleties [86]. Physically, the root can be interpreted as a reference frame internal to the system.

So far we have described the structure of the Hilbert space $\mathcal{H}_\triangle$ on a fixed triangulation. What is missing is the inductive limit construction of the continuum Hilbert space $\mathcal{H}_\Sigma$. Consider two triangulations $\triangle$ and $\triangle'$, such that $\triangle'$ is a refininement of $\triangle$, i.e. $\triangle \prec \triangle'$. Then, the inductive limit is based on the definition of embedding maps

$$\iota_{\triangle,\triangle'} : \mathcal{H}_\triangle \hookrightarrow \mathcal{H}_{\triangle'} . \tag{4.1}$$

Roughly speaking, in the BF representation, the embedding maps multiply the states in $\mathcal{H}_\triangle$ with a set of delta-functions—hence the relevance of the discrete measure on the group—enforcing the triviality of the holonomy around every additional cycle present in Γ' but not in Γ. Notice that there is one such cycle for every element of $\triangle'_0 \setminus \triangle_0$. This defines $\mathcal{H}_\Sigma$. However, we also need to define operators $\mathcal{O}$ compatible with the refinement procedure. This is easily done by requiring,

$$\mathcal{O}_{\triangle'} \circ \iota_{\triangle,\triangle'} = \iota_{\triangle,\triangle'} \circ \mathcal{O}_\triangle . \tag{4.2}$$

In [22, 96], such operators have been constructed and fully characterized. They are of two types. Firstly, there are holonomy operators along root-based closed cycles of Γ. These operators are labelled by a representation of $\mathcal{G}$ and act by multiplication in the obvious way. Secondly, there are so-called *exponentiated flux operators*. In (2+1)d, they are associated to edges of the triangulation $\triangle$ itself. They act by translating the holonomies associated to the links of Γ dual to the relevant edges of $\triangle$. Therefore, they act as exponentiated derivative operators, hence their name.[6] Notice that the holonomy translation by the action of the exponentiated fluxes induces curvature defects at some vertices of the triangulation. In other words, it introduces non-trivial monodromies around cycles of Γ dual to some vertices of $\triangle$. To obtain a state with a curvature defect at an arbitrary position $x \in \Sigma$, one just has to first refine $\triangle$ to $\triangle'$ in such a way that $x \in \triangle'_0$. Finally, we stress that the operators just described, and properly defined in [22, 86], are either gauge invariant or lead to gauge violations confined at the root.

This last remark is important because, in the present work, we will allow torsion degrees of freedom to be carried by the vertices of the triangulation. This means that more general gauge-invariance violations than in the setting presented above will be allowed. Although to avoid technicalities we will do this in the context of a finite group gauge theory, this generalization is conceptually of crucial importance for gravity (which is, of course, based on a Lie group). This is because, spinning particles induce torsion violation [98, 99]. The relevant operators, creating this more general type of excitations, have been introduced—albeit in a slightly different manner with respect to ours—by Kitaev, in [38]. He called them 'ribbon operators'. In the context of (2+1)d gravity, ribbon operators crucially provide Dirac observables. We draw from this further motivation for the present work, in that we want on the one hand to give a lattice-independent definition of ribbon operators, and on the other to use their eigenvalues to fully characterize a basis of the quantum gravity Hilbert space on Σ.

4.2.2 An alternative description of the BF representation

Here we present an alternative formulation of the BF-representation. Its advantages are multiple: First, its language is closer to that of the Turaev-Viro based representation [34]. Second, it translates

[6] In the ALI representation of loop quantum gravity, gravitational fluxes act as derivatives on the holonomies.

a range of techniques used in the context of string net models [37, 80] to an holonomy-based formalism. Finally, it provides a lattice-independent description of the Kitaev model [38], which can in turn be mapped onto an 'extended' string net model [93, 94].

The basic idea behind this alternative formulation is to replace the triangulation, its vertices and its dual graph, with a less rigid structure provided by punctured surfaces and general graphs on them. Introducing an equivalence class among graphs allows for a first step towards the continuum limit. We say 'a first step' because in this thesis we will work with the defects' locations, i.e. the punctures, kept fixed. The second, and last, step to the continuum limit would be to consider the inductive limit in which one allows for the addition of new punctures. A possible way to achieve this is sketched in app. A.1.

Let us now provide all the ingredients needed for the construction of this alternative description of the BF representation.

Finite group: As mentioned above, we will work with a finite gauge group $\mathcal{G}$, with $|\mathcal{G}| < \infty$ elements. Some of our results can be generalized to Lie groups, in both the BF and ALI representations. This would, however, require lengthy (measure theoretical) technical discussions. Here, we rather prefer to emphasize the underlying algebraic structures and the many analogies to the TV representation. Indeed, one can understand the q-deformation at root of unity characteristic of the TV representation, as in a certain sense turning SU(2) into a finite (quantum) group $\mathrm{SU}(2)_q$. Spin-foam models with finite groups are used to study the behaviour of spin-foams under coarse-graining [19, 60, 62, 100, 101], and we hope that the techniques developed here will be useful also in this context. We denote general elements of $\mathcal{G}$ by $G, H, g, u, \dots$ and variations thereof, and the identity element by $\mathbb{1}$. The delta-function on the group is normalized so that $\delta(g,h) \equiv \delta_{g,h} \equiv \delta_g(h) = 1$ if $g = h$ and vanishes otherwise.

Punctured surface: In our analysis we will for simplicity exclusively work in the case in which Σ is the two-sphere $\mathbb{S}_2$. Fix $\mathbb{S}_2$ to have a finite number $|p|$ of marked points, called punctures $\{p\}$. Define Σ^0_p to be the genus-0 surface $\mathbb{S}_2$ with one disc removed around each puncture and with one point marked on the boundary of each such discs. We will call these points *puncture-nodes*. This structure is needed to describe torsion defects and later-on to define the gluing of states along punctures. Now, consider finite directed graphs embedded into this surface. The graphs can have *open links*, i.e. links ending in a one-valent node, provided this node is a puncture-node. We require all other nodes to be two- or tri-valent.[7] This is just a choice, that leads to a triangulation as dual complex and furthermore makes a translation to string nets (via a standard group Fourier transform) more immediate. This restriction can however be easily dropped.[8]

Among all the possible graphs, there is a special subclass of *minimal graphs*. Minimal graphs on a punctured sphere are defined by the following properties: (i) They capture the first fundamental group of the punctured sphere, namely $\pi_1(\Sigma^0_p)$, (ii) they have no contractible faces, that is all their faces enclose a puncture, (iii) they have no two-valent node, and (iv) they have one open link associated to each puncture, see fig. 4.1 for examples. Given Σ^0_p, minimal graphs are by no means unique. From our definition, it is not difficult to see that a minimal graph on $\Sigma^0_{p>1}$ must have exactly $L = 1 + 2(p-2) + 3(p-1) = 5p - 6$ links, and $N = \frac{1}{3}(2L - p)$ internal nodes.

Hilbert Space $\mathcal{H}_p$: The configuration space underlying the BF representation is, exactly as before, given by the moduli space of flat connections on $\mathbb{S}_2$ minus some points (or, equivalently, discs). In

[7] Two-valent nodes are needed only as intermediate steps of the refining procedure.

[8] Notice the difference between this formulation and the one of the previous chapter as we are now working on graphs dual to triangulations while we were previously working on the one-skeleton of a given discretization.

Figure 4.1. Examples of minimal graphs on the twice-punctured $\mathbb{I}$ and thrice-punctured spheres $\mathbb{Y}$.

this case, this reads $\mathcal{V}^{\text{flat}}(\Sigma_p^0)$. This space is now completely characterized by the holonomies along the links of a minimal graph Γ. Hence, we define the Hilbert space $\mathcal{H}_\Gamma$ to be given by the set of gauge invariant functions $\{\psi\}$ on such a space of holonomies:

$$\psi : \mathcal{G}^L \to \mathbb{C} , \tag{4.3}$$

where L denotes the number of links of the minimal graph. Importantly, we require the gauge group to act only at the internal nodes, and not at the puncture-nodes. Indeed, imposing gauge invariance at the puncture-nodes would result in the trivialization of the dependence of the state from the group element associated to the only link ending there. In the following, it will become apparent that avoiding this trivialization is crucial to implement both torsion excitations and a consistent cutting-and-gluing scheme of the states. More specifically, a gauge transformation is parametrized by a choice $\{u_n\}_n \in \mathcal{G}^N$ where n denotes an internal node and N their number. It acts on a holonomy configuration $\{g_l\} \in \mathcal{G}^L$ as

$$\{u_n\}_n \triangleright \{g_l\}_l = \{u_{t(l)}^{-1}\, g_l\, u_{s(l)}\}_l , \tag{4.4}$$

where $s(l)$ and $t(l)$ denote the source and target nodes of the link l, respectively.[9] Finally, the inner product in $\mathcal{H}_\Gamma$ is defined by

$$\langle \psi_1, \psi_2 \rangle = \frac{1}{|\mathcal{G}|^L} \sum_{\{g_l\}} \overline{\psi_1\{g_l\}}\, \psi_2\{g_l\} . \tag{4.5}$$

To obtain a Hilbert space $\mathcal{H}_p$ associated directly to Σ_p^0, we need to show how to identify various $\mathcal{H}_{\Gamma'}$ for different choices of (possibly non-minimal) graphs Γ' in Σ_p^0 . We do this by declaring two states based on different graphs as equivalent if they are related by a combination of the four operations we are now going to describe. The idea is that via a minimal graph one can already characterize $\mathcal{V}^{\text{flat}}(\Sigma_p^0)$ completely: It gives access to the holonomies associated to all the non-contractible cycles (those around the punctures), as well as giving the holonomy (parallel transport) between any couple of punctures. Since the connection is locally flat, the path underlying each holonomy can be smoothly deformed. Also, we can refine the graph, provided we ensure that the holonomies associated to the contractible cycles are all trivial, and that gauge invariance is preserved. As a consequence of gauge invariance, we can freely remove two-valent nodes. Likewise for a non-minimal graph we can remove links, if the resulting graph still captures $\pi_1(\Sigma_p^0)$. Formally, the operations are:

- *Link deformation*—A link can be (smoothly) deformed as long as no other link, node or puncture is crossed. Two states ψ, ψ' based on two graphs Γ, Γ' related by a link deformation are defined to be equivalent if they are described by the same function, i.e. if $\psi(\{g\}) = \psi'(\{g\})$ as functions on $\mathcal{G}^L$.

[9] In the equation above, we left understood that $u_{s(l)} \equiv e$ if $s(l)$ is a puncture-node. Similarly for $t(l)$.

- *Link orientation flip*—After flipping the orientation of a link $l \to l^{-1}$, the state ψ' equivalent to ψ is

$$\psi'(g_{l^{-1}}, \dots) \;=\; \psi(g_l^{-1}, \dots) \,. \tag{4.6}$$

- *Link subdivision/union*—After the subdivision of a link $l \to l_2 \circ l_1$, the state $\psi'(g_{l_1}, g_{l_2}, \cdots)$ equivalent to $\psi(g_l, \cdots)$ is

$$\psi'(g_{l_1}, g_{l_2}, \dots) = \psi(g_{l_2} g_{l_1}, \dots) \,. \tag{4.7}$$

- *Face removal/addition*—After the addition of a new link l, the graph gains a new closed face (that is a contractible cycle) f with holonomy h_f (we are assuming that any link subdivision necessary to the addition of this new link has already been performed). Then the state $\psi'(\{g_{l'}\})$ on the new graph which is equivalent to the original $\psi(\{g_l\})$ is

$$\psi'(\{g_{l'}\}) = \sqrt{|\mathcal{G}|}\; \delta(\mathbb{1}, h_f)\, \psi(\{g_l\}) \,. \tag{4.8}$$

  where the factor $\sqrt{\mathcal{G}}$ in (4.8) has been introduced to ensure that equivalent states have the same norm.

At this point, it is a simple exercise to show that the inner product is independent of the choice of representative in the equivalence class described above. This concludes the construction of $\mathcal{H}_p$. Notice that the only information that is common to all $\mathcal{H}_\Gamma$, and therefore that is proper to $\mathcal{H}_p$ itself, is the embedding of the punctures. This mirrors the properties of the states in $\mathcal{H}_p$: Excitations are confined to the punctures and the state describe locally-flat gauge-invariant connections away from the punctures. To obtain a continuum Hilbert space allowing for excitations at arbitrary positions in Σ we have to consider the inductive limit over Hilbert spaces $\mathcal{H}_p$, where p stands not only for the number of punctures (denoted by $|p|$) but also for their embedding information. For a sketch on how to achieve this, we refer to app. A.1.

The construction presented here can be recast in a spin network language, essentially by decomposing the states ψ via the Peter-Weyl theorem onto a graph-dependent basis labeled by representation-theoretic data. In this formulation one would recover the so-called extended string nets [93, 94], and the conditions above would be rephrased in a completely algebraic and combinatorial language.

4.3 From Ocneanu's tube algebra to the Drinfel'd double

So far, we have been describing states in a graph-dependent and redundant fashion. Graph independence is then shown to be recovered thanks to the introduction of appropriate equivalence relations. It would be, however, much more efficient to characterize the states directly, with no reference to any choice of graph. To this end we turn our focus on the punctures and the excitations they carry. Let us start by analyzing the simplest cases, Σ_p^0 with $|p| = 1, 2, 3$.

We know $\mathbb{S}_2$ cannot carry excitations, since $\pi_1(\mathbb{S}_2)$ is trivial. Indeed, a minimal graph on $\mathbb{S}_2$ has one link l surrounding the puncture, and one link l' starting at $n = s(l) = t(l)$ and ending at the puncture-node; now, contractibility of l imposes $\psi(g_l, g_{l'}) = \delta(\mathbb{1}, g_l) f(g_{l'})$, while gauge invariance at n requires f to be constant. Thus, the simplest non-trivial case is that of the twice-punctured sphere, $\Sigma_2^0 \equiv \mathbb{I}$. The study of states on the cylinder is the subject of this section. The next-simplest case is the thrice-punctured sphere $\mathbb{Y} \equiv \Sigma_3^0$ whose study is the subject of the next section (sec. 4.4).

4.3.1 Characterizing the excitations

As explained in the previous chapter, cylinders play a special role in the characterization of 'basic' excitations since cylinders can be glued 'around a puncture' without changing the topology of Σ_p^0. By successively gluing cylinders onto one-another, it is straightforward to define a multiplication between cylinder states which leads to Ocneanu's tube algebra.

By visualizing the cylinder as an annulus of space, one can think of the gluing operation as the addition of 'more-space' around an excitation. Topological excitations relevant to 3d gravity should be stable under this operation. Therefore, they are characterized by idempotents of the tube algebra, or—equivalently—by its indecomposable (representation) modules [21, 32, 33]. As pointed out by Ocneanu [21, 32], this allows the interpretation of such idempotents as viable boundary conditions. In the next subsection, we will rederive how the tube algebra is nothing but the Drinfel'd double algebra $\mathcal{D}(\mathcal{G})$ [20] in the present context. Hence we conclude that excitations in 3d Euclidean gravity can be classified in terms of irreducible representation ρ of $\mathcal{D}(\mathcal{G})$. In the case $\mathcal{G} = \mathrm{SU}(2)$, the two labels defining such a ρ can be directly interpreted as the mass and the spin of the excitation.

This result is not new, see e.g. [102–105]. However, in previous treatments, it was a found as a consequence of the presence of group-valued constraints (moment maps). The gluing of cylinder states seems, however, to provide so far the simplest and most direct argument.

4.3.2 Twice-punctured sphere

A minimal graph Γ_2 on the twice-punctured two-sphere $\mathbb{I}$ possesses four links $\{l_i\}_{i=1,\dots,4}$. We fix the compositions $l_2^{-1} \circ l_4$ to be a closed loop winding once around the cylinder, and $l_3 \circ l_2 \circ l_1$ to go from the *source* puncture to the *target* puncture. Finally, label the links of the graph with group elements $\{g_{l_i} \in \mathcal{G}\}$. For brevity we set $g_{l_i} = g_i$:

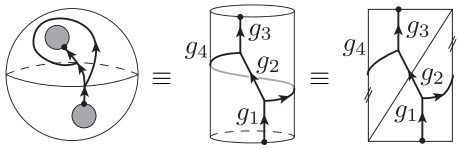

(4.9)

A state in $\mathcal{H}_{\Gamma_2}$ is given by a gauge invariant state

$$\psi^{\mathbb{I}}(g_1, g_2, g_3, g_4) = \psi^{\mathbb{I}}(ug_1, vg_2u^{-1}, g_3v^{-1}, vg_4u^{-1}) \,, \tag{4.10}$$

for any $u, v \in \mathcal{G}$. Taking advantage of the gauge invariance of $\psi^{\mathbb{I}}$, choosing $v = g_3$ and $u = g_3g_2$, we can fix $g_2 = \mathbb{1} = g_3$. A basis of $\mathcal{H}_{\Gamma_2}$ is then given by the gauge-fixed states

$$\psi^{\mathbb{I}}_{G,H}(g_1, g_4)_{|\text{g.f.}} = |\mathcal{G}|^{3/2}\delta(G, g_1)\delta(H, g_4) \equiv |\mathcal{G}|^{3/2}$$

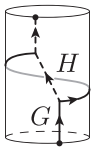

. (4.11)

where $|\mathcal{G}|^{3/2}$ is a normalization factor chosen for later convenience. In the above diagram, dashed lines represent gauge fixed group elements, while solid lines carry the group variables. In fully gauge-covariant form, these basis states read

$$\psi^{\mathbb{I}}_{G,H}(g_1, g_2, g_3, g_4) = |\mathcal{G}|^{3/2}\delta(G, g_3g_2g_1)\delta(H, g_3g_4g_2^{-1}g_3^{-1}) \,. \tag{4.12}$$

This basis can readily proved to be orthogonal:

$$\langle \psi^{\mathbb{I}}_{G,H} \, , \, \psi^{\mathbb{I}}_{\widetilde{G},\widetilde{H}} \rangle = \frac{1}{|\mathcal{G}|^4} \sum_{g_1,\dots,g_4} \overline{\psi^{\mathbb{I}}_{G,H}(g_1,\dots,g_4)} \psi^{\mathbb{I}}_{\widetilde{G},\widetilde{H}}(g_1,\dots,g_4) \, = |\mathcal{G}| \delta(G,\widetilde{G}) \delta(H,\widetilde{H}) \, .$$

Notice that the states $\psi^{\mathbb{I}}_{G,H}$ are not normalized. The reason for this choice will be made clear later. Henceforth, we will often keep the $\{g_i\}$ implicit, and denote the basis states simply $\psi^{\mathbb{I}}_{G,H}$.

A general element of $\mathcal{H}_2$ can then be written as

$$\psi^{\mathbb{I}} = \sum_{G,H \in \mathcal{G}} \alpha(G,H) \psi^{\mathbb{I}}_{G,H} \, . \tag{4.13}$$

In particular, we define the (unnormalized) $\mathbb{I}$ vacuum state to be

$$\psi^{\mathbb{I}}_0 \, = \, \delta(\mathbb{1}, g_4 g_2^{-1}) \, 1(g_1) \, 1(g_3) \, , \tag{4.14}$$

where $1(\bullet)$ denotes the constant function evaluating to 1 on any group element. Therefore, $\psi^{\mathbb{I}}_0$ is the following linear combination of basis states,

$$\psi^{\mathbb{I}}_0 = |\mathcal{G}|^{-3/2} \sum_{G \in \mathcal{G}} \psi^{\mathbb{I}}_{G,\mathbb{1}} \qquad \text{with} \qquad \langle \psi^{\mathbb{I}}_0, \psi^{\mathbb{I}}_0 \rangle = |\mathcal{G}|^{-1} \, . \tag{4.15}$$

4.3.3 Ocneanu's tube algebra

As we have already mentioned, a fundamental property of punctured manifolds is the possibility of gluing them together. As in the previous chapter, we denote the gluing operation by a $\star$. Then, denoting Σ^{g}_p the Riemann surface of genus g and p punctures, one has

$$\Sigma^{\mathsf{g}}_p \star \Sigma^{\mathsf{h}}_q = \Sigma^{\mathsf{g}+\mathsf{h}}_{p+q-2} \, . \tag{4.16}$$

This gluing procedure follows the same rules as exposed in the previous chapter but the graphs carrying the degrees of freedom are different. Clearly, gluing a cylinder $\mathbb{I} \equiv \Sigma^0_2$ to any other Σ^{g}_p gives back Σ^{g}_p. At the level of the graphs Γ^{g}_p and Γ^{h}_q, the gluing is defined by identifying the marked points associated to the punctures along which the gluing is performed and matching the two edges which end at these marked points. The marked points then become a single two-valent node n in the graph resulting from this matching step denoted by $\mathfrak{G}$. Even if the two original graphs on Σ^{g}_p and Σ^{h}_q were minimal, the resulting graph on $\Sigma^{\mathsf{g}+\mathsf{h}}_{p+q-2}$ is not. Indeed, it contains an extra closed face f, i.e. a face surrounding no puncture. Therefore, if we want the gluing to be mirrored at the level of the state spaces, this face must be associated with a trivial holonomy. The gluing operator on basis states based on graphs can be summarized as before as

$$\begin{array}{rccccc} \star : & \mathcal{H}_{\Gamma_1} \otimes \mathcal{H}_{\Gamma_2} & \xrightarrow{\mathfrak{G}} & \mathcal{H}_{\text{aux}} & \xrightarrow{\mathbb{A} \circ \mathbb{B}} & \mathcal{H}_{\Gamma_1 \cup \Gamma_2 / \sim} \\ & (\psi_1, \psi_2) & \longmapsto & \mathfrak{G}(\psi_1, \psi_2) & \longmapsto & \mathbb{A} \circ \mathbb{B} \triangleright \mathfrak{G}(\psi_1, \psi_2) \end{array} \tag{4.17}$$

where $\mathcal{H}_{\text{aux}}$ is the Hilbert space of functionals before enforcement of the constraints at the newly created bulk vertices and closed faces, and $\Gamma_1 \cup \Gamma_2 / \sim$ is the graph obtained after gluing of Γ_1 and Γ_2 up to equivalence relations. This can be extended by linearity to arbitrary states. Recall that the operator $\mathbb{A}$ projects onto gauge invariant states at the newly created two-valent node n of $\mathfrak{G}(\Gamma_1, \Gamma_2)$ and $\mathbb{B}$ projects onto states carrying trivial holonomies around the newly created closed face f.

To clarify the above construction, we will as in the previous chapter consider the important case of gluing two cylinders to one-another. The computation is sensibly more cumbersome than before

because of the additional structure, however it follows precisely the same steps. In this case, $\mathbb{I} \star \mathbb{I} = \mathbb{I}$, and the gluing defines a multiplication operation on $\mathcal{H}_2$. Notice that this is not a standard structure on a Hilbert space. In particular, thanks to the gluing operation, $\mathcal{H}_2$ carries a representation of algebra, named Ocneanu's tube algebra.

Consider two minimal states

$$\psi_1^{\mathbb{I}}(\{g_i\}),\ \psi_2^{\mathbb{I}}(\{g'_i\}) \in \mathcal{H}_2\ . \tag{4.18}$$

Then, following the prescriptions above, we obtain

$\mathfrak{G}(\psi_1^{\mathbb{I}}, \psi_2^{\mathbb{I}})(\{g_i, g'_i\}) =$ 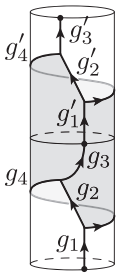

(4.19)

where the gray face is the new closed face f on which the flatness constraint has to be imposed. The node n is the one where the links l_3 and l'_1 meet. Gauge invariance at n can be imposed by group averaging:

$$\tilde{\Psi}(\{g_i, g'_i\}) := \Big(\mathbb{A} \triangleright \mathfrak{G}(\psi_1^{\mathbb{I}}, \psi_2^{\mathbb{I}})\Big)(\{g_i, g'_i\}) \tag{4.20}$$

$$= \frac{1}{|\mathcal{G}|} \sum_{k \in \mathcal{G}} \psi_2^{\mathbb{I}}(g'_1 k^{-1}, g'_2, g'_3, g'_4) \psi_1^{\mathbb{I}}(g_1, g_2, k g_3, g_4)\ . \tag{4.21}$$

Now, the flatness constraint at the new closed face f is readily imposed as

$$\psi_1^{\mathbb{I}} \star \psi_2^{\mathbb{I}} = \Big(\mathbb{B} \triangleright \tilde{\Psi}\Big)(\{g_i, g'_i\}) \ = \ \delta(\mathbb{1}, h_f) \tilde{\Psi}(\{g_i, g'_i\}) \tag{4.22}$$

where $h_f = g_3 g_4 g_2^{-1} g_3^{-1} g_1'^{-1} g_4'^{-1} g'_2 g'_1$. The state so constructed is not defined on a minimal graph. However, it is in $\mathcal{H}_{\Gamma \cup \Gamma'}$ and hence via the equivalence relation described above, can be identified with a state in $\mathcal{H}_2$.

Let us be even more specific, by gluing two basis states of $\mathcal{H}_2$. Graphically:

$\psi^{\mathbb{I}}_{G',H'} \star \psi^{\mathbb{I}}_{G,H} \ = \ |\mathcal{G}|^3$ 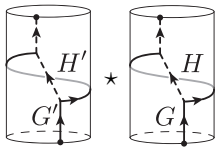

$\simeq |\mathcal{G}|^3\, \mathbb{A} \circ \mathbb{B} \triangleright \mathfrak{G}\Big($ 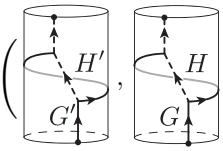

$\Big)$

but, on the other hand, the linked cylinder state is explicitly given by

$\mathfrak{G}\Big($ 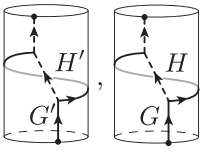

$\Big) =$ 

$=$

$$= \delta(G, g_3g_2g_1)\delta(H, g_3g_4g_2^{-1}g_3^{-1})\delta(G', g'_3g'_2g'_1)\delta(H', g'_3g'_4(g'_2)^{-1}(g'_3)^{-1})$$ 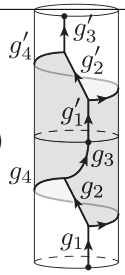

. (4.23)

Hence, applying the projectors and rearranging the delta functions, we obtain

$$|\mathcal{G}|^3 \mathbb{A} \circ \mathbb{B} \triangleright \mathfrak{G}\Big($$ 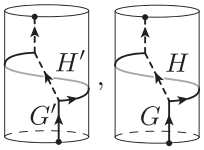

$$\Big) =$$

$$= |\mathcal{G}|^3 \frac{1}{|\mathcal{G}|} \sum_{k\in\mathcal{G}} \delta(G', g'_3g'_2g'_1k^{-1})\delta(g'_2g'_1g_3g_4g_2^{-1}g_3^{-1}(g'_1)^{-1}(g'_4)^{-1})$$
$$\times \delta(G'G, g'_3g'_2g'_1g_3g_2g_1)\,\delta(H, (G')^{-1}H'G')\,\delta(H', g'_3g'_4(g'_2)^{-1}(g'_3)^{-1})$$ 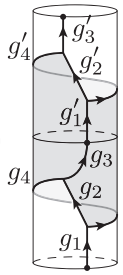

.

Now, we appeal to the equivalence relations of sec. 4.2 to remove the dependence on g_4 by removing the corresponding link (and associated face, see eq. (4.8)). We then undo three link subdivisions and declare $l'_1 \circ l_3 \circ l_2 \circ l_1$ to be the new link $\tilde{l}_1$. Hence, we finally obtain the following crucial result[10]

$$\psi^{\mathbb{I}}_{G',H'} \star \psi^{\mathbb{I}}_{G,H} \;=\; |\mathcal{G}|^{3/2}\delta(H, (G')^{-1}H'G') \;=\; \delta((G')^{-1}H'G', H)\psi^{\mathbb{I}}_{G'G,H'}\,. \tag{4.24}$$ 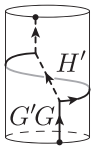

This multiplication law, together with the usual Hilbert space linear structure, defines the Ocneanu tube algebra. As a matter of fact, the $\star$ multiplication we have just constructed is exactly the multiplication law of the Drinfel'd double algebra $\mathcal{D}(\mathcal{G})$. The present construction can be readily generalized to the case where $m \geq 1$ links are allowed to end at the puncture, see app. A.3.

Now that we have recovered the Drinfel'd double structure in the present context of lattice gauge theories in the BF representations, we can adapt the procedure spelled out in chap. 3 to construct the fusion basis.

4.4 The fusion basis

In this section, we make use of the mathematical properties introduced in chap. 3 to construct the fusion basis for the Hilbert space $\mathcal{H}_p$. The idea is to label the punctures by its physical charges $\rho = (C, R)$, and to use the recoupling theory of $\mathcal{D}(\mathcal{G})$ to 'put these charges together' into singlet states on Σ^0_p.

[10] Note that we could have made different choices to simplify the final form of the state, but all choices would have led to the same result.

The result of this construction is a basis with a direct physical interpretation, which mathematically resembles a spin network basis where $\mathcal{G}$ has been replace by $\mathcal{D}(\mathcal{G})$. Thanks to the use of recoupling theory at the level of the defect charges, this basis will also trivialize the notion of merging—or coarse-graining—defects. Heuristically, we can imagine the merging of defects by replacing two punctures by a single one defined by a disc containing the two puncture-discs to be merged:

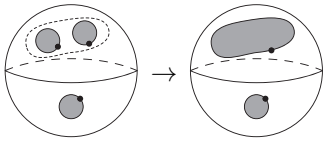

(4.25)

In practice, such a merging is realized by performing a fusion of the corresponding irreducible representations. For this reason, we refer to this basis as the *fusion basis* and label the corresponding basis states with an $\mathfrak{f}$. Since any surface Σ_p^0 can be decomposed into trinions (a.k.a. pair of pants or thrice-punctured two-sphere), it is only necessary to define the states $\psi^{\mathbb{I}}_{\mathfrak{f}}$ and $\psi^{\mathbb{Y}}_{\mathfrak{f}}$, as well as a procedure to glue them to one another.

4.4.1 The twice-punctured sphere

Consider the $\{\psi^{\mathbb{I}}_{G,H}\}$ basis of $\mathcal{H}_2$,

$$\psi^{\mathbb{I}}_{G,H}(g_1,\dots,g_4) = |\mathcal{G}|^{3/2}\delta(G, g_3g_2g_1)\delta(H, g_3g_4g_2^{-1}g_3^{-1}) \,. \tag{4.26}$$

Then, the following change of basis defines the fusion basis $\{\psi^{\mathbb{I}}_{\mathfrak{f}}[\rho, MN]\}$:

$$\begin{cases} \psi^{\mathbb{I}}_{\mathfrak{f}}[\rho, MN] = \dfrac{1}{|\mathcal{G}|}\displaystyle\sum_{G,H} \sqrt{d_\rho}\; D^\rho_{MN}(G\otimes\delta_H)\; \psi^{\mathbb{I}}_{G,H} \\ \psi^{\mathbb{I}}_{G,H} = \displaystyle\sum_{\rho}\sum_{M,N} \sqrt{d_\rho}\; \overline{D^\rho_{MN}(G\otimes\delta_H)}\; \psi^{\mathbb{I}}_{\mathfrak{f}}[\rho, MN] \end{cases} \tag{4.27}$$

With the above normalizations, the fusion basis can be shown to be orthonormal in $\mathcal{H}_2$:

$$\begin{aligned} &\big\langle \psi^{\mathbb{I}}_{\mathfrak{f}}[\rho, MN]\,,\, \psi^{\mathbb{I}}_{\mathfrak{f}}[\widetilde{\rho}, \widetilde{M}\widetilde{N}]\big\rangle \\ &\quad= \frac{1}{|\mathcal{G}|^6}\sqrt{d_\rho d_{\widetilde{\rho}}} \sum_{g_1,\dots,g_4}\sum_{\substack{G,H\\ \widetilde{G},\widetilde{H}}} \overline{\psi^{\mathbb{I}}_{G,H}(g_1,\dots,g_4)}\psi^{\mathbb{I}}_{\widetilde{G},\widetilde{H}}(g_1,\dots,g_4)\overline{D^\rho_{MN}(G\otimes\delta_H)}D^{\widetilde{\rho}}_{\widetilde{M}\widetilde{N}}(\widetilde{G}\otimes\delta_{\widetilde{H}}) \\ &\quad= \delta_{\rho,\widetilde{\rho}}\delta_{N,\widetilde{N}}\delta_{M,\widetilde{M}} \end{aligned} \tag{4.28}$$

The calculation above uses the explicit form of $\psi^{\mathbb{I}}_{G,H}$ and the orthogonality relation (3.29). Similarly, one can explicitly show that the basis is complete in $\mathcal{H}_2$:

$$\begin{aligned} &\sum_\rho\sum_{M,N} \psi^{\mathbb{I}}_{\mathfrak{f}}[\rho, MN](\{g\})\overline{\psi^{\mathbb{I}}_{\mathfrak{f}}[\rho, MN](\{\widetilde{g}\})} \\ &\qquad= |\mathcal{G}|^2\delta(g_3g_2g_1, \widetilde{g}_3\widetilde{g}_2\widetilde{g}_1)\delta(g_3g_4g_2^{-1}g_3^{-1}, \widetilde{g}_3\widetilde{g}_4\widetilde{g}_2^{-1}\widetilde{g}_3^{-1}) \,, \end{aligned} \tag{4.29}$$

where once more use was made of the explicit form of $\psi^{\mathbb{I}}_{G,H}$, as well as of the completeness the representation matrices.

This new basis diagonalize the $\star$-product:

$$\psi^{\mathbb{I}}_{\mathfrak{f}}[\rho_2, M_2N_2] \star \psi^{\mathbb{I}}_{\mathfrak{f}}[\rho_1, M_1N_1] = \frac{\delta_{\rho_1,\rho_2}}{\sqrt{d_{\rho_1}}}\; \delta_{N_2,M_1}\; \psi^{\mathbb{I}}_{\mathfrak{f}}[\rho_1, M_2N_1] \,. \tag{4.30}$$

This crucial relation is proven in app. A.2.1. The importance of such a basis is that it is labeled by the physically 'stable' properties of the punctures. In other words $\rho = (C, R)$ can be interpreted as the *charge* carried by the puncture. With a little stretch of the formalism, we could in principle consider $\mathcal{G} = \mathrm{SU}(2)$. Then, interpreting the punctures as point particles, $C \in [0, 2\pi]$ would correspond to the *mass* of the particle, as measured by the (curvature) conical defect it induces, and $R \in \mathbb{N}$ would correspond to its *spin*, i.e. the torsion defect.

4.4.2 The thrice-punctured sphere

Using the Clebsch-Gordan coefficients which play the role of intertwiners between the irreducible representations of $\mathcal{D}(\mathcal{G})$, one can now construct the fusion basis states for the thrice-punctured sphere. Once again, we start from the basis in the (G, H)-picture. After gauge-fixing, a basis of $\mathcal{H}_{\mathbb{Y}}$ is given by

$$\psi^{\mathbb{Y}}_{G_1,H_1|G_2,H_2}(\{g\},\{g'\})|_{\text{g.f.}} \;=\; |\mathcal{G}|^3 \cdot$$

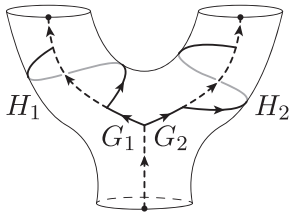

$$= \psi^{\mathbb{I}}_{G_1,H_1}(\{g\})|_{\text{g.f.}}\psi^{\mathbb{I}}_{G_2,H_2}(\{g'\})|_{\text{g.f.}} \,. \tag{4.31}$$

where we borrowed the notation of eq. (4.11). The definition on a non-gauge-fixed state is readily recovered by reintroducing the other group elements and averaging over the gauge action at the five internal nodes. Now, we perform the transformation to the $[\rho, MN]$-picture on each of the $\mathbb{I}$ factors:

$$\psi^{\mathbb{Y}}_{\rho_2,M_2N_2|\rho_1,M_1N_1} \;=\; \frac{1}{|\mathcal{G}|^2} \sum_{\substack{G_1,H_1\\G_2,H_2}} \sqrt{d_{\rho_2} d_{\rho_1}}\; D^{\rho_2}_{M_2N_2}(G_2 \otimes \delta_{H_2})\; D^{\rho_1}_{M_1N_1}(G_1 \otimes \delta_{H_1})\; \psi^{\mathbb{Y}}_{G_1,H_1|G_2,H_2} \tag{4.32}$$

where we have suppressed from our notation the dependence on $\{g, g'\}$. In this basis, the charges at the 'top' punctures 1 and 2 are fixed to ρ_1 and ρ_2. However, little can be said for what concerns the charge of the bottom puncture. Moreover, we are left with 'magnetic' indices of $\mathcal{D}(\mathcal{G})$, N_1 and N_2, associated with the 'bottom' of the two cylinders we are gluing, which—from the trinion perspective—'sit' in the very middle of the graph. What is needed, is therefore a unitary transformation that maps two magnetic indices into one representation label (the charge of the third puncture) and one magnetic index (now sitting at the bottom of the graph). This is exactly the job of the Clebsch-Gordan coefficients. Hence, we finally define the fusion basis of $\mathcal{H}_{\mathbb{Y}}$ as

$$\begin{cases} \psi^{\mathbb{Y}}_{\mathfrak{f}}\begin{bmatrix}\rho_1, M_1\\ \rho_2, M_2\\ \rho_3, N_3\end{bmatrix} \;=\; \dfrac{1}{|\mathcal{G}|^2} \displaystyle\sum_{N_1,N_2} \sum_{\substack{G_1,H_1\\G_2,H_2}} \left(\prod_{i=1}^{2} \sqrt{d_{\rho_i}}\; D^{\rho_i}_{M_iN_i}(G_i \otimes \delta_{H_i})\right) \mathcal{C}^{\rho_1\rho_2\rho_3}_{N_1N_2N_3}\; \psi^{\mathbb{Y}}_{G_1,H_1|G_2,H_2} \\[2ex] \psi^{\mathbb{Y}}_{G_1,H_1|G_2,H_2} \;=\; \displaystyle\sum_{\rho_3,N_3} \sum_{\substack{\rho_1,N_1\,M_1\\ \rho_2,N_2\,M_2}} \left(\prod_{i=1}^{2} \sqrt{d_{\rho_i}}\; \overline{D^{\rho_i}_{M_iN_i}(G_i \otimes \delta_{H_i})}\right) \overline{\mathcal{C}^{\rho_1\rho_2\rho_3}_{N_1N_2N_3}}\; \psi^{\mathbb{Y}}_{\mathfrak{f}}\begin{bmatrix}\rho_1, M_1\\ \rho_2, M_2\\ \rho_3, N_3\end{bmatrix} \end{cases} \tag{4.33}$$

To prove the consistency of the two formulas above, it is sufficient to use the orthogonality and completeness of both $\mathcal{C}^{\rho_1\rho_2\rho_3}_{I_1I_2I_3}$ and $D^{\rho}_{MN}(G \otimes \delta_H)$. The orthonormality of the basis,

$$\left\langle \psi^{\mathbb{Y}}_{\mathfrak{f}}\begin{bmatrix}\rho_1, M_1\\ \rho_2, M_2\\ \rho_3, N_3\end{bmatrix}, \psi^{\mathbb{Y}}_{\mathfrak{f}}\begin{bmatrix}\widetilde{\rho}_1, \widetilde{M}_1\\ \widetilde{\rho}_2, \widetilde{M}_2\\ \widetilde{\rho}_3, \widetilde{N}_3\end{bmatrix} \right\rangle = \delta_{\rho_1,\widetilde{\rho}_1}\delta_{\rho_2,\widetilde{\rho}_2}\delta_{\rho_3,\widetilde{\rho}_3}\delta_{M_1,\widetilde{M}_1}\delta_{M_2,\widetilde{M}_2}\delta_{N_3,\widetilde{N}_3} \,,$$

is proved in app. A.2.2, while its completeness follows from the completeness of the basis $\{\psi^{\mathbb{Y}}_{G_1,H_1|G_2,H_2}\}$ and the change of basis above.

4.4.3 States on Σ^0_p

Here we define the fusion basis states $\psi_{\mathfrak{f}}^{\Sigma^0_p}$ for the p-punctured sphere by generalizing the construction followed for the case of the thrice-punctured sphere. In particular, this means that the $\mathbb{I}$ factors associated with $p-1$ punctures are transformed to the $[\rho', MN]$-picture and then a fusion tree is constructed by contracting Clebsch-Gordan coefficients together. In the following subsection, we will present how such states can be recovered by gluing states defined on thrice-punctured spheres as outlined at the beginning of this section.

To make the construction more transparent, we introduce a more synthetic graphical notation. Since all the operations defined on the fusion basis states can be performed at the level of the representations, it is not necessary to look at the group variables $\{g\}$ in detail. Therefore, we represent the fusion basis state $\psi_{\mathfrak{f}}^{\mathbb{Y}}$ as follows

$$\psi_{\mathfrak{f}}^{\mathbb{Y}}\begin{bmatrix}\rho_1, M_1\\ \rho_2, M_2\\ \rho_3, N_3\end{bmatrix} =: \quad . \tag{4.34}$$

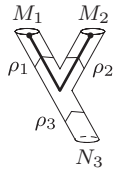

The tube structure provides the following combinatorial information:

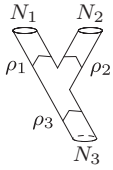

$$:= \mathcal{C}^{\rho_1\rho_2\rho_3}_{N_1N_2N_3} \tag{4.35}$$

such that the bold edge signals where the group variables are inserted (see eq. (4.31)), i.e., in a sense, where we consider the degrees of freedom to be. By this we mean that the lower cylinder in (4.34) 'does not carry any degree of freedom' because the flatness constraint tells us that a complete knowledge of the state is encoded in the knowledge of the upper tubes only. Nevertheless, it is possible to use the expression for the flatness constraint in order to rewrite the states on the thrice-punctured sphere in a more symmetric form (see eq. (4.40)), in which each tube is associated to a representation matrix.

To obtain the states on Σ^0_p, we first perform the transformation to the $[\rho', MN]$-picture using eq. (4.27) on each of the $p-1$ upper tubes respectively associated to $p-1$ punctures. The upper tubes are then connected to each other two by two via Clebsch-Gordan coefficients so as to form a fusion

tree. Using the graphical notation introduced above, the resulting states are given by

$$\psi_{\mathfrak{f}}^{\Sigma_p^0}\big[\{\rho_i\}_{i=1}^{2p-3},\{M_k\}_{k=1}^{p-1},N_p\big] = \tag{4.36}$$

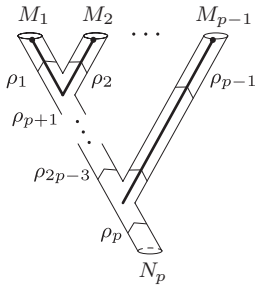

$$= \frac{1}{|\mathcal{G}|^{p-1}} \sum_{\{N\}} \sum_{\{G_k,H_k\}_{k=1}^{p-1}} \mathcal{C}^{\rho_1\rho_2\rho_{(p+1)}}_{N_1N_2N_{(p+1)}} \mathcal{C}^{\rho_{(2p-3)}\rho_{(p-1)}\rho_p}_{N_{(2p-3)}N_{(p-1)}N_p}\, \psi^{\mathbb{S}_p}_{\{G,H\}}$$
$$\times \prod_{k=1}^{p-1} \sqrt{d_{\rho_k}} D^{\rho_k}_{M_kN_k}(G_k\otimes\delta_{H_k}) \prod_{i=p+1}^{2p-4} \mathcal{C}^{\rho_i\rho_{(i-p+2)}\rho_{(i+1)}}_{N_iN_{(i-p+2)}N_{(i+1)}} \ .$$

The subindex $i\in\{1,\dots,2p-3\}$ labels the edges of the fusion tree. The subindex $k=\{1,\dots,p\}$ labels the p punctures, which are in one-to-one correspondence with the leaves of the fusion tree.

It is important to recall that the Clebsch-Gordan coefficients of $\mathcal{D}(\mathcal{G})$, $\mathcal{C}^{\rho_1\rho_2\rho_3}_{N_1N_2N_3}$, are not symmetric in all its indices, and $\{\rho_3,N_3\}$ actually play a distinguished role (see eq. (3.33)). Therefore the above graphs are directed. Different choices of root trees defining the states above are related by a change of basis, as it is most easily seen by going back to a group representation. Notice that this is just the simplest example of fusion tree. More refined construction can be built in a similar way, possibly with the idea in mind of reproducing the multi-scale design underlying the tensor network states. For this we refer to sec. 4.6.

4.4.4 Fusion basis via gluing

As we mentioned in the beginning of this section, every punctured sphere can be decomposed into trinions so that the fusion basis state for Σ_p^0 boils down to a *gluing* of states defined on thrice-punctured spheres.

To start with we want to represent the fusion basis for the thrice-punctured sphere in a more symmetric manner. To this end we use the equivalence relations in sec. 4.2.2 and express the state (4.31) on an extended graph

$$\psi^{\mathbb{Y}}_{G_1,H_1|G_2,H_2}(\{g\},\{g'\},\{g''\})|_{\text{g.f.}} = |\mathcal{G}|^{7/2} \sum_{G_3,H_3} \tag{4.37}$$

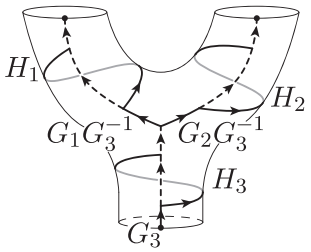

$$= |\mathcal{G}|^{7/2} \sum_{G_3,H_3} \delta(g_4,H_1)\delta(g_1,G_1G_3^{-1})\delta(g_4',H_2)\delta(g_1',G_2G_3^{-1})$$
$$\times \delta(g_4'',H_3)\delta(g_1'',G_3)\,\delta(G_3^{-1}H_3G_3,G_1^{-1}H_1G_1G_2^{-1}H_2G_2) \ .$$

Now, the following identity can be obtained from eq. (3.37), which spells out the relation of the Clebsch-Gordan coefficients to the flatness and Gauß constraints, by first setting $G_3 = \mathbb{1}$ and then summing over $H_3 \in \mathcal{G}$, that is by evaluating it on the Drinfel'd double identity $\mathbb{1}_{\mathcal{D}(\mathcal{G})} = \sum_{H_3} \mathbb{1} \otimes \delta_{H_3}$:

$$\sum_{N_1,N_2,N_3} D^{\rho_1}_{M_1N_1}(G_1 \otimes \delta_{H_1}) D^{\rho_2}_{M_2N_2}(G_2 \otimes \delta_{H_2})\, \mathcal{C}^{\rho_1\rho_2\rho_3}_{N_1N_2M_3} \tag{4.38}$$

$$= \sum_{N_1,N_2,N_3} D^{\rho_1}_{M_1N_1}(G_1G^{-1} \otimes \delta_{H_1}) D^{\rho_2}_{M_2N_2}(G_2G^{-1} \otimes \delta_{H_2})\, \mathcal{C}^{\rho_1\rho_2\rho_3}_{N_1N_2N_3} \times D^{\rho_3}_{N_3M_3}(G \otimes \delta_{GG_1^{-1}H_1G_1G_2^{-1}H_2G_2G^{-1}}) \,. \tag{4.39}$$

Using eq. (4.37) for the expression of $\psi^{\mathbb{Y}}_{G_1,H_1|G_2,H_2}$ on an extended graph, we can express the fusion state as

$$\begin{aligned}
\psi^{\mathbb{Y}}_{\mathfrak{f}}\begin{bmatrix}\rho_1, M_1\\ \rho_2, M_2\\ \rho_3, M_3\end{bmatrix}_{|\mathrm{g.f}} &= \frac{1}{|\mathcal{G}|^2} \sum_{N_1,N_2} \sum_{\substack{G_1,H_1\\ G_2,H_2}} \left(\prod_{i=1}^{2} \sqrt{d_{\rho_i}}\, D^{\rho_i}_{M_iN_i}(G_i \otimes \delta_{H_i})\right) \mathcal{C}^{\rho_1\rho_2\rho_3}_{N_1N_2M_3}\, \psi^{\mathbb{Y}}_{G_1,H_1|G_2,H_2|\mathrm{g.f}} \\
&= |\mathcal{G}|^{3/2} \sum_{N_1,N_2,N_3} \sum_{\substack{G_1,H_1\\ G_2,H_2,G_3,H_3}} \sqrt{d_{\rho_2}d_{\rho_1}}\, D^{\rho_2}_{M_2N_2}(G_2G_3^{-1} \otimes \delta_{H_2})\, D^{\rho_1}_{M_1N_1}(G_1G_3^{-1} \otimes \delta_{H_1}) \\
&\quad \times \mathcal{C}^{\rho_1\rho_2\rho_3}_{N_1N_2N_3}\, D^{\rho_3}_{N_3M_3}(G_3 \otimes \delta_{H_3})\, \delta(g_4, H_1)\delta(g_1, G_1G_3^{-1})\delta(g_4', H_2)\delta(g_1', G_2G_3^{-1}) \\
&\quad \times \delta(g_4'', H_3)\delta(g_1'', G_3)\, \delta(G_3^{-1}H_3G_3, G_1^{-1}H_1G_1G_2^{-1}H_2G_2) \,.
\end{aligned}$$

We first translate the summation variables $G_1 \to G_1G_3$ and $G_2 \to G_2G_3$, then we apply identity (3.37) again (this time with $G = \mathbb{1}$), hence 'reabsorbing" the delta function into the Clebsch-Gordan coefficient. In this way, we finally arrive at the following representation of the fusion state on $\mathbb{Y}$:

$$\begin{aligned}
\psi^{\mathbb{Y}}_{\mathfrak{f}}\begin{bmatrix}\rho_1, M_1\\ \rho_2, M_2\\ \rho_3, M_3\end{bmatrix}_{|\mathrm{g.f}} &= |\mathcal{G}|^{3/2} \sum_{N_1,N_2,N_3} \sum_{\substack{G_1,H_1\\ G_2,H_2,G_3,H_3}} \left(\prod_{i=1}^{2} \sqrt{d_{\rho_i}}\, D^{\rho_i}_{M_iN_i}(G_i \otimes \delta_{H_i})\right) \mathcal{C}^{\rho_1\rho_2\rho_3}_{N_1N_2N_3}\, D^{\rho_3}_{N_3M_3}(G_3 \otimes \delta_{H_3}) \\
&\quad \times \delta(g_4, H_1)\delta(g_1, G_1)\delta(g_4', H_2)\delta(g_1', G_2)\delta(g_4'', H_3)\delta(g_1'', G_3) \,.
\end{aligned} \tag{4.40}$$

We have thus obtained a more symmetric representation of the fusion state on the thrice-punctured sphere. Note however that the dimension factors d_ρ are still not equally distributed, which is due to an asymmetry in the Clebsch-Gordan coefficients.[11]

The fusion basis state on the thrice-punctured sphere is now expressed such that each leg carries a state that is locally equivalent to a cylinder state. We know how these states behave under gluing and thus we can now proceed to build a fusion state on the e.g. four-times-punctured sphere by gluing

[11] This can easily be arranged as in the previous chapter by considering the $3\rho M$-symbols instead of the Clebsch-Gordan coefficients.

two thrice-punctured sphere fusion states:

$$\psi_{\mathfrak{f}}^{\Sigma_4^0}[\{\rho_i\}_{i=1}^5,\{M\}_{i=1}^3,N_4] = \quad = \sqrt{d_{\rho_5}} \quad \star \quad = \sqrt{d_{\rho_5}}\ \psi_{\mathfrak{f}}^{\mathbb{Y}}\begin{bmatrix}\rho_1,M_1\\ \rho_2,M_2\\ \rho_5,N_5\end{bmatrix} \star \psi_{\mathfrak{f}}^{\mathbb{Y}}\begin{bmatrix}\rho_5,N_5\\ \rho_3,M_3\\ \rho_4,N_4\end{bmatrix} = \frac{1}{\sqrt{d_{\rho_5}}}\sum_{N_5}\psi_{\mathfrak{f}}^{\mathbb{Y}}\begin{bmatrix}\rho_1,M_1\\ \rho_2,M_2\\ \rho_5,N_5\end{bmatrix} \star \psi_{\mathfrak{f}}^{\mathbb{Y}}\begin{bmatrix}\rho_5,N_5\\ \rho_3,M_3\\ \rho_4,N_4\end{bmatrix}, \tag{4.41}$$

where in the first line we used that for the gluing of cylinder states the 'glued' indices have to coincide but drop out in the final result (see eq. (4.30)), while in the last line we summed over this index and included the corresponding normalization factor.

4.4.5 Gauge invariant projections of the fusion basis

The fusion basis state $\psi_{\mathfrak{f}}^{\Sigma_p^0}$ describes both curvature and torsion excitations at the punctures. Often we are interested in having only curvature excitations, that is states that are also gauge invariant at the punctures. We can obtain such states by applying the Gauß constraint projector $\mathbb{A}$ to the punctures.

Let us for example consider a fusion basis state on a cylinder

$$\psi_{\mathfrak{f}}^{\mathbb{I}}[CR,am,bn](g_1,\dots,g_4) = |\mathcal{G}|^{1/2}\sum_{G,H}\sqrt{d_{C,R}}\ \delta(H,c_a)\,\delta(c_a,Gc_bG^{-1})\,D^R_{mn}(q_a^{-1}Gq_b) \\ \times\,\delta(G,g_3g_2g_1)\delta(H,g_3g_4g_2^{-1}g_3^{-1}) \tag{4.42}$$

and apply $\mathbb{A}$ to the source node of the link carrying g_1, i.e. at the source puncture (s) of the cylinder state,

$$\mathbb{A}_{(s)}\triangleright\psi_{\mathfrak{f}}^{\mathbb{I}}[CR,am,bn] = |\mathcal{G}|^{-1/2}\sum_h\sum_{G,H}\sqrt{d_{C,R}}\ \delta(H,c_a)\,\delta(c_a,Gc_bG^{-1})\,D^R_{mn}(q_a^{-1}Gq_b) \\ \times\,\delta(G,g_3g_2g_1h)\delta(H,g_3g_4g_2^{-1}g_3^{-1})\,. \tag{4.43}$$

One finds (see app. A.2.3)

$$\mathbb{A}_{(s)}\triangleright\psi_{\mathfrak{f}}^{\mathbb{I}}[CR,am,bn] = \delta_{R,0}\delta_{a,0}\delta_{b,0}\frac{1}{|Q_C|}\sum_c\psi_{\mathfrak{f}}^{\mathbb{I}}[C0,a0,c0]\,. \tag{4.44}$$

Likewise, applying the projector $\mathbb{A}$ to the target puncture we find

$$\mathbb{A}_{(t)}\triangleright\psi_{\mathfrak{f}}^{\mathbb{I}}[CR,am,bn] = \delta_{R,0}\delta_{a,0}\delta_{b,0}\frac{1}{|Q_C|}\sum_c\psi_{\mathfrak{f}}^{\mathbb{I}}[C0,c0,b0]\,. \tag{4.45}$$

Note that the gauge averaged states have now norm equal to $1/|Q_C|$, to get normalized state we should multiply by $\sqrt{|Q_C|}$. This generalizes to the fusion basis for p-punctured spheres: applying a gauge averaging at a puncture p forces the corresponding labels R_p and M_p to be trivial and leads to an averaging over the a_p, b_p indices.

4.5 Ribbon operators

In the previous section we have introduced the fusion basis that gives immediate access to the excitation structure of a state. We are now going to construct operators that generate and measure these excitations. For reasons that will be clear soon, these operators are called *ribbon operators*. They come in two families: *open* ribbon operators that generate excitations, and *closed* ribbon operators that measure them. In particular, we will see that we can define operators that are diagonal in the fusion basis.

4.5.1 Open ribbon operators

Choosing as our configuration space group holonomies, that describe locally flat connections, we have at our disposal two types of operators. On the one hand, multiplication operators, known as *holonomy* or *Wilson path (loop) operators*, and on the other hand, *translation operators*, which translate an argument of the wave function either on the left or on the right.

Wilson path operators, W^f_γ, multiply wave functions by an $f : \mathcal{G} \to \mathbb{C}$,

$$(W^f_\gamma \triangleright \psi)(g_1, \dots, g_L) := f(h_\gamma)\psi(g_1, \dots, g_L) , \tag{4.46}$$

where $h_\gamma = g_{l_N} \cdots g_{l_1}$ is the holonomy associated to the path $\gamma = l_N \circ \cdots \circ l_1$ (clearly, care must be taken with respect to the orientation of the links). Being a multiplication operator, W^f_γ preserves any flatness constraints, which are multiplication operators themselves. Gauge invariance (i.e. Gauß constraints) is preserved only if γ is a loop and f a class function.

Translation operators $T_k[H]$ act by finite translations, and can therefore be thought of as the exponentiated version of momenta. In loop quantum gravity momenta are known as fluxes, hence the name of 'exponentiated flux'. A group translations can act either on the left or on the right. We choose to work with left multiplication:[12]

$$(T_k[H] \triangleright \psi)(\dots, g_k, \dots) = \psi(\dots, H^{-1} g_k, \dots) . \tag{4.47}$$

Note, however, that $T_k[H]$ in general violates all flatness constraints involving the group element g_k carried by the link l_k, as well as the Gauß constraints at the target node of l_k, $n = t(l_k)$. Thus, this operator in general takes a state out of its Hilbert space, and is therefore not viable as it is. Hence, we need to adjust the definitions of the above operators to correct this issue. Before doing so, however, we need to understand the structure of the constraint violations their action induces.

A translation of—say—the group element associated to the link l_1 will change the holonomies of the two faces—say—f_1 and f_2 which are adjacent to l_1. Now, by changing in a precise way also the holonomy associated to another link—say—$l_2 \in f_2$, it is clear that we can re-gain flatness at f_2. Nevertheless, this comes in general at the cost of changing the holonomy of a third face f_3, and so on. The argument can be used to push around Gauß constraint violations as well. To do so, we can first parallel transport the argument g_k which is about to be translated from its target node to another node n along a path γ. Once the translation is performed, we then transport back the translated holonomy. The resulting operators are denoted by $T_{k,\gamma}[H]$ and their action reads

$$(T_{k,\gamma}[H] \triangleright \psi)(\dots, g_k, \dots) = \psi(\dots, h_\gamma^{-1} H^{-1} h_\gamma g_k, \dots) \tag{4.48}$$

with h_γ the holonomy along the path γ. Notice how h_γ involves an implicit dependence on all the group elements g_l corresponding to links $l \in \gamma$.

[12] Right translation can be implemented by $(T_k[H] \triangleright \psi)(\dots, g_k, \dots) = \psi(\dots, g_k H, \dots)$.

What we actually learn from this discussion is that curvature excitations and Gauß constraint violations are always generated in pairs. Now, recall that—by construction—punctures are locations in Σ_p^0 where constraint violations are allowed. Therefore, we are led to considering operators that generate pairs of excitations whose positions coincide with a pair of punctures.[13] Also, Wilson path operators W_γ^f, which are associated to open paths γ, generate defects in pairs. In this case the defects are Gauß constraint violations that appear at the two ends of the Wilson path. Again, such violations are allowed if the Wilson path starts and ends at punctures.

Kitaev's ribbon operators: Kitaev, in [38], combined translation operators and Wilson path operators into so-called ribbon (or dyonic) operators. He also showed that ribbon operators carry an algebraic structure given by the Drinfel'd double of the underlying (discrete) gauge group. We first define ribbon operators on $\mathbb{I}$ (with a minimal graph), and generalize to more general punctured surfaces in a second moment. We show that ribbon operators generate the basis $\{\psi^{\mathbb{I}}_{G,H}\}$ (eq. (4.11)) of $\mathcal{H}_2$, thus revealing already a connection to the Drinfel'd double $\mathcal{D}(\mathcal{G})$.

Kitaev's ribbon on $\mathbb{I}$: Kitaev's ribbon operator on $\mathbb{I}$ is defined as the combination of a translation and a Wilson path operator. The translation operator acts at the link l_4, going *around* the cylinder. The translating element is parallel transported to the target puncture, i.e. the target node of l_3. We write this

$$(T_{4,3}[H] \triangleright \psi^{\mathbb{I}})(g_1, \ldots, g_4) \;:=\; \psi^{\mathbb{I}}(g_1, \ldots, g_3^{-1} H^{-1} g_3 g_4) \, . \tag{4.49}$$

After the action of $T_{4,3}[H]$ the inner vertices remain gauge invariant. The Wilson path operator involves the *longitudinal* holonomy in between the two punctures, and it is characterized by a function f which acts by multiplication. A basis for these operators is provided by delta functions $\{\delta(G, \bullet)\}_{G \in \mathcal{G}}$ such that

$$(W_{321}[G] \triangleright \psi^{\mathbb{I}})(g_1, \ldots, g_4) \;:=\; \delta(G, g_3 g_2 g_1)\, \psi^{\mathbb{I}}(g_1, \ldots, g_4) \, . \tag{4.50}$$

With these ingredients, we define on $\mathbb{I}$ the Kitaev's ribbon operator $\mathcal{R}[G,H]$ to be:

$$\mathcal{R}[G,H] := W_{321}[G] \circ T_{4,3}[H] \, . \tag{4.51}$$

Acting on the cylinder (global) vacuum state,

$$\psi_0^{\mathbb{I}}(g_1, \ldots, g_4) \;:=\; \delta(\mathbb{1}, g_4 g_2^{-1}) 1(g_1) 1(g_3) \tag{4.52}$$

with $1(\bullet)$ the constant function of value $1 \in \mathbb{C}$, we see that $T[H]$ and $W[G]$ generate the whole basis $\{\psi^{\mathbb{I}}_{G,H}\}$ of $\mathcal{H}_2$ (eq. (4.11)):

$$(\mathcal{R}[G,H] \triangleright \psi_0^{\mathbb{I}})(g_1, \ldots, g_4) \;=\; \left(W_{321}[G] \circ T_{4,3}[H] \triangleright \psi_0^{\mathbb{I}}\right)(g_1, \ldots, g_4) \tag{4.53}$$

$=$ 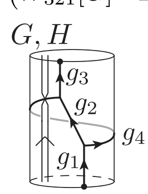

$=$ 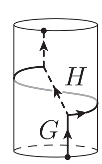

$= |\mathcal{G}|^{-3/2}\, \psi^{\mathbb{I}}_{G,H}$. (4.54)

[13] Operators generating curvature defects at the end of a certain path have been defined in [22, 86, 96] as (integrated) exponentiated flux operators.

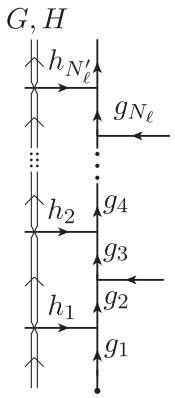

Figure 4.2. Action of the open ribbon operator.

Hence, ribbon operators $\mathcal{R}[G,H]$ generate all possible pairs of excitations at the punctures of $\mathbb{I}$. Let us briefly mention the fact that reversing the direction of the ribbon operator involves the antipode in $\mathcal{D}(\mathcal{G})$:

$$(\mathcal{R}_{\rm rev}[G,H] \triangleright \psi_0^{\mathbb{I}})(g_1,\dots,g_4) = (\mathcal{R}(S[G,H]) \triangleright \psi_0^{\mathbb{I}})(g_1,\dots,g_4)\,, \tag{4.55}$$

where $S([G,H]) = [G^{-1}, G^{-1}H^{-1}G]$ is the antipode of the Drinfel'd double element $G \otimes \delta_H$ as defined in eq. (3.24).

Kitaev's ribbon on Σ_p^0: The above considerations can be generalized, to ribbon operators on Σ_p^0 which start and end at two punctures. Consider two punctures connected by a directed link ℓ , possibly composed of several elementary links $\ell = l_{N_\ell} \circ \cdots \circ l_1$ with associated group elements $g_{N_\ell} \cdots g_1$, from which several links are departing to the right and to the left with respect to the orientation of ℓ. If necessary, we change orientations so that edges departing to the left are ingoing to ℓ, see fig. 4.2. Note that the graph underlying the state under consideration can be always brought into this form using the equivalences of sec. 4.2.2.

We can now define the action of a ribbon operator acting from the left. To this end, draw a ribbon to the left of the link ℓ, connecting the two punctures. It will be (over-)crossed by all the links departing to the left of ℓ. We denote the group elements associated to these links $h_1, \cdots, h_{N'_\ell}$ as in fig. 4.2. We also denote by g'_l the ordered products of the $\{g_l\}$ from the target of h_l to the target puncture of ℓ.

The (left) ribbon operator along ℓ, $\mathcal{R}_\ell[G,H]$, is then defined by

$$\begin{aligned}&(\mathcal{R}_\ell[G,H] \triangleright \psi)(g_1,\dots,g_{N_\ell},h_1,\dots,h_{N'_L},\dots) \\ &\quad = \delta(G, g_{N_\ell}\cdots g_1)\psi(g_1,\dots,g_{N_\ell},(g'_1)^{-1}H^{-1}g'_1h_1\ \cdots\ ,(g'_{N'_\ell})^{-1}H^{-1}g'_{N'_\ell}h_{N'_\ell},\dots)\,.\end{aligned} \tag{4.56}$$

As before the action of the ribbon operator splits into two parts: a Wilson path operator part that fixes to G the holonomy from the source to the target punctures of ℓ, and a translation operator part that translates by H^{-1} and from the left the (anti-clockwise) holonomy around the target puncture of ℓ:

$$(g'_{N'_\ell})h_{N'_\ell}\cdots(g'_{N'_\ell})^{-1} \quad\mapsto\quad H^{-1}\,(g'_{N'_\ell})h_{N'_\ell}\cdots(g'_{N'_\ell})^{-1}. \tag{4.57}$$

At the same time the (clockwise) holonomy around the source puncture of ℓ is changed by

$$\begin{aligned}(g'_1)^{-1}h_1\cdots g'_1 \;&\mapsto\; (g'_1)^{-1}(g'_2)^{-1}\cdots(g'_{N'_\ell})^{-1}H^{-1}g'_{N'_\ell}\cdots g'_2h_1\cdots g'_1\\ &= G^{-1}H^{-1}G\;(g'_1)^{-1}h_1\cdots g'_1\;.\end{aligned}\tag{4.58}$$

Note that the face holonomies stay trivial for any closed face. To ensure this, the prescription of how the group elements h_l are translated is essential: For any closed face being affected, there are always two group elements h_l and $(h_{l+1})^{-1}$ translated in an opposite manner, so that the net effect is leaving the face holonomy trivial.

In fact we can imagine that we slide the ribbon operator from one face (lying left to the link ℓ) to the next face, keeping the upper end fixed at the target puncture. Under this 'sliding', curvature and torsion excitations are moved from one face to the next, until one reaches the source puncture.

Charge ribbon operators: As we have seen, the ribbon operators $\mathcal{R}[G,H]$ generate the basis $\{\psi^{\mathbb{I}}_{G,H}\}$ of the twice-punctured sphere (eq. (4.11)). Then, the same transformation that allowed us to introduce the fusion basis can be used to define ribbon operators generating the basis $\{\psi^{\mathbb{I}}_{\mathfrak{f}}[\rho,MN]\}$ (eq. (4.27)). This is just a Fourier-Peter-Weyl transform performed from functions on the Drinfel'd double to functions on its representation labels:[14]

$$\begin{cases}\mathcal{R}[\rho,MN]=\dfrac{d_\rho}{|\mathcal{G}|}\displaystyle\sum_{G,H}\mathcal{R}[G,H]D^\rho_{MN}(G\otimes\delta_H)\\ \mathcal{R}[G,H]=\displaystyle\sum_{\rho}\sum_{M,N}\mathcal{R}[\rho,MN]\overline{D^\rho_{MN}(G\otimes\delta_H)}\end{cases}.\tag{4.59}$$

And

$$\psi^{\mathbb{I}}_{\mathfrak{f}}[\rho,MN]=\frac{|\mathcal{G}|^{3/2}}{\sqrt{d_\rho}}\;(\mathcal{R}[\rho,MN]\triangleright\psi_0)(g_1,\dots,g_4)\equiv\frac{|\mathcal{G}|^{3/2}}{\sqrt{d_\rho}}\;\rho$$

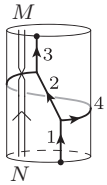

.

(4.60)

The fusion basis had projective (idempotence) properties under the gluing operation defining the $\star$-product for cylinder states. This qualified its labels as physical charges carried by the punctures. For this reason, we refer to $\mathcal{R}[\rho,MN]$ as the ρ-charge ribbon operator.

In calculations, the following expression of $\mathcal{R}[\rho,MN]$ is sometimes more useful

$$\begin{aligned}\mathcal{R}[CR;am,bn]&=\frac{d_{C,R}}{|\mathcal{G}|}\sum_{G,H}\delta(c_b,G^{-1}c_aG)\,\delta(H,c_a)D^R_{mn}(q_a^{-1}Gq_b)\,\mathcal{R}[G,H]\\ &=\frac{d_R}{|Z_C|}\sum_{z\in Z_C}D^R_{mn}(z)\,\mathcal{R}[q_azq_b^{-1},\,c_a]\,.\end{aligned}\tag{4.61}$$

It is straightforward to extend the definition of the charge ribbon operators to Σ^0_p. It is indeed enough to transform the $[G,H]$ labels of $\mathcal{R}_\ell[G,H]$ to $[\rho,MN]$.

[14] The factor d_ρ is not evenly distributed across the following two formulas in order to have eq. (4.66) to hold as it is, with no extra dimensional factors.

4.5.2 Properties of ribbon operators

In the following, we list some important properties of ribbon operators.

Deformation invariance of ribbons: The action of the ribbon operator $\mathcal{R}_\ell[G,H]$ between two punctures p_1 and p_2 along ℓ changes the quasi-local charges at the punctures. This action, however, does not depend on the precise path ℓ. Indeed, one can check that the action is invariant under isotopic deformations of the path (with regard to other punctures). On the one hand, only the holonomies around the punctures are changed by the ribbon. This translation is determined by the parameter H and the parallel transport along ℓ from p_1 to p_2. On the other hand, the state is multiplied by a delta-function, which fixes the holonomy from puncture p_1 to puncture p_2 along ℓ. And since we are dealing with locally flat states, only the isotopy class of ℓ matters, for both the parallel transport and the evaluation of the holonomies. This is the reason why the action of $\mathcal{R}_\ell[G,H]$ is invariant under isotopic deformations of ℓ.

Ribbon operators can be combined in different ways. We can glue two ribbons by their extremities and in this way define a lengthwise product. Or we can consider the operator product of two ribbons associated with the same path, which we call lateral product, obtaining a linear combination of ribbon operators. Again, these operations can be described by the structure of the Drinfel'd double of the gauge group [38].

Lengthwise product: To combine ribbons lengthwise, we consider a ribbon $\mathcal{R}_{\ell_1}[G_1,H_1]$ extending from a source puncture p_1 to a target puncture p_2, as well as a second ribbon $\mathcal{R}_{\ell_2}[G_2,H_2]$ extending from the (now) source puncture p_2 to a target puncture p_3. We assume that p_2 does not carry any excitation, i.e. Wilson loops around the puncture give trivial results, and the wave function has a trivial dependence on the holonomy associated to the link arriving at the puncture.[15]

We then demand that the lengthwise product should be such that it does not induce any excitation at the 'middle' puncture p_2. And hence, that this product in fact coincides with some (not self-crossing) ribbon operator along $\ell = \ell_2 \circ \ell_1$, directly going from p_1 to p_3. To achieve this, we enforce the flatness and Gauß constraints at the puncture p_2. This construction is analogous to the gluing of ribbons for the $\mathrm{SU}(2)_k$ case, as described in [34]. Moreover, as it will be apparent, this construction parallels the gluing of cylinder states.

If the links ℓ_1 and ℓ_2 are consistently oriented, to preserve the flatness at p_2 we need to require

$$H_1 \stackrel{!}{=} G_2^{-1} H_2 G_2 \,. \tag{4.62}$$

In order to avoid torsion excitations at p_2, we have to apply a group averaging to the resulting state. This operation eliminates the delta-function $\delta(G_1, g_{\ell_1})$ with g_{ℓ_1} is the holonomy along ℓ_1, which results from the action of $\mathcal{R}_{\ell_1}[G_1,H_1]$, but keeps the delta-function $\delta(G_2G_1, g_{\ell_2}g_{\ell_1})$ fixing the holonomy along the combined path $\ell = \ell_2 \circ \ell_1$. The resulting action of the procedure we just described is—as expected—equivalent (modulo normalizations) to that of a single ribbon operator acting along $\ell = \ell_2 \circ \ell_1$ and modifying the charge structure at p_1 and p_3:

$$|\mathcal{G}|\,(\mathbb{A}_{(p_2)} \circ \mathbb{B}_{(p_2)}) \circ \mathcal{R}_{\ell_2}[G_2,H_2]\mathcal{R}_{\ell_1}[G_1,H_1] = \delta(H_1, G_2^{-1}H_2G_2)\,\mathcal{R}_{\ell_2\circ\ell_1}[G_2G_1,H_2] \,. \tag{4.63}$$

App. A.4.1 exemplifies the gluing of two ribbons for states on the thrice-punctured sphere.

[15] Later, we will define closed ribbon operators that project onto wave functions with prescribed charges at a given puncture.

We now consider the lengthwise product of charge ribbon operators $\mathcal{R}_{\ell_2}[\rho, MN]$ and $\mathcal{R}_{\ell_1}[\rho, MN]$. Using (4.63) one finds (see app. A.4.2)

$$|\mathcal{G}|\,(\mathbb{A}_{(p_2)} \circ \mathbb{B}_{(p_2)}) \circ \mathcal{R}_{\ell_2}[\rho_2, M_2N_2]\mathcal{R}_{\ell_1}[\rho_1, M_1N_1] = \delta_{\rho_2,\rho_1}\delta_{N_2,M_1}\,\mathcal{R}_{\ell_2\circ\ell_1}[\rho_2, M_2N_1]\,. \tag{4.64}$$

Note that the resulting ribbon does not involve the indices $N_2 = M_1$ at the 'middle' puncture p_2. Thus, for the gluing of two charged ribbons, we can also define that the magnetic indices of the ribbons meeting at the puncture have to be contracted. This would introduce an extra factor $d_{\rho_1} = |C_1|d_{R_1}$ in the final result. Comparison with equations (4.24) and (4.30) immediately shows that there is a direct relation between the gluing of cylinders and the lengthwise multiplication of open ribbon operators. This means that the composition of ribbons agrees with the multiplication of the $\mathcal{D}(\mathcal{G})$ algebra. To make this completely explicit, we introduce a $\star$-product notation for the left-hand side of equations (4.63) and (4.64):

$$\mathcal{R}_{\ell_2}[G_2, H_2] \star \mathcal{R}_{\ell_1}[G_1, H_1] = \delta(H_1, G_2^{-1}H_2G_2)\mathcal{R}_{\ell_2\circ\ell_1}[G_2G_1, H_2] \tag{4.65}$$

and

$$\mathcal{R}_{\ell_2}[\rho_2, M_2N_2] \star \mathcal{R}_{\ell_1}[\rho_1, M_1N_1] = \delta_{\rho_1,\rho_2}\delta_{N_2,M_1}\,\mathcal{R}_{\ell_2\circ\ell_1}[\rho_2, M_2, N_1]\,. \tag{4.66}$$

Lateral product: We now consider the operator product of two ribbons based on the same path ℓ, which we name lateral product. Due to the deformation invariance of the ribbons this is equivalent to having the product of two ribbons that are based on paths parallel to each other, and which start as well as end at the same punctures. Hence, we can drop in this section the path label, from $\mathcal{R}[G_i, H_i],\ i = 1, 2$.

It is straightforward to verify that the lateral product of two ribbons is a third ribbon operator (of course based on the same path):

$$\mathcal{R}[G_2, H_2]\,\mathcal{R}[G_1, H_1] \;=\; \delta_{G_1,G_2}\,\mathcal{R}[G_1, H_2H_1]\,. \tag{4.67}$$

To prove the previous formula one can e.g. consider the consecutive action of two ribbons on the (global) vacuum state on $\mathbb{I}$:

$$(\mathcal{R}[G_2, H_2]\mathcal{R}[G_1, H_1] \triangleright \psi_0^{\mathbb{I}})(g_1, \ldots, g_4) =$$

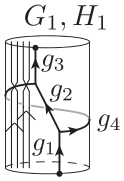

$$= \delta(G_1, g_3g_2g_1)(\mathcal{R}[G_2, H_2] \triangleright \psi_0^{\mathbb{I}})(g_1, \ldots, g_3^{-1}H_1^{-1}g_3g_4)$$

$$= \delta(G_1, g_3g_2g_1)\delta(G_2, g_3g_2g_1)\,\psi_0^{\mathbb{I}}(g_1, \ldots, g_3^{-1}H_1^{-1}H_2^{-1}g_3g_4) =$$

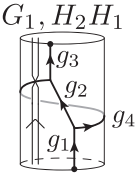

$$= \delta_{G_1,G_2}\,(\mathcal{R}[G_1, H_2H_1] \triangleright \psi_0^{\mathbb{I}})(g_1, \ldots, g_4)\,. \tag{4.68}$$

We can also consider the lateral product of two charge ribbons based, i.e. the operator product of two charge ribbons based on the same path. Here, the two ribbons generate two basic excitations at the

same puncture. We therefore expect that the resulting excitation should arise from a fusion of the two basic excitations. In fact, the lateral product involves the tensor product of the Drinfel'd double representations (and their dual):

$$\begin{aligned}
&\mathcal{R}[\rho_2, M_2N_2]\,\mathcal{R}[\rho_1, M_1N_1] \\
&\quad= \frac{d_{\rho_1}d_{\rho_2}}{|\mathcal{G}|^2} \sum_{\substack{G_1,H_1\\G_2,H_2}} D^{\rho_2}_{M_2N_2}(G_2\otimes\delta_{H_2}) D^{\rho_1}_{M_1N_1}(G_1\otimes\delta_{H_1}) \mathcal{R}[G_2,H_2]\,\mathcal{R}[G_1,H_1] \\
&\quad\overset{(4.67)}{=} \frac{d_{\rho_1}d_{\rho_2}}{|\mathcal{G}|^2} \sum_{\substack{G\\H_1,H_2}} D^{\rho_2}_{M_2N_2}(G\otimes\delta_{H_2}) D^{\rho_1}_{M_1N_1}(G\otimes\delta_{H_1}) \mathcal{R}[G,H_2H_1] \\
&\quad= \frac{d_{\rho_1}d_{\rho_2}}{|\mathcal{G}|^2} \sum_{\substack{G\\H_1,H_2}} \sum_{\rho_3} \sum_{N_3,M_3} D^{\rho_2}_{M_2N_2}(G\otimes\delta_{H_2}) D^{\rho_1}_{M_1N_1}(G\otimes\delta_{H_1}) \overline{D^{\rho_3}_{M_3N_3}(G\otimes\delta_{H_2H_1})} \mathcal{R}[\rho_3, M_3N_3] \\
&\quad= \frac{1}{|\mathcal{G}|} \sum_{\rho_3} \sum_{N_3M_3} \frac{d_{\rho_2}d_{\rho_1}}{d_{\rho_3}}\, \mathcal{C}^{\rho_2\rho_1\rho_3}_{M_2M_1M_3}\, \overline{\mathcal{C}^{\rho_2\rho_1\rho_3}_{N_2N_1N_3}}\, \mathcal{R}[\rho_3, M_3N_3]\,.
\end{aligned} \tag{4.69}$$

Note that the lateral product of two ribbons reflects an algebraic structure of the Drinfel'd double, namely its co-multiplication $\Delta(G\otimes\delta_H) = \sum_{H_2,H_1} \delta_{H_2H_1,H}(G\otimes\delta_{H_2})\otimes(H\otimes\delta_{H_1})$. Similarly, the lateral product allows us to write a given ribbon as a sum over all possible pairs of ribbon operators whose product is the desired one:

$$\mathcal{R}[G,H] \;=\; \frac{1}{|\mathcal{G}|} \sum_{H_2,H_1} \delta_{H_2H_1,H}\, \mathcal{R}[G,H_2]\,\mathcal{R}[G,H_1]\,. \tag{4.70}$$

4.5.3 Closed ribbons

By gluing the ends of an open ribbon, starting and ending at the same puncture, we obtain a closed ribbon. Closed ribbons do not generate excitations, they just measure the excitation content of the region they enclose. In the context of BF theory on a surface with fixed punctures (or higher genus), closed ribbon operators provide a complete basis of Dirac observables. This is because closed ribbons are defined in such a way to commute with the flatness and Gauß constraints. Moreover, the fusion basis constructed in sec. 4.4 diagonalizes the (charge) closed ribbon operators.

To explicitly construct a closed ribbon operator, we start with an open one as in sec. 4.5.1. It might be necessary to introduce an auxiliary puncture, at which the open ribbon starts and ends. By applying the refining operations detailed in sec. 4.2.2, we can always consider this puncture connected to the graph underlying the state under consideration via a link carrying a holonomy k (see fig. 4.3). The refined state would then be constant in k, i.e. not depend on this holonomy. The ribbon crosses L links with associated group elements $h_1,\dots,h_L$ which are incoming to a closed (circular) combination of links with associated holonomy $g'_L\cdots g'_2g'_1$. We also define $g'_{Ll} := g'_Lg'_{L-1}\cdots g'_l$, namely the parallel transport from the target node carrying h_l to the target node carrying h_1. Note that $g'_{L1} = g'_Lg'_{L-1}\dots g'_1$ is given by the holonomy going around the cycle defined by the ribbon. The (open) ribbon operator, then acts as

$$\begin{aligned}
&(\mathcal{R}[G,H]\triangleright\psi)\,(k,g'_1,\dots,h_1,\dots,\dots) \\
&\quad= \delta(G, kg'_{L1}k^{-1})\,\psi(g'_1,\dots,(g'_{L1})^{-1}k^{-1}H^{-1}kg'_{L1}\,h_1,\dots,(g'_L)^{-1}k^{-1}H^{-1}kg'_L\,h_L,\dots)\,.
\end{aligned} \tag{4.71}$$

We know that the ribbon will preserve both the flatness and Gauß constraints for every face, with the only exception given by (i) the flatness constraint for the face containing the auxiliary puncture, since

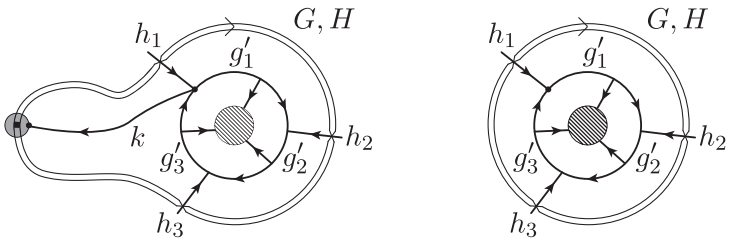

Figure 4.3. The construction of a closed ribbon operator. The left panel shows the auxiliary puncture and an auxiliary link with holonomy k going to this puncture. This holonomy plays no role in the final action of the closed ribbon operator as described in (4.74).

this face contains the holonomy combination $h_1^{-1} g'_L h_L$, and (*ii*) the Gauß constraint at the target node of the link carrying the holonomy k.

To deal with the flatness violation,[16] we first notice that the holonomy combination $h_1^{-1} g'_L h_L$ is shifted to

$$h_1^{-1} g'_L h_L \;\to h_1^{-1} (g'_{L1})^{-1} k^{-1} H k g'_{L1} g'_L (g'_L)^{-1} k^{-1} H^{-1} k g'_L h_L \tag{4.72}$$

$$= h_1^{-1} k^{-1} G^{-1} H G H^{-1} k g'_L h_L \; . \tag{4.73}$$

Therefore, to avoid a curvature excitation at the auxiliary puncture, we need to demand $GHG^{-1}H^{-1} = \mathbb{1}$, which can be taken care of by introducing an extra delta-function factor $\delta(GHG^{-1}H^{-1}, \mathbb{1})$. Then, we have to ensure gauge invariance at the target node of the link carrying k. This is achieved by applying the gauge averaging projector $\mathbb{A}$ for this node. Using that the initial state is gauge invariant, this results in

$$\begin{aligned}
&\big((\mathbb{A} \circ \mathbb{B} \circ \mathcal{R}[G,H]) \triangleright \psi\big)(k, g'_1, \dots, l'_1, \dots, \dots) \\
&\quad = \delta(GHG^{-1}H^{-1}, \mathbb{1}) \frac{1}{|\mathcal{G}|} \sum_h \delta(G, h k g'_{L1} k^{-1} h^{-1}) \psi(g'_1, \dots, (g'_{L1})^{-1} k^{-1} h^{-1} H^{-1} h k g'_{L1} l_1, \dots, \dots) \\
&\quad = \delta(GHG^{-1}H^{-1}, \mathbb{1}) \frac{1}{|\mathcal{G}|} \sum_h \big(\mathcal{R}[hGh^{-1}, hHh^{-1}]\, \psi\big)\, (g'_1, \dots, l'_1, \dots, \dots) \; .
\end{aligned} \tag{4.74}$$

Note that due to the group averaging the dependence on the (auxiliary) holonomy k disappears. Furthermore the (projected) closed ribbon operator does not depend anymore on the choice of face, among the faces crossed by the ribbon, at which the auxiliary puncture was inserted. Analogously to the open ribbons, the closed ribbons path dependence is limited to its isotopy class.

Note also that, due to the projections onto flatness and Gauß constraints, not all information contained in the pair (G, H) is actually relevant. To see this we first rewrite G using the notation of sec. 3.2.3 for the description of the Drinfel'd Double representations. This way we obtain, $G = q_a c_1 q_a^{-1}$, where c_1 is a representative of the conjugacy class C of G and $q_a \in Q_C = \mathcal{G}/Z_C$ with Z_C the centralizer group of c_1. Now, due to the delta function $\delta(GHG^{-1}H^{-1}, \mathbb{1})$ in (4.74) we see that H must be of the

[16] Even if the face we are considering here is a priori not closed, we can apply the refinement operations detailed in sec. 4.2.2, so that this face is closed. After applying the closed ribbon operator, we can go back to the coarser graph again, applying a coarse-graining transformation, to reach a state based on the initial graph.

form $H = q_a \tilde{z} q_a^{-1}$ for some $\tilde{z} \in Z_C$. Therefore, using the fact that G and H must commute, we have

$$\begin{aligned}\sum_{h\in\mathcal{G}} \mathcal{R}[hGh^{-1}, hHh^{-1}] &= \sum_{h\in\mathcal{G}} \mathcal{R}[hq_a^{-1}\, q_a c_1 q_a^{-1}\, q_a h^{-1}, hq_a^{-1} q_a \tilde{z} q_a^{-1} q_a h^{-1}] \\ &= \sum_{q_b\in Q_C} \sum_{z\in N_C} \mathcal{R}[q_b c_1 q_b^{-1},\, q_b z \tilde{z} z^{-1} q_b^{-1}] \\ &= |Z_D| \sum_{q_b\in Q_C} \sum_{d\in D} \mathcal{R}[q_b c_1 q_b^{-1},\, q_b d q_b^{-1}] \end{aligned} \tag{4.75}$$

where in the first step we shifted the summation argument by q_a, and in the second step we split the summation over $h \in \mathcal{G}$ into a one over $q_b \in Q_C$ and $z \in Z_C$.[17] In the third step, we split again the summation over Z_C into one over the stabilizer group $Z_D \subset Z_C$ and a conjugacy class D of the group Z_C.

Thus the group averaging over ribbons $\mathcal{R}[G, H]$ (with G and H commuting) does only depend on the conjugacy class C of $\mathcal{G}$ (such that $G \in C$) and a conjugacy class D of Z_C (such that H is conjugated to an element of D). Hence, we define closed ribbon operators as

$$\mathcal{K}[C, D] := \sum_{q_b\in Q_C} \sum_{d\in D} \mathcal{R}[q_b c_1 q_b^{-1},\, q_b d q_b^{-1}]\,, \tag{4.76}$$

where C is a conjugacy class of $\mathcal{G}$ and D is a conjugacy class of Z_C, the stabilizer group of $c_1 \in C$. We constructed closed ribbon operators from gluing open ribbons. We arrive at the same definition as in [106], where the closed ribbons $\mathcal{K}[C, D]$ are defined (via the third line of 4.75) based on more abstract reasoning.

Closed charge ribbon operators: In the case in which we consider punctured spheres only, the closed ribbon operators measure the excitation content of the region enclosed by the ribbon.[18] We are now going to construct closed ribbons with projective properties, which allow to project onto a region with a certain charge content. In this case, what is needed, is the projective property with respect to the lateral product, rather then the (lengthwise) $\star$-product.

Using (4.67) for $\mathcal{R}[G, H]$, we can deduce the lateral product for the closed ribbons:

$$\mathcal{K}[C_2, D_2]\, \mathcal{K}[C_1, D_1] = \sum_{\substack{q_a\in Q_{C_2}\\ q_b\in Q_{C_1}}} \sum_{\substack{d_2\in D_2\\ d_1\in D_1}} \delta(q_a c_1^{(2)} q_a^{-1}, q_b c_1^{(1)} q_b^{-1})\; \mathcal{R}[q_a c_1^{(2)} q_a^{-1}, q_a d_2 q_a^{-1} q_b d_1 q_b^{-1}] \tag{4.77}$$

$$= \delta_{C_2,C_1} \sum_{q\in Q_{C_2}} \sum_{\substack{d_2\in D_2\\ d_1\in D_1}} \mathcal{R}[q c_1^{(2)} q^{-1}, q d_2 d_1 q^{-1}]. \tag{4.78}$$

Defining coefficients $N_{D_2 D_1}^{D_3}$ via[19]

$$\sum_{\substack{d_2\in D_2\\ d_1\in D_1}} d_2 d_1 \;=\; \sum_{D_3} N_{D_2 D_1}^{D_3} \sum_{d_3\in D_3} d_3 \tag{4.79}$$

[17] There, we use that each group element has a unique representation of the form $h = q_b z$.

[18] On higher genus surfaces, the closed ribbons could wind around non-contractible cycles.

[19] The set $\{\sum_{d\in D} d\}_D$, where D is an index labelling the conjugacy classes of Z_C, gives a basis of (group algebra) elements commuting with all $z \in Z_C$. Thus also the product of $\sum_{d_2\in D_2} d_2$ with $\sum_{d_1\in D_1} d_1$ commutes with $z \in Z_C$ and can be expanded in this basis.

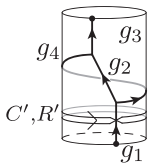

Figure 4.4. The closed ribbon operator applied to a state on a cylinder.

(both sides are to be understood as elements of the group algebra $\mathbb{C}[Z_{C_2}]$), we arrive at

$$\mathcal{K}[C_2, D_2]\,\mathcal{K}[C_1, D_1] = \delta_{C_2,C_1} \sum_{D_3} N^{D_3}_{D_2 D_1}\, \mathcal{K}[C_2, D_3]\ . \tag{4.80}$$

Therefore, the closed ribbon $\mathcal{K}[C, D]$ are already projective in C, but not in D. To reach fully projective closed ribbons under the lateral product, we define the charge closed ribbons via the formula

$$\mathcal{K}[C, R] := \frac{d_R}{|Z_C|} \sum_D \chi^R(D)\, \mathcal{K}[C, D]\ , \tag{4.81}$$

where R is an irrep of the stabilizer group Z_C (see also [106]—although, there slightly different conventions are used). The inverse transformation is given by

$$\mathcal{K}[C, D] = \frac{|Z_C|}{|Z_D|} \sum_R \frac{1}{d_R} \overline{\chi^R}(D)\ \mathcal{K}[C, R]. \tag{4.82}$$

Now, it is straightforward to check (see app. A.4.3) that the lateral product of two charge closed ribbons is simply

$$\mathcal{K}[C, R]\,\mathcal{K}[C', R'] = \delta_{C,C'}\delta_{R,R'}\mathcal{K}[C, R]. \tag{4.83}$$

Hence, the charge closed ribbons $\mathcal{K}[C, R]$ define a family of orthogonal projectors. We are now going to show that they do actually project precisely on the fusion basis states.

Diagonalization of closed ribbon operators: We consider the action of a closed charge ribbon $\mathcal{K}[C, R]$ applied to a fusion basis state on the cylinder. (We will later generalize to fusion basis states on Σ^0_p.) Using a minimal graph, the fusion basis state can be expressed in the holonomy representation as

$$\psi^{\mathbb{I}}_{\mathfrak{f}}[CR; am, bn] = |\mathcal{G}|^{1/2} \sqrt{d_{C,R}} \sum_{z \in Z_C} \delta(q_a z q_b^{-1}, g_3 g_2 g_1)\, \delta(c_a, g_3 g_4 g_2^{-1} g_3^{-1}) D^R_{mn}(z)\ . \tag{4.84}$$

We apply a closed ribbon $\mathcal{K}[C', R']$ that goes anti-clockwise around the cycle with holonomy $g_2^{-1} g_4$ and crosses only the link with holonomy g_1, as in fig. 4.4.
Then, the action of the closed ribbon $\mathcal{K}[C', R']$ on $\psi^{\mathbb{I}}_{\mathfrak{f}}[CR; am, bn]$ can be readily evaluated in the holonomy basis (see app. A.4.4). We expect that the closed ribbon does not change the charge content of the states. And indeed, the fusion basis states are eigenstates of the closed ribbon operator:

$$\mathcal{K}[C', R'] \triangleright \psi^{\mathbb{I}}_{\mathfrak{f}}[CR; am, bn] = \delta_{C,C'}\delta_{R,R'}\, \psi^{\mathbb{I}}_{\mathfrak{f}}[CR; am, bn]\ . \tag{4.85}$$

Or, more succinctly

$$\mathcal{K}[\rho'] \triangleright \psi^{\mathbb{I}}_{\mathfrak{f}}[\rho, MN] = \delta_{\rho,\rho'}\, \psi^{\mathbb{I}}_{\mathfrak{f}}[\rho, MN]\ . \tag{4.86}$$

Thus the closed charge ribbon operator $\mathcal{K}[C', R']$ projects onto the basis states $\psi^{\mathbb{I}}_{\dagger}[CR; am, bn]$.

This result can be immediately generalized to the fusion basis states on Σ^0_p. In this case, we consider a closed ribbon going around one leg of the trinion decomposition of Σ^0_p underlying the fusion basis. We can then choose the graph on this trinion to be the same as in fig. 4.4. Hence, the action of the closed charge ribbon can be evaluated in the same way as there. Again, the closed charge ribbon $\mathcal{K}[C, R]$ will project onto fusion basis states with charge labels (C, R) for the trinion leg in question.

4.5.4 An alternative closed ribbon operator

In the previous section we started with a ribbon $\mathcal{R}[G, H]$ based on a closed path, and then projected onto its flatness and gauge-invariance preserving component. We saw that the resulting operators only depend on the conjugacy class C of G and a conjugacy class D in the stabilizer group Z_C. Alternatively, we could also start with the charge ribbons $\mathcal{R}[\rho, MN]$, again based on a closed path, and project these. This provides an alternative basis of closed ribbon operators. We are going to discuss these here, as these ribbons mimic the closed ribbons discussed in [34] for the quantum group case $\mathrm{SU}(2)_{\mathrm{k}}$, where the group representation is not available. We will in particular see that the two types of closed ribbons are in a certain sense dual to each other: They are related by a specific transform that can be interpreted as Fourier transform within $\mathcal{D}(\mathcal{G})$ [88].

Recall the following expression of the charge ribbon operators

$$\mathcal{R}[CR; am, bn] = \frac{d_R}{|Z_C|} \sum_{z \in Z_C} D^R_{mn}(z)\, \mathcal{R}[q_a z q_b^{-1},\, c_a] \,. \tag{4.87}$$

Aiming at the definition of a closed ribbon operator, we sum over the indices $a = b$ and $m = n$:

$$\sum_{a,m} \mathcal{R}[C, R; am, bn] = \frac{d_R}{|Z_C|} \sum_{z \in Z_C} \chi^R(z) \sum_{q_a \in Q_C} \mathcal{R}[q_a z q_a^{-1}, q_a c_1 q_a^{-1}] \,. \tag{4.88}$$

As $c_a = q_a c_1 q_a^{-1}$ and z is in the stabilizer group of c_1 we see that $G = q_i z q_i^{-1}$ and $H = c_a$ do commute, and hence the flatness constraints are already satisfied. The contraction of the ribbon as defined in (4.88) is also invariant under the group averaging projector:

$$\begin{aligned}
\mathbb{A} \circ \sum_{a,m} \mathcal{R}[CR; am, bn] &= \frac{d_R}{|Z_C||\mathcal{G}|} \sum_{h \in \mathcal{G}} \sum_{z \in Z_C} \chi^R(z) \sum_{q_a \in Q_C} \mathcal{R}[h q_a z q_a^{-1} h^{-1}, h q_a c_1 q_a^{-1} h^{-1}] \\
&= \frac{d_R}{|Z_C|^2} \sum_{z \in Z_C} \chi^R(z) \sum_{q_b \in Q_C} \sum_{z' \in Z_C} \mathcal{R}[q_b z' z (z')^{-1} q_b^{-1}, q_b c_1 q_b^{-1}] \\
&= \frac{d_R}{|Z_C|} \sum_{\tilde{z} \in Z_C} \sum_{q_b \in Q_C} \chi^R(\tilde{z})\, \mathcal{R}[q_b \tilde{z} q_b^{-1}, q_b c_1 q_b^{-1}] \\
&= \sum_{a,m} \mathcal{R}[CR; am, am] \,.
\end{aligned} \tag{4.89}$$

In the above calculation, we first shifted the summation over h by q_a^{-1}, making the sum over $q_a \in Q_a$ superfluous. Then, we split again h as $h = q_b z'$ and redefined the variable z to $\tilde{z} = z' z (z')^{-1}$, hence making the sum over z' superfluous.

This shows that the following is a viable definition of an operator on $\mathcal{H}_p$, since it preserves both the flatness and Gauß constraints:

$$\tilde{\mathcal{K}}[C, R] := \sum_{a,m} \mathcal{R}[C, R; am, am] \,, \tag{4.90}$$

or, equivalently,

$$\tilde{\mathcal{K}}[\rho] := \sum_N \mathcal{R}[\rho; NN] \,. \tag{4.91}$$

In particular, the above formulas show that $\tilde{\mathcal{K}}[C,R]$, when expressed in terms of $\mathcal{R}[G,H]$, has essentially the same form as the ribbon operators $\mathcal{K}[C,R]$ defined at eq. (4.76) and (4.81). The only difference is that the role of the entries in the ribbon operator $\mathcal{R}[G,H]$ is exchanged. Indeed, the transformation between the two types of closed ribbon operators reveals why this is the case.

To express $\tilde{\mathcal{K}}[C,R]$ in terms of $\mathcal{K}[C',R']$ operators, we write

$$\begin{aligned}
\tilde{\mathcal{K}}[C,R] &= \mathbb{A} \circ \sum_{a,m} \mathcal{R}[C,R; am, am] \\
&= \frac{d_R}{|Z_C|} \sum_{z\in Z_C} \chi^R(z) \sum_{q_a \in Q_C} \mathbb{A} \circ \mathcal{R}[q_a z q_a^{-1}, q_a c_1 q_a^{-1}] \\
&\overset{(4.75)}{=} \frac{d_R}{|Z_C|} \sum_{z\in Z_C} \chi^R(z) \frac{|Z_{D(z,c_1)}|}{|Z_C|}\, \mathcal{K}[C_z, D_{z,c_1}] \\
&\overset{(4.81)}{=} \frac{d_R}{|Z_C|} \sum_{z\in Z_C} \chi^R(z) \sum_{R'} \frac{1}{d_{R'}} \overline{\chi^{R'}(D_{z,c_1})}\, \mathcal{K}[C_z, R'] \,,
\end{aligned} \tag{4.92}$$

where in the third line, we used the definition (4.75) of the ribbon operators $\mathcal{K}[C,D]$, and where we made use of the following notation: C_z stands for the conjugacy class of z in $\mathcal{G}$ and D_{z,c_1} for the conjugacy class in Z_{C_z}, which includes the element

$$q_{z,k}^{-1}\, c_1\, q_{z,k} \quad \text{where} \quad z = q_{z,k}\, c_{z,1}\, q_{z,k}^{-1} \quad \text{and} \quad q_{z,k} \in Q_{C_z},\ c_{z,1} \in C_z \,. \tag{4.93}$$

Therefore, we conclude that $\tilde{\mathcal{K}}[C,R]$ is a linear combination of operators $\mathcal{K}[C',R']$. This can be summarized with the formula,

$$\tilde{\mathcal{K}}[C,R] \;=\; \sum_{C',R'} \mathcal{S}_{CR,C'R'}\, \mathcal{K}[C',R'] \,, \tag{4.94}$$

where

$$\mathcal{S}_{CR,C'R'} = \frac{d_R}{d_{R'}\,|Z_C|} \sum_{z\in Z_C} \chi^R(z) \overline{\chi^{R'}(D_{z,c_1})}\, \delta_{C',C_z} \,. \tag{4.95}$$

This matrix turns out to be related to the so-called S-matrix of the Drinfel'd double $\mathcal{D}(\mathcal{G})$. This is defined as

$$\mathbf{S}_{CR,C'R'} \;=\; \frac{1}{|\mathcal{G}|} \sum_{\substack{h_a\in C \\ h'_b \in C'}} \delta(h_a h'_b,\, h'_b h_a)\, \overline{\chi^R(q_a^{-1} h'_b q_a)}\, \overline{\chi^{R'}((q'_b)^{-1} h_a q'_b)} \,. \tag{4.96}$$

where $h_a := q_a c_1 q_a^{-1}$ and $h'_b := q_b c'_1 q_b^{-1}$, with $c_1 \in C$, $c'_1 \in C'$ and $q_a \in Q_C$, $q'_b \in Q_{C'}$. As it is shown in app. A.5, the S-matrix $\mathbf{S}_{CR,C'R'}$ can be more succinctly be written as

$$\begin{aligned}
\mathbf{S}_{CR,C'R'} &= \frac{1}{|\mathcal{G}|} \sum_{h_a\in C} \sum_{z\in Z_C} \delta_{C',C_z}\, \overline{\chi^R(z)}\, \overline{\chi^{R'}(D_{z,c_1})} \\
&= \frac{1}{|Z_C|} \sum_{z\in Z_C} \delta_{C',C_z}\, \overline{\chi^R(z)}\, \overline{\chi^{R'}(D_{z,c_1})} \,,
\end{aligned} \tag{4.97}$$

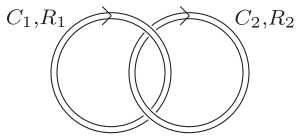

Figure 4.5. Two braided closed ribbon operators. These can be constructed by gluing open ribbon operators, which act in a certain order, e.g. under-crossing pieces of ribbons act before the over-crossing pieces of ribbons.

and thus

$$\mathcal{S}_{CR,C'R'} = \frac{d_R}{d_{R'}} \mathbf{S}_{CR^*,C'R'} \ , \tag{4.98}$$

where R^* denotes the contragredient representation to R. Using this result, it is straightforward to deduce the action of $\tilde{\mathcal{K}}[C,R]$ on the fusion basis. In the conventions of fig. 4.4, and with the usual short-hand notation:

$$\tilde{\mathcal{K}}[\rho'] \triangleright \psi[\rho, MN] = \mathcal{S}_{\rho,\rho'} \ \psi[\rho', MN] \ , \tag{4.99}$$

i.e. the fusion basis states are also eigenstates of $\tilde{\mathcal{K}}[C,R]$, but this time with eigenvalues determined by the entries of the S-matrix.

The relation between the two basis of closed ribbon operators and the fusion basis on the cylinder can be understood as follows. The label C in $\psi^{\mathbb{I}}_{\mathfrak{f}}[CR; am, bn]$ denotes the conjugacy class of the H–holonomy around the cylinder, whereas the representation label R encodes information about the functional dependence of the wave function on the G–holonomy along the cylinder. Going back to the construction of the closed charge ribbon $\mathcal{K}[C,R]$ (eq. (4.75) and (4.81)), we see that C is again the conjugacy class of the holonomy around the cylinder and R captures information about the holonomy along the cylinder. This explains why $\mathcal{K}[C,R]$ projects onto wave functions $\psi^{\mathbb{I}}_{\mathfrak{f}}[C,R;am,bn]$.

In turn, if we consider a closed ribbon $\tilde{\mathcal{K}}[C,R]$ going around the cylinder, C now captures information about the G–holonomy along the cylinder (the one crossed by the ribbon), whereas R encodes information about the holonomy going around the cylinder. In fact, on the two-torus $\mathbb{T}_2$—obtained e.g. by gluing the two punctures of the cylinder—we can consider closed ribbons associated to the two cycles generating the fundemental group. We can then define two different basis of $\mathcal{H}_{\mathbb{T}_2}$ diagonalizing the two different closed ribbons. The transformation between these two basis is given by the S-matrix. This is for the same reason why the S-matrix appears in the transformation between $\mathcal{K}$ and $\tilde{\mathcal{K}}$: It exchanges the role of the longitudinal and transverse holonomies. But, on the torus, the role of longitudinal and transverse holonomy is the same. Hence, the complete duality in this case.

At the level of the Drinfel'd double, $\mathcal{D}(\mathcal{G}) = \mathcal{F}(\mathcal{G})^* \otimes \mathcal{F}(\mathcal{G})$, the S-matrix defines a transform exchanging the role of $\mathcal{F}(\mathcal{G})$ and its dual $\mathcal{F}(\mathcal{G})^* \simeq \mathbb{C}[\mathcal{G}]$ [88]. In particular, this translates into the fact that the role of multiplication and co-mutiplication are also exchanged in a proper sense. This is why, in the analysis above, we have seen both the $\star$-multiplication and the co-multiplication structures appearing naturally in the context of lateral products.

Note finally that the S-matrix can also be defined as the eigenvalues of the operator defined by two interwoven closed $\tilde{K}$-ribbons (fig. 4.5). To define this interwoven operator one needs to build the closed ribbons by gluing open ribbons, after having applied the latter to the state in the appropriate order (see [34] for details).

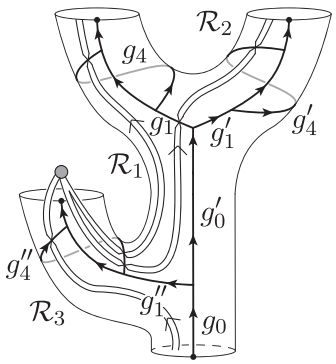

Figure 4.6. Construction of the fusion basis states on the thrice-punctured sphere using charge ribbon operators. An auxiliary puncture is introduced at which the three ribbons are fused via a Clebsch-Gordan coefficient.

4.5.5 Back to the fusion basis

We have previously shown that the charge ribbon operators generate the fusion basis on the cylinder, i.e.

$$\psi^{\mathbb{I}}_{\mathfrak{f}}[\rho, MN] = \frac{|\mathcal{G}|^{3/2}}{\sqrt{d_\rho}} (\mathcal{R}[\rho, MN] \triangleright \psi^{\mathbb{I}}_0)(g_1, \dots, g_4) \equiv \frac{|\mathcal{G}|^{3/2}}{\sqrt{d_\rho}} \; \rho \quad . \tag{4.100}$$

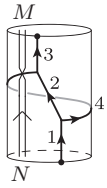

This statement can be generalized to spheres Σ^0_p with p punctures. Consider for instance the thrice-punctured sphere $\mathbb{Y} \equiv \Sigma^0_3$. We wish to obtain a fusion basis state by using the charge ribbon operators $\mathcal{R}_1[\rho_1, M_1, N_1]$, $\mathcal{R}_2[\rho_2, M_2, N_2]$ and $\mathcal{R}_3[\rho_3, M_3, N_3]$ for each of the legs of the thrice-punctured sphere. However the three ribbons need to be fused (or glued) at an auxiliary puncture, we therefore need to consider a four-punctured sphere, see fig. 4.6. Moreover, we need to contract the free indices arriving at the auxiliary puncture with a Clebsch-Gordan coefficient. By construction, the fusion procedure at the auxiliary puncture includes a projection of this puncture to vanishing electric and magnetic (curvature and torsion) charge. This allows us to understand the resulting state as a state on the thrice-punctured sphere again. As shown in app. A.4.5, this gives

$$\begin{aligned} &\sum_{N_1,N_2,N_3} \Big(\big(\mathcal{R}_1[\rho_1, M_1 N_1] \, \mathcal{R}_2[\rho_2, M_2 N_2] \, \mathcal{C}^{\rho_1\rho_2\rho_3}_{N_1 N_2 N_3} \big) \star \mathcal{R}_3[\rho_3, N_3 M_3] \Big) \triangleright \psi^{\mathbb{Y}}_0 \\ &\quad = \frac{1}{|\mathcal{G}|^3} \, d_{\rho_3} \sqrt{d_{\rho_1} d_{\rho_2}} \;\; \psi^{\mathbb{Y}}_{\mathfrak{f}} \begin{bmatrix} \rho_1, M_1 \\ \rho_2, M_2 \\ \rho_3, M_3 \end{bmatrix} . \end{aligned} \tag{4.101}$$

This construction can be easily generalized to spheres with more punctures.

4.6 Multi-scale design of states and coarse-graining

We finally come to applications of the fusion basis and the related ribbon operators. Here we discuss applications that make use of the multi-scale control the fusion basis offers.

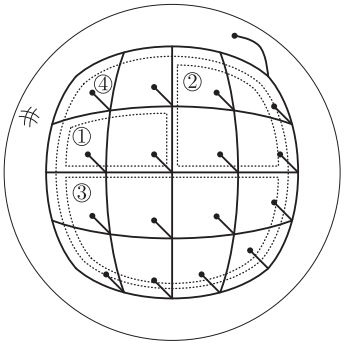

Figure 4.7. We can embed a regular square lattice on the sphere by closing it with an outer plaquette. Each plaquette, including the outer one, can carry an elementary curvature excitation. The solid lines represent the embedded graph while the dashed lines represent a possible scheme for coarse-graining the lattice.

4.6.1 Multi-scale design of states

In the previous sections, we constructed the fusion basis as well as ribbon operators which either generate it (open ribbon operators $\mathcal{R}$) or project onto it (closed ribbon operators $\mathcal{K}$). Crucially, the fusion basis is quite different from the spin network basis, since it allows a direct access to observables at different scales. In fact, the $\{\rho\}$ labels of a fusion basis state $\psi_{\mathfrak{f}}^{\Sigma^0_p}[\{\rho\},\{N\}]$ correspond to the ρ labels appearing in the set of closed ribbon operators $\{\mathcal{K}[\rho]\}$, which project onto the fusion basis state. In turn, such closed ribbon operators go around different number of punctures. This number provides us with a notion of 'scale', which we can associate to the closed ribbon operator $\mathcal{K}[\rho]$, and hence to the label ρ itself. In the case of gravity, the geometry is encoded in the states. Thus this notion of 'scale' is not a priori associated with a notion of length or metric. It is rather an auxiliary notion, from which one can however deduce a length scale, *once a choice of state is given*, see e.g. [15, 61].

Note that we are not forced to follow the linear construction of the fusion basis as indicated in sec. 4.4.3. We can indeed be more flexible. Take for example a regular square lattice[20] with $N \times N$ plaquettes, with $N = 2^K$ for some $K \in \mathbb{N}$. To obtain the topology of a punctured sphere[21] we close off this lattice with one *outer plaquette*, see fig. 4.7. This corresponds to the choice of free boundary conditions for the original lattice. The outer plaquette has 4 two-valent and $(4N-4)$ three-valent nodes along its boundary.

Each plaquette can then carry an elementary curvature (i.e. magnetic) excitations. The Gauß constraint violations (i.e. torsion or electric excitations) would usually sit on the nodes of the lattice.[22] However, for the regular square lattice, it is natural to move also these excitations onto the plaquettes. To do this, we restore gauge invariance at the two-, three- and four-valent nodes, but add an open link to all the four-valent nodes, pointing in one direction, toward the center of—say—the top-left plaque-

[20] This lattice (or graph) would of course have four-valent nodes. Nevertheless, the techniques developed in this chapter can be straightforwardly applied to graphs with nodes of valence higher than three. Alternatively, four-valent nodes can always be expanded into three-valent ones in a regular manner.

[21] Alternatively, we can allow for a punctured torus topology, for which one can also define a fusion basis. This implements periodic boundary conditions.

[22] In lattice gauge theories, as well as in loop quantum gravity, one restricts quite often attention to gauge invariant states, which would make the introduction of open links unnecessary. As we will see, coarse-graining of non-abelian gauge theories does however introduce torsion excitations, and one might want thus to include such cases in the discussion. On the other hand it is straightforward to restrict to a basis which is gauge invariant, by setting the torsion excitations for the initial plaquettes to zero.

tte. Thus, it is only the two-valent and three-valent nodes on the boundary of the outer plaquette, for which we ignore the Gauß constraint violations. To also allow for a Gauß constraint violation at the outer plaquette, we introduce an open link at one of its corners.

So each plaquette can be identified with a puncture, which can carry both curvature and torsion excitations. To define a fusion basis we have to decide on an ordering in which the punctures or plaquettes are fused to larger ones. To reach a homogeneous definition, we can first fuse pairs of plaquettes in x-direction and then pairs of plaquettes in y-direction (leaving the outer plaquette untouched). This coarse-graining procedure can be repeated until we remain with just two plaquettes, which represent the twice-punctured sphere. The fusion basis as defined earlier diagonalizes closed ribbon operators: $\mathcal{K}_1$ that go around single plaquettes, operators $\mathcal{K}_2$ that go around pairs (in x-direction) of plaquettes, operators $\mathcal{K}_4$ that enclose quadruples of plaquettes, and so on. Correspondingly, the different scales of the basis states are described by sets of representation labels $\{\rho_k^i\}$, where $k = 0, 1, 2, \dots, K$ indicates the scale given by the number 2^k of plaquettes surrounded.

Hence, we see that the fusion basis is ideal to design states with a prescribed multi-scale behavior of observables. We expect that this will help to design low-energy states for Yang-Mills (lattice) theory, by merging our tools with the techniques developed for this purpose in the context of tensor network states or MERA (multi-scale entanglement renormalization ansatz [107]), see [95] and also [108, 109] for some recent developments. The advantage of using the fusion basis is that it comes with multi-scale observables, that are automatically diagonalized by the fusion basis itself.

The fusion basis can also be useful in covariant (space-time) approaches to renormalization and coarse-graining of lattice gauge theories and spin-foams [19, 60, 62, 100, 101]. Here, the partition function associated to a space-time building block can be represented by a state on the boundary of this block [61, 65, 110]. Using the fusion basis to represent this state would allow to keep control in particular over the torsion excitations, which are generated by coarse-graining in non-abelian gauge theories, and which are rather difficult to handle in the spin network basis (see next section, and especially [19]).

4.6.2 Coarse-graining in terms of density matrices

We discuss here the coarse-graining of gauge theory and loop quantum gravity states, explain the intricacies of this procedure, and motivate the use of the fusion basis. We work in the context of a fixed (initial) graph, or lattice, thus the discussion in this section is independent of the question on which representation (ALI versus BF) we use. In the context of loop quantum gravity coarse-graining has been discussed in [18, 22, 23, 86, 111].

To start with, one considers a graph Γ and associates to it the Hilbert space $\mathcal{H}_\Gamma$ of functions $\psi \in \mathcal{F}(\mathcal{G}^L)$ of the graph connection. Here, L denotes the number of links, while the inner product in $\mathcal{H}_\Gamma$ is given by (7.17). Coarse graining in a canonical framework is usually discussed using density matrices, which we will here denote by $\mathfrak{D}$ (instead of ρ which we reserved for the representation labels of the Drinfel'd double $\mathcal{D}(\mathcal{G})$). Pure states are then represented in the holonomy basis by

$$\mathfrak{D} = \Big|\psi\Big\rangle\Big\langle\psi\Big| = \sum_{g,\tilde{g}} \mathfrak{d}\Big[\{g\},\{\tilde{g}\}\Big]\Big|\{g\}\Big\rangle\Big\langle\{\tilde{g}\}\Big| \,, \tag{4.102}$$

where

$$\mathfrak{d}\Big[\{g\},\{\tilde{g}\}\Big] \;=\; \psi(\{g\})\;\overline{\psi(\{\tilde{g}\})}\,. \tag{4.103}$$

The coarse-graining of a density matrix is defined as follows. First, choose a splitting of the holonomies $\{g\}$ attached to the links of the graph Γ under consideration, into two sets of finer $\{g^f\}$ and coarser

$\{g^c\}$ holonomies. Starting from a density matrix $\mathfrak{D}$ for the initial system, a coarser density matrix can then be defined by summing over the finer degrees of freedom,

$$\mathfrak{d}^c(\{g^c\},\{\tilde{g}^c\}) \;=\; \frac{1}{|\mathcal{G}|^{L_f}} \sum_{g^f} \mathfrak{d}(\{g^c\},\{g^f\},\{\tilde{g}^c\},\{g^f\}) \;, \tag{4.104}$$

where L_f denotes the number of finer links, i.e. those links carrying 'finer' holonomies.

In general, however, the graph under consideration will 'break apart' once the finer links are removed. To avoid this, we can first (unitarily) transform the state onto a lattice where all the finer links one wishes to integrate out are given by loops, see e.g. [18, 95].[23] This way, removing these loops leaves us with a connected coarser lattice. But this coarse-graining procedure has at least two major drawbacks.

(a) Despite providing a certain control over the coarser and finer variables in terms of the holonomies, it completely lacks control over their conjugated variables, i.e. the (electric) fluxes. This is an important issue, especially in the context of loop quantum gravity, where the fluxes encode the metrical information of the (spatial) geometry. From this perspective, one would rather be tempted to define a coarse-graining procedure in terms of both holonomies and flux variables.

(b) Moreover, the coarse density matrix is in general gauge invariant only under diagonal transformations, that is under those gauge transformations which agree in their action on the $\{g^c\}$ and $\{\tilde{g}^c\}$ variables. This is the case even if the finer density matrix was invariant under arbitrary gauge transformations at every single node. This full invariance holds in particular for pure density matrices constructed as in (4.102) from gauge invariant states. Note that this issue arises only in *non*-abelian gauge theories. Indeed, in abelian gauge theories it does not appear, if the finer variables are associated to loops, since gauge transformations act by adjoint action on holonomies associated to loops. In other terms, in this latter case, one has a simple procedure to coarse-grain gauge-invariant variables. On the contrary, for non-abelian gauge theories, the spin network basis for density matrices is not stable under coarse-graining, and is therefore quite inconvenient for this purpose.

Of course, one could consider an extension to non-gauge invariant spin network states as proposed in [18, 23], however, the main appeal of the spin network basis is the straightforward implementation of gauge invariance. A neat solution to issue (b) would consist in providing a basis which allows for a coarse-graining in terms of gauge-invariant variables. Here, one not only needs a maximally commuting subset of observables (which specifies a choice of basis), but also their conjugated observables, which brings us back to issue (a).

Before discussing a proposal for such a procedure, let us mention another possibility based on density matrix factorization. This consists in finding a transformation which decouples the finer holonomy variables (which we assume to be based on loops) from the rest of the state. That is, after the transformation, the density matrix takes the product form

$$\mathfrak{d}\Big[\{g^c\},\{g^f\},\{\tilde{g}^c\},\{g^f\}\Big] \;=\; \mathfrak{d}^c\Big[\{g^c\},\{\tilde{g}^c\}\Big] \times \mathfrak{d}^{\text{loops}}\Big[\{g^f\},\{g^f\}\Big]. \tag{4.105}$$

Upon coarse-graining, this would simply yield the density matrix $\mathfrak{D}^c$. In this case $\mathfrak{D}^c$ would be fully gauge invariant, provided this is the case for the initial density matrix $\mathfrak{D}$. However, such a transformation which allows us to cast density matrices into a product form, clearly depends on the

[23] In [95] such transformations are called *controlled rotation unitary gates*.

initial states. Therefore, the coarse-graining itself would not be controlled by a choice of coarser and finer observables, but rather by the form of the initial states. We mention this possibility here, because this type of decoupling of finer and coarser variables underlies the MERA approach [107].

4.6.3 Coarse-graining based on the splitting of the observable algebra

Let us now discuss a coarse-graining procedure in which the splitting of the observable algebra into coarser and finer variables is central. Here one can consider the kinematical, that is gauge covariant observable algebra, or the algebra of almost[24] gauge invariant observables. Such splittings of the observable algebra are also important for the construction of the continuum Hilbert spaces by an inductive limit [22] or projective techniques [112–114].

We use a phase space description, and to this end assume that $\mathcal{G}$ is a compact semi-simple Lie group. In this case, [25] the phase space associated with a graph is given by pairs (g_l, X_l) for each link l of the graph. $X_l \in \mathrm{Lie}(\mathcal{G})$ are the Lie algebra valued (electric) fluxes. We often express them in the basis τ^i as $X_l = \sum_i X_l^i \tau^i$. The phase space carries the canonical symplectic structure

$$\{g_l, g_{l'}\} = 0 \quad , \quad \{X_l^i, g_{l'}\} = \delta_{l,l'} g_l \tau^i - \delta_{l^{-1},l'} \tau^i g_{l'} \quad , \quad \{X_l^i, X_{l'}^j\} = \delta_{l,l'} \epsilon^{ijk} X_l^k \ . \tag{4.106}$$

Here, it is understood that we associate to an inverted link l^{-1} an hololonomy $g_{l^{-1}} = g_l^{-1}$ and a flux $X_{l^{-1}} = -g_l X_l g_l^{-1}$. Both fluxes and holonomies transform under gauge transformations, which are parametrized by $\{u_n \in \mathcal{G}\}_n$, with n labeling the nodes of the graph:

$$g_l \to u_{t(l)} g_l u_{s(t)}^{-1} \quad \text{and} \quad X_l \to u_{s(l)} X_l u_{s(l)}^{-1} \tag{4.107}$$

with $s(l)$ and $t(l)$ denote the source and target nodes of l, respectively.

A coarse-graining procedure based on gauge-covariant observables can be achieved in two steps, as follows. Firstly, find a canonical transformation such that the new variables split into coarser and finer sets of variables. Crucially, the sets of coarser and finer variables must commute with each other. Also, one should take care of preserving the form of the symplectic structure given by (4.106), since this is at the basis of the interpretation of the variables in terms of holonomies and fluxes. Secondly, as before, one can simply use a polarization of the wave functions in the new holonomy variables and integrate out the finer holonomy variables, while keeping the coarser holonomies fixed, as in (4.104). The coarser holonomies and the coarser fluxes give (conjugated) observables characterizing the coarser states. Therefore, this procedure is not different from the one described at the end of the previous section, but rather an amendment thereof. This amendment, which basically prescribes in more detail how to split the holonomies into coarser and finer sets, allows us, to gain control over the coarse-graining of the fluxes as well.

Now, one can ask what kind of transformations would preserve the symplectic structure (4.106), hence keeping the interpretation of the variables as holonomies and fluxes intact. Examples for such transformations are constructed in detail in [22, 86, 113]. We review the construction in [22, 86] shortly, as it is closely related to the construction of the ribbon operators. Holonomies are easy to treat, since we can simply consider compositions $g_{l'} = g_{l_n} \cdots g_{l_1}$ that result in 'new' holonomies $g_{l'}$ attached to 'new' links $l' = l_n \circ \cdots \circ l_1$ built out of the links on the initial graph. For the fluxes, we can consider combinations of the following type (see [22] for more detailed definitions)

$$X_{l'} := \sum_{l \in \{l'\}} g^{-1}_{s(l)s(l')} X_l \, g_{s(l)s(l')}. \tag{4.108}$$

[24] Since we will use a root that provides a global reference system.
[25] See e.g. [22] for a more detailed review of the phase space structures.

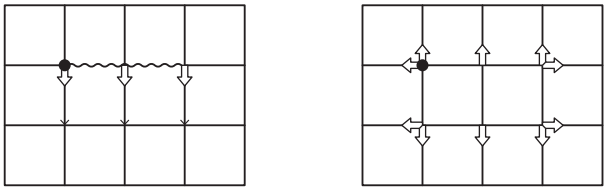

Figure 4.8. Each link of the graph is associated with an holonomy and the thick arrow represents the corresponding conjugated flux. The black dot represents the root at which gauge invariance is relaxed. The left panel shows an example of construction of a coarser flux. Fluxes are first parallel transported to the root following the path defined by the wiggly line and then added to form a coarser flux. The right panel shows an example of closed path. As before, fluxes must be first parallel-transported to a common frame before being added to each other. In presence of curvature, this sum will not be zero meaning that the Gauß constraint is violated.

Here, $\{l'\}$ is a set of links, so that the dual of these links form a connected path made out of edges of the triangulation, or more generally, out of edges of the dual complex to the graph under consideration. This connected path should be interpreted to be dual to a 'new' link l'. The holonomies $g_{s(l)s(l')}$ denote the parallel transport from a node $s(l')$, which will be the source node of the new link l' to the source node $s(l)$ of the link l. In this way, we sum up the fluxes in one and the same reference system, provided by $s(l')$. An explicit procedure to find phase space splittings into coarser and finer variables based on such transformations can be found in [22].

In a loop quantum gravity context, the fluxes are $\mathfrak{su}(2)$-valued and encode the edge vectors—for the edges dual to the links–in a reference frame associated with the nodes of the graph. This interpretation also holds for the coarse-grained fluxes (4.108) and thus justifies such a coarse-graining prescription.

The exponentiated action of the *coarser* or *integrated* fluxes, as defined in (4.108), agrees with the translation part of the open ribbon operators as discussed in sec. 4.5.1, see [86]. The holonomy (or multiplication) part of the ribbon operator is also constructed via a composition of holonomies, following the same prescription we employed in this section. Hence, ribbon operators use a coarse-graining of fluxes and holonomies analogous to the one described here. There is nevertheless an important difference. The holonomy part and the translational part of a ribbon operator commute with each other: The translational part corresponds to a flux integrated along a path of edges in the triangulation, and the holonomy part is associated to a path in the dual lattice. For the ribbon these two paths are parallel, whereas a holonomy and its conjugated flux are based on a link and an edge, that are transversal to each other.

So far, we have been discussing the gauge covariant phase space. The coarse-graining procedure described above would give us control over the coarser holonomy and flux variables, but would suffer also from a violation of (full) gauge invariance for the coarse density matrix. In the canonical formalism, gauge invariance is encoded in Gauß constraints associated to each node n,

$$G_n \;=\; \sum_{l:s(l)=n} X_l \;+\; \sum_{l:t(l)=n} X_{l^{-1}} \;. \tag{4.109}$$

Geometrically, these constraints demand the closure[26] into a polygon of the edges dual to the links ending or starting at n.

[26]Sometimes, Gauß constraints are renamed 'closure constraints'.

With such an interpretation, one might expect that the Gauß constraint are preserved under coarse-graining, as the coarser Gauß constraints would demand that the coarser edges of the coarser triangulation close, too. This is, however, generally not the case [22]. The reason is the following. The coarser fluxes have to be parallel transported to a common frame. Now, if this parallel transport has to go through a region with curvature, the coarser Gauß constraint will in general not hold. Hence, we effectively obtain torsion, defined as a violation of the Gauß constraint, due to the presence of curvature. Such an effect, which was named *curvature-induced torsion* in [22], is strictly related to the need of deforming the Gauß constraint in phase spaces describing piecewise homogeneously-curved (instead of piecewise flat) geometries [104, 115–118].[27] In terms of defect excitations, this is the statement that torsion excitations interpreted as spinning particles can arise from the fusion of two spinless defects, since two particles can have orbital angular momentum.

As mentioned, we could attempt to use gauge invariant variables for the coarse-graining, which would avoid loosing gauge invariance. At the phase space level, this would also mean that the Gauß constraints become redundant. In fact, implementing gauge invariance in phase space means to consider only the constraint hypersurface where the Gauß constraint is satisfied, and at the same time only gauge invariant functions on such phase space. But it is a very involved task to come up with a phase space description involving only completely gauge invariant observables. It is much easier to work with an almost gauge invariant set-up. This consists in choosing a node, called root r, as global reference frame, to which all fluxes and holonomies are parallel transported. In other words, in considering only root-based holonomies and fluxes. The resulting variables are invariant under all gauge transformations, except for those at the root that acts by adjoint action.

A further, necessary, step consists in identifying an independent set of observables. Indeed, the fluxes are related by the Gauß constraints (4.109), while holonomies along loops must satisfy certain algebraic relations. Such an independent set of variables can be obtained by choosing a rooted spanning-tree of the underlying graph Γ. This defines leaves ℓ, i.e., links which are not part of the tree. Each leaf ℓ defines a unique closed loop, which starts and ends at the root and which contains only links of the tree and the one leaf ℓ. Hence, each leaf defines an holonomy variable h_ℓ. Furthermore, for what concerns the fluxes, we can consider the leaf's flux X_ℓ parallel transported to the root: $\mathbf{X}_\ell = g^{-1}_{s(\ell)r} X_\ell \, g_{s(\ell)r}$. The set of variables $\{(h_\ell, \mathbf{X}_\ell)\}_\ell$, with ℓ running through all leaves, gives a complete parametrization of the almost gauge invariant phase space.[28] And they do so by essentially preserving the form of the symplectic structure of the gauge covariant phase space:

$$\{h_\ell, h_{\ell'}\} = 0 \quad , \quad \{\mathbf{X}^i_\ell, h_{\ell'}\} = \delta_{\ell,\ell'} h_\ell \tau^i - \delta_{\ell^{-1},\ell'} \tau^i h_{\ell'} \quad , \quad \{\mathbf{X}^i_\ell, \mathbf{X}^j_{\ell'}\} = \delta_{l,l'} \epsilon^{ijk} \mathbf{X}^k_\ell \, . \tag{4.110}$$

The coarse-graining procedure can now be run analoguesly to the gauge covariant case. In particular, there is a well defined sense in which both the graph and the tree are coarse-grained to a coarser graph and tree. Based on such a choice of coarser graph and tree, one can perform a split into coarser and finer variables, as needed for coarse-graining. All this is discussed in detail in [86].

Notice that within this procedure, one is working with an 'almost' gauge-invariant state space, which after coarse-graining still captures the 'almost' gauge-invariant observables. Therefore, we have in this way exhibited a structure which is stable under the coarse-graining procedure. This comes, however, at a price: While all the initial fluxes could have been reconstructed via the Gauß constraint, this is not the case at the level of the coarser fluxes. Of course, one could use some *ad hoc*

[27] See also [119–121], for an analysis in four dimensions.

[28] The leaf-associated loops allow the reconstruction of all other (root based) loops by construction. Furthermore we are only left with the fluxes associated to the leaves. The fluxes associated to the remaining links can be reconstructed using the Gauß constraints (see [22] for the procedure).

Gauß constraints of the form (4.109) to define fluxes associated to the links of the coarse tree. But these fluxes would not correspond to the fluxes one obtains via coarse-graining from the finer fluxes. In this sense, one looses important information, which in the case of loop quantum gravity encodes the coarser spatial metric. Once again, the underlying reason is that curvature can lead to torsion on a coarse-grained level. This is naturally taken into account in a coarse-graining scheme based on the fusion basis. We now turn to describing such a scheme.

4.6.4 Coarse-graining in the fusion basis

As discussed in sec. 4.6.1, the fusion basis diagonalizes operators which can be naturally interpreted as describing different coarse-graining scales. Therefore, the fusion basis $\psi_{\mathfrak{f}}[\{\rho_j\},\{N_k\}]$ comes equipped with a natural coarse-graining scheme, in which one sums directly over its $\mathcal{D}(\mathcal{G})$ representation labels.

Let us first review, what kind of observables these representation labels are related to. As discussed in sec. 4.5.3, the fusion basis diagonalizes the closed charge ribbon operators associated to the fusion tree structure. More generally, closed ribbon operators $\mathcal{K}_i[\rho']$ project onto states $\psi_{\mathfrak{f}}[\{\rho_j\},\{N_k\}]$ for which $\rho_i = \rho'$, where i and j label the branches in the fusion tree associated to the fusion basis, whereas k labels its one-valent nodes (i.e. its endpoints).

We want now to compare the coarse-graining procedure provided by the fusion basis and closed ribbon operators, to the one provided by the holonomy polarization in the almost gauge invariant set-up. To this end, we assume that we work with a p-punctured sphere Σ^0_p and a minimal graph, but do not have torsion excitations at the punctures, i.e. we have gauge invariant wave functions.

The holonomy polarization uses a basis which can be symbolically written as $\psi[\{G_\ell\}](\bullet) = \prod_\ell \delta(G_\ell,\bullet)$, where ℓ runs over the leaves of a spanning tree in the graph Γ, and the number of leaves is given by $|\ell| = p-1$. The operators diagonalizing this basis are given by root-based Wilson loop operators W^f. These Wilson loops need *not* be restricted to class functions, i.e. functions of the trace of the loop holonomy.

On the other hand, the closed ribbon operators $\mathcal{K}_j[C_j,R_j]$ are fully gauge invariant observables. In particular, the label C_j measures the conjugacy class (or trace) of the Wilson loop along the closed ribbons, instead of the full loop holonomy. While with the holonomy basis we describe holonomies only around a fundamental set of $(p-1)$ cycles, the subindex j of the fusion basis $\psi_{\mathfrak{f}}[\{\rho_j=(C_j,R_j)\},\{N_k=(n_k,b_k)\}]$ runs over $(2p-3)$ values and we have as many (not completely independent)[29] closed ribbon operators.

In addition to the holonomy information, the closed ribbon operators $\mathcal{K}_j[C_j,R_j]$ encode flux observables within the labels $\{R_j\}$. More precisely, these are integrated fluxes associated to a closed path. Note that in the almost gauge invariant phase space, discussed in the previous section, we only had fluxes associated to open paths,[30] provided we assume that the graph does not include loops (i.e. links with the same source and target node).

Another way to talk about the $\{R_j\}$ labels is to say that they measure torsion (electric charge). Indeed, if we assume a gauge invariant state we immediately find (see sec. 4.4.5) that R_j is equal to the trivial representations for those ribbons $\mathcal{K}_j[C_j,R_j]$ that go directly around the punctures. Notice that there are exactly p of such punctures. But for non-abelian groups, we can well have non-trivial

[29] The closed charge ribbon operators result *not* being completely independent, since their possible results are restricted by the coupling rules. E.g. for an abelian theory, all the coarser closed ribbon operators are determined by the finest closed ribbons around $p-1$ punctures.

[30] Before coarse-graining one can obtain fluxes associated to closed paths by combining the open paths fluxes and by using the Gauß constraints to reconstruct the fluxes associated to the tree links. The Gauß constraints are however not anymore valid for 'coarse-grained' nodes.

labels R_j for the remaining $(p-3)$ closed ribbons. These observables are crucial to keep track of how the Gauß constraint gets deformed under coarse-graining.

As explained in sec. 4.4.5, a basis for fully gauge invariant states satisfying the Gauß constraints at all punctures can be obtained from the fusion basis $\psi_{\mathfrak{f}}[\{\rho_j\},\{N_k\}]$ by setting the appropriate indices R_k equal to the trivial representation, denoted by 0. Furthermore, we also sum over the $\{b_k\}$ labels

$$\psi_{\mathfrak{f}}^{\text{g.i.}}[\{(C_m,R_j)\},\{C_k\}] \;=\; \left(\prod_k \frac{1}{\sqrt{|Q_{C_k}|}}\right) \sum_{\{b_k\}} \psi_{\mathfrak{f}}[\{(C_m,R_m)\},\{C_k,0\};\{b_k,0\}]. \tag{4.111}$$

In this formula, we have split the index j running over the edges of the fusion tree into two sets k and m, labelling the punctures (or leaves of the fusion tree) and the remaining edges of the fusion tree, respectively. Note that if one allows for states violating the Gauß constraints at the punctures, the $\{N_k\}$ labels encode only local information, and are measured by projective operators given by gluing cylinder fusion basis states $\psi_{\mathfrak{f}}^{\mathbb{I}}[\rho,N,N]$. The closed ribbon operators $\mathcal{K}_j[C_j,R_j]$ and the operation of gluing the cylinder fusion basis states give together a maximal commuting set of observables characterizing the fusion basis. Coarse-graining in the fusion basis means that these observables determine the splitting into coarser and finer ones.

In addition, there are conjugated observables, given by open ribbon operators extending from one puncture to another puncture. We leave it to future research to find a complete set of such independent operators. The coarse-graining scheme based on the fusion basis will also induce a splitting of the conjugated observables into a coarser and a finer set. To deduce this splitting one needs to study in more detail the commutation relations or the corresponding symplectic structure in phase space.

The coarse-graining is now given by summing over the finer variables, just as usual. Consider a density matrix defined using a fusion basis by

$$\mathfrak{D} \;=\; \sum_{\{\rho\},\{N\}} \sum_{\{\tilde\rho\},\{\tilde N\}} \mathfrak{d}\Big[\{\rho\},\{N\};\{\tilde\rho\},\{\tilde N\}\Big] \;\Big|\psi_{\mathfrak{f}}[\{\rho\},\{N\}]\Big\rangle\Big\langle\psi_{\mathfrak{f}}[\{\tilde\rho\},\{\tilde N\}\Big|\,. \tag{4.112}$$

This density matrix is adapted to the intended coarse-graining (or fusion) of punctures into new 'larger' punctures. That is the p punctures are partitioned into $p' \leq \frac{1}{2}p$ sets, each including at least two punctures. The fusion tree needs then to include a subtree for each set that describes the fusion of the punctures in this set. We label the variables attached to the subtrees with a super-index f, except for the pairs $(C_s,R_s)_{s=1}^{p'}$, which prescribe the excitations for the fused punctures. We label these pairs and the remaining variables with a super-index c.

Working in the polarization given by the fusion basis variables, the coarser density matrix is then defined by

$$\mathfrak{d}^c\Big[\{\rho^c\},\{\tilde\rho^c\}\Big] \;=\; \sum_{\{\rho^f\},\{N^f\}} \mathfrak{d}\Big[\{\rho^c\},\{\rho^f\},\{N^f\};\{\tilde\rho^c\},\{\rho^f\},\{N^f\}\Big]\,. \tag{4.113}$$

In this scheme we get rid of all indices N_k, assuming that these are all classified as finer information. An alternative scheme introduces new indices $N^c_{k'}$ for the coarser punctures. This scheme is based on an extension of the Hilbert space (before coarse-graining).

4.7 Concluding remarks

In this work we introduced the fusion basis for (2+1)-dimensional lattice gauge theories, in particular with non-abelian structure groups. The basis is well adapted for the weak coupling regime and for

describing topological BF theory with defects. The latter theory can also be taken as a description of (2+1)d gravity coupled to (possibly spinning) point particles.

In contrast to the spin network basis [16], the fusion basis is a multi-scale basis. It diagonalizes the traces of a certain multi-scale set of Wilson loop observables. This set does in itself not form a maximal set of commuting observables: For non-abelian gauge groups, one has rather to add further gauge-invariant observables describing electric excitations. Importantly, the electric (or torsion, in a gravitational context) excitation might emerge on larger scale even for gauge invariant states. This fact make it hard to control large scales in a spin network basis. For this reason, the fusion basis is ideally suited for coarse-graining in lattice gauge theories and loop quantum gravity [18, 19, 23, 60, 65, 100, 101, 108–110].

More specifically, we have seen that the fusion basis comes with a number of advantages: The fusion basis incorporates the notion of basic excitations and their fusion to coarse-grained excitations, hence making explicit the quasi-local structure of the excitations relative to the BF vacuum. It makes transparent the Drinfel'd double algebra structure, which in past (loop quantum gravity) discussions was rather hidden in the algebra of constraints [104, 105]. It incorporates a notion of cutting and gluing pieces of spatial manifolds along boundaries and thus comes automatically with a natural notion of local subsystems (see e.g. [122] for a different notion).

Moreover, in the context of (2+1)d loop quantum gravity coupled to point particles, the fusion basis provides naturally and directly the physical states of the theory, even for states including spinning particles (i.e. states with torsion), and diagonalizes the gauge and diffeomorphism invariant (Dirac) observables of the theory, which are given in terms of the closed ribbon operators. This shows that the fusion basis is a convenient tool for describing the coupling of multiple particles to $(2+1)$ dimensional gravity. It would be of particular interest to consider a thermodynamic or continuum limit, possibly resulting in gravity coupled to a matter field, see also [103]. A further question in this direction is whether the resulting system can be described by a matter field propagating on an effective non-commutative space-time, as derived in a covariant framework by [123].

The use of the fusion basis emphasizes the Drinfel'd algebra or quantum double structure of (2+1)d gravity coupled to point defects. This facilitates the comparison with other quantization schemes [124], such as the combinatorial quantization for Chern-Simons theory [125–127]. Let us also point out the recent work [128], which reformulates Kitaev models as a special case of combinatorial quantization via a reformulation of the latter in terms of a Hopf-algebra gauge theory.

Furthermore, in relation to coarse-graining, we emphasized that the fusion basis solves a deep problem related to coarse-graining in the spin network basis: In non-abelian gauge theories, coarse-graining generally leads to torsion degrees of freedom, even though these are not initially present, therefore the spin network basis cannot be stable under coarse-graining. The fusion basis, on the other hand, incorporates torsion degrees of freedom from the onset, hence allowing for a consistent coarse-graining scheme. Moreover, the fusion basis can be naturally used to design multi-scale states, in the sense that it diagonalizes a set of operators defined at all available scales (cf. e.g. [95]), a fact that makes it ideal for discussing coarse-graining schemes.

We hope to make all this explicit within a new tensor network coarse-graining framework, by generalizing the recently developed schemes of [61, 65]. One of our principal aims is studying the continuum limit and coarse-graining of spin-foam models. In the context of (2+1)-dimensional gravity models, a particularly intriguing question is how to flow via coarse-graining from models based on flat building blocks to models based curved building blocks, hence recovering in the quantum theory the classical result of [115, 116]. More specifically, for spin-foam models one expects a transition from $\mathrm{SU}(2)$ to the quantum deformed $\mathrm{SU}(2)_q$. This requires besides a condensation of curvature degrees of

freedom to a constant curvature state, also a condensation of torsion degrees of freedom. It is therefore important to have coarse-graining schemes which do not throw away the torsion degrees of freedom. Notice also that the fusion basis is already available for $\mathrm{SU}(2)_q$, with q root of unity, [34, 36] and has in some aspects even a simpler structure than in the finite group case. (Even more so, if one compares with SU(2), since the corresponding fusion category is not finite.) The finiteness of $\mathrm{SU}(2)_q$ makes this choice particularly attractive for numerical approaches to coarse-graining, see e.g. [63].

Finally recall that our study has been confined to lattice gauge theories with finite gauge groups. It is, however, an important point to generalize our analysis to Lie groups. For Lie groups there are two very different choices for the underlying topology of the state space and the related inner product. One possibility is to choose a discrete topology and measure on the gauge group, which is in fact necessary for the BF representation for *continuum* loop quantum gravity. In particular, this is needed for the BF vacuum to have a finite norm [86]. Alternatively, if one is only interested in lattice gauge theory with a fixed lattice or with a fixed number of excitations (i.e. of punctures), one can also adopt the usual (continuous) Haar measure on the gauge group. Drinfel'd double representations and their tensor product, based on this choice, have been discussed in the case of SU(2) in [88, 89, 129].

Chapter 5

Entanglement entropy for lattice gauge theories

As explained in the introduction, the non-locality of the observables inherent to lattice gauge theory prevents the factorization of the Hilbert space which is an obstruction to the computation of the entanglement entropy between two spacetime regions. Several approaches are available and, in this chapter, we employ the inherent hierarchal structure of the fusion basis, whose usefulness was demonstrated in the previous chapter in the context of the coarse-graining of lattice gauge theories, to encode a new notion of subsystems for lattice gauge theories and (2+1)d gravity coupled to point particles. This notion of subsystems can in turn be exploited to provide a notion of entanglement entropy.

The ambiguity in the notion of entanglement entropy for lattice gauge theories has been pointed out by Casini, Huerta and Rosabal (CHR) in [130] and discussed in a framework that focuses on the algebra of gauge invariant observables. This was fully developed only for abelian gauge theories in [130].[1]

In order to define a notion of entanglement entropy between two regions A and B in the algebraic framework one starts with the algebra $\mathcal{O}$ of (gauge invariant) observables and seeks to split this algebra into two mutually commuting subsets, associated to region A and B, respectively. The difficulty is, however, that due to the non-locality of gauge invariant observables, there is a set of observables that can be associated to both regions. This might be both due to (e.g. string like) observables crossing the boundary and due to observables being localized on the boundary. The ambiguity in the definition of entanglement entropy comes from a choice of a subset of such observables, which is *removed* from the observable algebra. The reduced algebra $\mathcal{O}_{\text{red}}$ features then (generically) a centre $\mathcal{Z}$, basically consisting of the observables conjugated to the removed ones. The resulting observable algebra should be such that the observables in the centre $\mathcal{Z}$ can be associated to the boundary, whereas the remaining observables $\mathcal{O}_{\text{red}}\backslash\mathcal{Z}$ can be associated to either region A or B.

The gauge-invariant Hilbert space that carries an (irreducible) representation of the algebra $\mathcal{O}$, will now feature superselection sectors with respect to $\mathcal{O}_{\text{red}}$: The common eigenspaces of the centre $\mathcal{Z}$ are left invariant by $\mathcal{O}_{\text{red}}$. At the same time, each eigenspace admits a factorization into Hilbert spaces associated to region A and B. The definition of entanglement entropy can be extended to

[1] The 'electric', as opposed to 'magnetic', prescription has been generalized to the non-abelian case by [131], and we will comment on this in sec. 5.2.2. In this work we will also generalize the 'magnetic' prescription, and show that it actually is not purely magnetic in the non-abelian case.

such cases with superselection sectors and thus provides the notion of entanglement entropy in this algebraic framework.

Furthermore, the superselection sectors label states with a definite choice of boundary conditions, that is with definite values for the observables in the centre $\mathcal{Z}$. The latter set is sometimes referred to as boundary observables, a viewpoint that is also reflected in the discussion of [122] on (classical) gauge systems with boundary. As we will argue in sec. 5.2, in the non-abelian case one can extend the set of gauge-invariant boundary observables by including non-gauge invariant frame information attached to the boundary.

The two most natural choices for boundary conditions in the abelian case consist in either fixing the electric fluxes on links transversal to the boundary, or the magnetic fluxes (Wilson loops) along the boundary. Correspondingly, CHR speak of an *electric* or *magnetic* choice of centre. This can also be matched to different ways of cutting the lattice into two parts, either *across* or *along* the links. We will show here that the generalization of the magnetic centre choice to the non-abelian case does also add an electric component to the centre, measuring the total electric flux through the boundary.[2] Note that, in the magnetic-centre case, no extended Hilbert space procedure was known. As recalled in the introduction, this other approach relies on an embedding of the Hilbert into an *extended* Hilbert space where gauge invariance violations are allowed at the boundary. Our proposal fills this gap in the abelian case and also provides the generalization to the non-abelian one.

What might appear surprising is the striking discrepancy in the behaviour of the entanglement entropy with respect to different choices of boundary conditions. This happens even when the entropies are calculated for the same state and on the same geometry. The authors of [130] argue that all these ambiguities disappear in the continuum limit, once only well-defined quantities such as relative entropies are considered. Let us, however, point out that—in a continuum limit appropriate to describe states of a topological field theory with defect excitations—the different procedures even yield finite or divergent results, respectively.

This brings us to the philosophy pursued here: We will focus our attention not so much on the lattice and how it is separated into two distinguished regions, but on the excitation content of the theory under consideration. Importantly the very notion of excitation depends on a choice of vacuum state. These are the two choices of totally squeezed vacua encountered before, namely the Ashtekar-Lewandowski (AL) [67, 68, 133] and BF vacua [22, 86, 96] that are related to the strong and weak coupling regime of lattice gauge theory, respectively.

Using such vacua, one can interpret states on a finite lattice as states with a finite number of excitations in a continuum theory. This is done by basically putting all degrees of freedom, finer than the lattice scale, into the chosen vacuum [110]. In this picture, the choice of boundary conditions specifying a notion of entanglement entropy should be adjusted to the choice of vacuum. For states that have almost everywhere vanishing electrical field we should choose electric boundary conditions. Considering states that have almost everywhere vanishing magnetic flux—or in the gravitational language have almost everywhere vanishing curvature—we should choose instead the magnetic centre. These choices are designed to give finite results in the continuum limit, whose result is by construction already fully captured at the level of a finite (fine enough) lattice.

Furthermore, our definition of excitations is rooted in the analysis of the properties that regions with boundaries manifest under gluing. In fact, we will also argue that the process of cutting a system in two and the related definition of an extended Hilbert space procedure should be understood as dual

[2] This observable is vanishing in the abelian case due to the Gauß constraints. In non-abelian gauge theories one might get 'effective' electric charges on larger scales without having an electric charge at the lattice scale. Such charges were called 'Cheshire charges' in [132].

to gluing. This brings into play techniques of extended topological field theory, *i.e.* topological field theory for manifolds with boundaries. Moreover, we already know that the choice of the BF vacuum will naturally lead us to consider the fusion basis which will allow to operationally specify regions by their excitation content. In this way we overcome the problems arising from defining a region independently of its content (something that would be in stark contrast with background independence), and we do so in a way that makes such a definition independent of the chosen regularizing lattice, thus directly avoiding the need of specifying the way we split it.

This proposal comes to full fruition in (2+1)d gravity where regions will now be specified by the point particles they contain. In this sense, our notion of entanglement theory characterizes the correlations between the excitation content of the different regions.

5.1 Gluing, splitting and extended Hilbert spaces

To define the entanglement entropy of a subregion, one first needs to specify how to associate the theory's degrees of freedom to it. In gauge theories, having to consider non-local gauge-invariant degrees of freedom leads to ambiguities.

The gauge-invariance condition manifests itself in terms of constraints, *i.e.* quantum versions of the elliptic equations a state must satisfy to represent valid initial data. In lattice gauge theories, this leads to Gauß constraints defined at the lattice nodes. The Gauß constraint at the node n involves all the links adjacent to it, links which carry gauge co-variant degrees of freedoms expressed in terms of parallel transports (holonomies) along open paths. As a consequence, a gauge-invariant wave function necessarily correlates the degrees of freedom across the links.

In turn, this prevents the splitting of the Hilbert space of gauge-invariant functions $\mathcal{H}$ into a tensor product $\mathcal{H}_A \otimes \mathcal{H}_B$, with the two factors associated to two complementary regions. The so-called extended Hilbert space procedure [30, 31] avoids this task, by considering an extended Hilbert space $\mathcal{H}_{\text{ext}}$, in which the Gauß constraints are relaxed along the boundary interface between the two regions. More precisely, this interface is defined to be transversal to the links of the lattice, and a two-valent node is introduced on each link cut by it. The Gauß constraints are then relaxed for these two-valent nodes only. This defines an extended Hilbert space, which does factorize $\mathcal{H}_{\text{ext}} = \mathcal{H}_A \otimes \mathcal{H}_B$ in a straightforward manner.

In this work, we show that the extended Hilbert space procedure can be generalized using a different set-up and also different sets of constraints. This generalized procedure is deeply connected to the theory of extended topological field theories presented in the previous chapters. There, indeed, one considered topological field theories on manifolds with boundaries[3] together with a procedure for gluing them to one-another. Splitting a manifold into two components thus arises as an inverse procedure. In the following, we describe the main idea and start with recalling briefly the notion of gluing states, defined on spatial manifolds with boundary. Dual to this gluing one can define a splitting procedure and the notion of extended Hilbert spaces.

[3] Here we are working in a Hamiltonian framework, therefore 'boundaries' have to be understood as codimension 2 surface, which-in a covariant context-are usually called *corners*.

5.1.1 Gluing

The gluing procedure considered here is a formal generalization of the one prescribed in the previous chapters to reveal the Drinfel'd double structure. To be concrete, we consider a theory where the (gauge co-variant) degrees of freedom are associated to the links of a graph Γ, as is the case in lattice gauge theories, where one has group elements g_l associated to the links l of Γ.

Let Γ_A and Γ_B be two graphs embedded into the hypersurfaces, Σ_A and Σ_B, respectively. We assume both Σ_A and Σ_B have boundaries and that the embedded graphs end at the boundaries by one or several open edges. The (gauge-covariant) wave functions defined on Γ_A and Γ_B, respectively, live in the kinematical Hilbert spaces $\mathcal{H}^{\text{kin}}_{\Gamma_A}$ and $\mathcal{H}^{\text{kin}}_{\Gamma_B}$. Let then $\{\mathscr{C}\}_A$ be a set of constraints that we require to be quasi-local, *i.e.* local *e.g.* with respect to the graph's nodes and faces and their adjacent structures, and $\mathcal{H}_A$ the subspace of wave functions in the Hilbert space $\mathcal{H}^{\text{kin}}_A$ which satisfies these constraints.[4] Likewise for $\{\mathscr{C}\}_B$. To every constraint $\mathscr{C}$, we assign a projector $\mathbb{P}_{\mathscr{C}}$ which projects onto the subspace of wave functions ψ satisfying the constraint: $\mathscr{C}\psi = 0$. One such constraint is the Gauß constraint, which acts only at the internal nodes of the graph imposing gauge invariance.

At the level of the surfaces, the gluing between Σ_A and Σ_B is obtained by identifying a portion of their boundaries. We denote the result of this operation $\Sigma_{A\cup B}$. At the level of the embedded graphs, it is analogously defined by connecting the links along which the gluing is performed. We denote the result $\Gamma_{A\cup B}$. Here we assume that the links ending at the two boundaries match under the gluing procedure.[5]

Given two wave functions $\psi_A \in \mathcal{H}_A$ and $\psi_B \in \mathcal{H}_B$, consider first the (usual $\mathbb{C}$-)product of wave functions $\psi_A \cdot \phi_B \equiv \mathfrak{G}(\psi_A, \psi_B)$, defined on the glued graph $\Gamma_{A\cup B}$. In general, this product wave function will *not* satisfy all the constraints $\{\mathscr{C}\}_{A\cup B}$, which will include $\{\mathscr{C}\}_A$ and $\{\mathscr{C}\}_B$ but also further constraints that result from the presence of new internal nodes and faces in $\Gamma_{A\cup B}$. Nevertheless, the set of wave functions of the form $\psi_A \cdot \psi_B$ will span the extended Hilbert space $\mathcal{H}_{\Gamma_A} \otimes \mathcal{H}_{\Gamma_B} =: \mathcal{H}_{\text{ext}}$, and hence the subspace $\mathcal{H}_{\Gamma_{A\cup B}}$ can be identified with the set of subspace of wave functions which satisfy all the constraints $\{\mathscr{C}\}_{A\cup B}$. Denoting the corresponding projector by $\mathbb{P}_{A\cup B}$ we finally define the star product as

$$\begin{array}{rccccc} \star: & \mathcal{H}_{\Gamma_A} \otimes \mathcal{H}_{\Gamma_B} & \xrightarrow{\mathfrak{G}} & \mathcal{H}_{\text{ext}} & \xrightarrow{\mathbb{A}\circ\mathbb{B}} & \mathcal{H}_{\Gamma_{A\cup B}/\sim} \\ & (\psi_A, \psi_B) & \longmapsto & \mathfrak{G}(\psi_A, \psi_B) & \longmapsto & \mathbb{P}_{A\cup B} \triangleright \mathfrak{G}(\psi_A, \psi_B) \end{array} \tag{5.1}$$

In the following we will denote for brevity, $C = A \cup B$. In the case where $\mathbb{P} = \mathbb{A} \circ \mathbb{B}$, we recover the gluing procedure defined earlier.

5.1.2 Splitting

Splitting is the 'inverse' operation of gluing. Given a surface Σ_C and embedded graph Γ_C we firstly have to introduce a boundary that splits Σ_C into Σ_A and Σ_B, and Γ_C into Γ_A and Γ_B, so that the gluing gives back the corresponding structures. (One might want to choose certain restrictions on which kinds of boundaries and graphs are allowed.)

To define the splitting of a wave function in $\mathcal{H}_C$ we are looking for an isometric embedding map

$$\mathcal{E} : \mathcal{H}_C \to \mathcal{H}_{\text{ext}} \simeq \mathcal{H}_A \otimes \mathcal{H}_B \,, \tag{5.2}$$

[4] Here we make the simplifying assumptions that the set of solutions to the constraints can inherit the inner product of $\mathcal{H}^{\text{kin}}_A$. This happens if zero is in the discrete spectrum of the constraints. If this is not the case a new inner product needs to be constructed, see *e.g.* [134–137], and the following procedure needs to be amended accordingly.

[5] This can be ensured by introducing marked points on the boundaries where the links are allowed to end.

such that $\star \circ \mathcal{E} = \mathrm{id}$ on $\mathcal{H}_C$. Note that this latter condition does not specify $\mathcal{E}$ uniquely, but we can demand that $\mathcal{E}$ maps $\mathcal{H}_C$ into $\mathcal{H}_C$ understood as a subspace of $\mathcal{H}_{\mathrm{ext}}$.[6] (Remember that $\mathcal{H}_C$ can be identified with the set of wave functions in $\mathcal{H}_{\mathrm{ext}}$ satisfying all the constraints $\{\mathscr{C}\}_C$.)

The embedding $\mathcal{E}$, therefore, maps wave functions in $\mathcal{H}_C$, which does not allow a straightforward splitting, into an extended Hilbert space $\mathcal{H}_{\mathrm{ext}} \simeq \mathcal{H}_{\Gamma_A} \otimes \mathcal{H}_{\Gamma_B}$, which comes with a natural tensor factorization associated to the splitting of Γ_C into Γ_A and Γ_B. Hence, to integrate out the degrees of freedom associated *e.g.* to Γ_B, one first uses the embedding, and then traces over $\mathcal{H}_{\Gamma_B}$.

5.1.3 Flatness constraint

We have already mentioned the Gauß constraint of gauge theories. However, for our proposal, the introduction of another constraint will be relevant. This is the flatness constraint, which acts at the faces of the graph and demands that these have a trivial holonomy,[7] *i.e.* a trivial magnetic flux through them. Again, we will have closed faces, necessarily internal to Σ, and open faces as well, necessarily including boundary components. We will demand the flatness constraints to hold for closed faces only.

At this point, the reader might wonder why we are interested in the flatness constraints. Firstly, we can allow for curvature by introducing punctures, that is by removing disks from Σ and thus introducing boundaries around which the flatness constraint does not need to hold. Introducing sufficiently many punctures we can regain all curvature degrees of freedom. Therefore, our procedure is not over-restrictive. On the other hand, the introduction of flatness constraints allows to achieve a certain independence from the lattice by putting the focus rather on the punctures themselves, which provide the support for the excitations. Secondly, with regard to the gluing and extension process, the flatness constraints allow us to trade all Gauß constraint violations, appearing in the extended Hilbert space as defined in [30, 31], for one flatness and Gauß constraint violation. The reason is that with the flatness constraints holding almost everywhere (except at the punctures) we can change the graph and its embedding without changing the physical content of the wave functions. Hence, in this way we can change the number of links crossing the boundary to just one link. In other words, the many local reference frames defined by the cut links are replaced by a global reference frame together with demanding a locally flat connection near the boundary. We will later see that this allows to define the (generalization of the) 'magnetic centre' choice [130] in terms of an extended Hilbert space procedure. Naturally, by proceeding like so, we are implicitly working in the BF representation presented in the previous chapter.

5.2 Entanglement entropy

We reviewed the issues arising when attempting the splitting of a Hilbert space $\mathcal{H}_C$ of wave functions satisfying a set of constraints $\{\mathscr{C}\}_C$ into a tensor product. Such a splitting can be performed by embedding the states in an extended Hilbert space $\mathcal{H}_{\mathrm{ext}} \simeq \mathcal{H}_A \otimes \mathcal{H}_B$ for which some constraints are relaxed. This is described by an embedding map $\mathcal{E} : \mathcal{H}_C \to \mathcal{H}_{\mathrm{ext}}$.

[6] In the case where we only take into account the Gauß constraint, this embedding map can also be expressed in terms of the fusion tensor product introduced in the first chapter. Indeed, given a link l whose Hilbert space is obtained as the fusion tensor product of two half-link Hilbert spaces, the embedding map reads

$$\mathcal{E} : \mathcal{H}_l \simeq \mathcal{H}_{l_L} \boxtimes_{\mathrm{SU}(2)} \mathcal{H}_{l_R} \longrightarrow \mathcal{H}_l^{\mathrm{ext}} \simeq \mathcal{H}_{l_L} \otimes \mathcal{H}_{l_R} \,. \tag{5.3}$$

[7] That is $g_{l_N} \cdots g_{l_1} = \mathbb{1}$ with $\mathbb{1}$ denoting the group unit and the group elements following clockwise or anti-clockwise order along the boundary of the face.

With a choice of embedding map at hand, we can define a notion of entanglement entropy for states in $\mathcal{H}_C$. To do so, we first use the map $\mathcal{E}$ to embed a given state $\psi \in \mathcal{H}_C$ into $\mathcal{H}_{\text{ext}} \simeq \mathcal{H}_A \otimes \mathcal{H}_B$. We then define the reduced density matrix

$$\mathfrak{D}^A_\psi = \text{tr}_B\big(\mathcal{E}(\psi)\overline{\mathcal{E}(\psi)}\big)\,, \tag{5.4}$$

from which the entanglement entropy can be readily evaluated

$$S_A(\psi) \;:=\; S_A(\mathcal{E}(\psi)) \;=\; -\text{tr}_A(\mathfrak{D}^A_\psi \ln \mathfrak{D}^A_\psi)\,. \tag{5.5}$$

Notice that both $\mathfrak{D}^A$ and S_A implicitly depend on $\mathcal{E}$.

In [28, 30, 31], a definition of entanglement entropy was proposed for both abelian and non-abelian gauge theories by Donnelly. His procedure was the type we just described—often referred to as the *extended Hilbert space* method—and made implicit use of a specific embedding map. In [130], CHR pointed out that (at least in the abelian case) Donnelly's procedure agrees with their *electric centre* prescription, but it was just one among other choices.

Here, we want to emphasize that, by choosing embedding maps different from Donnelly's, the extended Hilbert space construction can be generalized and is therefore not unique. In particular, the alternative procedure proposed here does reproduce CHR's *magnetic centre* prescription. This at least for abelian gauge theories, since we will see that the non-abelian case necessarily includes also an electric component. Hence, in so doing, we provide a tighter connection between CHR's algebraic constructions and the extended Hilbert space procedure. Moreover, by explicitly providing an extended Hilbert space procedure matching the *magnetic* centre prescription, we correct claims about its impossibility which have appeared in the literature [138].

In the rest of this section, we describe in detail the contributions to the entanglement entropy, as defined by the extended Hilbert space procedure, along the lines of Donnelly [31]. While his analysis was based on a specific embedding procedure (corresponding to a choice of spin network basis for the Hilbert spaces involved), we will instead allow for generic embeddings and associated choices of basis. With this toolbox at hand, we will relate the extended Hilbert space procedure to CHR's observable-algebra-based definition [130]. It is left to the forthcoming sections, the task of introducing the details of the fusion basis for (2+1)-dimensional lattice gauge theories [4], needed to parallel the magnetic centre choice, and the study of the corresponding embedding procedure and entanglement entropy.

5.2.1 Entanglement entropy from extended Hilbert spaces

Both the spin network basis and the fusion basis are indexed by representation labels, which we here will denote generically by ρ. Notice, however, that these are representations for different algebraic structures, namely for the group $\mathcal{G}$ and its Drinfel'd double $\mathcal{D}(\mathcal{G})$, respectively. As usual for basis-state labels, the ρ's encode the eigenvalues of a maximal set of commuting observables on the Hilbert space $\mathcal{H}_C$. This hints already at the connection to CHR's observable-algebra-based procedure as well as to more general choices of maximal sets of commuting observables.

We split the representation labels into three sets: $\{\rho_A\}$ associated to region A, $\{\rho_B\}$ associated to region B, and $\{\rho_\partial\}$ associated to the boundary $\partial A = \partial B$. In the case of the fusion basis we will just have one ρ_∂ associated to the boundary. Also, in case we allow torsion excitation at the punctures—that is violations of gauge invariance there—we have representation space indices M, N associated with these punctures. These can be associated either to region A or B and we therefore subsume them into the set of representation indices $\{\rho_A\}$ and $\{\rho_B\}$, respectively.

In the extended Hilbert space $\mathcal{H}_{\text{ext}} = \mathcal{H}_A \otimes \mathcal{H}_B$ we will have a basis that includes a doubling of the $\{\rho_\partial\}$ labels to $\{\rho_{\partial A}\}$ and $\{\rho_{\partial B}\}$. Furthermore, for each of these label sets, we have associated sets of representation-space labels[8] $\{N_{\partial A}\}$ and $\{N_{\partial B}\}$.

Denote $|\rho_A, \rho_B, \rho_\partial\rangle$ and $|\rho_A, \rho_{\partial A}, N_{\partial A}\rangle \otimes |\rho_B, \rho_{\partial B}, N_{\partial B}\rangle$ elements of an orthonormal basis of $\mathcal{H}_C$ and $\mathcal{H}_A \otimes \mathcal{H}_B$, respectively. The embedding map $\mathcal{E}$ is then given by[9]

$$\mathcal{E}\,|\rho_A, \rho_B, \rho_\partial\rangle = \frac{1}{\prod_\partial \sqrt{\dim(\rho_\partial)}} \sum_{N_\partial} |\rho_A, \rho_\partial, N_\partial\rangle \otimes |\rho_B, \rho_\partial, N_\partial\rangle \ . \tag{5.6}$$

Given a state

$$|\psi\rangle = \psi(\{\rho\})\,|\rho_A, \rho_B, \rho_\partial\rangle \ \in \ \mathcal{H}_C \ , \tag{5.7}$$

the corresponding density matrix $\mathfrak{D}^A_\psi$, defined in (5.4), has the following structure:

$$\mathfrak{D}^A_\psi = \bigoplus_{\rho_\partial} P(\rho_\partial) \left[\frac{|\rho_\partial, N_\partial\rangle\langle\rho_\partial, N_\partial|}{\prod_\partial \dim(\partial\rho)} \ \otimes \mathfrak{D}^A_\psi(\rho_\partial) \right] \ . \tag{5.8}$$

We see that $\mathfrak{D}^A$ is block diagonal, with each block labeled by a boundary-representation vector $|\rho_{\partial A} = \rho_\partial, N_{\partial A} = N_\partial\rangle$, and weighted by the probability distribution

$$P(\rho_\partial) = \sum_{\rho_A, \rho_B} \psi(\{\rho\})\overline{\psi(\{\rho\})} \ . \tag{5.9}$$

This distribution is constant over the N_∂ as a consequence of gauge invariance. On the other hand, the density matrix associated to each block (independent of N_∂) is

$$\mathfrak{D}^A_\psi(\rho_\partial) = \sum_{\rho_A, \tilde{\rho}_A, \rho_B} \frac{1}{P(\rho_\partial)} \psi(\rho_A, \rho_B, \rho_\partial)\overline{\psi(\tilde{\rho}_A, \rho_B, \rho_\partial)}\ |\rho_A\rangle\langle\tilde{\rho}_A| \ . \tag{5.10}$$

Now, given this decomposition, one finds that the entanglement entropy (5.5) has three contributions [30]

$$S_A \ = \ H(P(\rho_\partial)) \ + \ \sum_\partial \langle \ln \dim \rho_\partial \rangle \ + \ \langle S_A(\mathfrak{D}^A(\rho_\partial)) \rangle \ , \tag{5.11}$$

where $\langle \bullet \rangle$ stands for the expectation value with respect to the classical probability distribution $P(\rho_\partial)$, and $H(P(\rho_\partial))$ for its Shannon entropy,

$$H(P(\rho_\partial)) \ = \ -\sum_{\rho_\partial} P(\rho_\partial) \ \ln P(\rho_\partial) \ . \tag{5.12}$$

5.2.2 Relation to observable-algebra-based entanglement entropy

We now comment on the relation between this approach and the definition of entanglement entropy via the splitting of the observable algebra. CHR's original proposal [130] concerned only abelian gauge theories. We will comment below on the non-abelian generalizations.

[8] By this we mean the following. Call V_ρ the vector space supporting the representation ρ, then N labels the elements of a basis of V_ρ.

[9] The product is over the boundary elements. In the case of the fusion basis we will have only one boundary element and index ρ_∂. In the case of the spin network basis any edge cut by the boundary is a boundary element.

Given the algebra of observables $\mathcal{O}$, associated to the gauge-invariant Hilbert space $\mathcal{H}_C$, one chooses a commuting subalgebra of observable $\mathcal{Z}$, associated to the boundary $\partial A = \partial B$. This commuting subset $\mathcal{Z}$ of observables serves as centre of a new, reduced, observable algebra $\mathcal{O}_{\text{red}}$, which is obtained by removing all the observables, which do not commute with the designated centre $\mathcal{Z}$. The choice of $\mathcal{Z}$ must be done in such a way that $\mathcal{O}_{\text{red}}$ admits a splitting $\mathcal{O}_{\text{red}} = \mathcal{O}_A \cup \mathcal{O}_B$ into two mutually commuting subalgebras, which can be associated to the regions A and B, respectively. These subalgebras clearly have a non-vanishing intersection given by the centre, $\mathcal{O}_A \cap \mathcal{O}_B = \mathcal{Z}$.

Now, $\mathcal{H}_C$ (usually) provides an irreducible representation of the observable algebra $\mathcal{O}$. By removing observables from $\mathcal{O}$, one finds that the reduced algebra $\mathcal{O}_{\text{red}}$ features superselection sectors on $\mathcal{H}_C$. These superselection sectors are precisely labeled by the eigenvalues $\{\lambda\}_{\mathcal{Z}}$ for the observables in $\mathcal{Z}$. This is because the original Hilbert space has by construction the structure

$$\mathcal{H}_C = \bigoplus_{\{\lambda\}} \mathcal{H}_C^{\{\lambda\}} = \bigoplus_{\{\lambda\}} \mathcal{H}_A^{\{\lambda\}} \otimes \mathcal{H}_B^{\{\lambda\}} , \tag{5.13}$$

where each superselection sector $\mathcal{H}_C^{\{\lambda\}}$ can be readily factorized into $\mathcal{H}_A^{\{\lambda\}} \otimes \mathcal{H}_B^{\{\lambda\}}$. Clearly, $\mathcal{H}_A^{\{\lambda\}}$ ($\mathcal{H}_B^{\{\lambda\}}$) carries a representation of the algebra $\mathcal{O}_A$ ($\mathcal{O}_B$, respectively), with elements in $\mathcal{Z}$ acting trivially as multiples of the identity operator.

The observables in $\mathcal{Z}$ can be also understood as boundary conditions, characterizing each of the superselection sectors. This interpretation physically explains the 'classical' behaviour of these observables noticed by CHR. See also the discussion in [139].

At the beginning of this section, we introduced the basis $|\rho_A, \rho_B, \rho_\partial\rangle$ for $\mathcal{H}_C$. This basis immediately suggests one to choose the centre $\mathcal{Z}$ to be generated by the projectors $\mathbb{P}_{\rho_\partial}$ onto the subspaces spanned by the $|\rho_A, \rho_B, \rho_\partial\rangle$ with varying ρ_A, ρ_B but fixed ρ_∂. This is equivalent to requiring the eigenvalues $\{\lambda\}_{\mathcal{Z}}$ to be directly determined by the labels $\rho_\partial \equiv \{\rho_\partial\}_{\mathcal{Z}}$. Henceforth, with this choice in mind, we will replace the superindex $\{\lambda\}$ by ρ_∂.

The definition of entanglement entropy via the specification of a centre by CHR [130] did originally concern only the abelian case. It can also be generalized to the non-abelian case, albeit in two different manners. One choice corresponds to staying withing the algebraic framework based on gauge-invariant observables alone [131]. In this case one forms density matrices with a superselection structure as given by (5.13)

$$\mathfrak{D} = \bigoplus_{\rho_\partial} P(\rho_\partial)\, \mathfrak{D}(\rho_\partial) . \tag{5.14}$$

Factorizing each sector $\mathcal{H}^{\rho_\partial}$ into $\mathcal{H}_A^{\rho_\partial} \otimes \mathcal{H}_B^{\rho_\partial}$ one can compute the entanglement entropy $S_A(\mathfrak{D}^A(\rho_\partial))$ for each sector separately. The entanglement entropy for the entire system is then defined as

$$S_A := H(P(\rho_\partial)) + \langle S_A(\mathfrak{D}(\rho_\partial))\rangle, \tag{5.15}$$

where again $\langle\bullet\rangle$ stands for the averaging with respect to $P(\rho_\partial)$.

We see that this result does not completely reproduce the extended Hilbert space procedure (5.11), as in (5.15) we do not have the term $\langle \ln \dim \rho_\partial \rangle$ appearing (this term trivially vanishes for the abelian case). The source of the discrepancy is the following. In the extended Hilbert space procedure, the density matrices resulting from the embedding map $\mathcal{E}$, have also a superselection structure. But this superselection structure is more refined: additional subsectors appear that are related to the internal indices of the representation $N_\partial := N_{\partial A} = N_{\partial B}$. Consequently, the density matrices resulting form

the embedding procedure are *effectively* characterized by the following probability distribution

$$P(\rho_\partial, I_\partial) = \frac{P(\rho_\partial)}{\prod_\partial \dim \rho_\partial} \,, \tag{5.16}$$

and block density matrices

$$\mathfrak{D}^A(\rho_\partial, I_\partial) \;=\; \frac{\mathfrak{D}^A(\rho_\partial)}{\prod_\partial \dim \rho_\partial} \,. \tag{5.17}$$

The entanglement entropy for density matrices with such a superselection structure is given by

$$\begin{aligned} S_A &= H(P(\rho_\partial, N_\partial)) \;+\; \langle S_A(\mathfrak{D}^A(\rho_\partial, N_\partial))\rangle_{P(\rho_\partial, N_\partial)} \\ &= H(P(\rho_\partial)) \;+\; \sum_\partial \langle \ln \dim \rho_\partial \rangle_{P(\rho_\partial)} \;+\; \langle S_A(\mathfrak{D}^A(\rho_\partial))\rangle_{P(\rho_\partial)} \end{aligned} \tag{5.18}$$

where here $\langle \bullet \rangle_{P(\rho_\partial, N_\partial)}$ denotes averaging with respect to $P(\rho_\partial, N_\partial)$ and $\langle \bullet \rangle_{P(\rho_\partial)}$ averaging with respect to $P(\rho_\partial)$. This definition reproduces the splitting into three terms as in (5.11).

This second choice of superselection structure, which includes the magnetic indices N_∂, is not tied to the initial gauge invariant observable algebra, as the magnetic indices only arise after cutting the manifold. One can, however, argue that cutting the manifold one introduces a boundary, and that the magnetic indices should be part of the boundary data together with the ρ_∂, characterizing (sectors of) wave functions defined on manifolds with boundary. In other words, one could argue that the splitting of a system into subsystem requires the introduction of additional information about the reference frames at the boundary, as encoded in the magnetic indices, which is needed to perform a consistent gluing.

Thus, the first two contributions to the entanglement entropy in (5.18) are resulting from the superselection structure and are thus due to the classical probability distribution (5.16). Indeed, it was conjectured by CHR and proven by [131, 140] that only the third contribtion in (5.18) gives the so-called distillable entropy, which is defined to be the maximum number of Bell pairs that can be extracted by a so-called entanglement distillation. The latter process involves a choice of (local) operator algebra, which in [131, 140] is based on the reduced operator algebra $\mathcal{O}_{\text{red}}$. Thus the notion of distillable entropy also depends on the choice of reduced operator algebra or alternatively boundary conditions.

From a physical standpoint, what all this discussion is reminding us is that the concept of entropy is coarse-graining, *i.e.* observer, dependent. By varying the amount of information we know, or conversely, we would like to know about a system, we calculate different entropies. This can be summarized in the statement, that entropy is an epistemological quantity. And in sophisticated enough situations, also the entanglement entropy is such.

As mentioned above, the extended Hilbert space procedure was first proposed using spin network functions [28–31]. Here the representation labels ρ_∂ characterize the eigenvalues of electric flux operators associated to the links that are cut by the boundary (for non-abelian gauge theories one can take Casimir operators formed from the electric fluxes associated to each such link, see [131]). Thus, in the corresponding algebraic definition the centre is formed by these electric operators. Below, we focus on the extended Hilbert space procedure for the fusion basis, where ρ_∂ characterizes a so-called closed-ribbon operator along the boundary between the two regions A and B. In the case of an abelian theory (and considering only gauge-invariant wave functions), this ribbon operator reduces to a Wilson loop. Thus, in this case, the centre is given by a *magnetic* operator. For non-abelian gauge theories,

however, the closed-ribbon operator measures also an electric excitation, related to the total flux of the electric field flowing out of the enclosed region. Note that this can be non-trivial even for completely gauge invariant wave functions. Thus, for non-abelian theories, the magnetic centre gets naturally enlarged by a further *electric* operator.

5.3 Fusion basis for lattice gauge theories with fixed lattice

In this section, we review the construction of the fusion basis for a (2+1)-dimensional lattice gauge system for finite groups. However, this time, we work with a fixed lattice. Therefore, we are not explicitly working in the BF representation. As such, this is closer to the usual formulation of lattice gauge theories. As before, we fix the topology of the underlying two-dimensional hypersurface to be a puncture 2-sphere.

This section essentially provides a more detailed construction of the fusion basis for a fixed lattice as sketched at the end of the previous chapter. The reader should therefore expect some overlap between this section and sec. 4.6.

5.3.1 Different viewpoints

Let Γ be a graph embedded into $\mathbb{S}_2$. Γ being planar, we can unambiguously identify its plaquettes or faces. The shift of point of view we propose relies on the assumption that Γ carries excitations located at the faces. As we will explain presently, these excitations have to be understood with respect to the BF vacuum.

First, we consider curvature excitations since they are naturally carried by the faces of Γ. Indeed, they are characterized by the amount of curvature carried by every face, defined as the trace of the holonomy surrounding the face. In the electromagnetic case these are precisely the magnetic fluxes.

Then, we consider torsion excitations, that is violations of the Gauß constraints. In the electromagnetic case these excitations correspond to the presence of non-vanishing electric charges. Being associated with a Gauß constraint violations, these excitations are *a priori* located at the nodes of Γ, and not at its faces as we desired. To obviate this problem, we introduce extra links and nodes. More precisely, we introduce one new link and one new node for each face. For a given face, this new link starts at some node on its boundary and ends at a new one-valent node placed in its interior. The valency of an internal node is strictly bigger than one. In the same spirit, we call the links adjacent to the end nodes *open links*. Fig. 5.1 depicts such a construction in the case of a lattice with square faces.

The result of this construction is an extended graph Γ' which leads to a new Hilbert space $\mathcal{H}_{\Gamma'}$ equipped with an inner product of the same form as the previous one, see (7.17). As we already know, allowing for torsion excitations is a necessity in the case of non-abelian gauge theories, even in the case we do not allow them at the lattice scale. We restrict our focus on the subspace of $\mathcal{H}_p$ constituted by wave functions which are gauge invariant at all internal nodes, but not at the end node, where p stands for the number of end-nodes in Γ'.

Note that the Hilbert space $\mathcal{H}_p$ is unitarily equivalent to the subspace of wave functions in $\mathcal{H}_\Gamma$ which are gauge invariant at all nodes where one does *not* attach an open link. In other words, we can map the torsion excitations from $\mathcal{H}_p$ to $\mathcal{H}_\Gamma$ by associating them with the nodes to which one attaches an open link. For the example of the lattice depicted in fig. 5.1, gauge invariance violations at almost all nodes can be taken into account in the Hilbert space $\mathcal{H}_p$. Furthermore, one can also generalize the

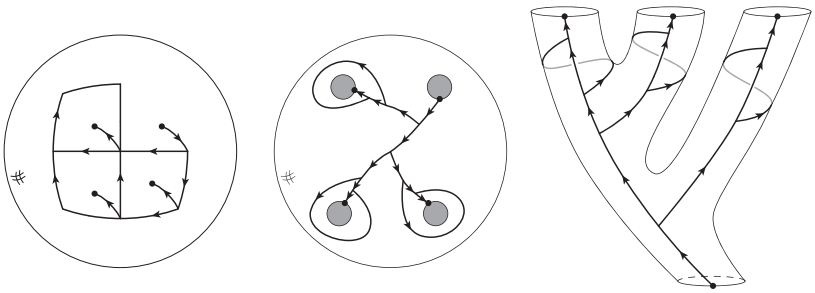

Figure 5.1. The left panel represents a lattice of three plaquettes embedded on a two-sphere by closing it with an outer plaquette. For every plaquette, including the outer one, an open edge going from the lattice to a marked point can carry torsion degrees of freedom. The middle panel represents an equivalent description where the plaquettes are replaced by punctures. The solid lines now represent a minimal graph embedded on the corresponding punctured sphere. The right panel finally proposes another graphical representation where the topology of the punctured sphere is deformed to obtain pairs of pants. This final representation is the preferential one for the construction of the fusion basis.

definition of $\mathcal{H}_p$, allowing more than one open link to end in a given face [4]. This allows to take into account all possible gauge invariance violations, starting from an arbitrary graph Γ.

The change of point of view we adopt here can be made more explicit by placing a puncture in the middle of each face. More precisely, instead of thinking of a lattice embedded in $\mathbb{S}_2$ and allow for some excitations, we can directly imagine a graph embedded onto a punctured sphere. In this case, we can map a lattice with p faces to a graph embedded on a p-punctured sphere. The face holonomy becomes the holonomy surrounding the puncture while the open edges now go from a node of the graph to one-valent node sitting at the puncture.

5.3.2 Holonomy basis for $\mathcal{H}_p$

We now construct a holonomy basis of the Hilbert space $\mathcal{H}_p$. As the name suggests, this basis is designed to diagonalize holonomy operators. These operators are demanded to be based on paths which start and finish at the end nodes. To define a maximal set of such holonomy operators, we join the two following subsets:

i) *G-holonomies*—First, we single out one end-node and call it the *root node*, n^{r}. We call the face enclosing this root node the *outer face*. We then need to choose a set of paths from the root node to each of the other end nodes $\{n^{\mathrm{e}}\}$. For this we pick a (connected) spanning tree in Γ' denoted $\mathcal{T}'$. Such a tree uniquely determines a path $\mathcal{P}'_n$ from the root node to any other node n, and *a fortiori* also to the end nodes of Γ'. The set of G–holonomies $\{G_{n^{\mathrm{e}}}\}$ is defined as the oriented product of holonomies following the paths $\mathcal{P}'_{n^{\mathrm{e}}}$:

$$G_{n^{\mathrm{e}}} \equiv \overrightarrow{\prod_{l \subset \mathcal{P}'_{n^{\mathrm{e}}}}} g_l \ . \tag{5.19}$$

This set automatically fixes all holonomy between pairs of end nodes along paths supported on $\mathcal{T}'$.

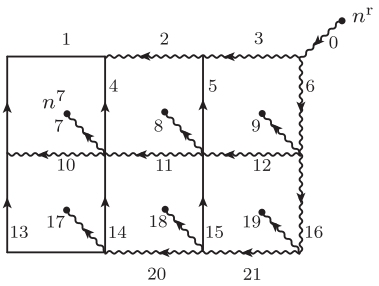

Figure 5.2. Example of lattice with six plaquettes embedded on the two-sphere $\S_2$ by introducing an outer plaquette. The wiggly lines represent the connected spanning tree $\mathcal{T}'$. For each plaquette we associate a G–holonomy defined as the product of holonomies going from the corresponding end node to the root following $\mathcal{T}'$ and a H–holonomy defined by going anti-clockwise around the face starting and ending at the end-point. For the upper-left face we have for instance $G_7 = h_7 h_{11} h_{12} h_6 h_0$ and $H_7 = h_7 h_4^{-1} h_1 h_{10} h_7^{-1}$.

ii) *H-holonomies*—The second set is constituted of holonomies $\{H_{n^{\mathrm{e}}}\}$ based on closed paths $\{\mathcal{L}'_{n^{\mathrm{e}}}\}$, going anti-clockwise along the boundary of every face containing a puncture n^{e} (all the others being trivial, anyway) and starting at the end-node n^{e} associated to the face itself,

$$H_{n^{\mathrm{e}}} \equiv \overrightarrow{\prod_{l \subset \mathcal{L}'_{n^{\mathrm{e}}}}} g_l \ . \tag{5.20}$$

Note that in order to obtain a maximal set of holonomies, it is not necessary to include the one around the outer face as long as we include the holonomies around all the other faces.

Thus, a basis wave-function turns out to be labeled by $(p-1)$ pairs $(G_{n^{\mathrm{e}}}, H_{n^{\mathrm{e}}}) \in \mathcal{G}^2$. Denote it $\psi_{\{G_{n^{\mathrm{e}}}, H_{n^{\mathrm{e}}}\}}$. fig. 5.2 depicts an example of such a construction. The wave functions can finally be written in a fully covariant form as a product over delta functions prescribing the G– and H–holonomies. For the sake of clarity, let us look at the minimal examples of a lattice with two faces. Replacing the faces by punctures, this corresponds to considering an embedded graph on the twice-punctured sphere. Since the twice-punctured sphere $\mathbb{I} \equiv \Sigma_2^0$ is topologically equivalent to a cylinder, we have the following gaphical correspondence:

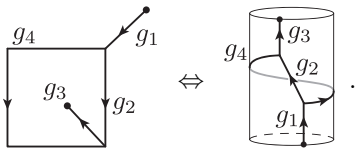

(5.21)

with the marked point at the bottom puncture chosen as the root node. Applying the previous prescriptions, the gauge covariant form for the holonomy basis states on the two-faces square lattice (or twice-punctured sphere $\mathbb{I}$) is given by

$$\psi_{G,H}(g_1, \ldots, g_4) \ = \ |\mathcal{G}|^{3/2} \delta(G, g_3 g_2 g_1) \delta(H, g_3 g_4 g^{-1} g_3^{-1}) \equiv$$

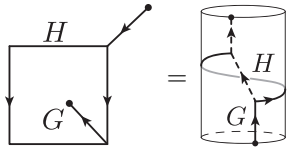

, (5.22)

where we have chosen a particular normalization that will turn out to be convenient later on.

5.3.3 Hierarchical set of ribbon operators

The holonomy basis $\{\psi_{\{G_{n^e},H_{n^e}\}}\}$ diagonalizes holonomy operators that are not gauge invariant at the end nodes and for this reason it is for now quite involved to specify a complete and independent subset of fully gauge invariant wave functions. Therefore, we first aim to find a (maximal) set of gauge-invariant operators and hence the basis which diagonalizes it.

Starting from the holonomy basis, the previous remark suggests that we should include into the set of gauge invariant operators the conjugacy class of the holonomies $\{h_{n^e}\}$. Let us for instance consider a lattice and two faces associated with the end nodes n_1^e and n_2^e. We denote $h_{n_2^e \cup n_1^e}$ the holonomy surrounding these two faces. If we have a non-abelian group $\mathcal{G}$, knowing only the conjugacy classes C_1 and C_2 of the two holonomies $h_{n_1^e}$ and $h_{n_2^e}$, will in general not determine the conjugacy class of $h_{n_2^e \cup n_1^e}$ uniquely. Therefore the conjugacy class of the holonomy going around two faces generally encodes more information than the one provided by the conjugacy classes of the individual faces. It turns out that, knowing the individual conjugacy classes, the set of conjugacy classes one can obtain for the holonomy around the two faces is determined by so-called fusion rules.

The fusion basis diagonalizes a hierarchical set of (gauge invariant) operators, detecting the conjugacy classes of loop based holonomies. This hierarchical set is described by a so-called fusion tree. We choose it to be rooted and binary (*i.e.* with three-valent internal vertices) such that the end vertices of this tree are associated to the faces (or punctures) together with their corresponding end nodes, and the root of the tree is associated to the outer face with the root node n^r. The combinatorial structure of the fusion tree determines which faces (or loops, or punctures) and in which order, are fused to form larger ones. Thus, the fusion tree determines for which hierarchical merging of loops one considers the associated closed holonomies. As an extra condition, we require the set of loops underlying the closed holonomies not to cross each other.

The hierarchical set of loops $\{\ell\}$ defined above prescribe gauge invariant functionals $\{f(g_\ell)\}$ which detect the conjugacy classes and therefore capture the curvature (or magnetic) degrees of freedom. In particular, this defines Wilson loop operators $\{W_\ell^f\}$. However, we would also like to have operators that characterize the torsion (or electric) degrees of freedom. Indeed, even if we consider completely gauge-invariant functionals without torsion degrees of freedom for the original faces, we might have 'emergent' torsion degrees of freedom which arise when applying the fusion scheme described above. This is the one reason why torsion excitations might appear under coarse-graining [4, 18, 22, 23, 141]. This feature is again characteristic of non-abelian groups and such effective torsion charges have been named Cheshire charges in [141]. Conveniently, the torsion degrees of freedom can be captured with operators based on the same hierarchical set of loops, as the one used for the curvature degrees of freedom. The difference is that these operators include the action of translation operators. As we already know, by putting together these two kinds of operators, we obtain the closed ribbon operators (see sec. 4.5).

A set of closed ribbon operators $\{\mathcal{K}_\beta[C,R]\}$ is mutually commuting as long as the ribbons do not cross each other. The fusion basis diagonalizes exactly a certain choice of such mutually commuting closed ribbon operators. This leads to a hierarchical set of ribbons. Indeed, first we consider the set of ribbons around the basic faces (or punctures), excluding the root face. These define the basic excitations. One then fuses two excitations by considering ribbons around fused faces or punctures. In each step one fuses two excitations, which can be either basic ones or excitations resulting themselves from a fusion. One proceeds until there is only the outer face or root puncture left. Since we consider a sphere the ribbon around the root puncture agrees with the ribbon around the remaining punctures modulo orientation. The choice of fusion scheme can be encoded in a fusion tree, where the end

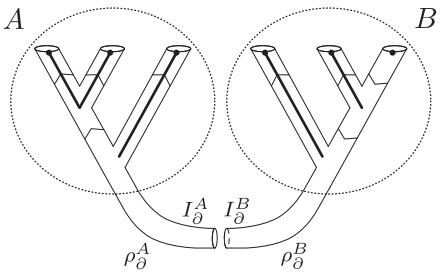

Figure 5.3. For a given fusion tree we identify the region A as a set of punctures and B its complement. The splitting is performed by cutting a cylinder of the fusion tree. This cut requires the introduction of additional punctures. Note that the fusion tree employed here is the same as the one appearing in the alternative fusion states defined in app. B.1.

vertices of the tree correspond to the end nodes of the graph, that is to its faces or punctures, and the root of the tree correspnds the root of the graph, that is to its outer face. The trivalent vertices of the tree encode the fusion of two excitations into a new one. The edges of the fusion tree are labeled by pairs (C_β, R_β) where $\beta \in \{1, \cdots, 2p-3\}$. These labels determine a set of fusion basis states, namely those fusion basis states the closed ribbon operators $\mathcal{K}_\beta[C_\beta, R_\beta]$ project onto.

These fusion basis states can be explicitly defined as in the previous chapter and we represent them as before (see e.g. eq. (4.36)). With such a graphical notation, it is clear that the usual lattice-based representation has been abandoned in favour of a representation relying exclusively on the excitations and the way they fuse together. Therefore it is natural at this point to define a region not so much in terms of the underlying lattice but only in terms of the excitations it contains. Note that a different choice of fusion tree would lead to a different fusion basis.

5.4 Entanglement entropy in lattice gauge theories

With the fusion basis at hand, we have all the ingredients to define a new notion of entanglement entropy through the procedure of sec. 5.2. There, we assumed to have a basis labeled by representation indices $\{\rho\}$, and that the system under scrutiny was divided in two regions generically associated to a set of representation labels $\{\rho_\partial\}$. Now, in the case of the fusion basis, and assuming that there is only one connected boundary, this set of labels can always be reduced so that it includes *only one* representation ρ_∂.

This representation label describes the outcomes of the closed ribbon operator going along the boundary between regions. The extension procedure described in sec. 5.1, introduces an extended Hilbert space $\mathcal{H}_{\text{ext}} = \mathcal{H}_A \otimes \mathcal{H}_B$, which factorizes into two Hilbert spaces. These two Hilbert spaces correspond to the two systems one obtains after splitting the surface Σ along the boundary, see the discussion in sec. 5.1.

Fig. 5.3 represents the cut into two regions in the picture using punctures and the fusion tree. In the usual lattice picture the cut proceeds along the boundary of the plaquettes. More precisely we can imagine to double the Wilson loop around *e.g.* the region A into two loops which go closely parallel to each other. The two Wilson loops are connected with one 'small' link, whereas the area between the two loops carries flat connection.[10] The cut proceeds then in-between the two Wilson loops and

[10]Demanding flat connection for this area and gauge invariance at the additional nodes, we can uniquely map the state on the original graph to the graph with the doubled Wilson loop.

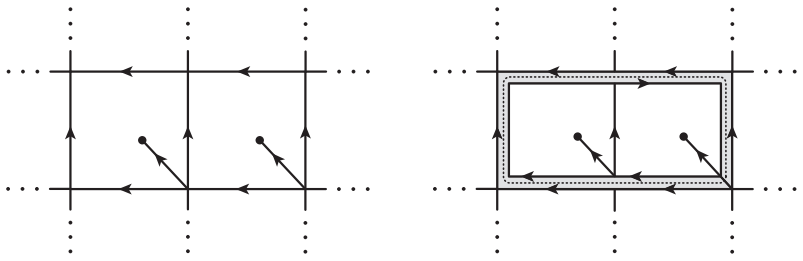

Figure 5.4. Example of splitting on a square lattice between two plaquettes and the complementary graph. First the plaquettes are isolated by doubling the boundary links. An extra link is added to connect the isolated plaquettes to the rest of the lattice. The group element on this extra link is determined by the flatness constraint imposed on the face represented in gray. The splitting is finally performed along the dashed line.

cuts the link connecting the two loops.

Let us mention some key differences between this extension procedure and the one which uses spin network states as in [28, 30, 31]. The use of the fusion basis emphasizes the role of the excitations with respect to the BF vacuum, which in turn prescribes gauge-invariant flat connection. In (2+1)d this means that only the position of the punctures matters, not the graph itself. This feature is particularly important for the application to (2+1)-dimensional gravity, where the BF vacuum, with defect excitations describing particles, give the physical states [124, 142].

The two procedures can be also compared in how 'big' the extension of the Hilbert spaces is. This can be quantified in terms of how many constraints are violated in the extended Hilbert space. In the case of the spin network basis this includes all the Gauß constraints at the two-valent nodes that result from the boundary cutting links. In the case of the fusion basis this includes only one Gauß constraint and one flatness constraint. In the picture described above, the Gauß constraint needs not to hold anymore for the link which is cut into two. And the flatness constraint that is violated in the extended Hilbert space is the one between the two Wilson loops arising from doubling the Wilson loop along the boundary.

This is, nonetheless, a sort of minimal choice which can always be made. A more general splitting can be introduced also for the fusion basis. This corresponds to choosing arbitrary more marked points along the boundary of the two regions. In this way, more Gauß constraint violations will be added (but no extra curvature violation, see [4]). From the observable algebra perspective, this corresponds to declaring observable a series of gauge-variant holonomies along a set of paths which partition the boundary. This extension will only introduce additional vector-space indices (*i.e.* new indices 'next to' the (M, N) in V_{ρ_∂}). Later, we will briefly discuss what kind of consequence this has for the entanglement entropy.

We are now going to explicitly calculate the entanglement entropy for some simple choices of states and regions. To remind the reader, the entanglement entropy has three contributions

$$S_A \;=\; H(P(\rho_\partial)) \;+\; \langle \ln \dim \rho_\partial \rangle \;+\; \langle S_A(\mathfrak{D}^A(\rho_\partial)) \rangle \;, \tag{5.23}$$

where $P(\rho_\partial)$ is the classical probability distribution

$$P(\rho_\partial) = \sum_{\substack{\rho_A, N_A \\ \rho_B, N_B}} \psi(\{\rho; N\}) \overline{\psi(\{\rho; N\})} \;, \tag{5.24}$$

while $\langle \bullet \rangle$ and $H(P(\rho_\partial))$ denotes the average with respect to $P(\rho_\partial)$ and its Shannon entropy respectively.

5.4.1 Entanglement entropy of fusion basis states (and BF vacuum)

We start with a fusion basis state on the p-times-punctured sphere Σ_p^0. Its expansion in the fusion basis of course gives

$$\Big(\psi_{\mathfrak{f}}[\{\rho^0; N^0\}]\Big)(\{\rho; N\}) \;=\; \prod_{\beta} \delta_{\rho_\beta, \rho^0_\beta} \prod_{\alpha} \delta_{N_\alpha, N^0_\alpha} \,. \tag{5.25}$$

Here β labels the edges of the fusion tree and α its endpoints. We partition the punctures into two sets A and B. We choose a fusion tree such that the A and B sets are only connected by one fusion tree edge labeled by $\rho_\partial = \rho^0_\partial$. That is we are only considering fusion basis states from a basis characterized by a tree which is 'compatible' with the prescribed splitting. Such a basis always exists (and in fact, there are many).

In this case the classical probability distribution $P(\rho_\partial)$ is peaked on one particular value $P(\rho_\partial) = \delta(\rho_\partial, \rho^0_\partial)$, thus the associated Shannon entropy vanishes. The density matrices $\mathfrak{D}^A(\rho_\partial)$ are defined to vanish for $\rho_\partial \neq \rho^0_\partial$, and the density matrix $\mathfrak{D}^A(\rho^0_\partial)$ has only one non-vanishing entry equal to 1 on the diagonal, and therefore gives no contribution to the entanglement entropy (5.23). Therefore, we are left with the middle term in (5.23)

$$S_A(\psi_{\mathfrak{f}}[\{\rho^0; N^0\}]) \;=\; \ln \dim \rho^0_\partial \,. \tag{5.26}$$

Notice that we find a vanishing entropy for the BF vacuum state, as in this case $\dim \rho^0_\partial = 1$. This agrees with the result found in [130] for abelian gauge theories with the magnetic centre choice on the BF vacuum state. For abelian structure groups, $\rho = (C, R)$ is labeled by a group element (as $C = \{g\}$) and an irreducible representation of its stabilizer, that is of the whole group. This irreducible representation is—the group being abelian—one-dimensional. Hence, in this case $\dim \rho = |C| \cdot \dim V_R = 1$, and the entanglement entropy vanishes for (compatible) fusion basis states.

We can also consider gauge invariant projections of fusion basis states, as defined in sec. 5.3. We can consider these states both in the Hilbert space $\mathcal{H}_p$ which allows for torsion excitations at the punctures, and its gauge invariant projection, where torsion excitations do not appear for the punctures (but can—in the non-abelian case—appear for internal edges of the fusion tree). In both cases the result is the same as in (5.26). The only difference could have been in the contributions from the density matrices $\mathfrak{D}^A(\rho_\partial)$, but these do describe pure states also after the action of gauge-averaging projectors. This is because such projectors act locally within one single region.

Let us shortly come to the extension mentioned at the end of this section's introduction. This extension consists in a generalization of the Hilbert space $\mathcal{H}_p$ and of the corresponding fusion basis to the case where more than one link is allowed to end on a given puncture (in this case the puncture that is identified with the boundary between the two regions, see [4]). It turns out that the corresponding fusion basis is still labeled with the same representations, the only difference is in the vector space indices N at the extended puncture: For each additional marked point accompanied with a link ending at the puncture the index range is multiplied by $|\mathcal{G}|$, the order of the group. Associated to this generalization of the fusion basis we can also consider a generalization of the gluing and extension procedure. Basically we can decide by how many graph links we wish to connect region A and region B. Note that this reintroduces a graph dependence[11] that previously we fixed by using an equivalence

[11] More precisely one decides on the number of marked points along the boundary through which the crossing links have to pass.

relation between states, that allowed us to change the underlying graphs. This enabled us to always reduce to the case that region A and region B are connected by only one link.

Using this generalized procedure the adjustment of the entropy formula is very simple. The result is that for each additional marked point the entanglement entropy increases by $\ln|\mathcal{G}|$. Interestingly, it turns out that the following relations between dimensions hold (see *e.g.* [4])

$$\dim \mathcal{D}(\mathcal{G}) = |\mathcal{G}|^2 = \sum_{\rho} (\dim \rho_{\mathcal{D}(\mathcal{G})})^2 \,, \tag{5.27}$$

where the first is a dimension of the Drinfel'd double seen as a vector space spanned by the basis $\{[G,H]\}$, the second is the cardinality (order) of the group $\mathcal{G}$, and the last one is again a dimension of a vector space, *i.e.* of V_ρ. The last term in the above equality is also known as the (square of the) 'total quantum dimension' of the fusion category given by the irreducible representations of $\mathcal{D}(\mathcal{G})$:

$$\Omega_{\mathcal{D}(\mathcal{G})} := \sqrt{\sum_{\rho} (\dim \rho_{\mathcal{D}(\mathcal{G})})^2} \,. \tag{5.28}$$

Hence, we find that for a (compatible) extended fusion basis state, with m marked points[12] at the boundary puncture, itself labeled by ρ_∂, the entanglement entropy amounts to

$$S_A(\psi_{\mathfrak{f}}^m[\{\rho^0; N^0\}]) \;=\; \ln \dim \rho_\partial^0 + (m-1)\ln \Omega_{\mathcal{D}(\mathcal{G})} \tag{5.29}$$

Notice, that by using such a graph-dependent formula, one obtains also a non-vanishing contribution for the BF vacuum state. This can be understood by realizing that the extended Hilbert space allows now a refined information on the gauge connection along the boundary. For example, with two links crossing the boundary we can specify the holonomy between the corresponding two marked points on the boundary. This holonomy can be non-trivial even if the holonomy along the complete boundary is trivial.

Remarkably, the result (5.29), applied to the BF vacuum with $\mathbb{Z}_2$ gauge group, does agree with the entanglement entropy defined via the Hilbert space extension based on the spin network basis (or with the electric centre choice) found in [30]. To this end one has to choose m, the number of links connecting regions A and B to agree in both procedures. As we pointed out however, with our procedure, based on the fusion basis we are free to perform the (BF representation based) continuum limit keeping m fixed, ensuring a finite (or vanishing if $m = 1$) entanglement entropy for the BF vacuum. In contrast, using the Ashtekar-Lewandowski representation, the continuum limit of the BF vacuum state requires to take m to infinity, thus leading to an infinite entropy in this limit. Nevertheless this agreement in results is striking and it would be interesting to see if this holds for more generic states.

5.4.2 States generated by the action of open charge ribbon operators

Let us go back to the usual Hilbert space $\mathcal{H}_p$ and consider another class of examples, namely states that are generated from the BF vacuum by applying a number of open ribbon operators, that are going from region B to region A. We start with the case of two charge ribbon operators $\mathcal{R}_1[\rho_1]$ and $\mathcal{R}_2[\rho_2]$, associated to two different paths. Thus we have to consider states on the 4-punctured sphere Σ_4^0.

[12] This number, m, includes also the marked point which is always supposed to be there. Hence $m \geq 1$ in this definition, and $m = 1$ for 'minimal' fusion basis states.

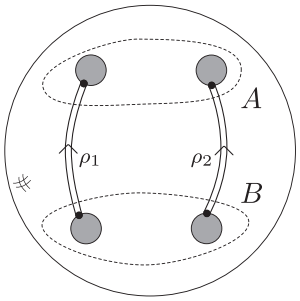

Figure 5.5. A class of states is generated from the BF vacuum by acting with several open ribbon operators going from a region B to a region A. The entanglement entropy for such states can be computed using the fusion basis construction.

In this case too, the contribution $S_A(\mathfrak{D}^A(\rho_\partial))$ vanishes as $\mathfrak{D}^A(\rho_\partial)$ describes again a pure state. As shown in more detail in app. B.2 the other two contributions to the entanglement entropy are determined by the probability distribution

$$P(\rho_\partial) \;=\; N_{\rho_1\rho_2}^{\rho_\partial}\,\frac{\dim\rho_\partial}{\dim\rho_1\,\dim\rho_2}\;. \tag{5.30}$$

Note that this agrees with the expectation value of the closed ribbon operator $\mathcal{K}[\rho_\partial]$ along the boundary of the two regions, *i.e.* $P(\rho_\partial) = \langle\mathcal{K}[\rho_\partial]\rangle$. One has indeed $\sum_{\rho_\partial} P(\rho_\partial) = 1$. With this probability distribution one can compute the entanglement entropy for the state under consideration to be

$$S_A \;=\; \ln\dim\rho_1 + \ln\dim\rho_2\;. \tag{5.31}$$

More generally, we can consider n non-intersecting ribbons $\mathcal{R}_a[\rho_a]$, $a = 1,\dots n$, all going from region B to region A. These will generate a state proportional to the normalized state (see app. B.2)

$$\sum_{\rho_{n+1},\dots,\rho_\partial} N_{\rho_1\rho_2}^{\rho_{(n+1)}}\,N_{\rho_{(n+1)}\rho_3}^{\rho_{(n+2)}}\cdots N_{\rho_{(2n-2)}\rho_n}^{\rho_\partial}\sqrt{\frac{d_{\rho_\partial}}{d_{\rho_1}\cdots d_{\rho_n}}}$$
$$\widehat{\psi}_{\mathfrak{f}}^{\Sigma^0_{2n}}[\{\rho_a\},\{\rho,\dots,\rho\}_{(n+1)}^{2(n-1)},\rho_\partial,\{\rho,\dots,\rho\}_{(n+1)}^{2(n-1)},\{\rho_a\};\{N_a\},\{M_a\}]\;, \tag{5.32}$$

where the states $\widehat{\psi}_{\mathfrak{f}}^{\Sigma^0_{2n}}$ are the orthonormal fusion basis states defined in app. B.1. Again the entanglement entropy is determined by the first two terms in (5.23) to be simply

$$S_A \;=\; \sum_a \ln\dim\rho_a\;. \tag{5.33}$$

We thus get the entropy to scale with the number of ribbon operators crossing the boundary. Note that we only get a non-vanishing entropy for these states due to the first two 'classical" contributions to the entanglement entropy (5.23). The distillable entanglement entropy would therefore be vanishing. This is probably due to the fact that the ribbon operators generating these states are not part of the reduced observable algebra $\mathcal{O}_{\text{red}}$, that underlies the definition of distillable entanglement entropy.

5.4.3 Comparison with the literature

A similar result to (5.33) was also obtained in [143, 144], which considered the entanglement entropy for Chern-Simons theory. Whereas [143] uses the replica trick in a covariant path integral approach

combined with surgery techniques, [144] employs again the replica trick but within the conformal field theory induced on the boundary.

In these two references, the entanglement entropy is also computed for states on the sphere as generated by the insertion of Wilson line operators. Notice, that the Chern-Simons Wilson lines involve holonomies of a Poisson non-commutative connection, which is therefore not the connection involved in our underlying states. At the same time, our states are generated by the action of ribbon operators, which are exactly Wilson lines for the double of the group. The analysis of [128, 145] actually shows explicitly that the quantization of BF theory with gauge group $\mathcal{G}$ is equivalent to the combinatorial quantization of Chern-Simons theory for the double $\mathcal{D}(\mathcal{G})$. This result[13] suggests that by appropriately identifying the structures in our computation and in theirs, they should match exactly, in the sense that they aim to compute the same physical quantities in two equivalent quantization schemes. After this premise, we can now compare the results.

First of all, while [143] finds finite answers, those of [144]—found through computations in the edge field theory—are divergent. This divergence is due to an offset proportional to the central charge of the dual conformal field theory, and can therefore be thought as being associated to its zero-point energy. We will come back to this term later, for the moment let us focus on the other terms on which [143] and [144] agree. These terms contain two contributions. The first contribution S_1 coincides with our result (5.33), while the second S_2 is another universal offset determined by the total quantum dimension Ω

$$S_2 = -\ln \Omega. \tag{5.34}$$

This can be interpreted as a 'vacuum contribution' to the entanglement entropy. It is a negative contribution. As such, it cannot result from a finite Hilbert space computation, and in fact we do not find it. (This term is also related to the so-called topological entropy [39, 146], whose study in the framework of [39] needs the application of the fusion basis technique to disconnected regions. We postpone this study to future investigations.)

Finally, coming back to the (positive) divergent term found using the dual field theory, it is interesting to speculate about its possible origin in the discrete framework. In Chern-Simons theory on a three-manifold with boundaries, the dual CFT living on the boundary is given by the WZNW model. If the three-manifold is a two-disk times an interval, a way to see the appearance of the WZNW model is by solving explicitly the flatness constraint in the bulk of the disk. In the standard notation $A_\mu(x) = g(x)^{-1}\partial_\mu g(x)$. This leaves us with the field $g(x)$ on the boundary, since its bulk contributions to the action essentially cancel out (modulo topological terms). Therefore, it is the choice of local frame $g(x)$ in which the flat gauge connection is evaluated which encodes the boundary CFT field (see also [147] for these derivations in relation to three-dimensional gravity). At this point, it is natural to draw a parallel between the frame $g(x)$ in the continuum theory and the local frames we introduce in the refined boundary-puncture picture. If this is done, it is clear that infinitely many refining points on the boundary-puncture are needed to fully capture the dual field theory. In this limit also our entropy diverges. But as our procedure and the regularization procedure used in [144] are completely different, a more precise relation is difficult to obtain at this stage. In spite of this, we find this question extremely interesting.

[13] Their result holds 'on-shell' as a quantization of the moduli space of flat connections. However their construction involves 'off-shell' quantities as well, and the claim we are going to make can be in principle checked rigorously. We postpone the study of this interesting question to future work.

5.4.4 TQFT based continuum limits

In sec. 5.3, we defined the Hilbert spaces $\mathcal{H}_p$ that capture $2p-2$ degrees of freedom of a gauge theory on a fixed graph or lattice embedded on the 2-sphere. The set-up taken here allows to embed these Hilbert spaces $\mathcal{H}_p$ into a continuum Hilbert space $\mathcal{H}_{\text{cont}}$.

This leads to the so-called BF representation [22, 86, 96], consisting of a Hilbert space which supports a representation of a continuum observable algebra, formed by the ribbon operators. The Hilbert space is based on the BF vacuum state, which is sharply peaked on flat connections, and is spanned by states that arise from the action of finitely many open ribbon operators on this vacuum state. The ribbon operators are then allowed to end at arbitrary points, which hence define the punctures. Such a Hilbert space can be constructed as an inductive limit from a family of Hilbert spaces based on fixed graphs (or more precisely equivalence classes of graphs, see [22, 86, 96]). In this latter viewpoint one puts all degrees of freedom, which are finer than the ones supported by the fixed graph, in the BF vacuum state.

This leads us to the following interpretation of the result (5.33). First of all, the vacuum state has a vanishing entanglement entropy. Then, each (charge ribbon) operator $\mathcal{R}[\rho]$ that connects the two regions contributes to the entanglement entropy with $\ln \dim \rho$. This is despite the fact that in our definition of entanglement entropy we make explicit use of a particular fusion basis, which involves only one ribbon crossing the boundary.

An analogous result holds for the *electric centre* choice, or its spin network based extension [31]. Here we can also introduce a continuum Hilbert space, known as Ashtekar-Lewandowski representation [67, 68, 133]. This Hilbert space is based on a vacuum state peaked on vanishing electric fluxes. Wilson loops and lines do now act as creation operators. In fact a spin network state results from the action of a network of Wilson lines connected via intertwiners. Using the spin network based extension, one also finds that the entanglement entropy of a spin network basis state is given by $\sum_a \ln \dim \rho_a$ where now ρ_a denotes the irreducible representation of $\mathcal{G}$ associated to the a-th spin network link which crosses the boundary. Again, one finds that the associated vacuum (the Ashtekar-Lewandowski vaucuum) has vanishing entanglement entropy.

However, if we express the BF vacuum in the spin network basis and use the procedure of [31] to define the entanglement entropy, we notice that the result depends on the underlying graph. In particular, taking a refinement limit for the graph we would find a divergent result. Such a refining limit is necessary in this case to fully (*i.e.* everywhere) describe the BF vacuum. In other words, the BF vacuum is an infinitely excited state with respect to the Ashtekar-Lewandowski one, and the entanglement entropy reflects this fact. On the other hand, using the fusion basis and the related Hilbert space extension we emphasize the excitations relative to the BF vacuum itself. This leads to a result which is graph independent, a fact that makes our method applicable to the case of $(2+1)$ dimensional gravity, which is described via a BF theory with defects describing point particles. Of course, attempting a description of the Ashtekar-Lewandowski vacuum (that is the strong coupling limit of Yang Mills theory) in terms of the fusion basis would also lead to results which are graph dependent or divergent.

Thus, we see that different notions of entanglement entropy are also adjusted to different notions of representations, or phases, or regimes. The BF representation corresponds to the (Yang Mills) weak coupling regime, and the Ashtekar-Lewandowski representation to the strong coupling regime. The excitations are in both cases (quasi-local) deviations from the weak coupling and strong coupling limit, respectively. In both cases, one deals with a topological theory with defect excitations.

We wish to emphasize that the vacua, both in the BF as well as in the Ashtekar-Lewandowski

representation, describe theories without propagating degrees of freedom. That is, one can define Hamiltonians for which these vacua are the lowest energy states, which are moreover gapped. It is, thus, consistent to associate a vanishing entanglement entropy to these states. To describe the vacua of theories with propagating degrees of freedom in the continuum limit, we would need to introduce infinitely many excitations with respect to either of the vacua. This would lead to the usual divergent behaviour for the entanglement entropy in quantum field theories with propagating degrees of freedom.

5.5 Entanglement entropy in gravity

The notion of entanglement entropy is usually (but not exclusively) associated to subsystems describing a region of space, which is specified by coordinates. One would like to link such a choice of region to a subset of observables, commuting with the remaining observables, but we have seen that this is already an ambiguous process for gauge systems. These difficulties are much more enhanced in general relativity.

In background independent theories, such as general relativity, regions specified by coordinates lack an a priori operational meaning. Alternatively, one can define regions through matter or metric fields. This is very similar to employing relational observables [148–151] as gauge invariant observables in general relativity. Here the metric or matter fields are used as a reference system, in which other fields can be expressed in [151–153]. Thus one can also attempt to specify 'physical regions' by employing a *physical reference system*.

Relational observables can be computed in an approximation scheme [154, 155], which also allows an understanding of how the standard observables of quantum field theory (on a fixed background) arise as approximations to fully gauge invariant observables. A crucial drawback of using matter or metric fields as reference system is that there will be phase space regions in which these fields are not suited as clocks and rods. In some systems smooth gauge invariant observables might not exist [156, 157]. Thus one expects that notions of locality can be realized only for a certain class of states [27] and are furthermore only approximate [138, 149].

Another key point is the question whether one can find a split of the observable algebra into mutually commuting sets describing (approximately local) subsystems [27, 138, 158]. For example, the approximation scheme developed in [154] regains the usual quantum field theoretical observables on a fixed background at lowest order, but at higher orders it includes non-local terms. Giddings and Donnelly argue that observables creating *e.g.* matter fields, need to be gravitationally dressed, in order to capture the accompanying gravitational field. In contrast to Yang-Mills theories, this dressing cannot be screened and leads to an inherent non-local structure [138].

Using relational observables, one can deduce the commutator algebra by using Dirac brackets [150]. Realistic (that is relativistic) matter fields allow, however, only for an approximate localization [149, 154]. Physical coordinates built from geometry (*e.g.* by using geodesics) lead, at least so far, to non-local algebras [154, 159].

The exploration of the diffeomorphism invariant observable algebra is very difficult, as it basically requires to understand and solve the dynamics of the system. This is, of course, a very challenging task for the four-dimensional theory. On the other hand three-dimensional general relativity is much simpler: It describes locally flat spacetimes (or homogeneously curved ones, in presence of a non-vanishing cosmological constant). This also means that one has no local degrees of freedom, but only global topological ones. Introducing matter changes this situation, but it requires again a solution of

the theory. To keep the system solvable, one can consider the coupling of point particles, which leads to a topological field theory with curvature and torsion defects, as discussed in this chapter.

In fact (Euclidean) 3d gravity without a cosmological constant can be described by a BF theory with SU(2) structure group. The coupling of point particles leads to curvature and torsion defects [98, 99, 142, 160]. In short, the formalism needed to describe 3d gravity is very close to the formalism used here. Moreover including a positive cosmological constant, one has to work with a $\mathrm{SU}(2)_q$ structure group, with q a root of unity. This leads to a finite dimensional Hilbert space, as in the finite group case we discussed. The fusion basis, ribbon operators, as well as gluing and cutting procedures are also available in the quantum group case [34].

The fusion basis diagonalizes a maximally commuting subset of gauge invariant (*i.e.* Dirac) observables, given by closed ribbon operators. A conjugated set of Dirac observables is provided by open ribbon operators going from one particle to another. Adopting the definition of entanglement entropy laid out here, a region is indeed specified by its matter content, that is by the particles contained in this region. Note that we do not have to specify the precise (geometric) position of the boundary, we only need to declare which particles belong to which regions. The geometric information is rather contained in the state under consideration.

Given two regions A and B, the algebra of observables associated with region A includes closed ribbons surrounding subsets of particles living in A, with the exception of the closed ribbon surrounding all particles in this region (and therefore also surrounding all the particles in the region B, since we consider spherical topology). This closed ribbon forms the centre of the algebra in the language of [130]. Additionally one can construct Dirac observables from open ribbon operators going from one A-particle to another A-particle. Ribbon operators crossing the boundary cross also the closed ribbon along the boundary and would therefore not commute with it. These operators cannot be associated to either the A or B region. Thus, although we can solve in this example the problem of how to define a region, we still have to modify the observable algebra, removing ribbons that cross from the A to the B regions from the operator algebra on which the entanglement entropy is being defined (if we follow the definition of [130]).

The notion of subsystems for 3d gravity used here differs in key points from the proposal (so far on the classical level) of [122]. There one introduces additional fields, that allow to fix the boundary in terms of embedding or coordinate functions. This has been motivated as a generalization of the extended Hilbert space construction (or rather its classical version). Here we point out that as there are different extension procedures in lattice gauge theories, this is also very likely to hold for gravity. The procedure laid out in this work can be applied to 3d gravity, and leads to much less extra structure compared to [122]. Furthermore, we can also state the definition of subsystems in terms of mutually commuting subsets of the Dirac observable algebra. This has still to be addressed within the proposal of [122], as was also remarked in [138]. Perhaps, the relevant suggestion is that this splitting of the observable algebra might not be only achieved by removing certain observables, but also allowing for (many) more observables via the introduction of a new unphysical 'boundary field'. This additional boundary structure might, in fact, be used to construct new local observables which otherwise would not be available [138].

5.6 Concluding remarks

Recent work has shown that the notion of entanglement entropy in gauge systems is ambiguous. The deep underlying reason is that due to the non-local features of the observable algebra in gauge systems,

a notion of subsystems needs to be defined first. The way this question is answered does not only affect the definition of entanglement entropy, but has much wider implications for our understanding of (quantum) systems with gauge symmetries [27, 122, 139, 161]. In particular, defining subsystems in background independent theories, *e.g.* gravity, leads to various completely open issues. The methods developed here lead to a new proposal for lattice gauge theories, that is also applicable to (2+1) dimensional gravity. The main feature of this proposal is to use defect excitations to localize regions, which in the case of (2+1) gravity means that regions are specified operationally by their particle content.

Furthermore, we clarified the relation between the different approaches put forward so far to define entanglement entropy, notably the extended Hilbert space approach [31], and the CHR approach [130], which focuses on the observable algebra. In particular, we showed that the extended Hilbert space approach can be generalized to match not only the *electric centre* choice of [130] but also the *magnetic centre* choice [130] (and its non-abelian generalization). In our view, the resulting notion for subsystems can, in both approaches, be fully characterized by a choice of boundary conditions. In the non-abelian case, the extended Hilbert space approach relies on the introduction of extra frame information at the boundary, which we argued could also be added in a generalized CHR approach. We have also seen that the proposal made here requires only the introduction of a global frame, which is then transported with a locally flat connection along the boundary. In contrast, the spin network based method of [31] necessarily introduces for each link cut by the boundary-and in the continuum limit to each point of the boundary-a local frame. Nevertheless, we observed that—if we wanted to—we could extend our framework as well, by allowing arbitrarily many frames along the boundary, leading to additional contributions to the entanglement entropy.

We have also pointed out that the different choices of boundary conditions, described by the *electric* vs. *magnetic* centre, are related to a choice of vacuum state. These vacuum states are of a *topological* nature, *i.e.* they arise as vacua of topological field theories with no local degrees of freedom. The states can be used to define continuum Hilbert spaces, that then describe the states of the related topological field theory with defect excitations. Thus, for states describing BF theory with defects, we have to choose the (generalized) 'magnetic centre' definition, in order to obtain an entanglement entropy which is regularization-(*i.e.* graph-)independent and finite.

The vacua we discussed here, are of a squeezed nature, which means they are sharply peaked either on flat connection (for the BF representation [22, 86, 96]) or vanishing electric fluxes (for the AL representation [67, 68, 133]). The relation to preferred boundary conditions arises for the following simple reason: for states sharply peaked on connection degrees of freedom, it is natural and appropriate to fix the connection degrees of freedom (or the curvature) at the boundary. Similarly, for states peaked on some value of the electric flux, the original extended Hilbert space procedure [31] based on spin networks is the most natural and appropriate one. Possible generalizations include q-deformed BF theory vacua [34], corresponding to (2+1)d gravity with a cosmological constant and, in condensed matter, to string net models [39]. Furthermore, we suspect that also vacua with non-vanishing background values (*e.g.* for the electric fluxes [162–164]) come with a preferred notion of entanglement entropy.

Chapter 6

Fusion basis in (3+1)d

In this chapter, we propose a generalization of the fusion basis for (3+1)d gauge models of topological phases. This generalization relies upon extracting the algebraic structure underlying the 3d excitations from the gluing operation of the 3d equivalents of the cylinder states. It leads to an algebraic structure which naturally extends the Drinfel'd double. Using the irreducible representations of this algebraic structure, we can define a generalization of the fusion basis for (3+1)d topological phases with defect excitations. To do so, we work within the formalism of chap. 3. In particular, this means that we consider the Hamiltonian realization of 4d BF theory for finite groups. Moreover, the graphical calculus we use follow the same rules as the one presented in chap. 3. This generalization could also be derived in the broader context of LGTs as in chap. 4. However, the lattice Hamiltonian formalism and the corresponding graphical notation turn out to be very convenient here.

6.1 Three-cylinder algebra

The definitions of chap. 3 still hold in (3+1)d. In particular, the lattice Hamiltonian is the same as before [47, 48, 54], but defined with respect to a 3d lattice. This means that gauge invariance is still enforced at the bulk vertices and every flux going through a face associated with a contractible cycle is zero. For instance, the Hilbert space $\mathcal{H}_{\mathbb{T}_3}$ of gauge invariant functionals on the space of flat connections on the three-torus $\mathbb{T}_3 = \mathbb{S}_1 \times \mathbb{S}_1 \times \mathbb{S}_1$ is given by

$$\mathcal{H}_{\mathbb{T}_3} = \Big\{ \frac{1}{|\mathcal{G}|} \sum_{x \in \mathcal{G}} |xgx^{-1}, xhx^{-1}, xkx^{-1}\rangle_{\mathbb{T}_3} \,|\, [g,h] = [g,k] = [h,k] = \mathbb{1}_{\mathcal{G}} \Big\} =: \Big\{$$

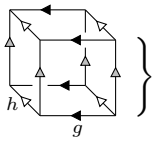

$$\Big\}$$

where the discretization of the three-torus is composed of one cube, three faces on which $\mathbb{B}_f$ acts, three edges corresponding to the three non-contractible cycles, and one bulk vertex on which $\mathbb{A}_v$ acts. In 2d, we obtained the cylinder (or twice-punctured two-sphere) $\mathbb{I}$ by cutting the two-torus along one direction. We proceed similarly in 3d so as to obtain the topology $\mathbb{S}_1 \times \mathbb{S}_1 \times I$, with I an interval. We will refer to the result of this cutting as the *three-cylinder* denoted by $\mathbb{I}_3$. The boundary of the three-cylinder $\mathbb{I}_3$ is the support of both point-like electric excitations and string-like magnetic excitations [47]. More precisely, the three-torus is bounded by two two-tori whose non-contractible cycles carry the magnetic excitations. Furthermore, each boundary torus carries two non-contractible marked cycles

which intersect at a marked point at which the Gauß constraint is relaxed so that the tori support both types of excitations.

Similarly to the 2d cylinder, which is obtained by removing two disks from the two-sphere, we can obtain the three-cylinder by removing two linked solid two-tori from the three-sphere $\mathbb{S}_3$. This follows from the fact that the three-sphere can be obtained as the identification of two solid two-tori (this is the genus-one Heegaard splitting of the three-sphere). Removing one solid torus leaves us with the other solid torus which becomes $\mathbb{I}_3$ after removing a second solid torus. Moreover, the three-cylinder is nothing but $\mathbb{I} \times \mathbb{S}_1$. We will restrict our analysis to the case where excitations are supported by torus boundaries.

The three-cylinder $\mathbb{I}_3$ is therefore discretized by one cube, three faces on which $\mathbb{B}_f$ acts, five edges, and two boundary vertices at which the Gauß constraint is relaxed. The Hilbert space $\mathcal{H}_{\mathbb{I}_3}$ thus reads[1]

$\mathcal{H}_{\mathbb{I}_3} =$ 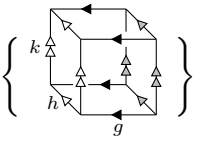 with 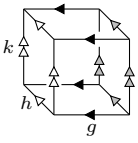 $\longleftrightarrow$ 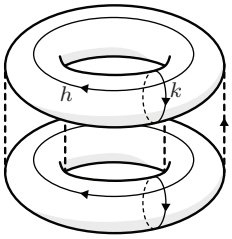 . (6.1)

Using these three-cylinder basis states, we can now repeat the gluing procedure in order to reveal the underlying structure of the excitations. The gluing follows the same rule as in two dimensions, however, during the identification step $\mathfrak{G}$, it is now necessary to identify the equatorial and the meridional non-contractible cycles of the boundary tori in addition to the marked points. Using our graphical representation for the states defined on the three-cylinder, the gluing reads

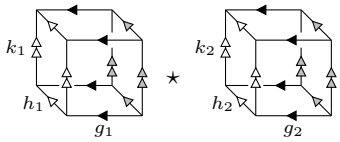 $= (\mathbb{A} \circ \mathbb{B}) \triangleright \mathfrak{G}\Big($ 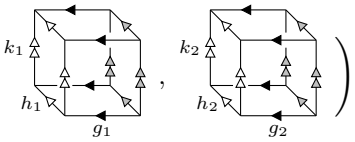 $\Big)$ (6.2)

$= \delta_{h_2, g_1^{-1} h_1 g_1} \delta_{k_2, g_1^{-1} k_1 g_1}$ 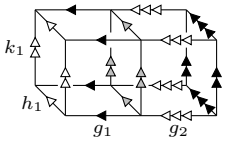 (6.3)

$\sim \delta_{h_2, g_1^{-1} h_1 g_1} \delta_{k_2, g_1^{-1} k_1 g_1}$ 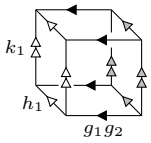 (6.4)

where the last step repeatedly makes use of the equivalence relations (3.14) and (3.15). We summarize

[1] Another way to visualize the three-cylinder is to think of it as a hollow two-torus so that the radial direction corresponds to the g–holonomy.

this gluing operation as

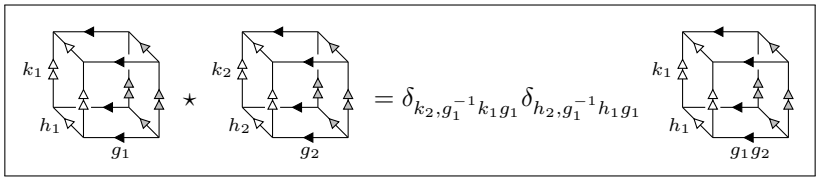

(6.5)

which is a (3+1)d generalization of Ocneanu's tube algebra. We will now describe how this gluing operation corresponds to the multiplication map of an algebraic structure which is a natural extension of the Drinfel'd double.

6.2 Quantum triple $\mathcal{T}(\mathcal{G})$

It is clear from (6.5) that if either $h = \mathbb{1}_{\mathcal{G}}$ or $k = \mathbb{1}_{\mathcal{G}}$, the algebra we are interested in reduces to the Drinfel'd double. We are therefore looking for an extension of the Drinfel'd double, denoted $\mathcal{T}(\mathcal{G})$, and referred to as the *quantum triple* following the suggestion of [44]. Similarly to $\mathcal{D}(\mathcal{G})$, which is obtained as the pairing between an algebra and its coalgebra with opposite comultiplication, $\mathcal{T}(\mathcal{G})$ can be thought as a trialgebra obtained from an algebra and two copies of its coalgebra. More generally, a trialgebra involves an associative algebra and two additional compatible algebraic structures such that the first one provides the bialgebra structure and the second one the trialgebra structure.

Let us now propose the defining properties of the quantum triple $\mathcal{T}(\mathcal{G})$. As a vector space, the quantum triple is isomorphic to

$$\mathcal{T}(\mathcal{G}) \simeq \mathbb{C}[\mathcal{G}] \otimes \mathcal{DF}(\mathcal{G}) \subset \mathbb{C}[\mathcal{G}] \otimes \mathcal{F}(\mathcal{G}) \otimes \mathcal{F}(\mathcal{G}) \tag{6.6}$$

where $\mathcal{DF}(\mathcal{G})$ denotes the abelian algebra of linear functions on $\mathcal{G} \times \mathcal{G}$ such that they have support on commuting holonomies only. A basis for $\mathcal{T}(\mathcal{G})$ is therefore provided by $\{g \otimes \delta_h \otimes \delta_k \,|\, [h,k] = \mathbb{1}_{\mathcal{G}}\}_{g,h,k \in \mathcal{G}}$. In the following, we will simply denote the basis elements by $g \otimes \delta_h \otimes_{\mathfrak{c}} \delta_k \equiv \delta_{hk,kh}(g \otimes \delta_h \otimes \delta_k)$ where $\mathfrak{c}$ is there to remind of the commutation between the group variables h and k. The quantum triple comes equipped with the maps:

- *Multiplication:*

$$(g_1 \otimes \delta_{h_1} \otimes_{\mathfrak{c}} \delta_{k_1}) \star (g_2 \otimes \delta_{h_2} \otimes_{\mathfrak{c}} \delta_{k_2}) := \delta_{k_2, g_1^{-1} k_1 g_1} \delta_{h_2, g_1^{-1} h_1 g_1} (g_1 g_2 \otimes \delta_{h_1} \otimes_{\mathfrak{c}} \delta_{k_1}) \tag{6.7}$$

  with corresponding unit element $\mathbb{1}_{\mathcal{T}(\mathcal{G})} = \sum_{h,k \in \mathcal{G}} \mathbb{1}_{\mathcal{G}} \otimes \delta_h \otimes_{\mathfrak{c}} \delta_k$.

- *Comultiplications:*

$$\begin{aligned} \Delta_{\mathrm{I}}(g \otimes \delta_h \otimes_{\mathfrak{c}} \delta_k) &:= \sum_{\substack{x,y \in \mathcal{G} \\ xy = h}} (g \otimes \delta_x \otimes_{\mathfrak{c}} \delta_k) \otimes (g \otimes \delta_y \otimes_{\mathfrak{c}} \delta_k) \\ \Delta_{\mathrm{II}}(g \otimes \delta_h \otimes_{\mathfrak{c}} \delta_k) &:= \sum_{\substack{x,y \in \mathcal{G} \\ xy = k}} (g \otimes \delta_h \otimes_{\mathfrak{c}} \delta_x) \otimes (g \otimes \delta_h \otimes_{\mathfrak{c}} \delta_y) \,. \end{aligned} \tag{6.8}$$

- *Antipodes:*

$$\begin{aligned} S_{\mathrm{I}}(g \otimes \delta_h \otimes_{\mathfrak{c}} \delta_k) &:= g^{-1} \otimes \delta_{g^{-1} h^{-1} g} \otimes_{\mathfrak{c}} \delta_{g^{-1} k g} \\ S_{\mathrm{II}}(g \otimes \delta_h \otimes_{\mathfrak{c}} \delta_k) &:= g^{-1} \otimes \delta_{g^{-1} h g} \otimes_{\mathfrak{c}} \delta_{g^{-1} k^{-1} g} \,. \end{aligned} \tag{6.9}$$

The idea behind the construction of this trialgebra relies upon the fact that if any of the coalgebras is 'trivialized', *i.e.* reduced to the algebra of linear functions on the trivial subgroup $\{\mathbb{1}_{\mathcal{G}}\}$, we are left with a Drinfel'd double structure. In other words, the defining maps (6.7)(6.8)(6.9) are such that they satisfy the defining axioms of an Hopf algebra when one of the coalgebras is trivialized. In particular, it follows straightforwardly from the compatibility conditions of the Drinfel'd double that the comultiplications Δ_{I} and Δ_{II} are algebra homomorphisms, *i.e.*

$$\Delta_{\mathrm{I,II}}\big((g_1 \otimes \delta_{h_1} \otimes_{\mathfrak{c}} \delta_{k_1}) \star (g_2 \otimes \delta_{h_2} \otimes_{\mathfrak{c}} \delta_{k_2})\big) = \Delta_{\mathrm{I,II}}(g_1 \otimes \delta_{h_1} \otimes_{\mathfrak{c}} \delta_{k_1}) \star \Delta_{\mathrm{I,II}}(g_2 \otimes \delta_{h_2} \otimes_{\mathfrak{c}} \delta_{k_2}) \,, \tag{6.10}$$

while the antipodes S_{I} and S_{II} are algebra antihomomorphisms, *i.e.*

$$S_{\mathrm{I,II}}\big((g_1 \otimes \delta_{h_1} \otimes_{\mathfrak{c}} \delta_{k_1}) \star (g_2 \otimes \delta_{h_2} \otimes_{\mathfrak{c}} \delta_{k_2})\big) = S_{\mathrm{I,II}}(g_2 \otimes \delta_{h_2} \otimes_{\mathfrak{c}} \delta_{k_2}) \star S_{\mathrm{I,II}}(g_1 \otimes \delta_{h_1} \otimes_{\mathfrak{c}} \delta_{k_1}) \,. \tag{6.11}$$

The fundamental difference between the quantum triple $\mathcal{T}(\mathcal{G})$ and the Drinfel'd double $\mathcal{D}(\mathcal{G})$ is the existence of two comultiplications. These two maps will naturally lead to two notions of tensor product, and *a fortiori*, to two different sets of fusion rules. Moreover, because of the existence of antihomomorphic antipode maps S_{I} and S_{II}, it is possible to define dual representations with respect to either Δ_{I} or Δ_{II}. Accordingly, we can also define two notions of trivial representations. But only one representation is trivial with respect to both Δ_{I} and Δ_{II}, and it is defined in terms of the counit $\epsilon(g \otimes \delta_h \otimes_{\mathfrak{c}} \delta_k) = \delta_{h,\mathbb{1}_{\mathcal{G}}} \delta_{k,\mathbb{1}_{\mathcal{G}}}$.

From the identification between the multiplication rule (6.7) of $\mathcal{T}(\mathcal{G})$ and the gluing map (6.5) of three-cylinder states, we deduce the correspondence

$\mathcal{H}_{\mathbb{I}_3} \ni$ 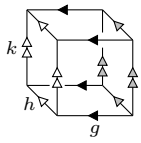

$\longleftrightarrow\ (g \otimes \delta_h \otimes_{\mathfrak{c}} \delta_k) \in \mathcal{T}(\mathcal{G})$ (6.12)

between three-cylinder (basis) states and quantum triple (basis) elements.

6.3 Representation theory of $\mathcal{T}(\mathcal{G})$

So far the properties of the quantum triple $\mathcal{T}(\mathcal{G})$ have followed closely the ones of the Drinfel'd double $\mathcal{D}(\mathcal{G})$. The same is true for the representation theory of $\mathcal{T}(\mathcal{G})$ which is a natural extension of the one of $\mathcal{D}(\mathcal{G})$.

Recall that the irreducible representations $\{\rho\}$ of $\mathcal{D}(\mathcal{G})$ are labeled by a conjugacy class $C(\mathcal{G})$ of the full group $\mathcal{G}$, and an irreducible representation $R(Z_C)$ of the centralizer Z_C of C, so that $\rho = (C(\mathcal{G}), R(Z_C))$. It turns out that the irreducible representations $\{\wp\}$ of $\mathcal{T}(\mathcal{G})$ are labeled by a conjugacy class $C(\mathcal{G})$ of $\mathcal{G}$, a conjugacy class $D(Z_C)$ of the centralizer Z_C of C, and an irreducible representation $R(Z_D)$ of the centralizer Z_D of D so that $\wp = (C(\mathcal{G}), D(Z_C), R(Z_D))$. Naturally, when $C(\mathcal{G}) = \{\mathbb{1}_{\mathcal{G}}\}$, the irreducible representations $\{\wp\}$ of $\mathcal{T}(\mathcal{G})$ reduce to the representations $\{\rho\}$ of $\mathcal{D}(\mathcal{G})$.

The elements of the conjugacy class $C(\mathcal{G})$ are denoted c_a and c_1 is chosen as representative so that the centralizer Z_C is defined as $\{g \in \mathcal{G} \,|\, gc_1 = c_1 g\}$. The elements of the quotient $P_C \simeq \mathcal{G}/Z_C$ are denoted p_a and they satisfy the relation $c_a = p_a c_1 p_a^{-1}$. The elements of the conjugacy class $D(Z_C)$ are denoted d_α and d_1 is chosen as representative so that the centralizer Z_D is defined as $\{g \in Z_C \,|\, gd_1 = d_1 g\}$. The elements of the quotient $Q_D \simeq Z_C/Z_D$ are denoted q_α and they satisfy the

relation $d_\alpha = q_\alpha d_1 q_\alpha^{-1}$. Finally, the matrix elements of the quantum triple element $g \otimes \delta_h \otimes_{\mathfrak{c}} \delta_k$ in the representation $\wp = (C(\mathcal{G}), D(Z_C), R(Z_D))$ are given by

$$\boxed{\begin{aligned} D^{C,D,R}_{a\alpha m, b\beta n}(g \otimes \delta_h \otimes \delta_k) &= \delta(k, c_a)\delta(c_a, g c_b g^{-1})\delta(hk, kh) \\ &\times \delta(p_a^{-1} h p_a, d_\alpha)\delta(d_\alpha, p_a^{-1} g p_b d_\beta p_b^{-1} g^{-1} p_a) D^R_{mn}(q_\alpha^{-1} p_a^{-1} g p_b q_\beta) \end{aligned}} \tag{6.13}$$

where $\delta(c_a, g c_b g^{-1})$ ensures that $p_a^{-1} g p_b$ belongs to Z_C and $\delta(d_\alpha, p_a^{-1} g p_b d_\beta p_b^{-1} g^{-1} p_a)$ ensures that $q_\alpha^{-1} p_a^{-1} g p_b q_\beta$ belongs to Z_D. It is easy to check explicitly, using the definition of c_a and d_α, that $q_\alpha^{-1} p_a^{-1} g p_b q_\beta$ commutes with both c_1 and d_1. Furthermore, since $hk = kh$, we have $p_a^{-1} h p_a \in Z_C$. Note that we dropped the label $\mathfrak{c}$ in the tensor product since the commutation of the group variables h and k is now encoded in the definition of the representations. Thereafter, the more compact notation $D^\wp_{MN} \equiv D^{C,D,R}_{a\alpha m, b\beta n}$ is used, such that $M \equiv a\alpha m$, $N \equiv b\beta n$ and $\wp \equiv (C, D, R)$. Interestingly, an alternative basis can be defined where the role of the group variables h and k is switched, i.e.

$$\begin{aligned} D^{D,C,R}_{a\alpha m, b\beta n}(g \otimes \delta_h \otimes \delta_k) &= \delta(h, c_a)\delta(c_a, g c_b g^{-1})\delta(hk, kh) \\ &\times \delta(p_a^{-1} k p_a, d_\alpha)\delta(d_\alpha, p_a^{-1} g p_b d_\beta p_b^{-1} g^{-1} p_a) D^R_{mn}(q_\alpha^{-1} p_a^{-1} g p_b q_\beta) \,. \end{aligned} \tag{6.14}$$

As we are about to see, both these bases are compatible with the algebraic structure, but each one of them is compatible with only one of the coalgebraic structures.

By definition, these representations are algebra homomorphisms (see app. C.1 for proof) *i.e.*

$$\sum_N D^\wp_{MN}(g_1 \otimes \delta_{h_1} \otimes \delta_{k_1}) D^\wp_{NO}(g_2 \otimes \delta_{h_2} \otimes \delta_{k_2}) = D^\wp_{MO}((g_1 \otimes \delta_{h_1} \otimes \delta_{k_1}) \star (g_2 \otimes \delta_{h_2} \otimes \delta_{k_2})) \,. \tag{6.15}$$

The set $\{\wp\}$ of irreducible representations is complete and orthogonal. The completeness relation reads

$$\sum_\wp \sum_{M,N} d_\wp D^\wp_{MN}(g_1 \otimes \delta_{h_1} \otimes \delta_{k_1}) \overline{D^\wp_{MN}(g_2 \otimes \delta_{h_2} \otimes \delta_{k_2})} = |\mathcal{G}| \delta_{g_1,g_2} \delta_{h_1,h_2} \delta_{k_1,k_2} \delta_{h_1 k_1, k_1 h_1} \tag{6.16}$$

while the orthogonality is provided by (*cf* app. C.2 for proof)

$$\frac{1}{|\mathcal{G}|} \sum_{g,h,k \in \mathcal{G}} D^{\wp_1}_{M_1 N_1}(g \otimes \delta_h \otimes \delta_k) \overline{D^{\wp_2}_{M_2 N_2}(g \otimes \delta_h \otimes \delta_k)} = \frac{\delta_{\wp_1,\wp_2}}{d_{\wp_1}} \delta_{M_1,M_2} \delta_{N_1,N_2} \tag{6.17}$$

where $d_\wp = d_{C,D,R} = d_R \cdot |C| \cdot |D|$ is the dimension of the representation $\wp$.

As a trialgebra, the quantum triple comes equipped with two compatible coalgebraic structures. In particular, this means there exists two different comultiplication maps which can be used to define two different kinds of tensor product of irreducible representations. Therefore, we can define two sets of fusion rules and intertwining maps, associated to each one of the comultiplication maps Δ_{I} and Δ_{II}. However, given a choice of basis for the representations, only one coalgebraic structure is compatible. Because of the obvious symmetry between Δ_{I} and Δ_{II}, it is enough to focus on Δ_{I} for instance. This is the choice compatible with the basis (6.13). In that case, the tensor product reads

$$(D^{\wp_1} \otimes_{\mathrm{I}} D^{\wp_2})(\Delta_{\mathrm{I}}(g \otimes \delta_h \otimes \delta_k)) = \sum_{\substack{x,y \in \mathcal{G} \\ xy = h}} (D^{\wp_1} \otimes_{\mathrm{I}} D^{\wp_2})((g \otimes \delta_x \otimes \delta_k) \otimes (g \otimes \delta_y \otimes \delta_k))$$

which can be decomposed into irreducible representations according to the fusion rules ${}_{\mathrm{I}}N^{\wp_3}_{\wp_1 \wp_2}$, *i.e.*

$$\wp_1 \otimes_{\mathrm{I}} \wp_2 = \bigoplus_{\wp_3} {}_{\mathrm{I}}N^{\wp_3}_{\wp_1 \wp_2} \, \wp_3 \,. \tag{6.18}$$

These fusion rules can be explicitly obtained in terms of the characters $\chi^{\wp}$. For instance, we have

$$ {}_{\mathrm{I}}N_{\wp_1\wp_2}^{\wp_3} = \frac{1}{|\mathcal{G}|}\sum_{g,h,k\in\mathcal{G}} \mathrm{tr}[D^{\wp_1}\otimes_{\mathrm{I}} D^{\wp_2}](\Delta_{\mathrm{I}}(g\otimes\delta_h\otimes\delta_k))\overline{\chi^{\wp_3}(g\otimes\delta_h\otimes\delta_k)} \tag{6.19} $$

$$ = \frac{1}{|\mathcal{G}|}\sum_{g,k\in\mathcal{G}}\sum_{h_1,h_2\in\mathcal{G}} \chi^{\wp_1}(g\otimes\delta_{h_1}\otimes\delta_k)\chi^{\wp_2}(g\otimes\delta_{h_1^{-1}h_2}\otimes\delta_k))\overline{\chi^{\wp_3}(g\otimes\delta_{h_2}\otimes\delta_k)}\,. \tag{6.20} $$

Several important remarks can be drawn from this last equation. The fusion of representations with respect to the comultiplication Δ_{I} vanish if the conjugacy class C is not the same for $\wp_1$, $\wp_2$ and $\wp_3$. This means that the fusion rules for the quantum triple effectively boil down to the ones of $\mathcal{D}(\mathcal{G})$, but they are parametrized by an additional conjugacy class. More precisely, in the case of the comultiplication Δ_{I} and for a given conjugacy class C, the fusion rules of $\mathcal{T}(\mathcal{G})$ boils down to the ones of the Drinfel'd double $\mathcal{D}(Z_C)$ for the subgroup Z_C. It therefore suggests that for the fusion category $\mathrm{Rep}[\mathcal{T}(\mathcal{G})]$ formed by the representations of $\mathcal{T}(\mathcal{G})$ the following grading holds:[2]

$$ \mathrm{Rep}[\mathcal{T}(\mathcal{G})] \simeq \bigoplus_C \mathrm{Rep}[\mathcal{D}(Z_C)]\,. \tag{6.21} $$

This obviously reminds of dimensional reduction which consists in expressing (3+1)d topological orders as a sum of (2+1)d topological orders via a compactification of one of the spatial directions. The conjugacy class C is associated to such compactified direction. The fact that the quantum triple is equipped with two comultiplication maps only translates the fact that we can think of either the h–holonomy or the k–holonomy of the three-cylinder as being along the compactified direction. This also determines a choice of basis for the representation matrices.

Thanks to the antipode map S_{I}, we can define the representations $\wp^{*_{\mathrm{I}}}$ dual to the representation $\wp$ with respect to the set of fusion rules defined above. The corresponding expressions for the matrix elements are provided by

$$ D^{\wp^{*_{\mathrm{I}}}}_{MN}(g\otimes\delta_h\otimes\delta_k) = D^{\wp}_{NM}(S_{\mathrm{I}}(g\otimes\delta_h\otimes\delta_k)) = D^{\wp}_{NM}(g^{-1}\otimes\delta_{g^{-1}h^{-1}g}\otimes\delta_{g^{-1}kg})\,. \tag{6.22} $$

Moreover, the fact that the comultiplications are algebra homomorphisms implies the existence of unitary maps

$$ {}_{\mathrm{I}}\mathcal{C}^{\wp_1\wp_2} : \bigoplus_{\wp_3\in\wp_1\otimes\wp_2} V_{\wp_3} \to V_{\wp_1}\otimes_{\mathrm{I}} V_{\wp_2} \tag{6.23} $$

which satisfy

$$ D^{\wp_1}_{M_1N_1}\otimes_{\mathrm{I}} D^{\wp_2}_{M_2N_2}(\Delta_{\mathrm{I}}(g\otimes\delta_h\otimes\delta_k)) = \sum_{\wp_3}\sum_{M_3,N_3} {}_{\mathrm{I}}\mathcal{C}^{\wp_1\wp_2\wp_3}_{M_1M_2M_3}\, D^{\wp_3}_{M_3N_3}(g\otimes\delta_h\otimes\delta_k)\,\overline{{}_{\mathrm{I}}\mathcal{C}^{\wp_1\wp_2\wp_3}_{N_1N_2N_3}}\,. $$

where (M_1M_2) and $(\wp_3M_3)$ have to be understood as the indices of the matrix ${}_{\mathrm{I}}\mathcal{C}^{\wp_1\wp_2}$. As in chap. 3, we define the more symmetric symbols

$$ \begin{pmatrix} \wp_1 & \wp_2 & \wp_3 \\ M_1 & M_2 & M_3 \end{pmatrix}_{\mathrm{I}} := \frac{1}{\sqrt{d_{\wp_3}}}{}_{\mathrm{I}}\mathcal{C}^{\wp_1\wp_2\wp_3^{*_{\mathrm{I}}}}_{M_1M_2M_3} \tag{6.24} $$

which we will refer to as the $3\wp M$-symbols. The intertwining maps whose coefficients are given by the $3\wp M$-symbols are denoted $\mathcal{I}_{\mathrm{I}}^{\wp_1\wp_2\wp_3}$. The unitarity of ${}_{\mathrm{I}}\mathcal{C}^{\wp_1\wp_2}$ yields the orthogonality relation

$$ \sum_{M_1,M_2}\begin{pmatrix} \wp_1 & \wp_2 & \wp \\ M_1 & M_2 & M \end{pmatrix}_{\mathrm{I}}\overline{\begin{pmatrix} \wp_1 & \wp_2 & \wp' \\ M_1 & M_2 & M' \end{pmatrix}_{\mathrm{I}}} = \frac{1}{d_\wp}\delta_{\wp,\wp'}\delta_{M,M'}, \tag{6.25} $$

[2]This isomorphism is not true at the level of the vector spaces since it would require the g–holonomy and the k-holonomy to commute in the definition of the basis elements.

as well as the completeness relation

$$\sum_{\wp}\sum_{M} d_{\wp}\left(\begin{smallmatrix}\wp_1 & \wp_2 & \wp\\ M_1 & M_2 & M\end{smallmatrix}\right)_{\mathrm{I}}\overline{\left(\begin{smallmatrix}\wp_1 & \wp_2 & \wp\\ N_1 & N_2 & M\end{smallmatrix}\right)_{\mathrm{I}}} = \delta_{M_1,N_1}\delta_{M_2,N_2}\ . \tag{6.26}$$

Finally, it follows directly from the definition that the $3\wp M$-symbols satisfy the invariance property

$$\left(\begin{smallmatrix}\wp_1 & \wp_2 & \wp_3\\ M_1 & M_2 & M_3\end{smallmatrix}\right)_{\mathrm{I}} = \sum_{h_1,h_2,k} D^{\wp_1}_{M_1N_1}(g\otimes\delta_{h_1}\otimes\delta_k)D^{\wp_2}_{M_2N_2}(g\otimes\delta_{h_2}\otimes\delta_k)D^{\wp_3}_{M_3N_3}(g\otimes\delta_{h_2^{-1}h_1^{-1}}\otimes\delta_k)\left(\begin{smallmatrix}\wp_1 & \wp_2 & \wp_3\\ N_1 & N_2 & N_3\end{smallmatrix}\right)_{\mathrm{I}} \tag{6.27}$$

which is proven in app. (C.4). In the following, we will use these intertwining maps to define a generalization of the fusion basis to (3+1)d. The existence of two sets of fusions rules, and their corresponding intertwining maps, suggests that there are two geometrically different ways of fusing torus-excitations. Nevertheless, we restrict our attention to one type of fusion rules only. This means that all the tensor products will be defined with respect to the same comultiplication, namely Δ_{I}.

6.4 Excitation basis for (3+1)d topological phases

As for the (2+1)d case, the representation theory of the quantum triple $\mathcal{T}(\mathcal{G})$ provides us with a natural way of defining the so-called fusion basis for excited states. The (2+1)d construction relied on the fact that any Riemann surface Σ^p_{g} can be decomposed into thrice-punctured two-sphere $\mathbb{Y}$. Such a general statement does not exist for 3d manifolds. Nevertheless, we have the following result: Any three-manifolds of the form $\Sigma^p_{\mathsf{g}}\times\mathbb{S}_1$ can be obtained by gluing several copies of the manifold $\mathbb{Y}\times\mathbb{S}_1$. As we shall see, this is reminiscent of the fact that the three-cylinder $\mathbb{I}_3$ can be obtained as $\mathbb{I}\times\mathbb{S}_1$. The manifold $\mathbb{Y}\times\mathbb{S}_1$ is bounded by three copies of the two-torus $\mathbb{T}_2$. Therefore, by considering manifolds of the form $\Sigma^p_{\mathsf{g}}\times\mathbb{S}_1$, we are constructing a basis for topological phases with defect excitations located at boundary two-tori.

To construct the generalization of the fusion basis to (3+1)d topological phases, we will follow step by step the previous construction. Everytime we considered a surface Σ in (2+1)d, we will now look at the manifold $\Sigma\times\mathbb{S}_1$. In other words, we could first define the fusion basis for Σ and then take the direct product with $\mathbb{S}_1$, hence lifting the Drinfel'd double elements to quantum triple elements. Naturally the basis states will now be labeled by irreducible representations of the quantum triple. The resulting basis will also be referred to as the *fusion basis*.

So far, we have defined basis states for the three-cylinder $\mathbb{I}_3$ and the three-torus $\mathbb{T}_3$ in terms of group holonomies. The correspondence (6.12) provides the fusion basis states for the three-cylinder as the 'Fourier transform' of the basis states (6.1):

$$|\wp, MN\rangle_{\mathbb{I}_3} = \frac{1}{|\mathcal{G}|}\sum_{g,h,k\in\mathcal{G}}\sqrt{d_\wp}D^{\wp}_{MN}(g\otimes\delta_h\otimes\delta_k)$$

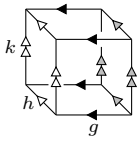

. (6.28)

By construction, these fusion basis states diagonalize the $\star$-multiplication:

$$|\wp_1, M_1N_1\rangle_{\mathbb{I}_3}\star|\wp_2, M_2N_2\rangle_{\mathbb{I}_3} = \frac{\delta_{\wp_1,\wp_2}}{\sqrt{d_{\wp_1}}}\delta_{N_1,M_2}|\wp_1, M_1N_2\rangle_{\mathbb{I}_3} \tag{6.29}$$

which confirms that the fusion basis states (6.28) on the three-cylinder are the states of elementary quasi-excitations. Analogously to (2+1)d, the conjugacy classes C and D are associated with fluxes and the representation R with charges. The obvious difference between (2+1)d and (3+1)d is therefore that the quasi-excitations carry two flux labels. Note however that these two labels are independent only in the case where the group $\mathcal{G}$ is abelian.

In particular, since the three-torus is nothing else than a three-cylinder with the pieces of its boundary identified, we deduce immediately that the fusion basis states for the three-torus read [48]

$$|\wp\rangle_{\mathbb{T}_3} = \frac{1}{|\mathcal{G}|}\sum_{g,h,k\in\mathcal{G}} \chi^{\wp}(g\otimes\delta_h\otimes\delta_k)$$ 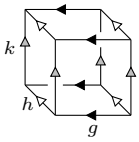 $$= \frac{1}{|\mathcal{G}|}\sum_{\substack{k\in C,\, h\in D(Z_k)\\ g\in Z_{h,k}}} \chi^{R_{h,k}}(g)|g,h,k\rangle_{\mathbb{T}_3} \tag{6.30}$$

where $Z_{h,k} = \{g\in\mathcal{G}\,|\,gh=hg\,,\,gk=kg\}$ denotes the centralizer of both the group elements h and k and $\chi^{R_{h,k}}$ the characters of the representation $R_{h,k}$ of $Z_{h,k}$ isomorphic to R. The two vertices which were located at the boundary of the three-cylinder are now identified so that the three-torus has a single bulk vertex at which $\mathbb{A}_v$ acts. The group averaging induces the contraction of the magnetic indices M and N which turns the representation matrix $D^{\wp}$ into the character $\chi^{\wp}$ defined as

$$\begin{aligned}\chi^{\wp}(g\otimes\delta_h\otimes\delta_k) = {}& \Theta_C(k)\Theta_D(p_{\iota_C(k)}^{-1}hp_{\iota_C(k)})\delta_{gh,hg}\delta_{gk,kg}\delta_{hk,kh}\\ & \times\chi^R\big(q^{-1}_{\iota_D(p^{-1}_{\iota_C(k)}hp_{\iota_C(k)})}p^{-1}_{\iota_C(k)}\,g\,p_{\iota_C(k)}q_{\iota_D(p^{-1}_{\iota_C(k)}hp_{\iota_C(k)})}\big)\end{aligned} \tag{6.31}$$

where $\Theta_C(\bullet)$ and $\Theta_D(\bullet)$ denote the characteristic functions of the conjugacy classes C and D, respectively, $\iota_C(\bullet)$ and $\iota_D(\bullet)$ are labeling functions for C and D defined such that $\iota_C(c_a)=a$ and $\iota_D(d_\alpha)=\alpha$, respectively. As in the (2+1)d, the ground-states on the three-torus are in one-to-one correspondence with the quasi-excitations defined on the three-cylinder. Remark that, as for the representation matrices, this is not the only basis possible. As a matter of fact we can define six equivalent bases which correspond to the six different ways to 'order' the variables g, h and k.

As explained above, in order to construct the fusion basis associated to surfaces of the form $\Sigma\times\mathbb{S}_1$, we need first to consider the fusion basis states for the manifold $\mathbb{Y}\times\mathbb{S}_1$. Knowing that the 'minimal' thrice-punctured two-sphere can be discretized by a triangular face whose vertices are identified, we deduce that $\mathbb{Y}\times\mathbb{S}_1$ can be minimaly discretized by a triangular prism whose six vertices are identified. The basis states associated to such a discretization are labeled by three group holonomies corresponding to the three non-contractible cycles and are represented by

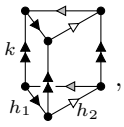 , (6.32)

where the dots represent identified vertices.

Recall furthermore that the manifold $\mathbb{Y}\times\mathbb{S}_1$ is bounded by three two-tori. Exactly as in the (2+1)d case, the discretization (6.32) is somewhat degenerate so that we would like to consider a slightly more complicated discretization which allows to associate a set of group holonomies $\{g,h,k\in\mathcal{G}\,|\,hk=kh\}$ with each of one of these tori. This discretization is obtained by gluing three three-cylinder $\mathbb{I}_3$ to each

one of the square faces of (6.32). The holonomies $\{h\}$ and $\{k\}$ then account for string-like magnetic degrees of freedom while the holonomies $\{g\}$ account for point-like electric degrees of freedom. Note however that because of the cube-geometry of the three-cylinder states, such a gluing can be performed in two different ways, or more precisely along two different orientations. Either we decide to associate the $\{k\}$-holonomies to the $\mathbb{S}_1$ direction, or the $\{h\}$-holonomies. In terms of representations, this determines the choice of comultiplication map. Because of the symmetry between the two coalgebraic structures, both possibilities are equivalent, however, for consistency requirements all the gluing must be performed according to the same orientation so that we obtain a topology of the form $\Sigma \times \mathbb{S}_1$. In the following, we will choose the orientation consistent with the graphical representation presented above so that the k-holonomy always refers the $\mathbb{S}_1$ direction. The comultiplication compatible with this choice is Δ_{I}. As such, the states defined above provide a geometrical interpretation of the fusion rules ${}_{\mathrm{I}}N$. In (2+1)d, the fusion of excitations can be imagined as replacing two punctures by a single one containing the original ones. The fusion of defects in (3+1)d boils down to the (2+1)d picture with an additional direct product with the circle.

Because of the zero-flux condition located at the triangle of the discretization (6.32), we know that, after gluing of the three $\mathbb{I}_3$ states, there will be the same constraint between $\{g\}$ and $\{h\}$-holonomies as in the (2+1)d case. There will be a further constraint which identifies the holonomies $\{g^{-1}kg\}$. This last constraint might seem surprising. It is actually reminiscent of the fact that we are working with a manifold of the form $\Sigma \times \mathbb{S}_1$ and therefore, there is only one independent holonomy in the $\mathbb{S}_1$ direction. This also justifies why we are working with comultiplication maps of the form (6.8). Indeed, we are dealing with fusion rules which ensure that the conjugacy class associated with one of the spatial directions always remain the same. This conjugacy class is the one associated with the $\mathbb{S}_1$ direction of the manifold under consideration.

It now remains to find the fusion basis states defined on the manifold $\mathbb{Y} \times \mathbb{S}_1$. The construction above suggests that one can obtain the basis states of $\mathcal{H}_{\mathbb{Y}\times\mathbb{S}_1}$ by gluing three three-cylinder fusion basis states $|\wp, MN\rangle_{\mathbb{I}_3}$ via an intertwining map $\mathcal{I}_{\mathrm{I}}^{\wp_1\wp_2\wp_3}$, *i.e.*

$$
\begin{aligned}
|\{\wp_i, M_i\}_{i=1}^3\rangle_{\mathbb{Y}} &= \mathrm{tr}_{\{V^\wp\}}\left[|\wp_1, M_1\rangle_{\mathbb{I}} \otimes_{\mathrm{I}} |\wp_2, M_2\rangle_{\mathbb{I}} \otimes_{\mathrm{I}} |\wp_3, M_3\rangle_{\mathbb{I}} \otimes \mathcal{I}_{\mathrm{I}}^{\wp_1\wp_2\wp_3}\right] \\
&= \sum_{\{N_i\}_{i=1}^3} |\wp_1, M_1N_1\rangle_{\mathbb{I}} \otimes_{\mathrm{I}} |\wp_2, M_2N_2\rangle_{\mathbb{I}} \otimes_{\mathrm{I}} |\wp_3, M_3N_3\rangle_{\mathbb{I}} \begin{pmatrix} \wp_1 & \wp_2 & \wp_3 \\ N_1 & N_2 & N_3 \end{pmatrix}_{\mathrm{I}} \\
&= \frac{1}{|\mathcal{G}|^3} \sum_{\{M_i\}_{i=1}^3} \sum_{\{g_i,h_i,k_i\}} \prod_{i=1}^3 \left(\sqrt{d_{\wp_i}} D^{\wp_i}_{M_iN_i}(g_i \otimes \delta_{h_i} \otimes \delta_{k_i}) \right.
\end{aligned}
$$

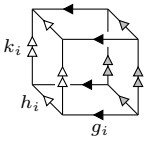

$$
\left. \begin{pmatrix} \wp_1 & \wp_2 & \wp_3 \\ N_1 & N_2 & N_3 \end{pmatrix}_{\mathrm{I}} \right) . \tag{6.33}
$$

Thanks to the invariance property (6.27) of the intertwining map $\mathcal{I}_{\mathrm{I}}^{\wp_1\wp_2\wp_3}$ and following exactly the

same steps as in (3.45), one has

$$
\begin{aligned}
&\sum_{\{N_i\}_{i=1}^3} \left(\prod_{i=1}^3 D^{\wp_i}_{M_i N_i}(g_i \otimes \delta_{h_i} \otimes \delta_{k_i})\right) \begin{pmatrix} \wp_1 & \wp_2 & \wp_3 \\ N_1 & N_2 & N_3 \end{pmatrix}_{\mathrm{I}} \\
&\quad = \sum_{p_1,p_2,k\in\mathcal{G}} \sum_{\{N_i\}_{i=1}^3} \sum_{\{O_i\}_{i=1}^3} \left(\prod_{i=1}^3 D^{\wp_i}_{M_i N_i}(g_i \otimes \delta_{h_i} \otimes \delta_{k_i})\right) \\
&\qquad\qquad \times D^{\wp_1}_{N_1 O_1}(g \otimes \delta_{p_1} \otimes \delta_k) D^{\wp_2}_{N_2 O_2}(g \otimes \delta_{p_2} \otimes \delta_k) D^{\wp_3}_{N_3 O_3}(g \otimes \delta_{p_2^{-1} p_1^{-1}} \otimes \delta_k) \begin{pmatrix} \wp_1 & \wp_2 & \wp_3 \\ O_1 & O_2 & O_3 \end{pmatrix}_{\mathrm{I}} \\
&\quad = \sum_{p_1,p_2,k\in\mathcal{G}} \sum_{\{O_i\}_{i=1}^3} \left(\prod_{i=1}^3 D^{\wp_i}_{M_i O_i}(g_i g \otimes \delta_{h_i} \otimes \delta_{k_i})\right) \\
&\qquad\qquad \times \delta_{p_1, g_1^{-1} h_1 g_1} \delta_{p_2, g_2^{-1} h_2 g_2} \delta_{p_2^{-1} p_1^{-1}, g_3^{-1} h_3 g_3} \delta_{k, g_1^{-1} k_1 g_1} \delta_{k, g_2^{-1} k_2 g_2} \delta_{k, g_3^{-1} k_3 g_3} \begin{pmatrix} \wp_1 & \wp_2 & \wp_3 \\ O_1 & O_2 & O_3 \end{pmatrix}_{\mathrm{I}} \\
&\quad = \sum_{\{O_i\}_{i=1}^3} \left(\prod_{i=1}^3 D^{\wp_i}_{M_i O_i}(g_i g \otimes \delta_{h_i} \otimes \delta_{k_i})\right) \delta(g_1^{-1} h_1 g_1 g_2^{-1} h_2 g_2 g_3^{-1} h_3 g_3, \mathbb{1}_{\mathcal{G}}) \\
&\qquad\qquad \times \delta_{g_1^{-1} k_1 g_1,\, g_2^{-1} k_2 g_2} \delta_{g_2^{-1} k_2 g_2,\, g_3^{-1} k_3 g_3} \begin{pmatrix} \wp_1 & \wp_2 & \wp_3 \\ O_1 & O_2 & O_3 \end{pmatrix}_{\mathrm{I}}
\end{aligned}
\tag{6.34}
$$

where we used the defining property of the representations of the quantum triple. By comparing the first and the last line of (6.34), we conclude that the $3\wp M$-symbols implicitly encode the zero-flux condition on the surface of $\mathbb{Y} \times \mathbb{S}_1$, the gauge invariance at the single bulk vertex, as well as the identification of the $\{g^{-1}kg\}$-holonomies along the $\mathbb{S}_1$ direction.

Using the states (6.33), we can construct the fusion basis for excited states defined on manifolds of the form $\Sigma \times \mathbb{S}_1$. To do so, we rely upon the fact that the manifold $\Sigma \times \mathbb{S}_1$ can be obtained as a sewing of several copies of $\mathbb{Y} \times \mathbb{S}_1$. The strategy is to perform such a decomposition of the manifold, associate a state $|\{\wp_i, M_i\}_{i=1}^3\rangle_{\mathbb{Y}\times\mathbb{S}_1}$ to each copy of $\mathbb{Y} \times \mathbb{S}_1$, and contract them to each other following the decomposition pattern. Equivalently, we can associate an intertwining map $\mathcal{I}^{\wp_1\wp_2\wp_3}$ to each copy of $\mathbb{Y} \times \mathbb{S}_1$ and contract them via three-cylinder fusion basis states $|\wp, MN\rangle_{\mathbb{I}_3}$. For a given manifold $\Sigma \times \mathbb{S}_1$, and for a given decomposition $\{\mathbb{Y} \times \mathbb{S}_1\}$, a formal expression for the corresponding fusion basis states therefore reads

$$
\boxed{\left|\{\wp_i\}_{i=1}^L\right\rangle_{\Sigma\times\mathbb{S}_1} = \mathrm{tr}_{\{V^\wp\}}\Big[\bigotimes_{\mathbb{I}_3} |\wp\rangle_{\mathbb{I}_3} \otimes \bigotimes_{\mathbb{Y}\times\mathbb{S}_1} \mathcal{I}^{\{\wp\}}\Big]}
\tag{6.35}
$$

where L is the number of 'connections' between the manifolds $\mathbb{Y} \times \mathbb{S}_1$. The fusion basis is *orthogonal* and *complete*. This follows directly from the orthogonality (6.17) and completeness (6.16) of the representation matrices as well as the orthogonality (6.25) and completeness (6.26) of the $3\wp M$-symbols coefficients.

6.5 Remarks and generalizations

Although the fusion basis for the three-torus, as presented in this chapter, appeared before, see *e.g.* [44, 48], the corresponding algebraic structure was yet to be explored. By following the strategy employed in (2+1)d to reveal the Drinfel'd double, we revealed this algebraic structure, namely the quantum triple $\mathcal{T}(\mathcal{G})$. In addition, we showed explicitly how the ground states on the three-torus are in one-to-one correspondence with the quasi-excitations defined on the manifold obtained by cutting the three-torus along one direction.

Furthermore, we presented a method to define the fusion basis for general excited states. In this construction, excitations are restricted to happen at boundary two-tori such that we are dealing with manifolds of the form $\Sigma \times \mathbb{S}_1$. The definition of the fusion basis relies upon the fact that such manifolds can be obtained as the sewing of several copies of $\mathbb{Y} \times \mathbb{S}_1$, namely the direct product between the thrice-punctured two-sphere and the circle. Such decomposition then dictates a simple way of constructing the basis: To each copy of $\mathbb{Y} \times \mathbb{S}_1$ we assign an intertwining map, which we contract to each other via three-cylinder basis states. The resulting states are labeled by two sets of conjugacy classes $\{C\}$ and $\{D\}$, representing fluxes, and a set of irreducible representations $\{R\}$, representing charges. The definition of the fusion basis is tied to the choice of comultiplication maps when constructing the quantum triple. Here we made a natural choice such that the fusion category of representations of the quantum triple $\mathcal{T}(\mathcal{G})$ reduces to fusion categories of representations of Drinfel'd doubles $\mathcal{D}(Z_C)$. As such, it turns out that our construction provides an algebraic translation of the dimensional reduction strategy. We could reproduce the construction presented here by replacing the three-cylinder with another manifold of the form $\Sigma \times I$. This would lead to another version of the 3d tube algebra yielding yet another algebraic structure.

The (2+1)d fusion basis associated to a given punctured surface, diagonalizes a set of closed ribbon operators [4, 84, 106]. These operators, which measure the excitation content of a given region, are constructed as a composition of Wilson loop operators and parallel-transported translation operators. We expect that the fusion basis for (3+1)d topological phases we proposed in this chapter also diagonalizes a set of analogous operators. These operators should be an extension of the ribbon operators in the same way as the quantum triple is an extension of the Drinfel'd double.

We focused our study on the case where the ground state is described by a BF theory. The natural next step of this work would be to generalize to Dijkgraaf-Witten theory which can be thought as a twisted BF theory such that the twist deforms the Gauß constraint. The twisted case differs from the non-twisted case in the definition of the local equivalence relations. In (2+1)d, when picking the graph to be the one-skeleton of a triangulation, the local equivalence relations can be defined in terms of Pachner moves. In particular, the 2–2 Pachner move is performed by a map which evaluates to a group 3-cocycle α in $H^3(\mathcal{G}, U(1))$. The tube algebra then requires three Pachner moves so that the multiplication is deformed by a phase

$$\theta_h(g_1, g_2) = \frac{\alpha(h, g_1, g_2)\alpha(g_1, g_2, (g_1 g_2)^{-1} h g_1 g_2)}{\alpha(g_1, g_1^{-1} h g_1, g_2)} \, .$$

It turns out that this phase is the slant product $i_h \alpha$ which pairs the group element h with the 3-cocycle α. Algebraically, this corresponds to turning the Drinfel'd double into a quasi Hopf algebra whose twist reads

$$\phi = \sum_{h_1, h_2, h_3} \alpha(h_1, h_2, h_3)^{-1} (\mathbb{1}_{\mathcal{G}} \otimes \delta_{h_1}) \otimes (\mathbb{1}_{\mathcal{G}} \otimes \delta_{h_2}) \otimes (\mathbb{1}_{\mathcal{G}} \otimes \delta_{h_3}) \, .$$

The same strategy generalizes to the three-cylinder algebra. The key is to realize that when working with a manifold of the form $\Sigma \times \mathbb{S}_1$ we can extend the (2+1)d construction to (3+1)d by replacing the cocycle α by the slant product $i_k \omega$ where ω is an element of $H^4(\mathcal{G}, U(1))$ and k is the holonomy along the compactified direction. Algebraically, this means deforming the quantum triple by the following twist

$$\phi = \sum_{h_1, h_2, h_3, k} i_k \omega(h_1, h_2, h_3)^{-1} (\mathbb{1}_{\mathcal{G}} \otimes \delta_{h_1} \otimes_{\mathfrak{c}} \delta_k) \otimes (\mathbb{1}_{\mathcal{G}} \otimes \delta_{h_2} \otimes_{\mathfrak{c}} \delta_k) \otimes (\mathbb{1}_{\mathcal{G}} \otimes \delta_{h_3} \otimes_{\mathfrak{c}} \delta_k)$$

In general, the result of the slant product $i_k \omega$ satisfies a so-called *twisted 3-cocycle condition*. However, thanks to the commutativity between h and k holonomies, it actually satisfies the usual group 3-cocycle

condition. This means that ϕ defines an associator, as for the Drinfel'd double, and can therefore be used in order to 'twist' the quantum triple. It finally follows from the consistency conditions satisfied by the twist ϕ that the multiplication and the comultiplications are deformed by twisted 2-cocyles obtained as slant products of $i_k\omega$. For instance, the twisted 2-cocyle deforming the multiplication rule is given by

$$\theta_{h,k}(g_1,g_2) = \frac{i_k\omega(h,g_1,g_2)i_k\omega(g_1,g_2,(g_1g_2)^{-1}hg_1g_2)}{i_k\omega(g_1,g_1^{-1}hg_1,g_2)}$$

so that the multiplication rule now reads

$$(g_1\otimes\delta_{h_1}\otimes_{\mathfrak{c}}\delta_{k_1})\star(g_2\otimes\delta_{h_2}\otimes_{\mathfrak{c}}\delta_{k_2}) := \delta_{k_2,g_1^{-1}k_1g_1}\delta_{h_2,g_1^{-1}h_1g_1}\theta_{h_1,k_1}(g_1,g_2)(g_1g_2\otimes\delta_{h_1}\otimes_{\mathfrak{c}}\delta_{k_1})$$

This generalization should be particularly interesting since it is believed that (3+1)d bosonic topological orders with bosonic point-like excitations are classified by a pair $(\mathcal{G},\omega)$, with $\mathcal{G}$ a finite group and ω a group 4-cocycle [54].

Chapter 7

Heegaard splitting and magnetic excitations in (3+1)d

We propose in this chapter a strategy to make some of the techniques developed for (2+1)d topological phases available to the (3+1)d case. This approach is more general than the one exposed in the previous chapter as it gives access to a richer structure/topology of defects, however it does not allow for a construction of excited states as systematic. The main idea is to use Heegaard splittings [165] of 3d manifolds representing spatial slices of (3+1)d space-time manifolds. Such a Heegaard splitting performs a splitting of the 3d surface into two handlebodies along a 2d surface referred to as the Heegaard surface. On this 2d Heegaard surface, the usual topological lattice models can be defined and in particular the 2d operators. By imposing additional flatness constraints, we can lift these 2d operators to (excitations generating) operators in 3d.[1] Hence we can study (magnetic) excitations for a 3d model without actually dealing with the 3d manifold itself. We will study in particular how different parameterizations of the space of flat connections on the 2d Heegaard surface lead to different gauge invariant bases for the 3d theory with magnetic excitations.

This strategy was applied in [52] in the context of (2+1)d Turaev-Viro theory where the input data is not a finite or Lie group but the quantum group $\mathrm{SU}(2)_k$, seen as a modular fusion category. In this case, different fusion bases on the 2d Heegaard surface lead, in particular, to two gauge invariant excitation bases for the (3+1)d theory, namely a quantum deformed spin network basis and a dual magnetic basis. In both cases, the parameterization of the basis states is such that it is easy to read off the local curvature (magnetic excitation). It turns out that the modularity of the category is crucial to achieve this. In this chapter, we aim to construct analogous bases in the finite group case. However, we will see that, in the case of the dual magnetic basis, it is much more complicated to obtain a local parametrization from which the excitation content can be easily read off.

Heegaard splittings and more generally handle decompositions [166] have been used to construct topological field theories in three and four dimensions e.g. [167, 168].[2] Here, however, we deal with topological field theories with defects in a *canonical* set-up, that is in a Hilbert space description where we are in particular looking for operators generating and measuring the defect excitations. To make

[1] As a matter of fact, the strategy presented here was first introduced in [6] as a systematic way to define operators generating excitations in (3+1)d.

[2] See also [169] for the use of Heegaard splitting and the associated reduction in dimension in quantum gravity models involving a sum over topologies.

the main idea clear we will focus, as in the previous chapters, on the special case of BF theory with a finite groups $\mathcal{G}$.

7.1 A simple example

Given a three-manifold $\mathcal{M}$, we are ultimately interested in bases for the Hilbert space of gauge invariant functionals on the space of locally flat connections on $\mathcal{M}$ with *line defects*. In this section, we illustrate the general idea of our construction based on Heegaard splittings with a simple example for which the computations are particularly straightforward. The rest of the chapter will be dedicated to generalizing this procedure and make some of the statements exposed in this section more precise.

7.1.1 Three-sphere with a line defect

Our aim is to define a Hilbert space of functionals on the space of flat connections for a three-manifold with defects. We will restrict our attention to the case where these topological defects are the support of *magnetic excitations*. Generally, flat connection have non-trivial holonomies along non-contractible loops only. As such, in order to obtain magnetic excitations, it is necessary to introduce defects which insert non-contractible loops.

For our first example, we choose the three-manifold to be the three-sphere $\mathbb{S}_3$. Let us consider a closed loop embedded in $\mathbb{S}_3$. By considering a regular neighborhood of this closed loop, we obtain a solid two-torus denoted by $\mathring{\mathbb{T}}_2$. It turns out that the manifold $\mathbb{S}_3\backslash\mathring{\mathbb{T}}_2$ is also isomorphic to a solid two-torus. This defines a decomposition of the three-sphere as $\mathbb{S}_3 = \mathring{\mathbb{T}}_2 \cup \mathbb{S}_3\backslash\mathring{\mathbb{T}}_2 \simeq \mathring{\mathbb{T}}_2 \cup \mathring{\mathbb{T}}_2$ which states that the three-sphere can be obtained as the gluing of two solid tori. This decomposition is referred to as the *genus-one Heegaard splitting* of the three-sphere (more detail about Heegaard splittings will be provided in sec. 7.3). The gluing of the two tori is performed along the boundary $\partial\mathring{\mathbb{T}}_2$ of the manifold $\mathring{\mathbb{T}}_2$ which is by definition isomorphic to a two-torus $\mathbb{T}_2$.

Most importantly, the manifold $\mathbb{S}_3\backslash\mathring{\mathbb{T}}_2$ contains one non-contractible cycle. States defined on such a manifold can therefore be understood as excited with respect to the ground states defined on $\mathbb{S}_3$. In order to construct explicitly these excited states, we follow two steps: (i) Define the Hilbert of gauge invariant functionals on the space of flat connections on the surface $\mathbb{T}_2$. (ii) Impose the holonomies along the contractible cycles in $\mathbb{S}_3\backslash\mathring{\mathbb{T}}_2$ to be flat. The 2d states living in the Hilbert space defined on $\mathbb{T}_2$ and satisfying these additional conditions can be interpreted as the 3d excited states we are looking for.

The two-torus is a genus one surface which carries two non-contractible cycles. These cyles which are represented in fig. 7.1.1 are referred to as the *meridional* and *equatorial* cycles. Let us denote by $|g,h\rangle_{\mathbb{T}_2}$ the graph-states defined on $\mathbb{T}_2$ where the group variables $g,h \in \mathcal{G}$ label the equatorial and the meridional cycles, respectively. As seen in chap. 3, the Hilbert space $\mathcal{H}_{\mathbb{T}_2}$ of gauge invariant functionals on the space of flat connections on $\mathbb{T}_2$ is then spanned by states

$$\mathcal{H}_{\mathbb{T}_2} = \Big\{ \frac{1}{|\mathcal{G}|} \sum_{x\in\mathcal{G}} |xgx^{-1}, xhx^{-1}\rangle \,|\, [g,h] = \mathbb{1} \Big\} \tag{7.1}$$

where $[g,h] := ghg^{-1}h^{-1}$ is the group commutator. Henceforth, we will refer to basis states defined in terms of group variables as being in the *holonomy representation*. It is now straightforward to determine the ground state degeneracy of the corresponding lattice Hamiltonian (as introduced in chap. 3) on the torus which is given as the dimension of the Hilbert space $\mathcal{H}_{\mathbb{T}_2}$, i.e.

$$\mathsf{GSD}_{\mathbb{T}_2} = \big|\{(g,h)\in\mathcal{G}^2\,,\,[g,h]=\mathbb{1}_{\mathcal{G}}\}/\mathcal{G}\big| \tag{7.2}$$

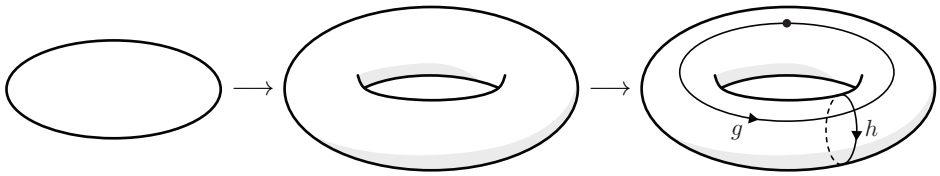

Figure 7.1. The left panel represents a closed line embedded on the three-sphere. The middle panel corresponds to a regular neighborhood of such closed line which is nothing else than a solid two-torus $\mathring{\mathbb{T}}_2$. The right panel represents a minimal graph on the boundary of the solid two-torus which capture the two non-contractible cycles of the two-torus.

where it is understood that the group $\mathcal{G}$ acts by conjugation.

Starting from the 2d ground states (7.1), it is simple to deduce the 3d excited states for $\mathbb{S}_3$ which are effectively the 3d ground states on the manifold $\mathbb{S}_3\backslash\mathring{\mathbb{T}}_2$. To do so, it is only necessary to identify the cycles which are non-contractible on $\mathbb{T}_2$ but contractible in $\mathbb{S}_3\backslash\mathring{\mathbb{T}}_2$. There is only one, namely the equatorial cycle labeled by the g–holonomy. We finally define the 3d excited states as the subset of states in $\mathcal{H}_{\mathbb{T}_2}$ satisfying $g = \mathbb{1}$. These states only depend on a conjugacy class C of $\mathcal{G}$ and are of the form

$$|C\rangle_{\mathbb{T}_2} := \frac{1}{|C|}\sum_{h\in C} |\mathbb{1}, h\rangle_{\mathbb{T}_2} \ . \tag{7.3}$$

We remark that the parametrization we choose for the states on the torus persists when defining the excited states. This suggests that different choices of parametrization may lead to excited states labeled by different set of variables. But as we already know, there is another basis of ground states for the torus, namely the fusion basis. Recall that this basis is parametrized by a conjugacy class C of $\mathcal{G}$ and an irreducible representation R of the centralizer Z_C of C which is defined as $\{g \in G \,|\, [g, c_1] = \mathbb{1}\}$. The expression of these alternate basis states reads

$$|R, C\rangle_{\mathbb{T}_2} = \frac{1}{|\mathcal{G}|}\sum_{\substack{h\in C\\ g\in Z_h}} \chi^R(g)\ |g, h\rangle_{\mathbb{T}_2} \ . \tag{7.4}$$

where $Z_h = \{g \in \mathcal{G} \,|\, [g, h] = \mathbb{1}\}$ is the centralizer of the group element h and χ^R denotes the character of the representation R. In such a parametrization, we can obtain the 3d excited states (7.3) as a superposition of the 2d ground states on the torus as parameterized in (7.4). Indeed, we have

$$\begin{aligned}\sum_R d_R |R, C\rangle_{\mathbb{T}_2} &= \frac{1}{|\mathcal{G}|}\sum_{\substack{h\in C\\ g\in Z_h}}\sum_R d_R\chi^R(g)\ |g, h\rangle_{\mathbb{T}_2}\\ &= \frac{1}{|C|}\sum_{h\in C} |\mathbb{1}, h\rangle_{\mathbb{T}_2} = |C\rangle_{\mathbb{T}_2}\end{aligned} \tag{7.5}$$

where we made use of the well-known identity for finite groups

$$\frac{1}{|Z_C|}\sum_R d_R\chi^R(g) = \delta_{g,\mathbb{1}} \ . \tag{7.6}$$

So, starting from the fusion basis parameterization for the ground states on the torus, we obtained excited states which are still parameterized by a conjugacy class C. However, there exists yet another alternate basis for the ground states on the two-torus which is still parameterized by the labels (C, R).

This basis is obtained via the so-called *S-transformation* which sends the graph state $|g,h\rangle_{\mathbb{T}_2}$ to $|h^{-1},g\rangle_{\mathbb{T}_2}$ and reads

$$|R,C\rangle_{\mathbb{T}_2} = \frac{1}{|\mathcal{G}|}\sum_{\substack{h\in C\\ g\in Z_h}} \chi^R(g)|h^{-1},g\rangle_{\mathbb{T}_2} \tag{7.7}$$

$$= \frac{1}{|\mathcal{G}|}\sum_{\substack{g^{-1}\in C\\ h\in Z_g}} \chi^R(h)|g,h\rangle_{\mathbb{T}_2}\ . \tag{7.8}$$

As before, we impose the contractibility of the cycle labeled by the g–holonomy in this last expression. But now, this imposes the conjugacy class C to be trivial so that the excited states are parameterized by an irreducible representation R over the full group, whose expression simply reads

$$|R\rangle_{\mathbb{T}_2} = \frac{1}{|\mathcal{G}|}\sum_{h\in\mathcal{G}} \chi^R(h)|\mathbb{1},h\rangle_{\mathbb{T}_2}\ . \tag{7.9}$$

The states $|R\rangle_{\mathbb{T}_2}$ which form a subset of the 2d ground states on the two-torus $\mathbb{T}_2$ correspond to 3d excited states living on $\mathbb{S}_3\backslash\mathring{\mathbb{T}}_2$ with respect to the 3d ground states defined on $\mathbb{S}_3$. In other words, the states $|C\rangle_{\mathbb{T}_2}$ and $|R\rangle_{\mathbb{T}_2}$ define bases for the 3d Hilbert space of gauge invariant functionals everywhere flat but along the meridional cycle of the two-torus. Note that the states $|R\rangle_{\mathbb{T}_2}$ are effectively spin network basis states for the 3d theory while the states $|C\rangle_{\mathbb{T}_2}$ define a dual gauge invariant (magnetic) basis.

The reason why it is possible to have the excited states labeled by either conjugacy classes or irreducible representations is because there is a well-known result in finite group theory which states that the number of conjugacy classes matches the number of irreducible representations. Furthermore, because both the set of states $\{|C\rangle_{\mathbb{T}_2}\}$ and $\{|R\rangle_{\mathbb{T}_2}\}$ define a basis of excited states, there must be a map which sends one basis to the other. Indeed, one has the following relation

$$\begin{aligned}\sum_R \overline{\chi^R(C)}|R\rangle_{\mathbb{T}_2} &= \frac{1}{|\mathcal{G}|}\sum_{h\in\mathcal{G}}\sum_R \overline{\chi^R(C)}\chi^R(h)|\mathbb{1},h\rangle_{\mathbb{T}_2}\\ &= \frac{|Z_C|}{|\mathcal{G}|}\sum_{h\in\mathcal{G}}\Theta_C(h)|\mathbb{1},h\rangle_{\mathbb{T}_2}\\ &= \frac{1}{|C|}\sum_{h\in C}|\mathbb{1},h\rangle_{\mathbb{T}_2} = |C\rangle_{\mathbb{T}_2}\end{aligned} \tag{7.10}$$

where $\Theta_C(h)$ is the characteristic function of the conjugacy class C. The second line follows from the completeness of the characters and in the last line we used the fact that $|\mathcal{G}| = |C|\cdot|Z_C|$. Conversely, we have

$$\begin{aligned}\frac{1}{|\mathcal{G}|}\sum_C |C|\chi^R(C)|C\rangle_{\mathbb{T}_2} &= \frac{1}{|\mathcal{G}|}\sum_C\sum_{h\in C}\chi^R(C)|\mathbb{1},h\rangle_{\mathbb{T}_2}\\ &= \frac{1}{|\mathcal{G}|}\sum_{h\in\mathcal{G}}\chi^R(h)|\mathbb{1},h\rangle_{\mathbb{T}_2} = |R\rangle_{\mathbb{T}_2}\ .\end{aligned} \tag{7.11}$$

In the rest of the paper, we will make the ideas presented in this example more precise in order to apply our procedure to more general topology and more general defect structures. In particular, we will be interested in studying in detail the dual gauge invariant magnetic basis and to which extent the corresponding parameterization sometimes fails to provide explicitly the curvature content associated with each edge of the defect skeletal structure.

7.1.2 Drinfel'd double and S-transformation

We defined above basis states for the Hilbert space of gauge invariant functionals on the space of flat connections on the torus. These basis states were parametrized by a pair (C, R) which labels the irreducible representations of the Drinfel'd double $\mathcal{D}(\mathcal{G})$. Making explicit use the Drinfel'd double, we can express some of the previous statements in algebraic terms.

Using the definition (3.41) for the characters χ^ρ of $\mathcal{D}(\mathcal{G})$, we saw in chap. 3 that we can rewrite the basis states (7.4) as follows:

$$|\rho\rangle^A_{\mathbb{T}_2} = \frac{1}{|\mathcal{G}|}\sum_{g,h}\chi^\rho(g\otimes\delta_h)|g,h\rangle_{\mathbb{T}_2}\ . \tag{7.12}$$

Using this definition, we can provide a simple formula for the matrix elements of the S-transformation. Recall that the map S is defined as sending the Drinfel'd double element $g\otimes\delta_h$ to $h^{-1}\otimes\delta_g$, or equivalently the state $|g,h\rangle_{\mathbb{T}_2}$ to $|h^{-1},g\rangle_{\mathbb{T}_2}$. Let us first rewrite the alternate fusion basis states on the torus (7.7) using the definition of the characters as

$$|\rho\rangle^B_{\mathbb{T}_2} = \frac{1}{|G|}\sum_{g,h}\chi^\rho(h\otimes\delta_{g^{-1}})|g,h\rangle_{\mathbb{T}_2}\ . \tag{7.13}$$

The transformation between the basis states $|\rho\rangle_{\mathrm{A}}$ and $|\rho\rangle_{\mathrm{B}}$ can therefore be written

$$\begin{aligned}
|\rho\rangle^{\mathrm{A}}_{\mathbb{T}_2} &= \frac{1}{|G|}\sum_{g,h}\chi^\rho(g\otimes\delta_h)\ |g,h\rangle_{\mathbb{T}_2}\\
&= \frac{1}{|G|}\sum_{g,h}\sum_{\widetilde{\rho}}\chi^\rho(g\otimes\delta_h)\overline{\chi^{\widetilde{\rho}}(h\otimes\delta_{g^{-1}})}\ |\widetilde{\rho}\rangle^{\mathrm{B}}_{\mathbb{T}_2}\\
&= \sum_{\widetilde{\rho}}\left(\frac{1}{|G|}\sum_{g,h}\overline{\chi^\rho(g\otimes\delta_h)}\ \overline{\chi^{\widetilde{\rho}}(h\otimes\delta_g)}\right)|\widetilde{\rho}\rangle^{\mathrm{B}}_{\mathbb{T}_2} =: \sum_{\widetilde{\rho}}S^{\rho\widetilde{\rho}}\ |\widetilde{\rho}\rangle^{\mathrm{B}}_{\mathbb{T}_2}
\end{aligned} \tag{7.14}$$

where we used the fact that $\overline{\chi^\rho(g\otimes\delta_h)} = \chi^\rho(g^{-1}\otimes\delta_h)$. Equation (7.14) provides the matrix elements $S^{\rho\widetilde{\rho}} \equiv S^{R\widetilde{R}}_{C\widetilde{C}}$ of the S-transformation. We can finally recover the transformations (7.10) and (7.11) as

$$|R\rangle^A_{\mathbb{T}_2} = \sum_{\widetilde{R},\widetilde{C}} S^{R\widetilde{R}}_{C_1\widetilde{C}}|\widetilde{R},\widetilde{C}\rangle^B_{\mathbb{T}_2} = \frac{1}{|G|}\sum_{\widetilde{C}}|\widetilde{C}|\chi^R(\widetilde{C})|\widetilde{C}\rangle^B_{\mathbb{T}_2} \tag{7.15}$$

$$|C\rangle^A_{\mathbb{T}_2} = \sum_R\sum_{\widetilde{R},\widetilde{C}} S^{R\widetilde{R}}_{C\widetilde{C}}d_R|\widetilde{R},\widetilde{C}\rangle^B_{\mathbb{T}_2} = \sum_{\widetilde{R}}\overline{\chi^{\widetilde{R}}(C)}|\widetilde{R}\rangle^B_{\mathbb{T}_2}\ . \tag{7.16}$$

7.2 Polarizations for the Hilbert space of flat connections

In the previous section, we illustrated with a simple example our strategy to define Hilbert spaces of excited states for three-dimensional topological phases. This strategy can be summarized as follows: Firstly, we define the Hilbert of gauge invariant functionals on the space of flat connections on a two-dimensional surface obtained from a Heegaard splitting (defined in detail in sec. 7.3). Secondly, we impose the holonomies along the contractible cycles in one of the two three-manifolds resulting from the Heegaard splitting to be trivial, in order to obtain a Hilbert space of excited states for the original three-manifold. In this section, we focus on the first step, namely the construction of the Hilbert space

of flat connection on two-dimensional surfaces. We have already explained how to define such Hilbert space in the previous chapters, however, we would like to emphasize that it can be parametrized in several ways. The reason why we are going through these explanations is because for topologies more complicated than the two-torus, the definition of the spin network basis and the dual magnetic basis is rather involved and requires to work in a special polarization for the initial 2d Hilbert space.

7.2.1 Hilbert space

Let $\mathcal{M}$ be a compact, oriented manifold, with or without boundary. We are interested in the Hilbert space $\mathcal{H}_{\mathcal{M}}$ of gauge invariant functionals on the space of flat connections on $\mathcal{M}$. Recall that by definition of flat connections, we can label the gauge field configurations by homeomorphisms of the fundamental group $\pi_1(\mathcal{M})$ to the finite group $\mathcal{G}$. Let Γ be a minimal graph embedded in $\mathcal{M}$ which captures at least the loops of the fundamental group $\pi_1(\mathcal{M})$. The configuration space is completely characterized by the holonomies along the edges of Γ.

The Hilbert space of (non-gauge invariant) functionals on the space of flat connections is spanned by the functionals $\psi : \mathcal{G}^L \to \mathbb{C}$ on the space of holonomies, where L denotes the number of links in Γ. Furthermore, this Hilbert space is equipped with an inner product defined as

$$\langle \psi_1, \psi_2 \rangle = \frac{1}{|\mathcal{G}|^L} \sum_{\{g_l\}} \overline{\psi_1(\{g_l\})}\, \psi_2(\{g_l\}) \tag{7.17}$$

where g_l denotes the group element corresponding to the holonomy along the link l.

Gauge transformations are parametrized by $\{u_n\}_n \in \mathcal{G}^N$, where n denotes a node of Γ and N the number of such nodes. A gauge transformation acts on a holonomy configuration $\{g_l\} \in \mathcal{G}^L$ as

$$(\{u_n\}_n \triangleright \psi)\,(\{g_l\}) \;=\; \psi(\{u_{t(l)}^{-1}\, g_l\, u_{s(l)}\})\;, \tag{7.18}$$

where $s(l)$ and $t(l)$ denote the source and target nodes of the link l, respectively. As usual, we will consider the subspace of functions which are invariant under gauge transformation at every node which is not located at the boundary of the manifold. We refer to such nodes as *bulk nodes* in opposition to the *boundary* nodes.

This definition is valid in any dimension but we will use it for two-dimensional closed manifolds $\Sigma^{\mathtt{g}}$ of genus-$\mathtt{g}$ serving as Cauchy-surfaces of a three-dimensional theory. This Hilbert space will then be used to construct a Hilbert space for a three-dimensional Cauchy hypersurface 'with defects'. We will now present several parameterizations for the space of flat connections on $\Sigma^{\mathtt{g}}$ modulo gauge transformations

7.2.2 Holonomy parametrization

The first parametrization is based on a minimal set of holonomies. Let $\Sigma^{\mathtt{g}}$ be a closed genus-$\mathtt{g}$ two-dimensional hypersurface. It is possible to represent $\Sigma^{\mathtt{g}}$ as a sphere with $\mathtt{g}$ handles glued to it (see fig. 7.2). More precisely, we can obtain $\Sigma^{\mathtt{g}}$ by gluing two-punctured two-spheres (or cylinders) to a $2\mathtt{g}$-punctured two-sphere. Choosing a base point n_b on the sphere, we construct a minimal graph by choosing for each handle i an oriented curve that starts and ends at n_b and by going along the handle i only. The orientation of the curve induces an orientation for the handle which allows to differentiate between the *source* and *target* punctures on the sphere to which the handle is glued.

Furthermore, to every curve going along a handle, we assign a node n_i which is located on the curve, as well as another curve starting and ending at n_i which goes around this (and only this) handle

once. The orientation of this curve is chosen such that it goes anti-clockwise around the corresponding source puncture as seen from the target puncture. The resulting graph is denoted by Γ (see fig. 7.2).

Let us now define a *graph connection* on this graph Γ by assigning $\{g_i\}$ holonomies to the links going from the base point n_b to the node n_i on the handle i and $\{h_i\}$ to the links going around the handle i from n_i to n_i. The remaining links, that is the links going from the nodes n_i to the base point n_b are associated with a trivial holonomy. This can be understood as a gauge fixing condition for the gauge action at the nodes n_i.

So far, we have defined a graph connection on Γ by assigning a set of group elements $\{g_i, h_i\}_{i=1}^{\mathsf{g}}$. But this connection is not necessarily flat. In order to enforce the flatness constraint, we need to impose that contractible cycles to be associated with trivial holonomies. There is a contractible path which goes around each of the punctures once and starts and ends at n_b. Such path can be contracted to a trivial path and therefore the corresponding holonomy must be trivial. This flatness condition can be also understood as imposing the Bianchi identity for the sphere. To give the flatness constraint explicitly we assume that the links from the base point to the handles i can be cyclically ordered around n_b, without any crossings, as follows: If we denote by l_i the link from n_b to n_i and by l_i' the link from n_i to n_b the cyclic ordering in the clockwise direction is given by $(l_1, l_1', l_2, l_2', \dots, l_{\mathsf{g}}, l_{\mathsf{g}}')$. The flatness constraint finally reads

$$\prod_{i=1}^{\mathsf{g}} [g_i, h_i] \;=\; \mathbb{1}\;. \tag{7.19}$$

Furthermore, there is a remaining gauge action at the base point n_b. This leads to an adjoint action on the both the group elements $\{g_i\}$ and $\{h_i\}$ since we assume that the gauge fixing discussed above remains intact:

$$\{g_i, h_i\}_{i=1}^{\mathsf{g}} \longrightarrow \{G g_i G^{-1}, G h_i G^{-1}\}_{i=1}^{\mathsf{g}}\;. \tag{7.20}$$

We notice in particular that such simultaneous action by conjugation preserves the flatness constraint (7.19). In summary, the space of flat connection on a genus g surface is parametrized by equivalence classes

$$(\mathcal{G}^{2\mathsf{g}})_{|\text{flat}}/\text{Ad}(\mathcal{G}) \tag{7.21}$$

such that the flatness constraint (7.19) is satisfied.

We will now present a parameterization which is based on a *non-minimal* graph. As we will see, the purpose of this is to go towards a more local description. Later, this will be used in an attempt to provide a parameterization for the 3d excited states from which the local curvature can be easily read off.

The first step consists in using the fact that every two-dimensional Riemann surface can be obtained as a gluing of thrice-punctured two-sphere denoted by $\mathbb{Y}$. More precisely, we can decompose a closed surface of genus g, with $\mathsf{g} \geq 2$, into $2\mathsf{g}-2$ thrice-punctured two-spheres $\mathbb{Y}$.[3] We label the thrice-punctured spheres by $k = 1, \dots, (2\mathsf{g}-2)$ and we choose a base node $n_k^{\mathbb{Y}}$ on each sphere. Furthermore, as before, we assign the $(3\mathsf{g}-3)$ cylinders which are glued to the punctures with an orientation so that we can define source and target punctures associated to a given cylinder. Source and target punctures are all equiped with a marked point living at the boundary of the corresponding disks. These marked

[3] This simply follows from Euler's formula which states that for a convex three-dimensional polyheron: $\#_{\text{loops}} = \#_{\text{edges}} - \#_{\text{vertices}} + 1$. Since we are looking for a decomposition into thrice-puncture spheres, have the further constraint that $3\#_{\text{vertices}} = 2\#_{\text{edges}}$. Setting $\#_{\text{loops}} = \mathsf{g}$, we finally obtain $\#_{\mathbb{Y}} = \#_{\text{vertices}} = 2\mathsf{g} - 2$.

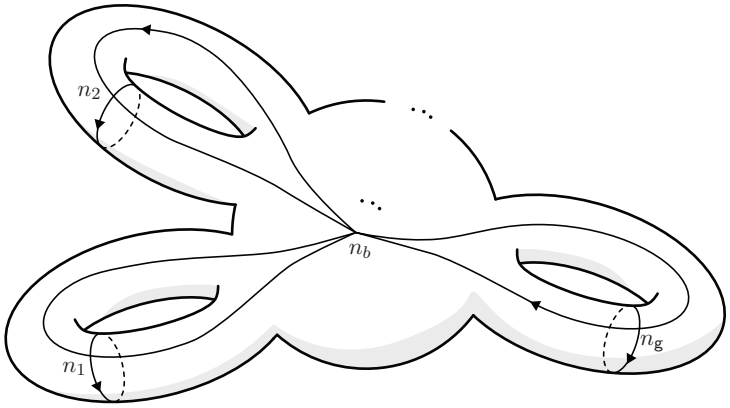

Figure 7.2. A genus-g two-dimensional hypersurface can be obtained by gluing g cylinders to a $2\mathsf{g}$-punctured two-sphere. We then define a graph Γ on the surface which captures all the non-contractible cycles.

points, which serve as nodes for the graph Γ, are denoted by $n^{\mathbb{I}}_{s(a)}$ and $n^{\mathbb{I}}_{t(a)}$ with $a = 1, \dots, (3\mathsf{g}-3)$. Putting everything together, we construct the graph[4] Γ together with a graph connection by choosing:

- For each of the source $s(a)$ and target punctures $t(b)$ on a given sphere k, a link from the base point $n^{\mathbb{Y}}_k$ to the marked points $n^{\mathbb{I}}_{s(a)}$ and $n^{\mathbb{I}}_{t(a)}$, respectively. We then associate a trivial holonomy to these links, or equivalently, we use the gauge freedom at the marked points in order to gauge fix them to the identity.
- For each cylinder a a link from its source node $n^{\mathbb{I}}_{s(a)}$ to its target node $n^{\mathbb{I}}_{t(a)}$. We associate a holonomy $g_a = g_{t(a)s(a)}$ to this link and such that the inverse holonomy g_a^{-1} is denoted by $g_{s(a)t(a)}$.
- For each cylinder a we define a link around the corresponding target puncture with *clockwise* orientation (as seen on the target sphere) which starts and ends at $n^{\mathbb{I}}_{t(a)}$. The corresponding holonomy is denoted by $h_{t(a)}$. Sometimes, it is also convenient to consider links around the source punctures so that the orientation matches the previous one. Flatness along the cylinder then imposes that the corresponding holonomy reads $h_{s(a)} := g_a^{-1} h_{t(a)}^{-1} g_a$ for these links.

The graph associated with a thrice-punctured two-sphere following these conventions is represented fig. 7.3.

As before, such a parametrization $\{g_a, h_a\}_{a=1}^{3\mathsf{g}-3}$ is over-complete since additional constraints and equivalence relations need to be imposed. Firstly, for each sphere there is a flatness constraint which can be interpreted as the Bianchi identity. Consider a sphere k and a clockwise ordering of the links around the base node $n^{\mathbb{Y}}_k$ given by $((a_1, o_1), (a_2, o_2), (a_3, o_3))$ where $o = s, t$ denotes whether the puncture is a *source* or *target* one, respectively. The flatness constraint is then given by

$$h_{o_3(a_3)} h_{o_2(a_2)} h_{o_1(a_1)} = \mathbb{1} \ . \tag{7.22}$$

Such expression typically involves g_a holonomies via the definition $h_{s(a)} := g_a^{-1} h_{t(a)}^{-1} g_a$. Secondly, there might be redundancies for the set of flatness constraints, e.g. for a genus three surface one finds only three independent flatness constraints. In general, we find that the number of independent flatness constraints matches the genus of the surface. Finally, we are looking for equivalence classes under

[4] We do not allow any crossing of the links accept at the nodes.

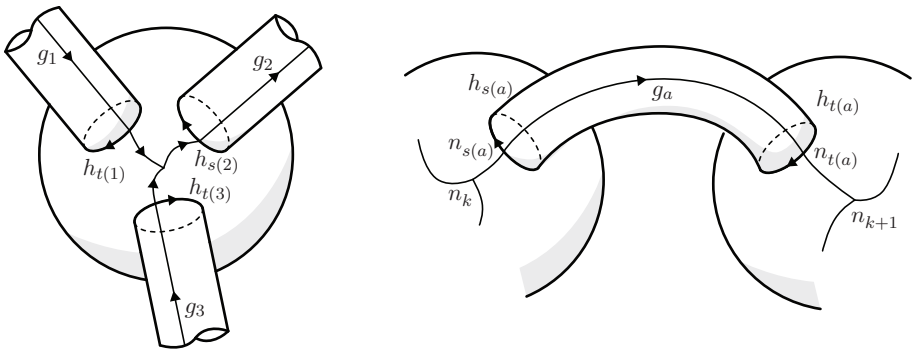

Figure 7.3. Example of thrice-punctured two-sphere $\mathbb{Y}$ with connected cylinders. The corresponding fusion basis state is given by $\mathrm{tr}\big[|\rho_1^*\rangle_{\mathbb{I}} \otimes |\rho_2\rangle_{\mathbb{I}} \otimes |\rho_3\rangle_{\mathbb{I}} \otimes C^{\rho_1^*\rho_2\rho_3}\big]$ where the Clebsch-Gordan coefficient encodes the flatness constraint as well as the gauge invariance.

gauge action at the base node $n_k^{\mathbb{Y}}$ of every thrice-punctured two-sphere. A transformation with gauge parameters $\{G_k\}_{k=1}^{2\mathsf{g}-2}$ acts as

$$\{g_{t(a)s(a)}, h_{t(a)}\}_{a=1}^{3\mathsf{g}-3} \longrightarrow \{G_{t(a)}^{-1} g_{t(a)s(a)} G_{s(a)}, G_{t(a)}^{-1} h_{t(a)} G_{t(a)}\}_{a=1}^{3\mathsf{g}-3} \,. \tag{7.23}$$

As before, it is always possible to preserve the gauge fixing for the holonomy going from $n_a^{\mathbb{I}}$ to the the marked point of the target puncture. To summarize, we now have a parametrization of flat graph connection by equivalence classes

$$(G^{6\mathsf{g}-6})_{|\mathrm{flat}}/G^{2\mathsf{g}-2} \tag{7.24}$$

where the holonomy configurations have to satisfy the flatness constraints (7.22) as well as the equivalences described by the gauge orbits defined in (7.23).

This description can be easily modified by contracting cylinders, which connect two different spheres, and thus joining these two spheres so as to obtain spheres carrying more than three punctures. A contraction of a cylinder removes a $(g_a, h_{t(a)})$ pair from the configuration space—which is consistent as one has also reduced the number of spheres, and thus the number of flatness constraints and gauge actions by one. We could also show that a contraction of cylinders along a maximal spanning tree (of the spine graph defined by taking the spheres as nodes and cylinders as edges) recovers consistently the *minimal* holonomy description given above.

7.2.3 Towards the Drinfel'd double parametrization

The *non-minimal holonomy parametrization* as defined above is not free, in the sense that many flatness constraints remain to be imposed on the holonomies, and we still have to factor out the gauge action. Starting from the holonomy parametrization which is based on a decomposition of the genus g surface into thrice-punctured two-spheres $\mathbb{Y}$, we will attempt to fix the gauge action and at the same time to solve for the flatness constraints associated with the spheres.[5]

Let us first consider the holonomies $\{h\}$ going around the punctures. The gauge invariance requires the parameterization to be invariant under adjoint action on such holonomies. Therefore, we can readily find a gauge invariant characterization in terms of the corresponding conjugacy classes. For

[5]Ultimately, this will be used to understand why the dual magnetic basis cannot typically be parameterized in terms of conjugacy classes only.

each $\mathbb{Y}$ we have three clockwise-ordered punctures labeled by $((a_1, o_1), (a_2, o_2), (a_3, o_3))$ with $o = s, t$. The corresponding holonomies $(h_{o_1(a_1)}, h_{o_2(a_2)}, h_{o_3(a_3)})$ then satisfy the flatness constraint (7.22).

A gauge invariant characterization of this triple of holonomies is obtained by using their conjugacy classes $(C_{o_1(a_1)}, C_{o_2(a_2)}, C_{o_3(a_3)})$. The flatness constraint then selects which triples of conjugacy classes are allowed to appear. In order to perform such selection, it is convenient to introduce *fusion rules* for the conjugacy classes. Let us consider the set

$$S = \{(h_{o_1(a_1)}, h_{o_2(a_2)}, h_{o_3(a_3)}) \in C_{o_1(a_1)} \times C_{o_2(a_2)} \times C_{o_3(a_3)} \,|\, h_{o_3(a_3)} h_{o_2(a_2)} h_{o_1(a_1)} = \mathbb{1}\} \,. \tag{7.25}$$

The number of orbits the set S splits into under simultaneous conjugation defines the so-called fusion rules denoted by $N_{C_{o_1 a_1} C_{o_2(a_2)} C_{o_3(a_3)}}$. The fusion rules are non-vanishing only when the triple of conjugacy classes is admissible. As the name suggests, we can indeed understand this statement as a condition for the magnetic excitations labeled by $C_{o_1(a_1)}$ and $C_{o_2(a_2)}$ to fuse so as to obtain a magnetic excitation labeled by $C_{o_3(a_3)^{-1}}$ which is defined to be the conjugacy class of the inverse of any element of $C_{o_3(a_3)}$. More precisely, the fusion rules counts the number of inequivalent ways of satisfying such a fusion. In the following, we will assume for notational convenience that for each allowed triple of conjugacy classes, there is only one representative triple of holonomies which satisfy the flatness constraint modulo a common adjoint action of the group, that is $N = 0, 1$. This amounts to assuming multiplicity freeness for the associated coupling.

Replacing the h–holonomies by their conjugacy classes C_h, and allowing for each thrice-punctured sphere only triplets of admissible conjugacy, is a first step towards a gauge-invariant parametrization. Note that if the target puncture of the cylinder is labeled by C_h, the source puncture is labeled by the conjugacy class $C_{h^{-1}}$. Let us now analyze the remaining gauge freedom in more detail. Let us consider an (ordered) triple of conjugacy classes (C_1, C_2, C_3) such that the corresponding fusion rules are non-vanishing and let us choose a representative (ordered) triplet of holonomies $(h_1, h_2, h_3) \in C_1 \times C_2 \times C_3$ satisfying $h_3 h_2 h_1 = \mathbb{1}$. We denote by $Z_{C_1 C_2 C_3}$ the stabilizer group with respect to a simultaneous adjoint action of this representative triplet. For each $\mathbb{Y}$, we equip the punctures with clockwise ordering and assign each ortiented cylinder with a conjugacy class so that the coupling conditions are satisfied. Assume that we have a configuration $\{g_{t(a)s(a)}, h_{t(a)}\}_{a=1}^{3\mathtt{g}-3}$ consistent with this choice of conjugacy classes. We can use the gauge freedom at each $\mathbb{Y}$ to transform each consistent triplet of holonomies $(h_{o_1(a_1)}, h_{o_2(a_2)}, h_{o_3(a_3)})$ into the representative triplet of holonomies determined by the triplet $(C_{o_1(a_1)}, C_{o_2(a_2)}, C_{o_3(a_3)})$ of conjugacy classes. This fixes all the gauge freedom but for the one given by the centralizer group $Z_{C_1 C_2 C_3}$ associated with every $\mathbb{Y}$.

So far we have been focusing on the h–holonomies, let us now consider the g–holonomies. More precisely, we want to determine how much freedom is left, after the above gauge fixing, in choosing the g–holonomies. The assignment of conjugacy classes to the cylinders, together with the above gauge fixing, determines uniquely all the $h_{s(a)}$ and $h_{t(a)}$ holonomies. For a given cylinder a with conjugacy class $C = C_a$ the choice of holonomy $g = g_a$ is restricted since the identity $h_s^{-1} := g^{-1} h_t g$ need to be satisfied so that it must take the form

$$g \;=\; q_{\iota_C(h_t)} \cdot z \cdot q^{-1}_{\iota_C(h_s^{-1})} \tag{7.26}$$

where $z \in Z_C$, the centralizer group of C, and ι_C is a labeling function such that $q_{\iota_C(h)}$ are elements of the quotient group G/Z_C satisfying $c_1 = q^{-1}_{\iota_C(h)} h q_{\iota_C(h)}$ with c_1 the representative of C.

Most importantly, it follows from the previous relation that for each cylinder a the freedom left in choosing g_a is parametrized by the centralizer group Z_{C_a} of the conjugacy class C_a associated with the cylinder. Together with the remaining gauge freedom given by the centralizer groups $Z_{C_1 C_2 C_3}$

associated with each thrice-punctured two-sphere, it turns out that the task of finding a gauge invariant parametrization leads to finding the irreducible representations of the so-called *Drinfel'd double*. It should now be clear that we are slowly reconstructing the fusion basis for a genus-$\mathtt{g}$ making this detailed description look a little bit cumbersome. However, we will make use of this non-minimal holonomy parametrization explicitly in the following.

7.2.4 The Drinfel'd double parametrization

Defining the Drinfel'd double parametrization amounts to constructing the fusion basis. Therefore, given a two-dimensional surface Σ, we obtain the Drinfel'd double parameterization as follows: (*i*) Choose a pant decomposition $\{\mathbb{Y}\}$ of the surface Σ. (*ii*) Associate with each $\mathbb{Y}$ a fusion basis state obtained as the gluing of three cylinder states via a Clebsch-Gordan coefficient. (*iii*) Glue all the fusion basis states together by summing over the corresponding vector space indices according to the pattern of the pant decomposition.

Thus to each cylinder one associates a Drinfel'd double irreducible representation $\rho = (C, R)$ where C denotes a conjugacy class of $\mathcal{G}$ and R an irreducible representation of the centralizer group Z_C of C. We have furthermore coupling conditions for each triple of representations ρ_1, ρ_2, ρ_3 (conjugated for each source puncture) meeting at a sphere. These coupling conditions are described by the fusion category resulting from considering the tensor product between the representations and entail the coupling conditions for the conjugacy classes alone.

The C_a-labels therefore agree with the one of the parameterization discussed above. The remaining labels R_a denote irreducible representations of the centralizer groups Z_{C_a} of C_a. Indeed we have seen in the previous section that the freedom in the g-connections is parametrized by the centralizer groups Z_{C_a}, but that there is a remaining gauge freedom given by the centralizer groups $Z_{C_1C_2C_3}$ associated to each thrice-punctured sphere. In fact, a further inspection of the Drinfel'd double representations reveals that they encode the g-connection into a spin network where the representation labels conditioned are not free but depend on the C-labels: The representation labeling a given edge of this spin network must be an irreducible representation of the centralizer group of the corresponding conjugacy class. This spin network description ensures gauge invariance with respect to the remaining gauge freedom given by the centralizers $Z_{C_1C_2C_3}$. Consequently, this means that the freedom in choosing the flat connection so that the gauge invariance is satisfied is parametrized by the labels of the irreducible representations of the Drinfel'd double. The corresponding basis is the fusion basis.

7.3 Lifting procedure to the (3+1)d case

We will now present the main result of this chapter, namely the construction of bases for topological phases with magnetic excitations. The first step of this construction consists in applying the previous procedure to define the Hilbert space of flat connections $\mathcal{H}_{\Sigma_\mathsf{H}}$ on a two-dimensional surface Σ_H obtained from a Heegaard splitting of a three-manifold $\mathcal{M}$. By imposing further constraints on the 2d states in $\mathcal{H}_{\Sigma_\mathsf{H}}$ we obtain a Hilbert space of 3d excited states for the three-manifold $\mathcal{M}$.

7.3.1 Heegaard splitting

A *Heegaard splitting* [166] is a decomposition of a compact three-manifold $\mathcal{M}$ into two handlebodies $\mathcal{M}_1$ and $\mathcal{M}_2$ such that $\mathcal{M} = \mathcal{M}_1 \cup \mathcal{M}_2$. This splitting is performed along the so-called Heegaard surface Σ_H, that is Σ_H is the boundary of each of the two handlebodies $\partial\mathcal{M}_1 = \partial\mathcal{M}_2 = \Sigma_\mathsf{H}$.

One way of obtaining such a splitting is via a triangulation. Let $\triangle$ be a trianguation of $\mathcal{M}$ and $\triangle_1$ its one-skeleton, i.e. the union of its vertices and edges. We then consider the regular neighbourhood $\mathbf{\Delta}_1$ of $\triangle_1$ obtained by blowing up the vertices and edges into a union of 3-balls and solid cylinders respectively. This regular neighbourhood provides the first handlebody $\mathcal{M}_1 \simeq \mathbf{\Delta}_1$ and $\mathcal{M}_2$ is defined as its complement in $\mathcal{M}$ i.e. $\mathcal{M}\backslash\mathbf{\Delta}_1$. The surface of this regular neighbourhood defines the Heegaard surface $\Sigma_{\mathsf{H}}(\triangle)$ associated with the triangulation $\triangle$.

Similarly we can consider the regular neighbourhood of the dual graph Υ to the triangulation that is homomorphic to $\mathcal{M}_2$ defined above, that is the complement of the regular neighbourhood of the one-skeleton $\mathbf{\Delta}_1$ in $\mathcal{M}$. The surface of the regular neighbourhood of the dual graph is homeomorphic to $\Sigma_{\mathsf{H}}(\triangle)$.

Let us now consider a graph Γ embedded on $\Sigma_{\mathsf{H}}(\triangle)$ which captures the non-contractible cycles of the fundamental group $\pi_1(\Sigma_{\mathsf{H}}(\triangle))$ of $\Sigma_{\mathsf{H}}(\triangle)$. We distinguish on the Heegaard surface $\Sigma_{\mathsf{H}}(\triangle)$ two sets of closed curves, which we denote by $\{\mathcal{C}_e\}$ and $\{\mathcal{C}_t\}$. The first set $\{\mathcal{C}_t\}_{t\subset\triangle}$ consists of the curves around the triangles, that is each triangle t contributes a curve $t\cap\Sigma_{\mathsf{H}}(\triangle)$. The second set $\{\mathcal{C}_e\}_{e\subset\triangle}$ is given by the curves around the edges e of the triangulation, that is for each edge we choose a disk d_e (of appropriate size) intersecting the edge e transversally and consider the curve $d_e\cap\Sigma_{\mathsf{H}}(\triangle)$.

The set $\{\mathcal{C}_t\}_{t\subset\triangle}$ generates all curves that are contractible in $\mathcal{M}\backslash\mathbf{\Delta}_1$ but are not contractible in $\mathbf{\Delta}_1$. Note that, as far as this generating property is concerned, the set $\{\mathcal{C}_t\}$ is in general over-complete. In terms of the holonomies associated with these curves, this over-completeness manifests itself as the Bianchi identities associated with each 3-simplex of $\triangle$. Conversely the set $\{\mathcal{C}_e\}_{e\subset\triangle}$ generates all curves that are contractible in $\mathbf{\Delta}_1$, but not in $\mathcal{M}\backslash\mathbf{\Delta}_1$. Again, this set is often over-complete which now corresponds to Bianchi identities associated with the vertices of the triangulation.

Let us now describe the space of flat connections on $\mathcal{M}\backslash\mathbf{\Delta}_1$ using the Heegaard surface $\Sigma_{\mathsf{H}}(\triangle)$: We do so by considering the Hilbert space $\mathcal{H}_{\Sigma_{\mathsf{H}}(\triangle)}$ and impose on this space additional flatness constraints. These flatness constraints demand that the holonomies along the curves in $\{\mathcal{C}_t\}$ are trivial. In the following we will refer to the set of flatness constraints associated with the curves in $\{\mathcal{C}_t\}$ as *two-handle constraints*.[6]

Thus, given a Hilbert space $\mathcal{H}_{\Sigma_{\mathsf{H}}(\triangle)}$ of wave functions of flat connections on $\Sigma_{\mathsf{H}}(\triangle)$ we can obtain a Hilbert space of wave functions of flat connections on $\mathcal{M}\backslash\mathbf{\Delta}_1$ by defining suitable operator versions of the two-handle constraints and projecting onto the subspace of functions satisfying these constraints. This subspace defines $\mathcal{H}_{\mathcal{M}\backslash\mathbf{\Delta}_1}$. We construct in a similar way the Hilbert space $\mathcal{H}_{\mathbf{\Delta}_1}$. These tasks are straightforward in the finite group case.[7]

We discussed in sec. 7.2.3 that to define a fusion basis on $\Sigma_{\mathsf{H}}(\triangle)$ we need to choose a pant decomposition for this surface. In the following we will consider two classes of such pant decompositions, which are adjusted to the one-skeleton $\triangle_1$ of the triangulation and the one-skeleton Υ_1 of the dual cell-complex, respectively.

[6] This is reminiscent of the fact that when blowing-up the one-skeleton of the triangulation $\triangle$, the blown-up edges form one-handles while the blown-up triangles form two-handles.

[7] For Lie groups the two-handle constraints are given by delta functions on the group. If one chooses a measure for $\mathcal{H}_{\Sigma_{\mathsf{H}}(\triangle)}$ constructed from the Haar measure on the group, wave functions satisfying these constraints will not be normalizable with respect to the inner product of $\mathcal{H}_{\Sigma_{\mathsf{H}}(\triangle)}$. Thus the space of solutions has to be equipped with a new inner product. Several methods are available [134–137] for the construction of such inner products. We will see that we regain the spin network basis, which is also well defined for the Lie group case and thus we expect that a suitable procedure can be found. Another possibility is to consider a discrete measure for $\mathcal{H}_{\Sigma_{\mathsf{H}}(\triangle)}$, which in fact arises if one wishes to work with continuum Hilbert spaces [22, 86, 96]. In this case the spectrum of the two-handle constraints will be discrete and thus the solutions to the constraints will be normalizable.

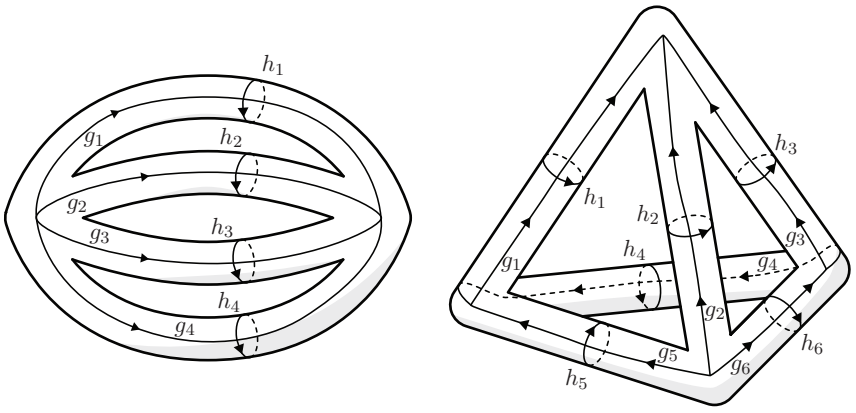

Figure 7.4. On the right panel, we consider the triangulation of the three-sphere $\mathbb{S}_3$ obtained by identifying two tetrahedra. By blowing up the one skeleton of this triangulation, we obtain a Heegaard splitting $\mathbb{S}_3 = \mathbf{\Delta}_1 \cup \mathbb{S}_3 \backslash \mathbf{\Delta}_1$. On the Heegaard surface $\Sigma_{\mathsf{H}}(\triangle)$, we construct a graph which capture all the non-contractible cycles on the surface. The cycles $\{\mathcal{C}_e\}_{e\subset\triangle}$, which go around the edges of the triangulation, are contractible in $\mathbf{\Delta}_1$ while the cycles $\{\mathcal{C}_t\}_{t\subset\triangle}$, which run along the edges of $\triangle$ and are homotopic to the triangles, are contractible in $\mathbb{S}_3\backslash\mathbf{\Delta}_1$. This means in particular that the line defects for $\mathbb{S}_3\backslash\mathbf{\Delta}_1$ run along $\{\mathcal{C}_e\}_{e\in\triangle}$. On the left panel, we represent the blown-up of the one skeleton Υ_1 of the dual cell-complex together with the corresponding embedded graph. The four-times-punctured spheres can be further split into two thrice-punctured sphere so as to obtain a pant decomposition

7.3.2 The spin network basis

In this section, we consider the case of a pant decomposition adjusted to Υ_1. We show that, in this case, the 2-handle constraints just pick out a subset of the fusion basis states in $\mathcal{H}_{\Sigma_{\mathsf{H}}(\triangle)}$. Such a pant decomposition can be obtained by first cutting the surface $\Sigma_{\mathsf{H}}(\triangle)$ along the triangle curves $\{\mathcal{C}_t\}_{t\in\triangle}$. This decomposes the surface into four-punctured spheres, each one of them being associated with a 3-simplex of the triangulation. These spheres are connected by cylinders which surround the edges of the dual graph Υ_1. Each four-punctured sphere can then be decomposed—in one of the three possible ways—into two thrice-punctured spheres in order to obtain a pant decomposition.

The fusion basis associated with such pant decomposition will assign labels (C_{e^*}, R_{e^*}) to each dual edge $e^* = t$. Furthermore, to each vertex v^* dual to a 3-simplex of the triangulation, we assign a pair of labels (C_{v^*}, R_{v*}) which labels the *virtual* cylinder connecting the thrice-punctured spheres after decomposing the four-punctured ones.

The C_{e^*}–labels provide the conjugacy classes associated with the holonomies going around the dual edges, that is around the triangles of $\triangle$. This means that the 2-handle constraints are satisfied if and only if $\{C_{e*} = \{\mathbb{1}\}\}$ for all the dual edges e^*. By doing so, for every thrice-punctured sphere, two punctures carry labels with a trivial conjugacy class. It then follows from the fusion rules of the conjugacy classes that the conjugacy classes associated with the remaining punctures must be trivial as well, i.e. $\{C_{v^*} = \{\mathbb{1}\}\}$ for all dual vertices v^*.

Since all conjugacy classes are trivial, the corresponding centralizer groups always coincide with the full group $\mathcal{G}$ and *a fortiori* the representation labels $\{R\}$ stand for irreducible representations of this group. In summary, we have $\mathcal{G}$-representation labels $\{R_{e^*}\}$ associated with the edges of the dual graph together with representation labels $\{R_{v^*}\}$ associated with the dual vertices. This latter

set can be interpreted as a label for the four-valent intertwiner associated with a dual vertex.[8] We have therefore reconstructed the spin network basis [16]. This can be easily confirmed by considering the group Fourier transform. Indeed, it follows from equations (3.27) and (3.33) that the irreducible representations and the Clebsch-Grodan coefficients for $\mathcal{D}(\mathcal{G})$ reduce to the ones for the group $\mathcal{G}$ when the conjugacy class is always trivial.

7.3.3 Dual magnetic basis

Let us now consider the case of a pant decomposition adjusted to $\triangle_1$. In this case, the projection procedure is far more involved. In particular, it involves a sum over the R-labels of the basis states, whereas the C labels 'survive' the projection.[9] Nevertheless, in general, some information about the set of R-labels is retained and added to the set of C-labels.

A pant decomposition associated with $\triangle_1$ can be obtained by cutting the Heegaard surface along the set of curves $\{\mathcal{C}_e\}_{e\in\triangle}$. By doing so, we associate with each m-valent vertex of the triangulation a m-punctured sphere. We can again freely decompose these m-punctured spheres into thrice-punctured ones. In order to discuss the imposition of the two-handle constraints, we will make use of the parametrization of the space of flat connections developed in sec. 7.2.2 and 7.2.3.

Let us recall the definition of the holonomies used in the parametrization of the space of flat connection. In particular, we want to clarify their meaning for the pant decomposition at hand. We start from the picture where to each oriented cylinder a appearing in the pant decomposition, we associate a holonomy $h_{t(a)}$ and a holonomy $g_a = g_{t(a)s(a)}$. This determines another holonomy associated with the source puncture of the cylinder whose expression reads $h_{s(a)} = g_a^{-1} h_{t(a)}^{-1} g_a$.

A subset of cylinders can be identified with the edges of the triangulation. We choose an orientation for these edges and denote the corresponding cylinders by e instead of a. The remaining cylinders are associated with the vertices of the triangulation. For each m-valent vertex of $\triangle$, we have $(m-3)$ pairs of variables $(h_{t(v,j)}, g_{v,j})_{j=1}^{m-3}$ arising from the decomposition of the associated m-punctured spheres into thrice-punctured ones. These variables can be also interpreted as belonging to (oriented) cylinders connecting the thrice-punctured spheres. We will refer to these as vertex-links and label them by (v,j) with $j = 1,\dots,m-3$. So the $h_{t(v,j)}$ variables give the holonomies around a set of edges starting from the same vertex v. The $g_{v,j}$ variables complete the information about the parallel transport on the punctured spheres, so that the set of g–holonomies provide a graph connection along the blown-up one-skeleton $\boldsymbol{\Delta}_1$. Note that is important to keep track of how the g–holonomies wind around the puntures of a given sphere.

The set of holonomies we just described can be used to define a flat connection on $\Sigma_{\mathsf{H}}(\triangle)$. It is subject to contraints. Firstly we have all the flatness constraints (Bianchi identities) for the punctured spheres involving the h–holonomies. As explained in sec. 7.2.3, these can be solved by associating to each cylinder $a = e$ or $a = (v,j)$ conjugacy classes C_a so that the coupling conditions are satisfied.

Additionally, we have the 2-handle constraints which we impose so as to project the states in $\mathcal{H}_{\Sigma_{\mathsf{H}}(\triangle)}$ onto the Hilbert space $\mathcal{H}_{\mathcal{M}\setminus\boldsymbol{\Delta}_1}$. To identify which holonomies are set to the identity, we need to consider for each triangle $t \in \triangle$ the triangle curve $\mathcal{C}_t$ and *isotopically deform this curve* so that it matches a path along the chosen graph Γ on $\Sigma(\triangle)$. Since the triangle curves necessarily go along the edges of the triangulation, the 2-handle constraints must involve the g–holonomies. However, in order to obtain paths which are isotopically equivalent to the triangle curves, it might be necessary to

[8] Remember that we assumed multiplicity freeness for the tensor product of two Drinfel'd double representations, which implies multiplicity freeness for the tensor product of two group representations.

[9] In some exceptional cases constraints on the C–labels may arise.

include some windings around the punctures. In such case, the 2-handle constraints will also involve some h–holonomies.

In sec. 7.2.3, we described how, given a consistent set of conjugacy classes $\{C_a\}_a$, we can construct a partial gauge fixing that determines uniquely all the h–holonomies. This partial gauge fixing is such that g_a-holonomies are restricted to be of the form

$$g_a \;=\; q_{\iota_{C_a}(h_t)} \cdot z_a \cdot q^{-1}_{\iota_{C_a}(h_s^{-1})} \equiv q_{\iota_a} \cdot z_a \cdot q^{-1}_{\iota'_a} \tag{7.27}$$

where the remaining freedom is parametrized by $z_a \in Z_{C_a}$ and $q_{\iota_C(h)}$ is defined as in (7.26). Henceforth, we will make use of the shorthand notation $q_{\iota_a} \equiv q_{\iota_{C_a}(h_t)}$ and $q_{\iota'_a} \equiv q_{\iota_{C_a}(h_s^{-1})}$. Recall finally that, when performing the partial gauge fixing, for a given consistent set of conjugacy classes $\{C_a\}_a$, there is some remaining gauge freedom given by the groups $Z_{C_1C_2C_3}$ associated with the thrice-punctured spheres.

For a given configuration $\{C_a\}_a$ of conjugacy classes, we will therefore understand the two-handle constraints as (flatness) conditions on the variables $\{z_a \in Z_{C_a}\}_a$. There are the following obvious possibilities:

(1) The two-handle constraints admit no solution, in which case we have to exclude the configuration $\{C_a\}_a$. In this case we have to conclude that a basis state with a curvature configuration $\{C_a\}_a$ does not exist.

(2) The two-handle constraints admit a unique solution modulo the gauge action given by the stabilizer groups $Z_{C_1C_2C_3}$ associated to the thrice-punctured spheres. In this case we can conclude that there is a unique basis state peaked on a curvature configuration $\{C_a\}_a$.

(3) There are several (left-over gauge) orbits satisfying the two-handle constraints so that we need to introduce additional quantum numbers $\{Q_N\}_N$ which label such orbits. We will use $\mathcal{Q}$ to label the different solution orbits, i.e. $\mathcal{Q}$ summarizes all the possible values of the quantum numbers $\{Q\}_N$.[10]

Intuitively, one would expect the scenario (3) to occur for manifolds $\mathcal{M}$ with non-trivial $\pi_1(\mathcal{M})$. Indeed, in the extreme case of vanishing magnetic excitations $\{C_a = \{\mathbb{1}\}\}$, for all a, we should still be left with the space of flat connections described by homomorphisms of $\pi_1(\mathcal{M})$ into $\mathcal{G}$ (modulo the adjoint action). Conversely, for a trivial $\pi_1(\mathcal{M})$, one will find a unique basis state with configuration $\{C_a = \{\mathbb{1}\}\}$. We will however see in the next section that all three cases do appear when we choose the three-dimensional surface to be the three-sphere $\mathbb{S}_3$ whose fundamental group is trivial.

7.4 Examples

In this section, we present several examples of our construction based on Heegaard splittings. In order to perform the computations explicitly, we consider the non-abelian symmetry group of three elements denoted by $\mathcal{S}_3$.

7.4.1 Preliminaries: Symmetric group $\mathcal{S}_3$

The symmetric group $\mathcal{S}_3$ is the simplest example of finite non-abelian group. It is the symmetry group of an equilateral triangle. This group is generated by the rotations by $2\pi/3$ angle as well as

[10] One can define closed holonomy operators $\mathcal{O}_N$, i.e. operators measuring the conjugacy class of holonomies associated to certain loops, that differentiate between these orbits. Furthermore, it is possible to choose such operators such that they have eigenvalues given by $\{Q_N\}_N$ on the corresponding basis states.

the reflections with respect to any of the three medians. The groups associated with these two sets of symmetry transformations are the cyclic groups $\mathbb{Z}_2$ and $\mathbb{Z}_3$ so that the symmetry group $\mathcal{S}_3$ can be expressed as the semi-direct product $\mathcal{S}_3 = \mathbb{Z}_2 \ltimes \mathbb{Z}_3$. We denote the generators of $\mathbb{Z}_2$ and $\mathbb{Z}_3$ by r and s, respectively, such that $r^2 = \mathbb{1}$ and $s^3 = \mathbb{1}$. The six group elements of $\mathcal{S}_3$ then read

$$\mathcal{S}_3 = \{r^i s^j\}_{i=0,1}^{j=0,1,2} = \{\mathbb{1}, r, rs, rs^2, s, s^2\} \,. \tag{7.28}$$

Using the defining relation of the generators r and s together with the relation $rs = s^2 r$, we can generate the following multiplication table:

$\cdot$	$\mathbb{1}$	r	rs	rs^2	s	s^2
$\mathbb{1}$	$\mathbb{1}$	r	rs	rs^2	s	s^2
r	r	$\mathbb{1}$	s	s^2	rs	rs^2
rs	rs	s^2	$\mathbb{1}$	s	rs^2	r
rs^2	rs^2	s	s^2	$\mathbb{1}$	r	rs
s	s	rs^2	r	rs	s^2	$\mathbb{1}$
s^2	s^2	rs	rs^2	r	$\mathbb{1}$	s

The group elements can be classified according to whether they are *odd* or *even*, that is, whether their expression contains an odd number of r elements or an even number. Correspondingly, the determinant in the fundamental representation is equal to -1 for odd elements and equal to $+1$ for even elements. There are only three distinct conjugacy classes

$$\mathcal{T} = \{\mathbb{1}\} \quad , \quad \mathcal{O} = \{r, rs, rs^2\} \quad , \quad \mathcal{E} = \{s, s^2\} \,, \tag{7.29}$$

the trivial conjugacy class $\mathcal{T}$, the conjugacy class $\mathcal{O}$ containing all odd elements and the conjugacy class $\mathcal{E}$ containing the even elements except for the unit $\mathbb{1}$. The corresponding centralizers are

$$\begin{aligned} Z_{\mathcal{T}} &\simeq \mathcal{S}_3 \,, \\ Z_{\mathcal{O}} &= \{\mathbb{1}, r\} \simeq \mathbb{Z}_2 \,, \\ Z_{\mathcal{E}} &= \{\mathbb{1}, s, s^2\} \simeq \mathbb{Z}_3 \end{aligned} \tag{7.30}$$

which are defined with respect to the following conjugacy class representatives: $c_1(\mathcal{T}) = \mathbb{1}$, $c_1(\mathcal{O}) = r$ and $c_1(\mathcal{E}) = s$.

Recall that the fusion rules for the conjugacy classes are defined as the number of orbits the set

$$\{(h_1, h_2, h_3) \in C_1 \times C_2 \times C_3 \,|\, h_3 h_2 h_1 = \mathbb{1}\}$$

split into under simultaneous conjugation. For $\mathcal{S}_3$ there are 11 non-vanishing fusion rules for which there exists a triplet (h_1, h_2, h_3) of group elements with $h_i \in C_i$ and $h_3 h_2 h_1 = \mathbb{1}$. Furthermore, for the group $\mathcal{S}_3$ it holds that for a given (C_1, C_2, C_3) all such triplets of group elements are related by a common adjoint action transformation. Therefore there is a one-to-one correspondence between each ordered triplet (h_1, h_2, h_3) satisfying the flatness condition and the corresponding triplet of allowed conjugacy classes (C_1, C_2, C_3). We summarize below these 11 configurations

$\otimes$	$\mathcal{T}$	$\mathcal{O}$	$\mathcal{E}$
$\mathcal{T}$	$\mathcal{T}$	$\mathcal{O}$	$\mathcal{E}$
$\mathcal{O}$	$\mathcal{O}$	$\mathcal{T} \oplus \mathcal{E}$	$\mathcal{O}$
$\mathcal{E}$	$\mathcal{E}$	$\mathcal{O}$	$\mathcal{T} \oplus \mathcal{E}$

(7.31)

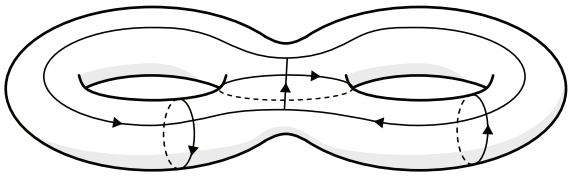

Figure 7.5. Example of embedded graph on a genus-2 surface. By cutting the surface along the curves going around the cylinders, we obtain a pant decomposition.

Finally, we make a choice of basis in which the standard representation matrix of s is diagonal. In this basis, the standard representation of the group elements r and s is

$$\rho^2(r) = \begin{pmatrix} 0 & 1 \\ 1 & 0 \end{pmatrix} \quad , \quad \rho^2(s) = \begin{pmatrix} \exp(\frac{2\pi i}{3}) & 0 \\ 0 & \exp(-\frac{2\pi i}{3}) \end{pmatrix}. \tag{7.32}$$

The representations for each group element are summarized in the following table

$D^\rho(g)$	$\mathbb{1}$	r	rs	rs^2	s	s^2
$\rho = 0$	1	1	1	1	1	1
$\rho = 1$	1	-1	-1	-1	1	1
$\rho = 2$	$\begin{pmatrix} 1 & 0 \\ 0 & 1 \end{pmatrix}$	$\begin{pmatrix} 0 & 1 \\ 1 & 0 \end{pmatrix}$	$\begin{pmatrix} 0 & \overline{\omega} \\ \omega & 0 \end{pmatrix}$	$\begin{pmatrix} 0 & \omega \\ \overline{\omega} & 0 \end{pmatrix}$	$\begin{pmatrix} \omega & 0 \\ 0 & \overline{\omega} \end{pmatrix}$	$\begin{pmatrix} \overline{\omega} & 0 \\ 0 & \omega \end{pmatrix}$

(7.33)

where $\omega = \exp(\frac{2\pi i}{3})$.

7.4.2 Genus-2 defect

In sec. 7.1, we considered the simplest example of our construction, namely a loop defect embedded in the three-sphere. A slightly more complicated example consists in a genus 2 defect embedded in the three-sphere.

Let us consider a graph embedded in $\mathbb{S}_3$ which consists of three edges and two vertices so as to form a θ-shape. By blowing up this graph we obtain a double torus that defines a Heegaard surface $\Sigma_{\mathsf{H}}(\triangle)$. The solid double torus corresponds to the manifold we denoted by $\mathbf{\Delta}_1$ earlier, and its complement in $\mathbb{S}_3$ is $\mathbb{S}_3 \backslash \mathbf{\Delta}_1$. This defines the so-called genus-2 Heegaard splitting of the three-sphere. We represent fig. 7.5 the Heegaard surface together with an embedded graph. By cutting the surface along the links going around the cylinders, we obtain a pant decomposition of the surface. Following sec. 7.2.4, we can then construct basis states in the Drinfel'd double representation for the Hilbert space $\mathcal{H}_{\Sigma_{\mathsf{H}}(\triangle)}$. To each thrice-punctured two-sphere $\mathbb{Y}$ resulting from the pant decomposition, we associate $3\rho M$-symbols which are then connected to each other via cylinder states. The result reads

$$\begin{aligned} |\rho_1, \rho_2, \rho_3\rangle &:= \sum_{\{M,N\}} |\rho_1, M_1 N_1\rangle_{\mathbb{I}} \otimes |\rho_2, M_2 N_2\rangle_{\mathbb{I}} \otimes |\rho_3, M_3 N_3\rangle_{\mathbb{I}} \otimes \begin{pmatrix} \rho_1 & \rho_2 & \rho_3^* \\ N_1 & N_2 & M_3 \end{pmatrix} \begin{pmatrix} \rho_2^* & \rho_1^* & \rho_3 \\ M_1 & M_2 & N_3 \end{pmatrix} \\ &= \frac{1}{|\mathcal{G}|^3} \sum_{\{g,h\}} \sum_{\{M,N\}} \left(\prod_{i=1}^{3} \sqrt{d_{\rho_i}} D^{\rho_i}_{M_i N_i}(g_i \otimes \delta_{h_i}) \right) \begin{pmatrix} \rho_1 & \rho_2 & \rho_3^* \\ N_1 & N_2 & M_3 \end{pmatrix} \begin{pmatrix} \rho_2^* & \rho_1^* & \rho_3 \\ M_1 & M_2 & N_3 \end{pmatrix} \otimes_{i=1}^{3} |g_i, h_i\rangle_{\mathbb{I}} \,. \end{aligned} \tag{7.34}$$

Using the invariance (3.37), we can perform a 'gauge fixing' so that the basis states now read

$$\begin{aligned} |\rho_1, \rho_2, \rho_3\rangle = \frac{1}{|\mathcal{G}|^3} \sum_{\{g,h\}} \sum_{\{M,N\}} & \sqrt{d_{\rho_1} d_{\rho_2} d_{\rho_3}} D^{\rho_1}_{M_1 N_1}(g_1 g_3 \otimes \delta_{h_1}) D^{\rho_2}_{M_2 N_2}(g_2 g_3 \otimes \delta_{h_2}) \delta(h_3, g_3 h_1 h_2 g_3^{-1}) \\ & \times \begin{pmatrix} \rho_1 & \rho_2 & \rho_3^* \\ N_1 & N_2 & M_3 \end{pmatrix} \begin{pmatrix} \rho_2^* & \rho_1^* & \rho_3 \\ M_1 & M_2 & N_3 \end{pmatrix} \otimes_{i=1}^{3} |g_i, h_i\rangle_{\mathbb{I}} \,. \end{aligned} \tag{7.35}$$

We can now impose the 2-handle constraints so as to obtain a basis for the Hilbert space $\mathcal{H}_{\mathcal{M}\setminus\mathbf{\Delta}_1}$ which amounts to setting the holonomies labeled by g_1g_3 and g_2g_3 to be trivial. It is straightforward to see that, after imposing the two-handle constraints, we naturally obtain a parameterization of the Hilbert space of excited states in terms of the two holonomies h_1 and h_2 modulo adjoint action. For $\mathcal{S}_3$, we find 11 such configurations. This is the holonomy parameterization presented in 7.2.2.

Now, from the expression (7.34) and projecting onto the subspace of states satisfying the two-handle constraints, we can also obtain a parameterization of the Hilbert space $\mathcal{H}_{\mathcal{M}\setminus\mathbf{\Delta}_1}$ of excited states in terms of conjugacy classes only. Basis states are then labeled by the conjugacy classes C_1, C_2 and C_3. Only the configurations of conjugacy classes allowed by the fusion rules are permitted. As seen from the expression (7.34), and because for $\mathcal{S}_3$ the conjugacy classes of a group element and its inverse are the same, the fusion rules at the thrice-punctured two-spheres are identical. We find therefore as many excited states as non-vanishing fusion rules $N_{C_1C_2}^{C_3}$, namely 11 (see tab. (7.31)). As expected, this matches the number obtained from the holonomy parameterization. This is a rare example where we can obtain a more local parameterization in terms of conjugacy classes only. In general, we would need to introduce additional quantum numbers $\{Q_N\}$ as explained in details in sec. 7.3.3.

7.4.3 Defects along a tetrahedral skeleton

We now consider a tetrahedron $\triangle$ embedded into the three-sphere. We then perform a Heegaard splitting of the three-sphere such that the Heeagaard surface $\Sigma_{\mathsf{H}}(\triangle)$ is obtained as the blow-up of the one skeleton of the tetrahedon. The result is a genus-3 two-dimensional surface which we equip with a flat connection. By performing a pant decomposition, we obtain $\Sigma_{\mathsf{H}}(\triangle)$ as a gluing of four $\mathbb{Y}$ associated with the vertices of $\triangle$ labeled by $k = 1, \dots, 4$. For each sphere we choose a base node n_k. The spheres are glued to each other via tubes labeled by $a = 21, 31, 41, 32, 42, 43$. Each tube intersect its source and target $\mathbb{Y}$ at punctures which possess a marked point on their boundary. These marked points define the nodes $n_{s(a)}$ and $n_{t(a)}$ and between these nodes we have a link going from $n_{s(a)}$ to $n_{t(a)}$. Furthermore, for each sphere k we choose a link from the base node k to all the $n_{s(a)}$ and $n_{t(a)}$ on this sphere. Finally we choose links going around (clockwise) both ends of each tube and starting and ending at $n_{s(a)}$ and $n_{t(a)}$. Putting everything together, we obtain a graph Γ on $\Sigma(\triangle)$. These conventions are summarized in fig. 7.3.

We can now define a flat connection on $\Sigma_{\mathsf{H}}(\triangle)$ by assigning group elements $\{g_a\}$ to each link running along the cylinders a from $n_{s(a)}$ to $n_{t(a)}$, as well as holonomies $\{h_{t(a)}\}$ going along the links encircling the target punctures of the cylinders. The holonomies from n_k to the adjacent $n_{s(a)}$ and $n_{t(b)}$ are gauge fixed to the identity by using the gauge freedom at these latter nodes.

Following this procedure, we obtain a parametrization which depends on six pair of group elements $\{g_a, h_{t(a)}\}$. This parametrization is over-complete since, on the one hand, there is a remaining gauge freedom for the base nodes $\{n_k\}$ and, on the other hand, the Bianchi identity holds at each $\mathbb{Y}$. To express this systematically, it is convenient to introduce the holonomies around the source puctures of the tubes, namely $\{h_{s(a)} = g_a^{-1}h_{t(a)}^{-1}g_a\}$. For instance, for the sphere no. 1 one has

$$h_{s(31)}h_{s(41)}h_{s(21)} \;\Rightarrow\; h_{t(41)} = g_{41}g_{21}^{-1}h_{t(21)}g_{21}\, g_{31}^{-1}h_{t(31)}g_{31}g_{41}^{-1}\,. \tag{7.36}$$

Using the Bianchi identities for the spheres $k = 1, 2, 3$ we can solve for $h_{t(41)}, h_{t(42)}$ and $h_{t(43)}$ in terms of $h_{t(21}, h_{t(32)}, h_{t(31)}$ and the g–holonomies. The Bianchi identity for the remaining sphere $k = 4$ is then automatically satisfied. The resulting parameterization still has some gauge freedom. This can be almost completely gauge fixed by imposing for instance the conditions $g_{13} = g_{23} = g_{42} = \mathbb{1}$. Putting everything together, we are left with a parametrization in terms of three h-variables and three g-variables. Only the residual global action is left to be taken into account.

With this parameterization on the space of flat connections at hand, we can impose the two-handle constraints—that is the constraints that impose flatness for the holonomies around the triangles of $\triangle$. There are four triangles but due to the Bianchi identity for the tetrahedron, we have only three independent constraints. Furthermore, it is possible to choose the graph so that these constraints involve only g–holonomies, e.g. for the triangle (124) we have $g_{41}^{-1} g_{42} g_{21} = \mathbb{1}$. With our gauge fixing we have a unique solution to these flatness constraints given by $g_a = \mathbb{1}$ for all a.

Imposing the two-handle constraints leads to a first parametrization of the state space of flat holonomies on the three-sphere with a tetrahedral defect structure: It is given by (ordered) triples of group elements $(h_{t(21)}, h_{t(32)}, h_{t(31)})$ up to a global adjoint action. For the group $\mathcal{S}_3$ there are 49 such equivalence classes. Therefore, the Hilbert space of excited states possesses 49 basis states.

We now would like to derive a more local parametrization, which would in particular allow us to read off directly the curvature (or magnetic charge) associated to each edge of the tetrahedral skeleton. As in the case of the genus-2 defect structure we could hope that labeling the edges a of the tetrahedron with the conjugacy classes C_a of the holonomies $h_{t(a)}$ gives a one-to-one parametrization of the set of equivalence classes described above. These C_a would naturally have to satisfy the coupling rules (7.31) at each vertex of the tetrahedron. However, it turns out that the number of all such configurations allowed by the coupling rules is only 47. Therefore, such parameterization would not be enough to capture the whole space of excited states.

To investigate in more detail the failure of the parametrization by the conjugacy classes, it is convenient to write down explicitly the admissible configurations of the six holonomies $\{h_{t(a)}\}$ and of the conjugacy classes $\{C_a\}$. Doing so we notice that the failure of the more local parametrization in terms of conjugacy classes is due to the fact that for one configuration $\{C_a\}$ there does not exist a g-connection satisfying the 2-handle constraints (case (1) in sec. 7.3.3), and that for three other configurations there are, modulo residual gauge transformation, two such g-connections (case (3)). For all other (43) configurations there exists a unique (modulo residual gauge transformation) g-connection satisfying the 2-handle constraints (case (2)).

7.4.4 Three-torus

Next, we wish to consider an example where the 3d manifold into which the defect structure is embedded in has a non-trivial topology. We take this 3d manifold to be the three-torus $\mathbb{T}_3$, which is discretized by a lattice consisting of only one cube with periodic boundary conditions. Due to the periodic identification of the various elements, this lattice only has three faces, three edges associated with the three non-contractible cycles, and one six-valent vertex. We allow for curvature defects along the edges of this one-cube lattice. We are thus interested in the space of flat connection on the three-torus with a thickening of the one-skeleton of the one-cube lattice removed.

The surface of the thickening of this one-skeleton defines a Heegaard surface for the three-torus. A convenient representation of this surface is shown in fig. 7.6. The sphere surrounding the one vertex with its six punctures is represented as a disk with five punctures, with the boundary of the disc defining the sixth puncture. Pairs of punctures $(i, i+1)$ with $i = 1, 3, 5$ are connected by tubes (or one-handles) and we have therefore a genus-3 surface. We can find a parametrization of the space of flat connections on this surface by choosing a base node n_0, links from n_0 to the marked points n_j, $j = 1, \ldots, 6$ of the six punctures, links around the punctures starting and ending in n_j, and links along the tubes from n_i to n_{i+1} (see fig. 7.6).

We associate holonomies h_j, $j = 1, \ldots, 6$ to the (clockwise) links around the punctures and holonomies $g_{i+1,i}$ to the links from the puncture $i = 1, 2, 3$ to the puncture $(i+1)$. Furthermore,

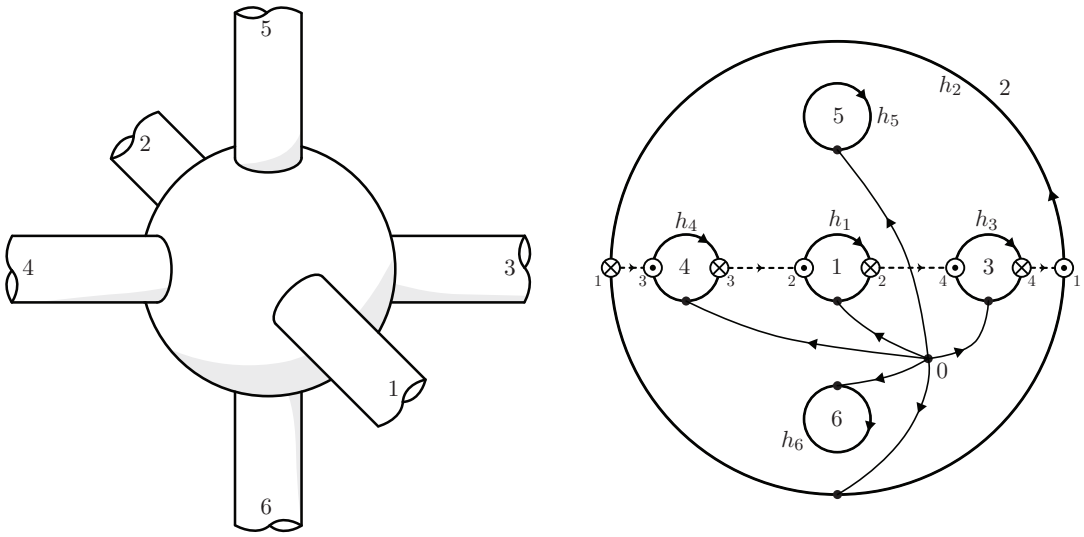

Figure 7.6. The three-torus can be discretized as a cube with opposite faces identified so that the discretization contains one six-valent vertex, three edges associated with the non-contractible cycles and three faces. The Heegaard surface is obtained by blowing-up the one skeleton of this discretization so that the single vertex becomes a six-times punctured two-sphere as represented on the left panel. The edges are also blown-up into cylinders connecting the spheres 1 to 2, 3 to 4 and 5 to 6, respectively. The same object is depicted in a different representation on the right panel as a disk with five punctures, the boundary of the disk corresponding to the sixth puncture.

holonomies from the base node n_0 to the marked points n_j are gauge fixed to the identity. Finally, the holonomies $\{h_j\}$ are not independent since

$$h_{i+1} = g_{i+1,i} h_i^{-1} g_{i+1,i}^{-1} \,. \tag{7.37}$$

We have therefore a parametrization of the space of flat connections on the genus-3 Heegaard surface by three pairs of holonomies $\{h_i, g_{i+1,i}\}_{i=1,3,5}$. This set of holonomies is subject to the Bianchi constraint associated with the six-times punctured two-sphere

$$g_{43} h_3^{-1} g_{43}^{-1}\, g_{65} h_5^{-1} g_{65}^{-1}\, g_{21} h_1^{-1} g_{21}^{-1}\, h_3\, h_2\, h_1 = \mathbb{1} \tag{7.38}$$

together with a left-over gauge action (at the base node n_0) that results into a diagonal adjoint action on the set $\{h_i, g_{i+1,i}\}_{i=1,3,5}$.

We can now consider the 2-handle constraints, which demand that the holonomies around the faces of the cube are flat. At this stage some care needs to be taken in determining a path that is homotopy equivalent to the intersection of the Heegaard surface with the faces, see fig. 7.6. It turns out that such a paths does not only involve links along the tubes but needs also to wind around one of the remaining punctures. Thus, each of the three 2-handle constraints involves one of the h_i-holonomies and can be used to fix these h_i-holonomies in terms of commutators of the corresponding g–holonomies:

$$\begin{aligned} h_1 &= g_{65}^{-1} g_{43} g_{65} g_{43}^{-1} \\ h_3 &= g_{21} g_{65}^{-1} g_{21}^{-1} g_{65} \\ h_5 &= g_{65}^{-1} g_{21} g_{43} g_{21}^{-1} g_{43}^{-1} g_{65} \,. \end{aligned} \tag{7.39}$$

These relations impose automatically the Bianchi identity (7.38). These relations imply that the space of flat connections on the 3-torus with the one-skeleton of the one-cube lattice removed is parametrized by the set of three holonomies $\{g_{21}, g_{43}, g_{65}\}$ modulo a diagonal adjoint action. For the group $\mathcal{S}_3$ this amounts to 49 configurations (the same number as for the tetrahedron).

In the case of the three-torus, the holonomies $\{g_{i+1,i}\}$ encode global topological observables, i.e. they are associated with paths that are topologically non-trivial even without removing the blown-up one-skeleton of the discretization. Due to the small lattice, it turns out that these observables also determine completely the holonomies around the edges of the cubical discretization. Nevertheless, in order to illustrate the effects of a non-trivial underlying three-dimensional manifold, we will discuss what happens if we seek a more local parametrization. To this end, we choose to include the conjugacy classes of the h–holonomies as parameters for the excited states:

$$\begin{aligned} C_1 = C_{h_1} \quad , \quad C_3 = C_{h_3} \quad , \quad C_5 = C_{h_5} \quad , \quad C_{35} = C_{h_3 h_5} \quad , \\ C_{62} = C_{g_{65} h_5^{-1} g_{65}^{-1} g_{21} h_1^{-1} g_{21}^{-1}} \quad , \quad C_{351} = C_{h_3 h_5 h_1} = C_{462} \ . \end{aligned} \tag{7.40}$$

The parameters $\{C_1, C_3, C_5, C_{35}, C_{62}, C_{351}\}$ alone fail to give an effective description of the 3-torus configurations due to again the appearances of the cases (1) and (3) listed in sec. 7.3.3.

Recall that case (1) refers to the impossibility of finding g-connections satisfying the 2-handle constraints for certain configurations of conjugacy classes which are allowed by the coupling rules. This is evident from the form of the h–holonomies (7.39) in terms of the g–holonomies: If a given h–holonomy includes a g–holonomy, it must include its inverse as well. Therore, all h–holonomies have to be even elements, hence the absence of the conjugacy class $C = \mathcal{O}$ of odd elements.

We also have occurences of case (3) appearing when there are several equivalence classes of g-connections for a given configuration of conjugacy classes. But for a non-trivial topology, there can be non-trivial g–holonomies along the non-contractible cycles even in the absence of excitations, that is when all holonomies around the edges of the lattice are trivial. In the case of the three-torus, there are 21 such equivalence classes of g-connections for trivial h–holonomy configurations. This is the number of locally flat holonomies on the three-torus for the group $\mathcal{S}_3$. Furthermore, degeneracies also appear for non-trivial values for the set of conjugacy classes. As before, it is possible to add obervables to the parameterization in order to resolve the degeneracy. In particular, we can choose to add the conjugacy classes $C_{g_{21}}$, $C_{g_{43}}$, $C_{g_{65}}$ and $C_{g_{21}g_{43}}$, $C_{g_{43}g_{65}}$, $C_{g_{21}g_{65}}$. This does indeed get rid of all degeneracies, but at the price of over-parametrization.

This example illustrates the ineffectiveness of such local parametrization in the case where all the holonomies are determined by global parameters. If we would refine the lattice, we expect the local parametrization to be more useful. Nevertheless, in the case of a non-trivial topology for the three-manifold carrying the defects, we will always have to take into account the non-triviality of the vacuum sector.

7.5 Ribbon operators

In this section, we present how the procedure defined previously for states also applies to operators. In particular, we show how ribbon operators defined on the Heegaard surface can be lifted so as to define excitation-generating operators for the 3d manifold. But before discussing this lifting, we briefly review the construction of the ribbon operators in the present context. We first discuss the open ones from which we can obtain the closed ones, which are the relevant ones for the 3d interpretation.

7.5.1 Ribbon operators on the Heegaard surface

In chap. 4, ribbon operators were defined as the composition of a Wilson loop operator $W^f_{\gamma'}$ and a translation operator $T_{k,\gamma}[H]$ such that

$$(W^f_{\gamma'} \triangleright \psi)(g_1, \dots, g_L) \;=\; f(h_{\gamma'})\psi(g_1, \dots, g_L), \tag{7.41}$$

where $h_{\gamma'} = g_{l_N} \cdots g_{l_1}$ is the holonomy associated to the path $\gamma' = l_N \circ \cdots \circ l_1$ and

$$(T_{k,\gamma}[H] \triangleright \psi)(\dots, g_k, \dots) = \psi(\dots, h_\gamma^{-1} H^{-1} h_\gamma g_k, \dots) \tag{7.42}$$

with h_γ the holonomy along the path γ and k labels the holonomy crossed by the ribbon operator.

Let Γ be the graph embedded on $\Sigma_{\mathsf{H}}(\triangle)$. Let us assume that the path γ is such that it intersects links of Γ transversally and does avoid the nodes of the graph. We also assume that all crossing links have the same orientation with respect to γ, namely if the direction of γ is upwards, then the links should cross from left to right. Note that by a variable transformation $g_{l^{-1}} = g_l^{-1}$ for the wave functions we can always adjust the orientation of the links accordingly. We furthermore need to specify, without loss of generaliy, one link l_1 crossed by γ as initial link. To the path γ we associate a *shadow* path γ' which has to be *isotopy equivalent* to γ and to run along Γ, i.e. γ' is composed from links of Γ. More specifically γ' has to connect the target nodes of the links $l \subset \Gamma$ which are crossed by γ and is not allowed to cross γ itself. In some rare case, these conditions cannot be satisfied for a given γ and a given graph Γ. It is then necessary to refine Γ so as to obtain an appropriate γ'. With these definitions, we can picture γ and γ' as the left and right boundary of a ribbon, respectively, such that the right boundary of this ribbon needs to be aligned to links of the graph Γ.

Let us now write down explicitly the action of the operators in this context. We denote the links crossed by the closed path γ by l_i, $i = 1, \dots, l_{N(\gamma)}$ and the associated holonomies by g_i. Furthermore $h'_i := h_{t(l_1)t(l_i)}$ is the holonomy from the target node of the link l_i along and in the direction of γ' to the target node of l_1. For $i = 1$, we define $h'_1 = h_{\gamma'}$ to be the holonomy of γ' starting and ending at the target node of l_1. We can finally write the action of the operator $T_\gamma[H]$ as

$$(T_\gamma[H] \triangleright \psi)(\{g\}) = \psi\big(\{(h'_i)^{-1} H^{-1} h'_i g_{l_i}\}_{l=l_i}, \{g_l\}_{l\neq l_i}\big)\,. \tag{7.43}$$

Ultimately, we want to use this translation operator to define a ribbon operator on the space of flat connections on $\Sigma_{\mathsf{H}}(\triangle)$. As such it must preserve the flatness constraints associated with the contracticle cycles of $\Sigma_{\mathsf{H}}(\triangle)$. This requires closed ribbon operators. Recall from chap. 4, that the operator (7.43) leaves almost all flatness constraints intact. The exceptional cycle is associated with the face, into which γ enters via crossing the last link $l_{N(\gamma)}$. Thus γ leaves the same face by crossing l_1. The action of the shifts on two links usually cancels out for the face holonomy, but in this case one might encounter a non-trivial result as the holonomy h_f is changed by

$$h_f = \cdots g_{l_1}^{-1} h'_{N(\gamma)} g_{l_{N(\gamma)}} \;\longrightarrow\; \cdots g_{l_1}^{-1} (h'_1)^{-1} H h'_1 H^{-1} h'_{N(\gamma)}\, g_{l_{N(\gamma)}}\,. \tag{7.44}$$

This is due to the fact that the parallel transport for the shift of l_1 involves $h'_1 = h_{\gamma'}$, that is the holonomy associated to the cylce γ, whereas the parallel transport for $l_{N(\gamma)}$ only involves $h'_{N(\gamma)}$, the holonomy from the target node of $l_{N(\gamma)}$ to the target node of l_1.

The flatness at such a face is preserved if H and $h_{\gamma'}$ do commute. One way to ensure this is to combine the translation operator $T_\gamma[H]$ with a holonomy operator $W^f_{\gamma'}$ where $f(\bullet) = \delta(G, \bullet)$ and such that G and H commute, i.e. $[G, H] = \mathbb{1}$. We are therefore working with ribbon operator of the form

$$\mathcal{K}_\gamma[G, H] = \delta(GH, HG)\, W_{\gamma'}[G] \circ T_\gamma[H]\,. \tag{7.45}$$

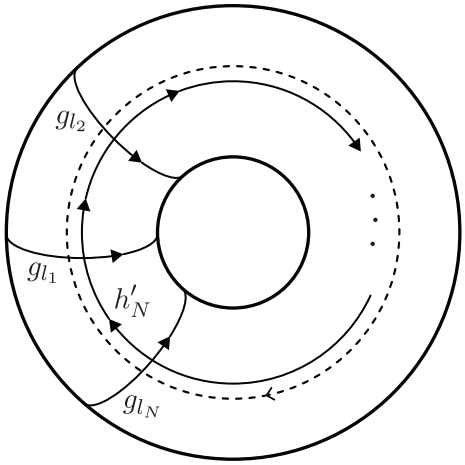

Figure 7.7. Example of ribbon operator along a non-contractible cycle on a one-torus. The dashed line represents the path γ'.

If $G \neq \mathbb{1}$ and γ (and therefore γ') is a contractible cycle, the ribbon operator (7.45) annihilates all states in the Hilbert space. Recall, furthermore, that a gauge averaging must be enforced to ensure that the ribbon operator preserves the gauge invariance at the node $t(l_1)$. The final result is the so-called closed ribbon operator:

$$\begin{aligned}\left(\mathcal{K}_\gamma[D,\, C] \triangleright \psi\right)(\{g_l\}) &:= \sum_{u\in\mathcal{G}} \left(\mathcal{K}_\gamma[u^{-1}Gu,\, u^{-1}Hu] \triangleright \psi\right)(\{g_l\}_l) \\ &= \sum_{u\in\mathcal{G}} \delta(G, uh_{\gamma'}u^{-1})\ \psi(\{(h'_i)^{-1}u^{-1}H^{-1}uh'_i g_{l_i}\}_{l=l_i}, \{g_l\}_{l\neq l_i})\end{aligned} \tag{7.46}$$

with C the conjugacy class of H in $\mathcal{G}$ and D the conjugacy class of G in the centralizer Z_H of H in $\mathcal{G}$. Since the ribbon operator preserves flatness for the contractible cycles. It can thus change only the holonomies associated to non-contractible cycles, which are crossed by γ. Furthermore, one can see that the action of the ribbon on the cycle holonomies is invariant under isotopic deformations of γ and thus the ribbon operator does only depend on the isotopy class of γ. Ribbon operators with $G = \mathbb{1}$ (or $D = \{\mathbb{1}\}$) with γ non-contractible plays a special role in our construction. In this case there is no restriction on H or on the conjugacy class C.

7.5.2 Excitation-generating ribbons in 3d

Let us now lift the operators defined above on the Heegaard surface $\Sigma_{\mathsf{H}}(\triangle)$ to excitations-generations ribbon operators for the manifold $\mathcal{M}\backslash\mathbf{\Delta}_1$. Remember that the space of flat connections on $\mathcal{M}\backslash\mathbf{\Delta}_1$ can be identified with the space of flat connections on $\Sigma_{\mathsf{H}}(\triangle)$ satisfying the two-handle constraints. We will make use in the following of the *non-minimal holonomy parameterization* of the space of flat connections as exposed in sec. 7.2.2. However, contrary to sec. 7.2.2, it will be more convenient not to impose the holonomies along the links going from the based point n_k of each $\mathbb{Y}$ to the marked points $n^{\mathbb{I}}_s(a), n^{\mathbb{I}}_{t(a)}$ to be trivial. These holonomies are denoted by k and their labeling follows from the one of the g–holonomies.

The operators we are looking for are the ribbon operators defined on $\Sigma_{\mathsf{H}}(\triangle)$ which in addition to leaving the flatness conditions associated with the contractible cycles in $\Sigma_{\mathsf{H}}(\triangle)$ intact, leaves the

two-handle constraints associated with the contractible cycles in $\mathcal{M}\backslash\mathbf{\Delta}_1$ intact. An obvious class of operators for which this holds are Wilson loop operators: These act by multiplication on the function space of holonomies and thus commute with any flatness constraints. Another class is given by a special kind of closed ribbon operators $\mathcal{K}_\gamma[G,H]$: We choose γ (and *a fortioti* γ') to be isotopic to the curve $t\cap\Sigma_{\mathsf{H}}(\triangle)$ for some triangle t of the triangulation.[11] To preserve the constraints $h_{\gamma'}=\mathbb{1}$, we will only consider the ribbon operators $\mathcal{K}_\gamma[D,C]$ with $D=\{\mathbb{1}\}$. We denote the resulting operators by $\mathcal{K}_t[C]$.

The operators $\mathcal{K}_t[C]$ leave all the two-handle constraints invariant: It is clear that $\mathcal{K}_t[C]$ leaves the flatness constraint coming from t itself invariant. Furthermore the closed curves $t\cap\Sigma_{\mathsf{H}}(\triangle)$ and $t'\cap\Sigma_{\mathsf{H}}(\triangle)$ for two different triangles t and t' do not intersect each other on $\Sigma_{\mathsf{H}}(\triangle)$. Thus even if $\mathcal{K}_t[C]$ goes along a curve γ that does intersect $t'\cap\Sigma_{\mathsf{H}}(\triangle)$ it has to intersect it an even number of times as γ needs to be isotopy equivalent to $t\cap\Sigma_{\mathsf{H}}(\triangle)$ which does not intersect $t'\cap\Sigma_{\mathsf{H}}(\triangle)$. Hence the holonomy associated to $t'\cap\Sigma_{\mathsf{H}}(\triangle)$ (or to a curve isotopy equivalent to $t'\cap\Sigma_{\mathsf{H}}(\triangle)$) will not be affected by the translational part of the action of $\mathcal{K}_t[C]$. We can thus associate to each triangle t ribbon operators $\mathcal{K}_t[C]$, labeled by a conjugacy class C of $\mathcal{G}$. This ribbon operator changes the holonomies around the edges bounding the triangle t. This is the same action as for the (gauge averaged) integrated flux operator associated to a triangle t and defined in [22, 86].

We can also consider ribbon operators associated to more general curves than thus arising from one triangle t: For instance we can take two adjacent triangles t,t' and consider their induced curves $t\cap\Sigma_{\mathsf{H}}(\triangle)$ and $t'\cap\Sigma_{\mathsf{H}}(\triangle)$. We can then isotopically deform e.g. $t'\cap\Sigma_{\mathsf{H}}(\triangle)$ to a curve β such that β agrees with $t\cap\Sigma_{\mathsf{H}}(\triangle)$ on the part of the curve running on the cylinder surrounding the edge shared by t and t'. This defines a merging of the curves $t\cap\Sigma_{\mathsf{H}}(\triangle)$ and β, denoted by $(t\circ t')\cap\Sigma_{\mathsf{H}}(\triangle)$ and given by the set $(t\cap\Sigma_{\mathsf{H}}(\triangle))\cup\beta/((t\cap\Sigma_{\mathsf{H}}(\triangle))\cap\beta)$. We can then consider a ribbon operator $\mathcal{K}_{t\circ t'}[C]$ associated to the curve $(t\circ t')\cap\Sigma_{\mathsf{H}}(\triangle)$. This ribbon operator will shift the h–holonomies around the edges adjacent to the triangles t and t' but for the one edge shared by t and t' and along which we merged the two triangle curves to one curve. (Even if the two triangles have more than one edge in common it might not be possible to merge further parts of their curve, see the following discussion.)

This procedure of merging the curves induced by the triangles can be generalized to an arbitrary number of triangles. In this way we can consider ribbon operators associated to curves going around a number of triangles. Note however that it is *in general not* possible to merge the curves arising from triangles meeting at a sphere k, so that the merged curve does not visit this sphere anymore. There might be punctures on k preventing such a merging. One can nevertheless consider a curve, e.g. resulting from the maximally possible merging of three triangles t,t',t'' meeting at a vertex. However even if the three triangles close around a sphere k to a surface we might not be able to merge the three triangles along all the (three) shared edges.

In short, we see that the ribbon operators associated to the merging of several triangle curves will not only depend on the triangles itself, but also on the details on how we merge the associated triangle curves. This determines along which path the group element H is parallel transported, by which we translate each of the holonomies that are crossed by the ribbon. Note that this dependence does also appear for the integrated flux operators in (3+1)d defined in [22, 86]. There, the exponentiated flux operators are associated to a surface glued from triangles. But for each such surface we also have to specify a tree that describes the parallel transport of the translational parameter H for each of the triangles of the surface.

In both, the Heegaard surface and the 3d description, we can also consider a closed surface made

[11] We will later consider more generalized operators.

out of triangles. However, for the reasons discussed above, in the ribbon case we will in general *not* be able to merge the curves induced by the triangles, so that the merged curve is equivalent to a contractible curve on $\Sigma_{\mathsf{H}}(\triangle)$ and the associated ribbon therefore trivial. We will rather have a merged curve visiting some or (in general) all of the spheres adjacent to the triangles making up the glued surface. In general the closed surface made out of triangles is cut open by a connected and spanning tree made out of the edges of the surface. The merged curve runs along the tubes surrounding the edges of the tree and furthermore traverses these tubes twice in opposite directions. The action of the ribbon associated to the merged curve is only non-trivial because of the difference in parallel transport for the two parts of the curve traversing each tube.

Also the exponentiated flux operators associated to closed surfaces as defined in [22, 96] have in general a non-trivial action due to the difference in parallel transport along some cut of the surface. This difference is only relevant if there is curvature, and, as the closed surface operators measure torsion, this effect has been named *curvature-induced torsion* in [22].

7.6 Example: 4-simplex triangulation of $\mathbb{S}_3$

As an example we consider the three-sphere $\mathbb{S}_3$ triangulated by the boundary of a 4-simplex $\triangle = \sigma^4$. We can identify $\mathbb{S}_3$ with the compactified space $\mathbb{R}^3$. This allows us to think of the boundary of the 4-simplex as embedded into $\mathbb{R}^3$. The one-skeleton of the triangulation agrees then with the one-skeleton obtained by subdividing one 3-simplex into four 3-simplices. The four 3-simplices agree with four of the five 3-simplices of the 4-simplex, the fifth 3-simplex is given by the outside region of the subdivided tetrahedron (or by the complement of the subdivided 3-simplex in $\mathbb{S}_3$). The Heegaard surface is finally obtained by blowing-up this one-skeleton.

The cylinders carry one link of the graph that has to coincide with the part of a curve $t \cap \Sigma_{\mathsf{H}}(\triangle)$ induced by one of the triangles. For each edge of the triangulation, that is for each cylinder of the Heegaard surface, we have therefore to select one triangle t adjacent to this edge. We make the following choice: For the edges of the subdivided 3-simplex we choose the links to go along the inside facing part of the tubes. That is for a cylinder $a = ij$ with $i, j = 1, \ldots, 4$ we choose the triangle $t(ij5)$. For cylinders $a = i5$ with $i = 1, 2, 3$ we choose the triangle $t(i54)$, and for $a = 45$ we choose the triangle $t(451)$.

In order to better represent the graph on the punctured spheres, we can draw the punctured spheres associated each vertex of the triangulation in a planar way, see fig. 7.8. In all cases we have four-times-punctured spheres. The four punctures are forming the four vertices of a flattened (on top view of a) 3-simplex. The edges of this (auxiliary) 3-simplex do indeed represent the curves resulting from the triangles of the triangulation cutting the punctured sphere in question. With our choice of links along the cylinders connecting the spheres we have also chosen the *marked points* of the punctures, that is the point on the boundary of the puncture at which the link coming from the cylinder will emerge. For each punctured sphere, we have to choose one node and four links connecting this node to the marked points on the punctures. We present such a choice in fig. 7.8.

There is one further choice to make, namely how to isotop the parts of the curves resulting from triangles cutting the Heegaard surfaces, which do not run already along the links of the graphs. (This has to be done in particular for the part of the curves running along the cylinders.) We indicate in fig. 7.8 in which way the triangle curves are isotoped around the punctures of a given sphere.

For the sake of clarity, let us consider the sphere number 1 denoted by $\mathfrak{S}_1$ in more detail. (As we have made all choices similar for the other spheres the same conclusions will hold there.) The four

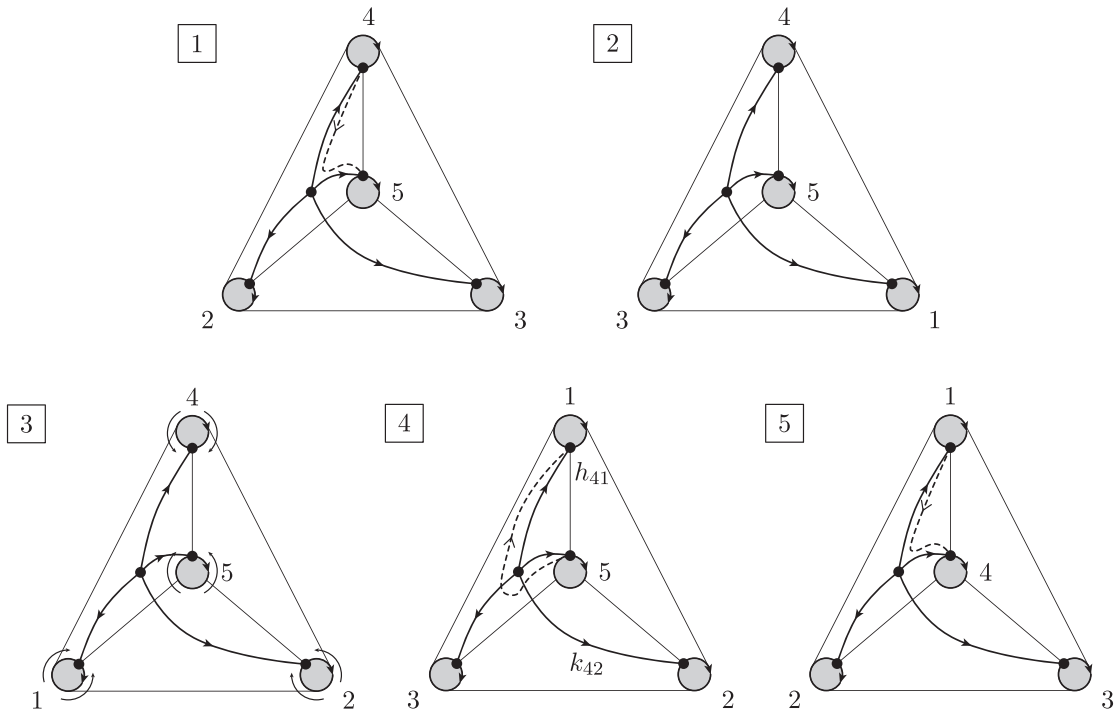

Figure 7.8. This figure shows the five punctured spheres $\mathfrak{S}_i$, $i = 1, \ldots, 5$ (in a planar representation) and the links of Γ on these spheres. The punctures are shown as grey disks. The spheres are glued to tubes, surrounding the edges of the triangulation, via the punctures. Thus each puncture on the sphere $\mathfrak{S}_i$ can be labeled by the sphere $\mathfrak{S}_j$ to which the glued tubes lead. The punctures are surrounded by links oriented clockwise as shown for the sphere $\mathfrak{S}_4$. The thin lines connecting the punctures show how the triangles cut through the punctured spheres and lead to curves on the Heegaard surface. In the picture for $\mathfrak{S}_3$ we have indicated how to deform the curves induced by the triangles so that these curves run along the links of the graph Γ. The dashed line represents the path α defining the action of the ribbon operator $\mathcal{R}_{451}[H]$.

punctures of the sphere can be labeled by the vertices which are connected (through tubes) to these punctures. In trying to construct a path along the graph which is isotopic to the curve induced by a given triangle we have to be careful in how the triangle curve, which emerges from one puncture and goes to another one, surrounds the remaining punctures. For instance we see that the curve given by $t(214) \cap \mathfrak{S}_1$ is isotopic to the following path along the graph Γ: We follow the link from puncture 4 to the 4-valent 'central' node and then follow the link to the marked point of the puncture 2. This holds also for the triangles $t(213), t(415), t(215)$. That is for four out of six triangles we can just follow the canonical path along the graph. (Note that this holds only for the corners of the triangles at v_1, the same triangles will in general involve more complicated paths at other vertices.) To get however a path along the graph that is isotopic to $t(413) \cap \mathfrak{S}_1$, we do however have to—in addition to the link from the puncture 4 to the central node and from the central node to the puncture 3—include a cycle around the puncture 5. Also for the triangle $t(513)$ we have to include a cycle around the puncture 5 itself.

In fact for each of the five spheres we have four triangles which induce curves which are already isotopic to the canonical path along the graph. For the remaining two triangles we need however to include a cycle around a puncture, which is always the central puncture in the figures 7.8.

Absorbing the k–holonomies into the g– and h–holonomies as follows

$$\begin{aligned}\tilde{g}_{ij} &= k_{ij}^{-1} g_{ij} k_{ji} \,, \\ \tilde{h}_{ij} &= k_{ij}^{-1} h_{ij} k_{ij} \,. \end{aligned} \tag{7.47}$$

we obtain holonomies $\tilde{g}$ and $\tilde{h}$ which start and end at the central nodes. We can now give the holonomies along the curves induced by the triangles. With $t(kji)$ we denote the curve going along the cylinders ij, jk and ki. The flatness constraints induced by the triangles are as follows:

$$\begin{aligned}
&t(231): \quad \tilde{g}_{12}\tilde{g}_{23}\tilde{g}_{31} = \mathbb{1} \quad , \quad t(125): \quad \tilde{g}_{25}\tilde{g}_{51}\tilde{g}_{12}\tilde{h}_{25} = \mathbb{1} \,, \\
&t(514): \quad \tilde{g}_{45}\tilde{g}_{51}\tilde{g}_{14} = \mathbb{1} \quad , \quad t(234): \quad \tilde{g}_{34}\tilde{g}_{42}\tilde{g}_{23}\tilde{h}_{35} = \mathbb{1} \,, \\
&t(524): \quad \tilde{g}_{45}\tilde{g}_{52}\tilde{g}_{24}\tilde{h}_{45} = \mathbb{1} \quad , \quad t(314): \quad \tilde{g}_{14}\tilde{g}_{43}\tilde{g}_{31}\tilde{h}_{15} = \mathbb{1} \,, \\
&t(354): \quad \tilde{g}_{54}\tilde{g}_{43}\tilde{g}_{35}\tilde{h}_{54} = \mathbb{1} \quad , \quad t(315): \quad \tilde{g}_{15}\tilde{h}_{54}^{-1}\tilde{g}_{53}\tilde{g}_{31}\tilde{h}_{15} = \mathbb{1} \,, \\
&t(235): \quad \tilde{g}_{35}\tilde{g}_{52}\tilde{g}_{23}\tilde{h}_{35} = \mathbb{1} \quad , \quad t(124): \quad \tilde{g}_{24}\tilde{h}_{45}\tilde{g}_{41}\tilde{g}_{12}\tilde{h}_{25} = \mathbb{1} \,.
\end{aligned} \tag{7.48}$$

These conditions determine 6 variables $\tilde{g}_{ij}$ in terms of the $\tilde{h}_{ij}$ and the remaining four $\tilde{g}_{ij}$. Choosing these four variables to be $\tilde{g}_{12}, \tilde{g}_{13}, \tilde{g}_{14}$ and $\tilde{g}_{15}$ (corresponding to an allowed gauge-fixing) we obtain

$$\tilde{g}_{23} = \tilde{g}_{21}\tilde{g}_{13} \tag{7.49}$$

$$\tilde{g}_{45} = \tilde{g}_{41}\tilde{g}_{15} \tag{7.50}$$

$$\tilde{g}_{43} = \tilde{g}_{41}(\tilde{h}_{15})^{-1}\tilde{g}_{13} \tag{7.51}$$

$$\tilde{g}_{24} = (\tilde{h}_{25})^{-1}\tilde{g}_{21}\tilde{g}_{14}(\tilde{h}_{45})^{-1} \tag{7.52}$$

$$\tilde{g}_{25} = (\tilde{h}_{25})^{-1}\tilde{g}_{21}\tilde{g}_{15} \tag{7.53}$$

$$\tilde{g}_{35} = (\tilde{h}_{35})^{-1}\tilde{g}_{31}\tilde{g}_{12}(\tilde{h}_{25})^{-1}\tilde{g}_{21}\tilde{g}_{15} \,. \tag{7.54}$$

The remaining 4 equations in (7.48) are redundant, for instance by leading to the Bianchi identity $\tilde{h}_{51}\tilde{h}_{52}\tilde{h}_{53}\tilde{h}_{54} = \mathbb{1}$.

Let us now discuss the action of the ribbon operators associated to the triangles. We start with a simple case, the ribbon associated to the triangle $t(431)$.

t(431):
Consider $\mathcal{K}_{431}[C]$, the ribbon around the triangle $t(431)$ with base node the marked point of puncture 1 so that we have a path γ given by the sequence of cylinders

$$13 \to 34 \to 41 \,. \tag{7.55}$$

The corresponding two-handle flatness constraints is

$$\mathbb{1} = \tilde{g}_{14}\tilde{g}_{43}\tilde{g}_{31}\tilde{h}_{15} \,. \tag{7.56}$$

One can follow the path (7.55) such that the links of the graph are always to the right of γ. This path will only cross h_{ij}-holonomies with $i, j \neq 5$. Thus all the triangle flatness constraints will be preserved. More in detail, we can again express the shift of $\tilde{h}$ and $\tilde{g}$ variables performed by the ribbon operator

$\mathcal{K}_{431}[C]$:

$$\begin{cases} \tilde{h}_{13}^{-1} \to (\tilde{g}_{13}\tilde{g}_{34}\tilde{g}_{41})\, H^{-1}\, (\tilde{g}_{14}\tilde{g}_{43}\tilde{g}_{31})\, \tilde{h}_{13}^{-1} \\ \tilde{h}_{31} \to (\tilde{g}_{34}\tilde{g}_{41})\, H^{-1}\, (\tilde{g}_{14}\tilde{g}_{43})\, \tilde{h}_{31} \\ \tilde{h}_{34}^{-1} \to (\tilde{g}_{34}\tilde{g}_{41})\, H^{-1}\, (\tilde{g}_{14}\tilde{g}_{43})\, \tilde{h}_{34}^{-1} \\ \tilde{h}_{43} \to (\tilde{g}_{41})\, H^{-1}\, (\tilde{g}_{14})\, \tilde{h}_{43} \\ \tilde{h}_{41}^{-1} \to (\tilde{g}_{41})\, H^{-1}\, (\tilde{g}_{14})\, \tilde{h}_{41}^{-1} \\ \tilde{h}_{14} \to H^{-1}\, \tilde{h}_{14}\ . \end{cases} \tag{7.57}$$

To make the ribbon operator gauge invariant, the group element H is group averaged (by adjoint action), so that only the information on the conjugacy class C remains. The ribbons $\mathcal{K}_{423}, \mathcal{K}_{124}$ and $\mathcal{K}_{213}$ function analogously. Next we discuss a case in which the ribbon also affects $\tilde{h}_{i5}$ holonomies and thus might a priori violate the triangle flatness constraints.

t(451):
We consider the path γ

$$15 \to 54 \to 41\ . \tag{7.58}$$

We see that some $\tilde{h}_{i5}$ holonomies are shifted but also the k_{42} and k_{43} holonomies. Despite this we can again express everything in terms of $\tilde{h}$ and $\tilde{g}$ variables. The crossing of the ribbon over links carrying h–holonomies leads to the following shifts: (We will make use of the triangle flatness constraint $\tilde{g}_{14}\tilde{g}_{45}\tilde{g}_{51} = \mathbb{1}$.)

$$\begin{cases} \tilde{h}_{15}^{-1} \to H^{-1}\, \tilde{h}_{15}^{-1} \\ \tilde{h}_{51} \to \tilde{g}_{51}\, H^{-1}\, \tilde{g}_{15}\, \tilde{h}_{51} \\ \tilde{h}_{54}^{-1} \to \tilde{g}_{51} H^{-1} \tilde{g}_{15}\, \tilde{h}_{54}^{-1} \\ \tilde{h}_{45} \to \tilde{g}_{41}\, H^{-1} \tilde{g}_{14}\, \tilde{h}_{45} \\ \tilde{h}_{41}^{-1} \to \tilde{g}_{41}\, H^{-1} \tilde{g}_{14}\, \tilde{h}_{41}^{-1} \\ \tilde{h}_{14} \to H^{-1}\, \tilde{h}_{14}\ . \end{cases} \tag{7.59}$$

Furthermore the crossing of the k_{42} and k_{43} variables influences the following variables:

$$\begin{cases} \tilde{g}_{24} \to \tilde{g}_{24}\, \tilde{g}_{41} H \tilde{g}_{14} \\ \tilde{h}_{42} \to \tilde{g}_{41} H^{-1} \tilde{g}_{14} \tilde{h}_{42} \tilde{g}_{41} H \tilde{g}_{14} \\ \tilde{g}_{34} \to \tilde{g}_{34} \tilde{g}_{41} H \tilde{g}_{14} \\ \tilde{h}_{43} \to \tilde{g}_{41} H^{-1} \tilde{g}_{14} \tilde{h}_{43} \tilde{g}_{41} H \tilde{g}_{14}\ . \end{cases} \tag{7.60}$$

The shifts do affect a priori the triangle flatness constraints (7.51) and (7.52). One can check however that the shifts of the various holonomies involved cancel out, and thus the triangle flatness constraints remain invariant. Again the ribbons associated to the triangles $t(524), t(512), t(523)$ and $t(354)$ work similarly. As the last slightly more subtle case we discuss the ribbon associated to the triangle $t(513)$.

t(513):
Let us now consider the ribbon operator whose path path γ is given by

$$53 \to 31 \to 15\ . \tag{7.61}$$

The corresponding triangle flatness constraint reads

$$\tilde{g}_{51}\tilde{h}_{15}^{-1}\tilde{g}_{13}\tilde{g}_{35}\tilde{h}_{54} = \mathbb{1}\,. \tag{7.62}$$

This example is more cumbersome than the previous ones since the ribbon crosses the link h_{15} which is part of the shadow path γ'. In order to circumvent this difficulty, we introduce additional links and decorate them with auxiliary holonomies. Doing so we must ensure that the flatness constraint as well as the gauge invariance are still satisfied and therefore the number of degrees of freedom is preserved. This refining of the graph is performed around the puncture 5 and can be graphically represented as follows

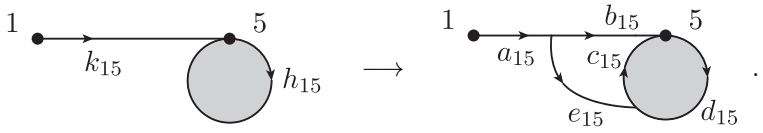

(7.63)

Furthermore, the enforcement of the constraints impose the following expressions between the original variables and the auxiliary ones

$$k_{15} = b_{15}a_{15} \quad , \quad h_{15} = c_{15}d_{15} \quad , \quad e_{15}c_{15}b_{15}^{-1} = \mathbb{1}\,. \tag{7.64}$$

It is now possible to define a ribbon which does not cross any holonomy appearing in the definition of the path γ'. Indeed, let us for instance consider the following ribbon

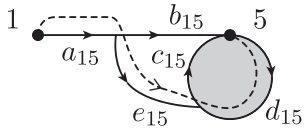

(7.65)

which crosses the links decorated by the holonomies b_{15} and c_{15} whereas the corresponding path γ' is associated to the holonomy $d_{15}^{-1}e_{15}a_{15}$. Putting everything together, we obtain that the ribbon operator produces the following shifts:

$$\begin{cases} \tilde{h}_{53}^{-1} \to (\tilde{g}_{53}\tilde{g}_{31}\tilde{h}_{15}\tilde{g}_{15})H^{-1}(\tilde{g}_{51}\tilde{h}_{15}^{-1}\tilde{g}_{13}\tilde{g}_{35})\tilde{h}_{53}^{-1} \\ \tilde{h}_{35} \to (\tilde{g}_{31}\tilde{h}_{15}\tilde{g}_{15})H^{-1}(\tilde{g}_{51}\tilde{h}_{15}^{-1}\tilde{g}_{13})\tilde{h}_{35} \\ k_{32}^{-1} \to (\tilde{g}_{31}\tilde{h}_{15}\tilde{g}_{15})H^{-1}(\tilde{g}_{51}\tilde{h}_{15}^{-1}\tilde{g}_{13})k_{32}^{-1} \\ \tilde{h}_{31}^{-1} \to (\tilde{g}_{31}\tilde{h}_{15}\tilde{g}_{15})H^{-1}(\tilde{g}_{51}\tilde{h}_{15}^{-1}\tilde{g}_{13})\tilde{h}_{31}^{-1} \\ \tilde{h}_{13} \to (\tilde{h}_{15}\tilde{g}_{15})H^{-1}(\tilde{g}_{51}\tilde{h}_{15}^{-1})\tilde{h}_{13} \\ k_{12}^{-1} \to (\tilde{h}_{15}\tilde{g}_{15})H^{-1}(\tilde{g}_{51}\tilde{h}_{15}^{-1})k_{12}^{-1} \\ k_{14}^{-1} \to (\tilde{h}_{15}\tilde{g}_{15})H^{-1}(\tilde{g}_{51}\tilde{h}_{15}^{-1})\tilde{k}_{14}^{-1} \\ \tilde{h}_{51} \to H^{-1}\tilde{h}_{51} \end{cases} \quad \text{and} \quad \begin{cases} k_{15} \to h_{15}g_{15}k_{51}H\tilde{g}_{51}\tilde{h}_{15}^{-1} \\ h_{15} \to h_{15}g_{15}k_{51}Hk_{51}^{-1}g_{51} \end{cases} \tag{7.66}$$

such that the shifts of the k–holonomies k_{32}, k_{12}, k_{14} and k_{15} and the h–holonomy h_{15} influence the

following variables:

$$\begin{cases} \tilde{g}_{32} \to (\tilde{g}_{31}\tilde{h}_{15}\tilde{g}_{15})H^{-1}(\tilde{g}_{51}\tilde{h}_{15}^{-1}\tilde{g}_{13})\tilde{g}_{32} \\ \tilde{h}_{32} \to (\tilde{g}_{31}\tilde{h}_{15}\tilde{g}_{15})H^{-1}(\tilde{g}_{51}\tilde{h}_{15}^{-1}\tilde{g}_{13})\tilde{h}_{32}(\tilde{g}_{31}\tilde{h}_{15}\tilde{g}_{15})H(\tilde{g}_{51}\tilde{h}_{15}^{-1}\tilde{g}_{13}) \\ \tilde{g}_{12} \to (\tilde{h}_{15}\tilde{g}_{15})H^{-1}(\tilde{g}_{51}\tilde{h}_{15}^{-1})\tilde{g}_{12} \\ \tilde{h}_{12} \to (\tilde{h}_{15}\tilde{g}_{15})H^{-1}(\tilde{g}_{51}\tilde{h}_{15}^{-1})\tilde{h}_{12}(\tilde{h}_{15}\tilde{g}_{15})H(\tilde{g}_{51}\tilde{h}_{15}^{-1}) \\ \tilde{g}_{14} \to (\tilde{h}_{15}\tilde{g}_{15})H^{-1}(\tilde{g}_{51}\tilde{h}_{15}^{-1})\tilde{g}_{14} \\ \tilde{h}_{14} \to (\tilde{h}_{15}\tilde{g}_{15})H^{-1}(\tilde{g}_{51}\tilde{h}_{15}^{-1})\tilde{h}_{14}(\tilde{h}_{15}\tilde{g}_{15})H(\tilde{g}_{51}\tilde{h}_{15}^{-1}) \\ \tilde{g}_{15} \to (\tilde{h}_{15}\tilde{g}_{15})H^{-1}(\tilde{g}_{51}\tilde{h}_{15}^{-1})\tilde{g}_{15} \\ \tilde{h}_{15} \to \tilde{h}_{15}\tilde{h}_{15}\tilde{g}_{15}H\tilde{g}_{51}\tilde{h}_{15}^{-1} \end{cases} \tag{7.67}$$

Despite these additional shifts, the flatness constraints are not violated. Indeed, the different shifts cancel each other such that all the flatness constraints presented earlier remain invariant. In particular, we have the following trivial transformations

$$\begin{cases} \tilde{g}_{12}\tilde{g}_{23}\tilde{g}_{31} = \mathbb{1} \to \tilde{h}_{15}\tilde{g}_{15}H^{-1}\tilde{g}_{51}\tilde{h}_{15}^{-1}\tilde{g}_{12}\tilde{g}_{23}\tilde{g}_{31}\tilde{h}_{15}\tilde{g}_{15}H\tilde{g}_{51}\tilde{h}_{15}^{-1}\tilde{g}_{13}\tilde{g}_{31} = \mathbb{1} \\ \tilde{g}_{35}\tilde{g}_{52}\tilde{g}_{23}\tilde{h}_{35} = \mathbb{1} \to \tilde{g}_{35}\tilde{g}_{52}\tilde{g}_{23}\tilde{g}_{31}\tilde{h}_{15}\tilde{g}_{15}H\tilde{g}_{51}\tilde{h}_{15}^{-1}\tilde{g}_{13}\tilde{g}_{31}\tilde{h}_{15}\tilde{g}_{15}H^{-1}\tilde{g}_{51}\tilde{h}_{15}^{-1}\tilde{g}_{13}\tilde{h}_{35} = \mathbb{1} \\ \tilde{g}_{15}\tilde{h}_{54}^{-1}\tilde{g}_{53}\tilde{g}_{31}\tilde{h}_{15} = \mathbb{1} \to \tilde{h}_{15}\tilde{g}_{15}H^{-1}\tilde{g}_{51}\tilde{h}_{15}^{-1}\tilde{g}_{15}\tilde{h}_{54}^{-1}\tilde{g}_{53}\tilde{g}_{31}\tilde{h}_{15}\tilde{h}_{15}\tilde{g}_{15}H\tilde{g}_{51}\tilde{h}_{15}^{-1} = \mathbb{1} \end{cases} \tag{7.68}$$

and one can check the remaining ones similarly.

Merging of two triangles:
We can now consider the case of a ribbon associated with the merging of two triangles. Let us for instance consider the triangles $t(431)$ and $t(412)$ which have in common the tube going from the puncture 1 to the puncture 4. We are looking for a ribbon operator $\mathcal{K}_{4312}[H]$ associated to the curve going around the two triangles so that we have the following path γ

$$21 \to 13 \to 34 \to 42\ . \tag{7.69}$$

The flatness constraints for the triangle $t(431)$ and $t(412)$ are given by $\tilde{g}_{14}\tilde{g}_{43}\tilde{g}_{31}\tilde{h}_{15} = \mathbb{1}$ and $\tilde{g}_{24}\tilde{h}_{45}\tilde{g}_{41}\tilde{g}_{12}\tilde{h}_{25} = \mathbb{1}$, respectively, so that the flatness constraint assiociated with the merging of the two triangles reads

$$\tilde{g}_{24}\tilde{h}_{45}\tilde{g}_{43}\tilde{g}_{31}\tilde{h}_{15}\tilde{g}_{12}\tilde{h}_{25} = \mathbb{1}\ . \tag{7.70}$$

The action of the ribbon then produces the following shifts of holonomies

$$\begin{cases} \tilde{h}_{21}^{-1} \to (\tilde{g}_{21}\tilde{h}_{15}^{-1}\tilde{g}_{13}\tilde{g}_{34}\tilde{h}_{45}^{-1}\tilde{g}_{42})H^{-1}(\tilde{g}_{24}\tilde{h}_{45}\tilde{g}_{43}\tilde{g}_{31}\tilde{h}_{15}\tilde{g}_{12})\tilde{h}_{21}^{-1} \\ \tilde{h}_{12} \to (\tilde{h}_{15}^{-1}\tilde{g}_{13}\tilde{g}_{34}\tilde{h}_{45}^{-1}\tilde{g}_{42})H^{-1}(\tilde{g}_{24}\tilde{h}_{45}\tilde{g}_{43}\tilde{g}_{31}\tilde{h}_{15})\tilde{h}_{12} \\ k_{14}^{-1} \to (\tilde{h}_{15}^{-1}\tilde{g}_{13}\tilde{g}_{34}\tilde{h}_{45}^{-1}\tilde{g}_{42})H^{-1}(\tilde{g}_{24}\tilde{h}_{45}\tilde{g}_{43}\tilde{g}_{31}\tilde{h}_{15})k_{14}^{-1} \\ \tilde{h}_{13}^{-1} \to (\tilde{g}_{13}\tilde{g}_{34}\tilde{h}_{45}^{-1}\tilde{g}_{42})H^{-1}(\tilde{g}_{24}\tilde{h}_{45}\tilde{g}_{43}\tilde{g}_{31})\tilde{h}_{13}^{-1} \\ \tilde{h}_{31} \to (\tilde{g}_{34}\tilde{h}_{45}^{-1}\tilde{g}_{42})H^{-1}(\tilde{g}_{24}\tilde{h}_{45}\tilde{g}_{43})\tilde{h}_{31} \\ \tilde{h}_{34}^{-1} \to (\tilde{g}_{34}\tilde{h}_{45}^{-1}\tilde{g}_{42})H^{-1}(\tilde{g}_{24}\tilde{h}_{45}\tilde{g}_{43})\tilde{h}_{34}^{-1} \\ \tilde{h}_{43} \to (\tilde{h}_{45}^{-1}\tilde{g}_{42})H^{-1}(\tilde{g}_{24}\tilde{h}_{45})\tilde{h}_{43} \\ k_{41}^{-1} \to (\tilde{h}_{45}^{-1}\tilde{g}_{42})H^{-1}(\tilde{g}_{24}\tilde{h}_{45})k_{41}^{-1} \\ \tilde{h}_{42}^{-1} \to \tilde{g}_{42}H^{-1}\tilde{g}_{24}\tilde{h}_{42}^{-1} \\ \tilde{h}_{24} \to H^{-1}\tilde{h}_{24} \end{cases} \tag{7.71}$$

The only remarkable feature is the fact that the ribbon operator acts on both k_{14}^{-1} and k_{41}^{-1} which is not the case when considering the independent actions on triangles $t(431)$ and $t(412)$. For the action of the ribbon on $\tilde{g}_{14}$ both transformation compensate so that $\tilde{g}_{14}$ remains unchanged. Indeed, we have

$$\tilde{g}_{14} \to (\tilde{h}_{15}^{-1}\tilde{g}_{13}\tilde{g}_{34}\tilde{h}_{45}^{-1}\tilde{g}_{42})H^{-1}(\tilde{g}_{24}\tilde{h}_{45}\tilde{g}_{43}\tilde{g}_{31}\tilde{h}_{15})\tilde{g}_{14}(\tilde{h}_{45}^{-1}\tilde{g}_{42})H(\tilde{g}_{24}\tilde{h}_{45}) = \tilde{g}_{14} \tag{7.72}$$

where we have used twice the flatness constraint on the triangle $t(413)$. Also h_{14} and h_{41} are not changed by the ribbon operator. We do have however a change of $\tilde{h}_{14} = k_{14}^{-1}h_{14}k_{14}$ and $\tilde{h}_{41} = k_{41}^{-1}h_{41}k_{41}$ due to the shift of k_{14} and k_{41}. Note however that this change is by an adjoint action, so the (gauge invariant) conjugacy classes of $\tilde{h}_{14}$ and $\tilde{h}_{41}$ do not change. Therefore, as previously discussed in the general case, the ribbon operator changes the holonomies associated with the edges adjacent to the triangles but for the edge shared by the triangles. Furthermore, since the remaining shifts are only about h–holonomies which do not influence the flatness constraints, we can confirm that the ribbon operator for the merging of two triangles as defined here is consistent.

7.7 Remarks

In this work, we explained how the Hilbert space and operators for a (2+1)d theory of flat connections lead to a Hilbert space and operators for a (3+1)d theory of flat connections with curvature defects. A crucial point is to use the Heegaard surface that arises from the Heegaard splitting of the 3d manifold, describing the equal time hypersurface of a (3+1)d manifold. The Heegaard splitting can be based on a triangulation (or other polyhedral lattice), the curvature defects are then confined to the one-skeleton of this triangulation. The theory of flat connections on the 3d manifold can then be described in terms of the theory of flat connections on the 2d Heegaard surface, but equipped with additional flatness constraints. In particular, starting from the fusion basis on the 2d Heegaard surface, we obtain two basis of 3d excited states, namely the spin network basis and the dual magnetic basis. The former is obtained as a subset of the fusion basis states, while the latter is obtained via superpositions of fusion basis states involving a sum over the R–labels. Furthermore, we can express operators generating curvature defects for the 3d theory as (ribbon) operators acting on the space of flat connections on the 2d surface, satisfying the additional flatness constraints.

This presents an interesting example where a (2+1)d dimensional topological quantum field theory can be used to construct a Hilbert space, with a (triangulation independent) vacuum state and excitations for a (3+1)d dimensional theory. We believe that this technique can be applied to a wide range of (2+1)d TQFTs and thus would allow the construction and understanding of a wide range of (3+1)d TQFTs with defects. In [52], the same construction was applied to the case Turaev-Viro TQFT for a modular fusion category. A similar analysis was carried out and the analogues of the spin network basis and the dual magnetic basis were defined. Interestingly, in that case, the parameterization of the basis states in both case is such that the local curvature content can be immediately read-off. This situations does not quite occur in the finite group case considered in this chapter as the structure of the excitations is more complicated. In the case of the magnetic basis, this translates into the fact that conjugacy classes alone do not completely parametrize the space of 3d excited states.

Apart from generalizing this construction to additional (2+1)d TQFTs, there are several interesting research directions. The most obvious one is to consider Heegaard splittings of three-dimensional manifold with boundaries. This would result in Heegaard surfaces with punctures, which, as we have extensively studied, allows for the introduction of torsion (or electric) defects. We could then use this framework in order to define a gluing of 3d excited states. A special case of this constructions should yield the quantum triple algebra presented in the previous chapter. Furthermore, following chap. 5, this could also be used to define a notion of entanglement entropy for 3d topological phases with defects.

Bibliography

[1] C. Delcamp, L. Freidel and F. Girelli, *Dual loop quantizations of 3d gravity*, 1803.03246.

[2] C. Delcamp, *Excitation basis for (3+1)d topological phases*, *JHEP* **12** (2017) 128, [1709.04924].

[3] C. Delcamp and A. Tiwari, *From gauge to higher gauge models of topological phases*, 1802.10104.

[4] C. Delcamp, B. Dittrich and A. Riello, *Fusion basis for lattice gauge theory and loop quantum gravity*, *JHEP* **02** (2017) 061, [1607.08881].

[5] C. Delcamp, B. Dittrich and A. Riello, *On entanglement entropy in non-Abelian lattice gauge theory and 3D quantum gravity*, *JHEP* **11** (2016) 102, [1609.04806].

[6] C. Delcamp and B. Dittrich, *From 3D topological quantum field theories to 4D models with defects*, *J. Math. Phys.* **58** (2017) 062302, [1606.02384].

[7] A. Ashtekar, *New variables for classical and quantum gravity*, *Phys. Rev. Lett.* **57** (Nov, 1986) 2244–2247.

[8] J. F. Barbero G., *Real Ashtekar variables for Lorentzian signature space times*, *Phys. Rev.* **D51** (1995) 5507–5510, [gr-qc/9410014].

[9] C. Rovelli, *Quantum Gravity*. Cambridge Monographs on Mathematical Physics. Cambridge University Press, 2004.

[10] A. Ashtekar and J. Lewandowski, *Background independent quantum gravity: A Status report*, *Class. Quant. Grav.* **21** (2004) R53, [gr-qc/0404018].

[11] K. G. Wilson, *Confinement of quarks*, *Phys. Rev. D* **10** (Oct, 1974) 2445–2459.

[12] J. Smit, *Introduction to Quantum Fields on a Lattice*. Sept., 2002.

[13] B. Dittrich, *How to construct diffeomorphism symmetry on the lattice*, *PoS* **QGQGS2011** (2011) 012, [1201.3840].

[14] B. Dittrich, *Diffeomorphism symmetry in quantum gravity models*, *Adv. Sci. Lett.* **2** (2008) 151, [0810.3594].

[15] B. Dittrich, *The continuum limit of loop quantum gravity - a framework for solving the theory*, in *Loop Quantum Gravity: The First 30 Years* (A. Ashtekar and J. Pullin, eds.), pp. 153–179. 2017. 1409.1450. DOI.

[16] C. Rovelli and L. Smolin, *Spin networks and quantum gravity*, *Phys. Rev.* **D52** (1995) 5743–5759, [gr-qc/9505006].

[17] R. Loll, *Independent SU(2) loop variables*, *Nucl. Phys.* **B368** (1992) 121–142.

[18] E. R. Livine, *Deformation Operators of Spin Networks and Coarse-Graining*, *Class. Quant. Grav.* **31** (2014) 075004, [1310.3362].

[19] C. Delcamp and B. Dittrich, *Towards a phase diagram for spin foams*, *Class. Quant. Grav.* **34** (2017) 225006, [1612.04506].

[20] V. G. Drinfel'd, *Quantum groups*, *Journal of Soviet Mathematics* **41** (1988) 898–915.

[21] A. Ocneanu, *Chirality for operator algebras*, *Subfactors (Kyuzeso, 1993)* 39–63.

[22] B. Dittrich and M. Geiller, *Flux formulation of loop quantum gravity: Classical framework*, *Class. Quant. Grav.* **32** (2015) 135016, [1412.3752].

[23] C. Charles and E. R. Livine, *The Fock Space of Loopy Spin Networks for Quantum Gravity*, *Gen. Rel. Grav.* **48** (2016) 113, [1603.01117].

[24] P. Calabrese and J. L. Cardy, *Entanglement entropy and quantum field theory*, *J. Stat. Mech.* **0406** (2004) P06002, [hep-th/0405152].

[25] L. Amico, R. Fazio, A. Osterloh and V. Vedral, *Entanglement in many-body systems*, *Rev. Mod. Phys.* **80** (May, 2008) 517–576.

[26] H. Casini and M. Huerta, *Entanglement entropy in free quantum field theory*, *J. Phys.* **A42** (2009) 504007, [0905.2562].

[27] S. B. Giddings, *Hilbert space structure in quantum gravity: an algebraic perspective*, *JHEP* **12** (2015) 099, [1503.08207].

[28] W. Donnelly, *Entanglement entropy in loop quantum gravity*, *Phys. Rev.* **D77** (2008) 104006, [0802.0880].

[29] P. V. Buividovich and M. I. Polikarpov, *Entanglement entropy in gauge theories and the holographic principle for electric strings*, *Phys. Lett.* **B670** (2008) 141–145, [0806.3376].

[30] W. Donnelly, *Decomposition of entanglement entropy in lattice gauge theory*, *Phys. Rev.* **D85** (2012) 085004, [1109.0036].

[31] W. Donnelly, *Entanglement entropy and nonabelian gauge symmetry*, *Class. Quant. Grav.* **31** (2014) 214003, [1406.7304].

[32] A. Ocneanu, *Operator algebras, topology and subgroups of quantum symmetry*, *Adv. Studies in Pure Math* (2001) 235–263.

[33] T. Lan and X.-G. Wen, *Topological quasiparticles and the holographic bulk-edge relation in (2+1) -dimensional string-net models*, *Phys. Rev.* **B90** (2014) 115119, [1311.1784].

[34] B. Dittrich and M. Geiller, *Quantum gravity kinematics from extended TQFTs*, 1604.05195.

[35] N. Bultinck, M. Mariën, D. J. Williamson, M. B. Şahinoğlu, J. Haegeman and F. Verstraete, *Anyons and matrix product operator algebras*, *Annals of Physics* **378** (2017) 183–233.

[36] R. Koenig, G. Kuperberg and B. W. Reichardt, *Quantum computation with Turaev-Viro codes*, *Annals of Physics* **325** (Dec., 2010) 2707–2749, [1002.2816].

[37] Y. Hu, N. Geer and Y.-S. Wu, *Full Dyon Excitation Spectrum in Generalized Levin-Wen Models*, 1502.03433.

[38] A. Yu. Kitaev, *Fault tolerant quantum computation by anyons*, *Annals Phys.* **303** (2003) 2–30, [quant-ph/9707021].

[39] M. A. Levin and X.-G. Wen, *String net condensation: A Physical mechanism for topological phases*, *Phys. Rev.* **B71** (2005) 045110, [cond-mat/0404617].

[40] A. Kitaev and L. Kong, *Models for Gapped Boundaries and Domain Walls*, *Communications in Mathematical Physics* **313** (July, 2012) 351–373, [1104.5047].

[41] T. Lan, L. Kong and X.-G. Wen, *A classification of 3+1D bosonic topological orders (I): the case when point-like excitations are all bosons*, *ArXiv e-prints* (Apr., 2017) , [1704.04221].

[42] A. Kirillov, Jr. and B. Balsam, *Turaev-Viro invariants as an extended TQFT*, *ArXiv e-prints* (Apr., 2010) , [1004.1533].

[43] A. Kirillov, Jr, *String-net model of Turaev-Viro invariants*, 1106.6033.

[44] J. Wang and X.-G. Wen, *Non-Abelian string and particle braiding in topological order: Modular SL(3,$\mathbb{Z}$) representation and (3+1) -dimensional twisted gauge theory*, *Phys. Rev.* **B91** (2015) 035134, [1404.7854].

[45] K. Walker and Z. Wang, *(3+1)-TQFTs and topological insulators*, *Frontiers of Physics* **7** (Apr., 2012) 150–159, [1104.2632].

[46] C. Wang and M. Levin, *Braiding statistics of loop excitations in three dimensions*, *Physical review letters* **113** (2014) 080403.

[47] H. Moradi and X.-G. Wen, *Universal Topological Data for Gapped Quantum Liquids in Three Dimensions and Fusion Algebra for Non-Abelian String Excitations*, *Phys. Rev.* **B91** (2015) 075114, [1404.4618].

[48] Y. Wan, J. C. Wang and H. He, *Twisted Gauge Theory Model of Topological Phases in Three Dimensions*, *Phys. Rev.* **B92** (2015) 045101, [1409.3216].

[49] A. Bullivant, M. Calada, Z. Kdr, P. Martin and J. F. Martins, *Topological phases from higher gauge symmetry in 3+1 dimensions*, *Phys. Rev.* **B95** (2017) 155118, [1606.06639].

[50] X.-G. Wen, *Exactly soluble local bosonic cocycle models, statistical transmutation, and simplest time-reversal symmetric topological orders in 3+1 dimensions*, *Phys. Rev.* **B95** (2017) 205142, [1612.01418].

[51] C. Delcamp and B. Dittrich, *From 3D TQFTs to 4D models with defects*, 1606.02384.

[52] B. Dittrich, *(3 + 1)-dimensional topological phases and self-dual quantum geometries encoded on Heegaard surfaces*, *JHEP* **05** (2017) 123, [1701.02037].

[53] D. J. Williamson and Z. Wang, *Hamiltonian models for topological phases of matter in three spatial dimensions*, *Annals Phys.* **377** (2017) 311–344, [1606.07144].

[54] T. Lan, L. Kong and X.-G. Wen, *A classification of 3+1D bosonic topological orders (I): the case when point-like excitations are all bosons*, *ArXiv e-prints* (Apr., 2017) , [1704.04221].

[55] D. V. Else and C. Nayak, *Cheshire charge in (3+1)-D topological phases*, *ArXiv e-prints* (Feb., 2017) , [1702.02148].

[56] A. Riello, *On a self-dual phase space for 3+1 lattice Yang-Mills theory*, 1706.07811.

[57] N. Tantivasadakarn, *Dimensional Reduction and Topological Invariants of Symmetry Protected Topological Phases*, 1706.09769.

[58] J. C. Baez, *Spin foam models*, *Class. Quant. Grav.* **15** (1998) 1827–1858, [gr-qc/9709052].

[59] A. Perez, *The Spin Foam Approach to Quantum Gravity*, *Living Rev. Rel.* **16** (2013) 3, [1205.2019].

[60] B. Dittrich, F. C. Eckert and M. Martin-Benito, *Coarse graining methods for spin net and spin foam models*, *New J. Phys.* **14** (2012) 035008, [1109.4927].

[61] B. Dittrich, *From the discrete to the continuous: Towards a cylindrically consistent dynamics*, *New J. Phys.* **14** (2012) 123004, [1205.6127].

[62] B. Bahr, B. Dittrich, F. Hellmann and W. Kaminski, *Holonomy Spin Foam Models: Definition and Coarse Graining*, *Phys. Rev.* **D87** (2013) 044048, [1208.3388].

[63] B. Dittrich, M. Martin-Benito and S. Steinhaus, *Quantum group spin nets: refinement limit and relation to spin foams*, *Phys. Rev.* **D90** (2014) 024058, [1312.0905].

[64] B. Bahr, *On background-independent renormalization of spin foam models*, *Class. Quant. Grav.* **34** (2017) 075001, [1407.7746].

[65] B. Dittrich, S. Mizera and S. Steinhaus, *Decorated tensor network renormalization for lattice gauge theories and spin foam models*, *New J. Phys.* **18** (2016) 053009, [1409.2407].

[66] B. Bahr and S. Steinhaus, *Numerical evidence for a phase transition in 4d spin-foam quantum gravity*, *Phys. Rev. Lett.* **117** (Sep, 2016) 141302.

[67] A. Ashtekar and C. J. Isham, *Representations of the holonomy algebras of gravity and nonAbelian gauge theories*, *Class. Quant. Grav.* **9** (1992) 1433–1468, [hep-th/9202053].

[68] A. Ashtekar and J. Lewandowski, *Representation theory of analytic holonomy C* algebras*, gr-qc/9311010.

[69] A. Ashtekar and J. Lewandowski, *Projective techniques and functional integration for gauge theories*, *J. Math. Phys.* **36** (1995) 2170–2191, [gr-qc/9411046].

[70] A. Perez, *Introduction to loop quantum gravity and spin foams*, in *2nd International Conference on Fundamental Interactions (ICFI 2004) Domingos Martins, Espirito Santo, Brazil, June 6-12, 2004*, 2004, gr-qc/0409061.

[71] C. Thiemann, *Introduction to Modern Canonical Quantum General Relativity*. Cambridge University Press, 2007.

[72] G. Ponzano and T. Regge, *Semiclassical limit of racah coefficients.*, *pp 1-58 of Spectroscopic and Group Theoretical Methods in Physics. Block, F. (ed.). New York, John Wiley and Sons, Inc., 1968.* (Oct, 1969) .

[73] J. W. Barrett and I. Naish-Guzman, *The Ponzano-Regge model*, *Class. Quant. Grav.* **26** (2009) 155014, [0803.3319].

[74] E. Fradkin, *Field theories of condensed matter physics*. Cambridge University Press, 2013.

[75] X.-G. Wen, *Quantum field theory of many-body systems: from the origin of sound to an origin of light and electrons*. Oxford University Press on Demand, 2004.

[76] D. Gaiotto and T. Johnson-Freyd, *Symmetry Protected Topological phases and Generalized Cohomology*, 1712.07950.

[77] R. Dijkgraaf and E. Witten, *Topological gauge theories and group cohomology*, *Communications in Mathematical Physics* **129** (1990) 393–429.

[78] D. S. Freed and F. Quinn, *Chern-Simons theory with finite gauge group*, *Commun. Math. Phys.* **156** (1993) 435–472, [hep-th/9111004].

[79] A. Kitaev, *Anyons in an exactly solved model and beyond*, *Annals Phys.* **321** (2006) 2–111.

[80] M. A. Levin and X.-G. Wen, *String net condensation: A Physical mechanism for topological phases*, *Phys. Rev.* **B71** (2005) 045110, [cond-mat/0404617].

[81] Y. Hu, Y. Wan and Y.-S. Wu, *Twisted quantum double model of topological phases in two dimensions*, *Phys. Rev.* **B87** (2013) 125114, [1211.3695].

[82] A. Mesaros and Y. Ran, *Classification of symmetry enriched topological phases with exactly solvable models*, *Phys. Rev.* **B87** (2013) 155115, [1212.0835].

[83] R. Dijkgraaf and E. Witten, *Topological gauge theories and group cohomology*, *Comm. Math. Phys.* **129** (1990) 393–429.

[84] A. Yu. Kitaev, *Fault tolerant quantum computation by anyons*, *Annals Phys.* **303** (2003) 2–30, [quant-ph/9707021].

[85] Y. Hu, Y. Wan and Y.-S. Wu, *Twisted quantum double model of topological phases in two dimensions*, *Physical Review B* **87** (2013) 125114.

[86] B. Bahr, B. Dittrich and M. Geiller, *A new realization of quantum geometry*, 1506.08571.

[87] R. Dijkgraaf, V. Pasquier and P. Roche, *Quasi hope algebras, group cohomology and orbifold models*, *Nuclear Physics B Proceedings Supplements* **18** (Jan., 1991) 60–72.

[88] T. H. Koornwinder, B. J. Schroers, J. K. Slingerland and F. A. Bais, *Fourier transform and the Verlinde formula for the quantum double of a finite group*, *J. Phys.* **A32** (1999) 8539–8549, [math/9904029].

[89] T. H. Koornwinder, F. A. Bais and N. M. Muller, *Tensor product representations of the quantum double of a compact group*, *Commun. Math. Phys.* **198** (1998) 157–186, [q-alg/9712042].

[90] G. Alagic, S. P. Jordan, R. König and B. W. Reichardt, *Estimating turaev-viro three-manifold invariants is universal for quantum computation*, *Physical Review A* **82** (2010) 040302.

[91] Y. Hu, S. D. Stirling and Y.-S. Wu, *Ground State Degeneracy in the Levin-Wen Model for Topological Phases*, *Phys. Rev.* **B85** (2012) 075107, [1105.5771].

[92] A. Baratin, B. Dittrich, D. Oriti and J. Tambornino, *Non-commutative flux representation for loop quantum gravity*, *Class. Quant. Grav.* **28** (2011) 175011, [1004.3450].

[93] O. Buerschaper, M. Christandl, L. Kong and M. Aguado, *Electric-magnetic duality of lattice systems with topological order*, *Nucl. Phys.* **B876** (2013) 619–636, [1006.5823].

[94] O. Buerschaper and M. Aguado, *Mapping Kitaev's quantum double lattice models to Levin and Wen's string-net models*, 0907.2670.

[95] A. Milsted and T. J. Osborne, *Quantum Yang-Mills theory: an overview of a programme*, 1604.01979.

[96] B. Dittrich and M. Geiller, *A new vacuum for Loop Quantum Gravity*, *Class. Quant. Grav.* **32** (2015) 112001, [1401.6441].

[97] V. G. Turaev and O. Y. Viro, *State sum invariants of 3 manifolds and quantum 6j symbols*, *Topology* **31** (1992) 865–902.

[98] P. de Sousa Gerbert, *On spin and (quantum) gravity in (2+1)-dimensions*, *Nucl. Phys.* **B346** (1990) 440–472.

[99] L. Freidel and D. Louapre, *Ponzano-Regge model revisited I: Gauge fixing, observables and interacting spinning particles*, *Class. Quant. Grav.* **21** (2004) 5685–5726, [hep-th/0401076].

[100] B. Bahr, B. Dittrich and J. P. Ryan, *Spin foam models with finite groups*, *J. Grav.* **2013** (2013) 549824, [1103.6264].

[101] B. Dittrich, M. Martn-Benito and E. Schnetter, *Coarse graining of spin net models: dynamics of intertwiners*, *New J. Phys.* **15** (2013) 103004, [1306.2987].

[102] L. Freidel and D. Louapre, *Ponzano-Regge model revisited II: Equivalence with Chern-Simons*, gr-qc/0410141.

[103] K. Noui and A. Perez, *Three-dimensional loop quantum gravity: Coupling to point particles*, *Class. Quant. Grav.* **22** (2005) 4489–4514, [gr-qc/0402111].

[104] V. Bonzom, M. Dupuis, F. Girelli and E. R. Livine, *Deformed phase space for 3d loop gravity and hyperbolic discrete geometries*, 1402.2323.

[105] F. Cianfrani, J. Kowalski-Glikman, D. Pranzetti and G. Rosati, *Symmetries of quantum spacetime in three dimensions*, *Phys. Rev.* **D94** (2016) 084044, [1606.03085].

[106] H. Bombin and M. A. Martin-Delgado, *A Family of Non-Abelian Kitaev Models on a Lattice: Topological Confinement and Condensation*, *Phys. Rev.* **B78** (2008) 115421, [0712.0190].

[107] G. Vidal, *Class of Quantum Many-Body States That Can Be Efficiently Simulated*, *Physical Review Letters* **101** (Sept., 2008) 110501, [quant-ph/0610099].

[108] L. Tagliacozzo, A. Celi and M. Lewenstein, *Tensor Networks for Lattice Gauge Theories with continuous groups*, *Phys. Rev.* **X4** (2014) 041024, [1405.4811].

[109] L. Tagliacozzo and G. Vidal, *Entanglement renormalization and gauge symmetry*, *Phys. Rev. B* **83** (Mar, 2011) 115127.

[110] B. Dittrich and S. Steinhaus, *Time evolution as refining, coarse graining and entangling*, *New J. Phys.* **16** (2014) 123041, [1311.7565].

[111] S. Ariwahjoedi, J. S. Kosasih, C. Rovelli and F. P. Zen, *How many quanta are there in a quantum spacetime?*, *Class. Quant. Grav.* **32** (2015) 165019, [1404.1750].

[112] J. Kijowski, *Symplectic geometry and second quantization*, *Reports on Mathematical Physics* **11** (Feb., 1977) 97–109.

[113] S. Lanry and T. Thiemann, *Projective Loop Quantum Gravity I. State Space*, *J. Math. Phys.* **57** (2016) 122304, [1411.3592].

[114] S. Lanry and T. Thiemann, *Projective Limits of State Spaces II. Quantum Formalism*, *J. Geom. Phys.* **116** (2017) 10–51, [1411.3590].

[115] B. Bahr and B. Dittrich, *Improved and Perfect Actions in Discrete Gravity*, *Phys. Rev.* **D80** (2009) 124030, [0907.4323].

[116] B. Bahr and B. Dittrich, *Regge calculus from a new angle*, *New J. Phys.* **12** (2010) 033010, [0907.4325].

[117] M. Dupuis, F. Girelli and E. R. Livine, *Deformed Spinor Networks for Loop Gravity: Towards Hyperbolic Twisted Geometries*, *Gen. Rel. Grav.* **46** (2014) 1802, [1403.7482].

[118] C. Charles and E. R. Livine, *The closure constraint for the hyperbolic tetrahedron as a Bianchi identity*, *Gen. Rel. Grav.* **49** (2017) 92, [1607.08359].

[119] H. M. Haggard, M. Han, W. Kaminski and A. Riello, *SL(2,C) Chern-Simons Theory, Flat Connections, and Four-dimensional Quantum Geometry*, 1512.07690.

[120] H. M. Haggard, M. Han, W. Kamiski and A. Riello, *SL(2,C) ChernSimons theory, a non-planar graph operator, and 4D quantum gravity with a cosmological constant: Semiclassical geometry*, *Nucl. Phys.* **B900** (2015) 1–79, [1412.7546].

[121] H. M. Haggard, M. Han, W. Kamiski and A. Riello, *Four-dimensional Quantum Gravity with a Cosmological Constant from Three-dimensional Holomorphic Blocks*, *Phys. Lett.* **B752** (2016) 258–262, [1509.00458].

[122] W. Donnelly and L. Freidel, *Local subsystems in gauge theory and gravity*, 1601.04744.

[123] L. Freidel and E. R. Livine, *Ponzano-Regge model revisited III: Feynman diagrams and effective field theory*, *Class. Quant. Grav.* **23** (2006) 2021–2062, [hep-th/0502106].

[124] C. Meusburger and K. Noui, *The Hilbert space of 3d gravity: quantum group symmetries and observables*, *Adv. Theor. Math. Phys.* **14** (2010) 1651–1715, [0809.2875].

[125] V. V. Fock and A. A. Rosly, *Poisson structure on moduli of flat connections on Riemann surfaces and r matrix*, *Am. Math. Soc. Transl.* **191** (1999) 67–86, [math/9802054].

[126] A. Yu. Alekseev, H. Grosse and V. Schomerus, *Combinatorial quantization of the Hamiltonian Chern-Simons theory. 2.*, *Commun. Math. Phys.* **174** (1995) 561–604, [hep-th/9408097].

[127] C. Meusburger and B. J. Schroers, *The quantisation of Poisson structures arising inChern-Simons theory with gauge group $G \ltimes \mathfrak{g}^*$*, *Adv. Theor. Math. Phys.* **7** (2003) 1003–1043, [hep-th/0310218].

[128] C. Meusburger and D. K. Wise, *Hopf algebra gauge theory on a ribbon graph*, 1512.03966.

[129] T. H. Koornwinder and N. M. Muller, *Quantum double of a (locally) compact group*, q-alg/9605044.

[130] H. Casini, M. Huerta and J. A. Rosabal, *Remarks on entanglement entropy for gauge fields*, *Phys. Rev.* **D89** (2014) 085012, [1312.1183].

[131] R. M. Soni and S. P. Trivedi, *Aspects of Entanglement Entropy for Gauge Theories*, *JHEP* **01** (2016) 136, [1510.07455].

[132] F. A. Bais, P. van Driel and M. de Wild Propitius, *Quantum symmetries in discrete gauge theories*, *Phys. Lett.* **B280** (1992) 63–70, [hep-th/9203046].

[133] A. Ashtekar, *New variables for classical and quantum gravity*, *Phys. Rev. Lett.* **57** (Nov, 1986) 2244–2247.

[134] A. Ashtekar and R. S. Tate, *An Algebraic extension of Dirac quantization: Examples*, *J. Math. Phys.* **35** (1994) 6434–6470, [gr-qc/9405073].

[135] D. Marolf, *Refined algebraic quantization: Systems with a single constraint*, gr-qc/9508015.

[136] B. Dittrich and T. Thiemann, *Testing the master constraint programme for loop quantum gravity. I. General framework*, *Class. Quant. Grav.* **23** (2006) 1025–1066, [gr-qc/0411138].

[137] B. Dittrich and T. Thiemann, *Testing the master constraint programme for loop quantum gravity. V. Interacting field theories*, *Class. Quant. Grav.* **23** (2006) 1143–1162, [gr-qc/0411142].

[138] W. Donnelly and S. B. Giddings, *Observables, gravitational dressing, and obstructions to locality and subsystems*, 1607.01025.

[139] H. Gomes and A. Riello, *The Observer's Ghost: a field-space connection-form and its application to gauge theories and general relativity*, 1608.08226.

[140] K. Van Acoleyen, N. Bultinck, J. Haegeman, M. Marien, V. B. Scholz and F. Verstraete, *The entanglement of distillation for gauge theories*, 1511.04369.

[141] M. de Wild Propitius and F. A. Bais, *Discrete gauge theories*, in *Particles and fields. Proceedings, CAP-CRM Summer School, Banff, Canada, August 16-24, 1994*, pp. 353–439, 1995, hep-th/9511201.

[142] K. Noui, *Three Dimensional Loop Quantum Gravity: Particles and the Quantum Double*, *J. Math. Phys.* **47** (2006) 102501, [gr-qc/0612144].

[143] S. Dong, E. Fradkin, R. G. Leigh and S. Nowling, *Topological Entanglement Entropy in Chern-Simons Theories and Quantum Hall Fluids*, *JHEP* **05** (2008) 016, [0802.3231].

[144] X. Wen, S. Matsuura and S. Ryu, *Edge theory approach to topological entanglement entropy, mutual information and entanglement negativity in Chern-Simons theories*, *Phys. Rev.* **B93** (2016) 245140, [1603.08534].

[145] C. Meusburger, *Kitaev lattice models as a Hopf algebra gauge theory*, 1607.01144.

[146] A. Kitaev and J. Preskill, *Topological entanglement entropy*, *Phys. Rev. Lett.* **96** (2006) 110404, [hep-th/0510092].

[147] S. Carlip, *Conformal field theory, (2+1)-dimensional gravity, and the BTZ black hole*, *Class. Quant. Grav.* **22** (2005) R85–R124, [gr-qc/0503022].

[148] C. Rovelli, *Partial observables*, *Phys. Rev.* **D65** (2002) 124013, [gr-qc/0110035].

[149] S. B. Giddings, D. Marolf and J. B. Hartle, *Observables in effective gravity*, *Phys. Rev.* **D74** (2006) 064018, [hep-th/0512200].

[150] B. Dittrich, *Partial and complete observables for Hamiltonian constrained systems*, *Gen. Rel. Grav.* **39** (2007) 1891–1927, [gr-qc/0411013].

[151] B. Dittrich, *Partial and complete observables for canonical general relativity*, *Class. Quant. Grav.* **23** (2006) 6155–6184, [gr-qc/0507106].

[152] K. V. Kuchar and C. G. Torre, *Gaussian reference fluid and interpretation of quantum geometrodynamics*, *Phys. Rev.* **D43** (1991) 419–441.

[153] J. D. Brown and K. V. Kuchar, *Dust as a standard of space and time in canonical quantum gravity*, *Phys. Rev.* **D51** (1995) 5600–5629, [gr-qc/9409001].

[154] B. Dittrich and J. Tambornino, *A Perturbative approach to Dirac observables and their space-time algebra*, *Class. Quant. Grav.* **24** (2007) 757–784, [gr-qc/0610060].

[155] B. Dittrich and J. Tambornino, *Gauge invariant perturbations around symmetry reduced sectors of general relativity: Applications to cosmology*, *Class. Quant. Grav.* **24** (2007) 4543–4586, [gr-qc/0702093].

[156] B. Dittrich, P. A. Hoehn, T. A. Koslowski and M. I. Nelson, *Chaos, Dirac observables and constraint quantization*, 1508.01947.

[157] B. Dittrich, P. A. Hoehn, T. A. Koslowski and M. I. Nelson, *Can chaos be observed in quantum gravity?*, 1602.03237.

[158] W. Donnelly and S. B. Giddings, *Diffeomorphism-invariant observables and their nonlocal algebra*, *Phys. Rev.* **D93** (2016) 024030, [1507.07921].

[159] N. Bodendorfer, P. Duch, J. Lewandowski and J. wieewski, *The algebra of observables in Gauian normal spacetime coordinates*, *JHEP* **01** (2016) 047, [1510.04154].

[160] G. 't Hooft, *Canonical quantization of gravitating point particles in (2+1)-dimensions*, *Class. Quant. Grav.* **10** (1993) 1653–1664, [gr-qc/9305008].

[161] R. Oeckl, *A 'General boundary' formulation for quantum mechanics and quantum gravity*, *Phys. Lett.* **B575** (2003) 318–324, [hep-th/0306025].

[162] T. A. Koslowski, *Dynamical Quantum Geometry (DQG Programme)*, 0709.3465.

[163] T. Koslowski and H. Sahlmann, *Loop quantum gravity vacuum with nondegenerate geometry*, *SIGMA* **8** (2012) 026, [1109.4688].

[164] H. Sahlmann, *On loop quantum gravity kinematics with non-degenerate spatial background*, *Class. Quant. Grav.* **27** (2010) 225007, [1006.0388].

[165] J. Johnson, *Notes on heegaard splittings*, *Preprint* (2006) .

[166] R. E. Gompf and A. Stipsicz, *4-manifolds and Kirby calculus*. No. 20. American Mathematical Soc., 1999.

[167] J. Roberts, *Skein theory and turaev-viro invariants*, *Topology* **34** (1995) 771 – 787.

[168] M. Brenz and J. Barrett, *Dichromatic state sum models for four-manifolds from pivotal functors*, 1601.03580.

[169] J. P. Ryan, *Tensor models and embedded Riemann surfaces*, *Phys. Rev.* **D85** (2012) 024010, [1104.5471].

[170] R. Dijkgraaf, C. Vafa, E. Verlinde and H. Verlinde, *The operator algebra of orbifold models*, *Communications in Mathematical Physics* **123** (1989) 485–526.

Appendix A

Technical details about the (2+1)d fusion basis

A.1 Inductive limit on $\{\mathcal{H}_p\}$

In this appendix, we explain how to construct an inductive limit of the Hilbert spaces $\mathcal{H}_p$ over the number of punctures $|p|$. Here, the index p in Σ^0_p and $\mathcal{H}_p$ will not only denote the number of punctures (which we here denote by $|p|$) but also the embedding information of the punctures. Importantly, this embedding information includes not only the position of the punctures, which themselves are infinitesimally small disks removed from the manifold, but also a marked point on the boundary of each of these small disks. Alternatively, a puncture can be described by a point in the manifold equipped with a tangent vector at this point [43]. The open links of the graphs have to end at the marked points of the small disks (in one description) or to approach the punctures tangential to the associated vector (in the other description). This additional structure of the punctures allows the inclusion of torsion defects and is also crucial in order to make the gluing operation well defined. It leads, however, to an entire family of continuum Hilbert spaces constructed via the inductive limit, as we will now explain.

We fix once and for all a coordinate atlas for the two-sphere $\mathbb{S}_2$. For the inductive limit, we need to specify a partial ordering of a label set. This label set will be given by the punctures, including their embedding (and marked points) information. Given two punctured spheres Σ^0_p and $\Sigma^0_{p'}$ we say that $\Sigma^0_{p'}$ is a refinement of Σ^0_p, denoted by $p \prec p'$, if all the punctures of Σ^0_p are punctures of $\Sigma^0_{p'}$. That is there are $|p|$ punctures in $\Sigma^0_{p'}$ whose positions and marked points agree with those of the punctures in Σ^0_p. Therefore, we have a family of Hilbert spaces $\mathcal{H}_p$, labelled by the embedding information p of a set of $|p|$ punctures. Theses labels are now equipped with a directed partial order $\prec$. What is needed for completing the definition of an inductive Hilbert space is the specification of (consistent) embedding maps $\iota_{pp'} : \mathcal{H}_p \to \mathcal{H}_{p'}$ for any pair $p \prec p'$.

We construct such an embedding map as follows: Given a state ψ on Σ^0_p we can w.l.o.g. assume that this state is defined on a minimal graph Γ_p. We add links and nodes to Γ_p so that is becomes a minimal graph for $\Gamma_{p'}$. This is done in $|p'| - |p|$ steps and we denote the graph after each step by $\Gamma_{p+i}, i = 1, \ldots, |p'| - |p|$. We label the new punctures with $i = 1, \ldots, |p'| - |p|$. For a new puncture added in the i-th step we do the following: We enclose the new punctures with a cycle and furthermore add a path (composed out of links) that connects the marked point of the puncture to some (new)

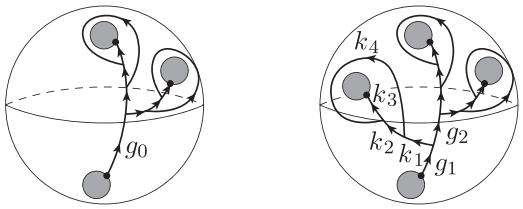

Figure A.1. Adding a puncture and extending correspondingly the minimal graph.

node on the graph Γ_{p+i-1}, see fig. A.1.

The embedding map from $\mathcal{H}_p$ to $\mathcal{H}_{p'}$ can be given as a composition of maps $\iota_{p_1 p_2}$ with $|p_2| = |p_1|+1$. For $|p'| = |p| + 1$ the refinement of the graph adds the following additional holonomies:

- One link l_0 of Γ_p needs to be subdivided into two links $l = l_2 \circ l_1$ with a new two-valent node n. Correspondingly we will have two new holonomies g_{l_1}, g_{l_2} satisfying $g_{l_0} = g_{l_2} g_{l_1}$.
- There will be a new path consisting of three new links $l'_3 \circ l'_2 \circ l'_1$ starting from the new node n to the marked point of the puncture. We will denote the associated holonomies by k_1, k_2, k_3.
- Furthermore there is one additional link l'_4 starting at the target node of l'_1 surrounding the new puncture and ending at the target node of l'_2. We denote the corresponding holonomy by k_4.

The embedding $\iota_{pp'} : \mathcal{H}_p \to \mathcal{H}_{p'}$ mapping a state $\psi(g_{l_0}, \{g_l\}_{l \neq l_0})$ is then given as

$$\iota_{pp'}(\psi)(g_{l_1}, g_{l_2}, \{g_l\}_{l\neq l_0}, k_1, \ldots, k_4) \;=\; \sqrt{\mathcal{G}}\, \delta(e,\, k_2^{-1} k_4)\; \psi(g_{l_2} g_{l_1},\, \{g_l\}_{l \neq l_0})\;. \tag{A.1}$$

That is the refined state describes a trivial holonomy for the cycle around the new puncture, whereas it is totally spread on the holonomy $k = k_3 k_2 k_1$, that gives the parallel transport from the added node on the coarser graph to the new puncture. In summary the new puncture carries neither a curvature nor a torsion excitation. The embedding maps are consistent, that is reaching a given refinement via different smaller steps, leads to the same result. We have further chosen the pre–factor in (A.1) so that the embedding map is isometric.

Consider now a family of Hilbert spaces $\{\mathcal{H}_p\}_{\{p\in\mathcal{P}\}}$, so that $\mathcal{P}$ carries a directed partial order. The inductive limit Hilbert space $\mathcal{H}_\mathcal{P}$ is defined as the (closure) of the union over all Hilbert spaces $\mathcal{H}_p$ with the following equivalence relation imposed: two states $\psi \in \mathcal{H}_p$ and $\psi' \in \mathcal{H}_{p'}$ if they can be made equal under some refinement. That is, if there exist a p'' with $p \prec p''$ and $p \prec p'$ such that

$$\iota_{pp''}(\psi) \;=\; \iota_{p'p''}(\psi')\;. \tag{A.2}$$

On this inductive limit Hilbert space one can define an inner product between as well as the addition of two states $\psi \in \mathcal{H}_p$ and $\psi' \in \mathcal{H}_{p'}$ by first embedding these two states in a common refinement Hilbert space $\mathcal{H}_{p''}$ with $p \prec p''$ and $p' \prec p''$.

Note that the inductive limit Hilbert space $\mathcal{H}_\mathcal{P}$ depends on the set of labels $\mathcal{P}$ and that we demanded that this set is directed. The latter property means that we can find for each two elements p, p' a common refinement p''. By construction, this excludes the case that p, p' have a puncture position in common, for which the marked points disagree, since in this case there is no common refinement.[1] Also, for $\mathcal{H}_\mathcal{P}$ to describe a sensible continuum limit one can demand for $\mathcal{P}$ to include some regular and infinite family of refinements.

[1] Alternatively, one can introduce a refinement of the punctures itself, i.e. allow that an arbitrary number of open links end at a given puncture. We will discuss the consequences of this choice elsewhere.

A.2 Properties of (2+1)d fusion basis

A.2.1 Diagonalization of the star-product

As an algebra, the Drinfel'd double is semi-simple so that a decomposition into irreducible modules is provided via an idempotent decomposition with respect to the multiplication. Considering two basis states labeled by the irreducible representations ρ_1 and ρ_2, respectively, we have indeed:

$$\begin{aligned}
&\psi^{\mathbb{I}}_{\mathfrak{f}}[\rho_2, M_2N_2] \star \psi^{\mathbb{I}}_{\mathfrak{f}}[\rho_1, M_1N_1] = \\
&= \frac{\sqrt{d_{\rho_1} d_{\rho_2}}}{|\mathcal{G}|^2} \sum_{\substack{G_1,H_1\\G_2,H_2}} D^{\rho_2}_{M_2N_2}(G_2 \otimes \delta_{H_2}) D^{\rho_1}_{M_1N_1}(G_1 \otimes \delta_{H_1}) \psi^{\mathbb{I}}_{G_2,H_2} \star \psi^{\mathbb{I}}_{G_1,H_1} \\
&= \frac{\sqrt{d_{\rho_1} d_{\rho_2}}}{|\mathcal{G}|^2} \sum_{\substack{G_1,H_1\\G_2,H_2}} \sum_{\rho_3} \sum_{M_3,N_3} D^{\rho_2}_{M_2N_2}(G_2 \otimes \delta_{H_2}) D^{\rho_1}_{M_1N_1}(G_1 \otimes \delta_{H_1}) \delta(G_2^{-1} H_2 G_2, H_1) \\
&\qquad \times \sqrt{d_{\rho_3}} \psi^{\mathbb{I}}_{\mathfrak{f}}[\rho_3, M_3N_3] \overline{D^{\rho_3}_{M_3N_3}(G_2G_1 \otimes \delta_{H_2})} \\
&= \frac{\sqrt{d_{\rho_1} d_{\rho_2}}}{|\mathcal{G}|^2} \sum_{\substack{G_1,H_1\\G_2,H_2}} \sum_{\rho_3} \sum_{M_3,N_3} \sum_{O_3} D^{\rho_2}_{M_2N_2}(G_2 \otimes \delta_{H_2}) D^{\rho_1}_{M_1N_1}(G_1 \otimes \delta_{H_1}) \sqrt{d_{\rho_3}} \\
&\qquad \times \overline{D^{\rho_3}_{M_3O_3}(G_2 \otimes \delta_{H_2})}\, \overline{D^{\rho_3}_{O_3N_3}(G_1 \otimes \delta_{H_1})} \psi^{\mathbb{I}}_{\mathfrak{f}}[\rho_3, M_3N_3] \\
&= \frac{\delta_{\rho_1,\rho_2}}{\sqrt{d_{\rho_1}}} \delta_{N_2,M_1}\, \psi^{\mathbb{I}}_{\mathfrak{f}}[\rho_1, M_2N_1]\,. \qquad \text{(A.3)}
\end{aligned}$$

A.2.2 Orthonormality of the fusion basis states

The basis states $\{\psi^{\mathbb{Y}}_{\mathfrak{f}}\}$ defined on the three-punctured sphere are orthonormal with respect to the inner product of $\mathcal{H}_3$ (this is defined in (7.17) and the following pages):

$$\begin{aligned}
&\left\langle \psi^{\mathbb{Y}}_{\mathfrak{f}} \begin{bmatrix} \rho_1, M_1 \\ \rho_2, M_2 \\ \rho_3, N_3 \end{bmatrix}, \psi^{\mathbb{Y}}_{\mathfrak{f}} \begin{bmatrix} \widetilde{\rho}_1 \tilde{M}_1 \\ \widetilde{\rho}_2, \tilde{M}_2 \\ \widetilde{\rho}_3, \tilde{N}_3 \end{bmatrix} \right\rangle = \\
&= \frac{1}{|\mathcal{G}|^{13}} \sum_{\substack{g_0,g_1,\dots,g_4\\g'_1,\dots,g'_4}} \sum_{\substack{G_1,H_1,\widetilde{G}_1,\widetilde{H}_1\\G_2,H_2,\widetilde{G}_2,\widetilde{H}_2}} \sum_{\substack{N_1,\tilde{N}_1\\N_2,\tilde{N}_2}} \overline{\psi^{\mathbb{Y}}_{\{G\},\{H\}}(\{g_k\},\{g'_k\})} \psi^{\mathbb{Y}}_{\{\widetilde{G}\},\{\widetilde{H}\}}(\{g_k\},\{g'_k\}) \\
&\qquad \times \prod_{k=1}^{2} \sqrt{d_{\rho_k} d_{\widetilde{\rho}_k}} \prod_{k=1}^{2} \overline{D^{\rho_k}_{M_kN_k}(G_k \otimes \delta_{H_k})} D^{\widetilde{\rho}_k}_{\tilde{M}_k\tilde{N}_k}(\widetilde{G}_k \otimes \delta_{\widetilde{H}_k}) \overline{\mathcal{C}^{\rho_1\rho_2\rho_3}_{N_1N_2N_3}} \cdot \mathcal{C}^{\widetilde{\rho}_1\widetilde{\rho}_2\widetilde{\rho}_3}_{\tilde{N}_1\tilde{N}_2\tilde{N}_3} \\
&= \frac{1}{|\mathcal{G}|^2} \sum_{\substack{G_1,H_1,\widetilde{G}_1,\widetilde{H}_1\\G_2,H_2,\widetilde{G}_2,\widetilde{H}_2}} \sum_{\substack{N_1,\tilde{N}_1\\N_2,\tilde{N}_2}} \prod_{k=1}^{2} \delta(G_k,\widetilde{G}_k)\delta(H_k,\widetilde{H}_k) \\
&\qquad \times \prod_{k=1}^{2} \sqrt{d_{\rho_k} d_{\widetilde{\rho}_k}} \prod_{k=1}^{2} \overline{D^{\rho_k}_{M_kN_k}(G_k \otimes \delta_{H_k})} D^{\widetilde{\rho}_k}_{\tilde{M}_k\tilde{N}_k}(\widetilde{G}_k \otimes \delta_{\widetilde{H}_k}) \overline{\mathcal{C}^{\rho_1\rho_2\rho_3}_{N_1N_2N_3}} \cdot \mathcal{C}^{\widetilde{\rho}_1\widetilde{\rho}_2\widetilde{\rho}_3}_{\tilde{N}_1\tilde{N}_2\tilde{N}_3} \\
&= \frac{1}{|\mathcal{G}|^2} \sum_{\substack{G_1,H_1\\G_2,H_2}} \sum_{\substack{N_1,\tilde{N}_1\\N_2,\tilde{N}_2}} \prod_{k=1}^{2} \sqrt{d_{\rho_k} d_{\widetilde{\rho}_k}} \prod_{k=1}^{2} \overline{D^{\rho_k}_{M_kN_k}(G_k \otimes \delta_{H_k})} D^{\widetilde{\rho}_k}_{\tilde{M}_k\tilde{N}_k}(G_k \otimes \delta_{H_k}) \overline{\mathcal{C}^{\rho_1,\rho_2,\rho_3}_{N_1,N_2,N_3}} \cdot \mathcal{C}^{\widetilde{\rho}_1\widetilde{\rho}_2\widetilde{\rho}_3}_{\tilde{N}_1\tilde{N}_2\tilde{N}_3} \\
&= \sum_{N_1,N_2} \mathcal{C}^{\rho_1\rho_2\rho_3}_{N_1N_2N_3} \cdot \mathcal{C}^{\rho_1\rho_2\widetilde{\rho}_3}_{N_1N_2\tilde{N}_3} \delta_{M_1,\tilde{M}_1}\delta_{M_2,\tilde{M}_2}\delta_{\rho_1,\widetilde{\rho}_1}\delta_{\rho_2,\widetilde{\rho}_2} = \delta_{N_3,\tilde{N}_3}\delta_{M_1,\tilde{M}_1}\delta_{M_2,\tilde{M}_2}\delta_{\rho_3,\widetilde{\rho}_3}\delta_{\rho_1,\widetilde{\rho}_1}\delta_{\rho_2,\widetilde{\rho}_2}\,.
\end{aligned}$$

Here, we used the orthogonality of the irreducible representations together with the orthogonality relation (3.35) of the Clebsch-Gordan coefficients. Similarly, the completeness relation for the fusion basis on the thrice-punctured sphere follows from the completeness relation of the twice-punctured sphere together with the orthogonality relation (3.36)). These properties generalize to the fusion basis states on the p-times-punctured sphere.

A.2.3 Gauge invariant projection of the fusion basis

Here we consider the Gauß constraint projector $\mathbb{A}$ applied to a fusion basis state on a cylinder:

$$\begin{aligned}\mathbb{A} \triangleright \psi_{\mathfrak{f}}^{\mathbb{S}_2}[CR, am, bn] &= |\mathcal{G}|^{-1/2} \sum_h \sum_{G,H} \sqrt{d_{CR}}\ \delta(H, c_a)\, \delta(c_a, G c_b G^{-1})\, D^R_{mn}(q_a^{-1} G q_b) \\ &\quad \times \delta(G, g_3 g_2 g_1 h^{-1}) \delta(H, g_3 g_4 g_2^{-1} g_3^{-1}) \\ &= |\mathcal{G}|^{-1/2} \sum_h \sum_{G,H} \sqrt{d_{CR}}\ \delta(H, c_a)\, \delta(c_a, G h c_b h^{-1} G^{-1})\, D^R_{mn}(q_a^{-1} G h q_b) \\ &\quad \times \delta(G, g_3 g_2 g_1 h) \delta(H, g_3 g_4 g_2^{-1} g_3^{-1})\ . \end{aligned} \tag{A.4}$$

One now writes h as $h = q_e z q_b$ and splits the sum over $h \in \mathcal{G}$ into a sum over $z \in Z_C$ and $q_e \in Q_C$. We have thus

$$h c_b h^{-1} = c_e \quad , \quad h q_b = q_e z\ . \tag{A.5}$$

Hence the summation variable z only appears in $D^R_{mn}(q_a^{-1} G h q_b) = D^R_{mn}(q_a^{-1} G q_e z)$ which gives ($q_a^{-1} G q_e$ is in Z_C due to the delta function in (A.4))

$$\frac{1}{|Z_C|} \sum_{z \in Z_C} D^R_{mn}(q_a^{-1} G q_e z) \ = \ \delta_{R,0} \delta_{m,0} \delta_{n,0}\ \delta(q_a^{-1} G q_e, \mathbb{1})\ . \tag{A.6}$$

where we denote the trivial representation of Z_C by $R = 0$. We are left with the summation over q_e which leads to the final result

$$\begin{aligned}\mathbb{A} \triangleright \psi_{\mathfrak{f}}^{\mathbb{I}}[CR, am, bn] &= |\mathcal{G}|^{1/2} \sum_{G,H} \sqrt{d_{C0}}\ \delta(H, c_a)\, \frac{1}{|Q_C|} \sum_{q_e} \delta(c_a, G q_e c_1 q_e^{-1} G^{-1}) \\ &\quad \times \delta(G, g_3 g_2 g_1 h^{-1}) \delta(H, g_3 g_4 g_2^{-1} g_3^{-1}) \\ &= \delta_{R,0} \delta_{m,0} \delta_{n,0} \frac{1}{|Q_C|} \sum_e \psi_{\mathfrak{f}}^{\mathbb{I}}[C0, a0, e0]\ . \end{aligned} \tag{A.7}$$

A.3 Generalized fusion basis

Here we discuss an extension of the fusion basis, resulting from a generalization of the gluing procedure of sec. 4.3.3. There, using the fact that the gluing of two cylinders is another cylinder, we found that such a gluing procedure defines at the level of the states (defined modulo appropriate equivalence relations, as in sec. 4.2.2) a multiplication mirroring that of the Drinfel'd algebra:

$$\widetilde{G} \otimes \delta_{\widetilde{H}} \star G \otimes \delta_H = \delta_{\widetilde{H}, \widetilde{G} H \widetilde{G}^{-1}} \widetilde{G} G \otimes \delta_{\widetilde{H}}\ . \tag{A.8}$$

In defining the gluing procedure of cylinders and states, it was necessary to specify a marked point on the boundary of the punctures at which a link of the underlying graph terminates. This prescription can be readily generalized by introducing several, say $m \geq 1$, marked points at a given puncture,

prescribing now where m different links can terminate. We will refer to such a puncture as a m-puncture. We can then consider the gluing of manifolds along two m-punctures. As an example, consider a cylinder with two 2-punctures denoted a and b. Labeling the marked points at a by a_1, a_2 and at b by b_1, b_2, we can associate four independent holonomies to such a cylinder such that

$$G = h(b_1, a_1) \quad , \quad H = h(b_1, b_2)h(b_2, b_1) \quad , \quad K' = h(b_2, b_1) \quad , \quad K = h(a_2, a_1) \, , \tag{A.9}$$

where $h(y, x)$ denotes the holonomy from the marked point x to the marked point y. All other holonomies between the marked points can be reconstructed using the flatness condition, *e.g.*

$$h(a_2, b_2) = K'GK^{-1} \, . \tag{A.10}$$

Considering a minimal embedded graph for the cylinder with two marked points at each puncture, we can define the following basis states via gauge fixing

$\psi^{\mathbb{I}}_{G,H,K',K} =$ 

, (A.11)

where the graphical notation is the same as in the main text. We can thus label a (basis) element of the algebra describing these cylinder states by $[G, H, K', K]$. Compared to the cylinder basis state with simple 1-punctures, these states contain additional information given by the holonomies between the two marked points at each of the punctures. In this sense, these are 'refined' punctures. Consider now gluing two such cylinders:

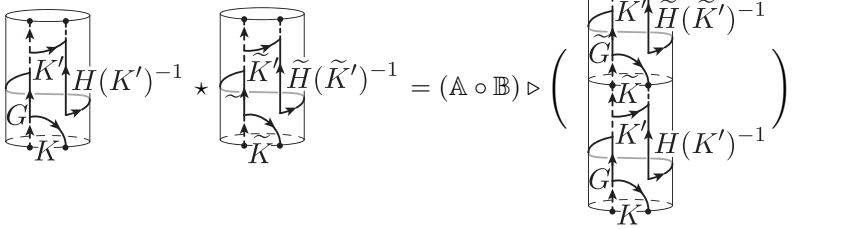

(A.12)

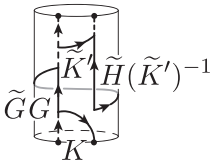

(A.13)

That is,

$$[\widetilde{G}, \widetilde{H}, \widetilde{K'}, \widetilde{K}] \star [G, H, K', K] = \delta_{\widetilde{K},K'} \delta_{\widetilde{H},\widetilde{G}H\widetilde{G}^{-1}} \ [\widetilde{G}G, \widetilde{H}, \widetilde{K'}, K] \, . \tag{A.14}$$

Note that this new multiplication rule (A.12) is essentially the same as the original Drinfel'd algebra multiplication (A.8): The $[G, H; \bullet, \bullet]$ part multiply precisely as in the Drinfel'd algebra, while the $[\bullet, \bullet, K', K]$ part functions as a factor with trivial multiplication rule

$$[\bullet, \bullet, \widetilde{K'}, \widetilde{K}] \star [\bullet, \bullet, K', K] = \delta_{\widetilde{K},K'} \ [\bullet, \bullet, \widetilde{K'}, K] \, . \tag{A.15}$$

In a way, this part already behaves like matrix indices in a representation. It is therefore not difficult to see, that the representations of this new algebra are given by a trivial extension of the Drinfel'd algebra representations $V^{(C,R)}$. It is indeed enough to extend the representation spaces to $V^{(C,R)}_{\text{ext}}$ whose basis $|c_a, m, k\rangle$ is the tensor product of the basis $|c_a, m\rangle$ of $V^{(C,R)}$ with the basis $|k\rangle$ of the group algebra $\mathbb{C}[\mathcal{G}]$, $k \in \mathcal{G}$. This leads to the matrix elements

$$(D^{C,R}_{\text{ext}})_{amk',bnk}([G,H,K',K]) \;=\; \delta(k,K)\delta(k',K')D^{C,R}_{am,bn}(G,\otimes\delta_H)\;. \tag{A.16}$$

It is easy to see that the representation property holds, as well as the generalizations of the orthogonality and completeness relations. Thus, it follows that the basis states for the cylinder with $(m=2)$-punctures carry an additional label $k \in \mathcal{G}$, which can again be absorbed into an extended multi-index M. This construction gives straightforwardly an extended fusion basis, which distinguishes itself from the original one only by its extended index structure associated to the punctures.

Generalizations to $(m>2)$-punctures is obvious: for each additional marked point at a given puncture one obtains an additional index $k \in \mathcal{G}$, describing the holonomy between two consecutive marked points. The generalization of the cylinder algebra and its representations is also obvious. In particular, the dimension of the corresponding extended representation is given by $|C| \times \dim(R) \times |\mathcal{G}|^{m-1}$. Therefore, we see that the physical content of the states, which is encoded in the set of charges $\rho = (C,R)$, is not altered at all by a refined puncture structure. This mirrors the Morita equivalence of tube algebras (with different number of open legs) discussed in [33]. What changes is only the 'amount of information' retained at the gluing interfaces.

A.4 Properties of ribbon operators

A.4.1 Gluing of Ribbons

Here we consider the gluing of two ribbons $\mathcal{R}_i[G_i,H_i]$, $i=1,2$ at a puncture. We assume that the state does not carry charges at this puncture. Applying a ribbon $\mathcal{R}_1$ ending at a puncture p and then a ribbon $\mathcal{R}_2$ starting at the puncture p we obtain

$$(\mathcal{R}_2[G_2,H_2]\mathcal{R}_1[G_1,H_1]) \triangleright \psi = \tag{A.17}$$

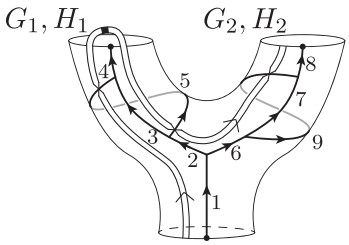

$$\begin{aligned}
&= \delta(G_2, g_8g_7g_6g_2^{-1}g_3^{-1}g_4^{-1})\,\delta(G_1, g_4g_3g_2g_1)\\
&\quad\times \psi(\ldots, g_4^{-1}H_1^{-1}g_4g_5(g_8g_7g_6g_2^{-1})^{-1}H_2g_8g_7g_6g_2^{-1}, \ldots, g_8^{-1}H_2^{-1}g_8g_9)\\
&= \delta(G_2G_1, g_8g_7g_6g_1)\delta(G_1, g_4g_3g_2g_1)\\
&\quad\times \psi(\ldots, g_4^{-1}H_1^{-1}g_4g_5g_3^{-1}g_4^{-1}G_2^{-1}H_2G_2g_4g_3, \ldots, g_8^{-1}H_2^{-1}g_8g_9)\;.
\end{aligned}$$

where $\mathcal{R}_1$ shifts g_5 and $\mathcal{R}_2$ shifts g_9 and g_5^{-1}.

A state without any charge at the puncture p_2 would have a g_5 dependence of the form $\delta(g_3^{-1}g_5)$. For this factor to be left invariant we need $H_1 = G_2^{-1}H_2G_2$. Thus the flatness projector $\mathbb{B}$ at the

puncture p leads to the corresponding delta function. Also, we can now use that $g_2^{-1}g_5^{-1}g_3g_2 = \mathbb{1}$ in the first delta–function on the (last) r.h.s of (A.17) so that for a state $\psi = \delta(g_3^{-1}g_5)\psi'$ we have

$$(\mathbb{B} \circ \mathcal{R}_2[G_2, H_2]\mathcal{R}_1[G_1, H_1]) \triangleright (\delta(g_3^{-1}g_5)\psi') \tag{A.18}$$

$$= \delta(H_1, G_2^{-1}H_2G_2)\delta(G_2G_1, g_8g_7g_6g_2^{-1}g_5^{-1}g_3g_2g_1)$$

$$\times\, \delta(G_1, g_4g_3g_2g_1)\delta(g_3^{-1}g_5)\,\psi'(\cdots, g_8^{-1}H_2^{-1}g_8g_9)\,. \tag{A.19}$$

We also apply a group averaging at the puncture

$$|\mathcal{G}|\,(\mathbb{A} \circ \mathbb{B} \circ \mathcal{R}_2[G_2, H_2]\mathcal{R}_1[G_1, H_1]) \triangleright (\delta(g_3^{-1}g_5)\psi') \tag{A.20}$$

$$= \sum_h \delta(H_1, G_2^{-1}H_2G_2)\delta(G_2G_1, g_8g_7g_6g_2^{-1}g_5^{-1}g_3g_2g_1) \tag{A.21}$$

$$\times\, \delta(G_1, hg_4g_3g_2g_1)\delta(g_3^{-1}g_5)\,\psi'(\cdots, g_8^{-1}H_2^{-1}g_8g_9)$$

$$= \delta(H_1, G_2^{-1}H_2G_2)\delta(G_2G_1, g_8g_7g_6g_2^{-1}g_5^{-1}g_3g_2g_1)\delta(g_3^{-1}g_5)\,\psi'(\cdots, g_8^{-1}H_2^{-1}g_8g_9)\,, \tag{A.22}$$

where we used that ψ' is gauge invariant at the target node of l_4, i.e. cannot depend on g_4. The r.h.s of (A.20) can now be written as

$$\delta(H_1, G_2^{-1}H_2G_2)\mathcal{R}_3[G_2G_1, H_2](\delta(g_3^{-1}g_5)\psi')\,, \tag{A.23}$$

where the path underlying $\mathcal{R}_3$ is as follows

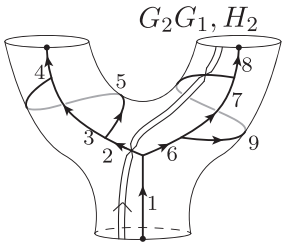

.

The ribbon does also cross the link l_2 and hence should shift the holonomy g_2. However we assumed that $\psi = \delta(g_3^{-1}g_5)\psi'$ does not carry charges at the puncture p and that means that ψ' does not depend on g_2 (and also not on g_4, as we used earlier). We conclude that for a gluing of ribbons at an (auxiliary) puncture which does not carrying any charge, we have

$$|\mathcal{G}|\,\mathbb{A} \circ \mathbb{B} \circ \mathcal{R}_2[G_2, H_2]\mathcal{R}_1[G_1, H_1] = \delta(H_1, G_2^{-1}H_2G_2)\mathcal{R}_3[G_2G_1, H_2]\,. \tag{A.24}$$

A.4.2 Gluing of charge ribbon operators

Using the previous result, equation (A.24), we can now repeat the same construction in the case of two charge ribbon operators

$$
\begin{aligned}
&|\mathcal{G}|\,\mathbb{A}\circ\mathbb{B}\circ\mathcal{R}_2[C_2,R_2;a_2m_2,b_2n_2]\mathcal{R}_2[C_1,R_1;a_1m_1,b_1n_1]\\
&\quad=\frac{d_{R_2}}{|Z_{C_2}|}\frac{d_{R_1}}{|Z_{C_1}|}\sum_{z_1,z_2}D^{R_2}_{m_2n_2}(z_2)D^{R_1}_{m_1n_1}(z_1)\,\delta(c^{(1)}_{a_1},c^{(2)}_{b_2})\,\mathcal{R}[q_{a_2}z_2q_{b_2}^{-1}q_{a_1}z_1q_{b_1}^{-1},c^{(2)}_{a_2}]\\
&\quad=\delta_{C_1,C_2}\frac{d_{R_2}}{|Z_{C_2}|}\frac{d_{R_1}}{|Z_{C_1}|}\sum_{z_1,z_2}D^{R_2}_{m_2n_2}(z_2)D^{R_1}_{m_1n_1}(z_1)\,\mathcal{R}[q_{a_2}z_2z_1q_{b_1}^{-1},c^{(2)}_{a_2}]\\
&\quad=\delta_{C_1,C_2}\frac{d_{R_2}}{|Z_{C_2}|}\frac{d_{R_1}}{|Z_{C_1}|}\sum_{z_1,z,o_2}D^{R_2}_{m_2o_2}(z)\overline{D^{R_2}_{n_2o_2}(z_1)}D^{R_1}_{m_1n_1}(z_1)\,\mathcal{R}[q_{a_2}nq_{b_1}^{-1},c^{(2)}_{a_2}]\\
&\quad=\delta_{C_1,C_2}\delta_{R_2,R_1}\delta_{n_2m_1}\frac{d_{R_2}}{|Z_{C_2}|}\sum_{z}D^{R_2}_{m_2n_1}(z)\;\mathcal{R}[q_{a_2}nq_{b_1}^{-1},c^{(2)}_{a_2}]\\
&\quad=\delta_{C_1,C_2}\delta_{R_2,R_1}\delta_{b_2a_1}\delta_{n_2m_1}\,\mathcal{R}[C_2,R_2;a_2m_2,b_1n_1]\;.
\end{aligned}
\tag{A.25}
$$

The delta function in the second line enforces $b_2=a_1$, which we used in the third line. Furthermore, it requires that $C_2=C_1$. We then performed a variable transformation and used orthogonality of the representation matrix elements.

A.4.3 Lateral product of closed ribbons

Here we consider the lateral product of two charge closed ribbons as defined in (4.81):

$$\mathcal{K}[C,R]\mathcal{K}[C',R']=\frac{d_R}{|Z_C|}\frac{d_{R'}}{|Z_{C'}|}\sum_{D,D'}\chi^R(D)\,\chi^{R'}(D')\,\mathcal{K}[C,D]\mathcal{K}[C',D'] \tag{A.26}$$

$$=\delta_{C,C'}\frac{d_Rd_{R'}}{|Z_C|^2}\sum_{D,D'}\sum_{q\in Q_C}\sum_{\substack{d\in D\\ d'\in D'}}\chi^R(D)\,\chi^{R'}(D')\,\mathcal{R}[qc_1q^{-1},qdd'q^{-1}] \tag{A.27}$$

$$
\begin{aligned}
&=\delta_{C,C'}\frac{d_Rd_{R'}}{|Z_C|^2}\sum_{q\in Q_C}\sum_{d,d'\in Z_C}\chi^R(d)\chi^{R'}(d')\;\mathcal{R}[qcq^{-1},qdd'q^{-1}]\\
&=\delta_{C,C'}\frac{d_Rd_{R'}}{|Z_C|^2}\sum_{q\in Q_C}\sum_{d,d''\in Z_C}\chi^R(d)\;\chi^{R'}(d^{-1}d'')\;\mathcal{R}[qcq^{-1},qd''q^{-1}]\\
&=\delta_{C,C'}\delta_{R,R'}\frac{d_R}{|Z_C|}\sum_{q\in Q_C}\sum_{d''\in Z_C}\chi^R(d'')\;\mathcal{R}[qcq^{-1},qd''q^{-1}]\\
&=\delta_{C,C'}\delta_{R,R'}\mathcal{K}[C,R]\;.
\end{aligned}
\tag{A.28}
$$

In the first step we used the result (4.78). We then rearranged the sums according to $\sum_D\sum_{d\in D}=\sum_{d\in Z_C}$, together with the fact that $\chi^R(D)=\chi^R(d)$ for all $d\in D$. Finally, we performed a change of variables and used the orthogonality of the irreducible representations for the stabilizers. Thus, we conclude that the closed ribbons $\mathcal{K}[C,R]$ define a family of orthogonal projectors under the above lateral product.

A.4.4 Action of closed ribbons on cylinder states

Here we consider the action of a closed ribbon on a fusion basis state on the cylinder. The minimal graph we use as well as the specific ribbon are indicated in fig. 4.4. Using the expression (4.84) for a

fusion basis state on the cylinder and the definitions (4.76, 4.81) for the closed ribbon we obtain

$$\begin{aligned}&\mathcal{K}[C',R']\triangleright\psi_{\mathfrak{f}}^{\mathbb{I}}[CR;am,bn] \qquad\qquad (A.29)\\ &=|\mathcal{G}|^{1/2}\sqrt{d_{R,C}}\frac{d_{R'}}{|Z_{C'}|}\sum_{z\in Z_C}\sum_{q\in Q_{C'}}\sum_{z'\in Z_{C'}}\chi^{R'}(z')D^R_{mn}(z)\delta(qc_1'q^{-1},\,g_2^{-1}g_4)\,\delta(c_a,\,g_3g_4g_2^{-1}g_3^{-1})\\ &\qquad\qquad\times\delta(q_azq_b^{-1},\,g_3g_2g_4^{-1}g_2q(z')^{-1}q^{-1}g_2^{-1}g_4g_1)\,.\end{aligned}$$

To lighten the formulas we will evaluate the resulting wave function in a gauge-fixed form s.t. $g_3 = g_2 = \mathbb{1}$. Hence,

$$\begin{aligned}&\Big(\mathcal{K}[C',R']\triangleright\psi_{\mathfrak{f}}^{\mathbb{S}_2}[CR;am,bn]\Big)_{|\text{g.f.}}\\ &=|\mathcal{G}|^{1/2}\sqrt{d_{R,C}}\frac{d_{R'}}{|Z_{C'}|}\sum_{z\in Z_C}\sum_{q\in Q_{C'}}\sum_{z'\in Z_{C'}}\chi^{R'}(z')D^R_{mn}(z)\delta(qc_1'q^{-1},\,g_4)\,\delta(c_{i'},\,g_4)\\ &\qquad\qquad\times\delta(q_{i'}zq_i^{-1},\,g_4^{-1}q(z')^{-1}q^{-1}g_4g_1)\,. \qquad\qquad (A.30)\end{aligned}$$

The first two delta functions on the RHS of (A.30), enforce $C = C'$, and also allow us to determine q from the condition

$$qc_1'q^{-1} \;=\; qc_1q^{-1} \;=\; q_ac_1q_a^{-1}\,, \qquad\qquad (A.31)$$

which in turn follows from the definition $c_a = q_ac_1q_a^{-1}$. Indeed, we find $q = q_a$ (as now both $q, q_a \in Q_C$).Next, we turn to the last delta function in (A.30). Using $g_4 = qc_1'q^{-1} = qc_1q^{-1}$, one can show that g_4 and $q(z')^{-1}q^{-1}$ do commute (since $z' \in Z_C$). Therefore, the condition enforced by the last delta function simplifies to

$$q_azq_b^{-1} \;=\; q(z')^{-1}q^{-1}g_1\,. \qquad\qquad (A.32)$$

This can in turn be solved for z':

$$z' = q^{-1}g_1q_bz^{-1}q_a^{-1}q \;=\; q_a^{-1}g_1q_bz^{-1}\,. \qquad\qquad (A.33)$$

Now, apart from determining $n \in Z_C$, equation (A.33) also requires that

$$q_{i'}^{-1}g_1q_i \;\in\; Z_C\,. \qquad\qquad (A.34)$$

We encode this into a characteristic function

$$\Theta_{Z_C}(g) \;=\; \begin{cases}1 & \text{if } g\in Z_C\\ 0 & \text{otherwise}\end{cases} \qquad\qquad (A.35)$$

Now, (A.30) can be written as

$$\begin{aligned}&\big(\mathcal{K}[C',R']\triangleright\psi_{\mathfrak{f}}^{\mathbb{I}}[CR;am,bn]\big)_{|\text{gf}} \qquad\qquad (A.36)\\ &=\delta_{C,C'}|\mathcal{G}|^{1/2}\sqrt{d_{R,C}}\frac{d_{R'}}{|Z_{C'}|}\sum_{z\in Z_C}\chi_{R'}(q_a^{-1}g_1q_bn^{-1})D^R_{mn}(z)\delta(c_a,\,g_4)\,\Theta_{Z_C}(q_a^{-1}g_1q_b)\\ &=\delta_{C,C'}\delta_{R,R'}|\mathcal{G}|^{1/2}\sqrt{d_{R,C}}\;D^R_{mn}(q_a^{-1}g_1q_b)\,\Theta_{Z_C}(q_a^{-1}g_1q_b)\,\delta(c_a,\,g_4)\\ &=\delta_{C,C'}\delta_{R,R'}\;\psi_{\mathfrak{f}}^{\mathbb{I}}[CR;am,bn]_{|\text{gf}}\,. \qquad\qquad (A.37)\end{aligned}$$

Thus the closed ribbon operator $\mathcal{K}[C,R]$ projects onto states $\psi[CR;am,bn]$. In particular, the projective cylinder states are eigenstates for the closed ribbons $\mathcal{K}$.

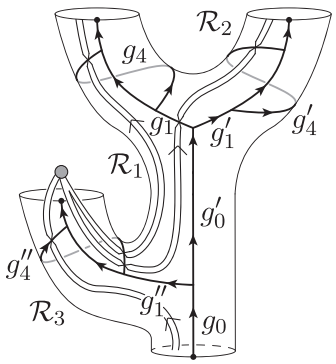

Figure A.2. Construction of the fusion basis states on the thrice-punctured sphere using charge ribbon operators. An auxiliary puncture is introduced at which the three ribbons are fused via a Clebsch-Gordan coefficient.

A.4.5 Constructing the fusion basis via charge ribbon operators

Here we construct the fusion basis on the three–punctured sphere by applying three charge ribbon operators, ending at an auxiliary puncture, see fig. A.2.

We start with a vacuum on the three punctured sphere, which in gauge fixed form is given by

$$\psi_{0\,|\text{g.f.}}^{\mathbb{Y}} \;=\; \delta(g_4,\mathbb{1})\delta(g_4',\mathbb{1})\;. \tag{A.38}$$

We now introduce an auxiliary puncture, using the embedding map detailed in (A.1):

$$\psi_0^{3\to 4}{}_{|\text{g.f.}} := (\iota_{pp'}(\psi_0^{\mathbb{Y}}))_{|\text{g.f.}} \;=\; |\mathcal{G}|^{1/2}\delta(g_4,\mathbb{1})\delta(g_4',\mathbb{1})\delta(g_4'',\mathbb{1})\;. \tag{A.39}$$

This allows us to apply three ribbon operators, as indicated in figure A.2:

$$\begin{aligned}&\big(\mathcal{R}_1[G_1,H_1]\mathcal{R}_2[G_2,H_2]\mathcal{R}_3[G_3,H_3]\triangleright\psi_0^{3\to 4}\big)_{|\text{g.f.}}\\ &\quad=|\mathcal{G}|^{1/2}\delta(g_1''g_0,G_3)\delta(g_4''G_1^{-1}H_1G_1G_2^{-1}H_2G_2,H_3)\;\delta(g_1'(g_1'')^{-1},G_2)\delta(g_4',H_2)\\ &\qquad\times\;\delta(g_1(g_1'')^{-1},G_1)\delta(g_4,H_1)\;.\end{aligned} \tag{A.40}$$

To glue the ribbons together we apply the flatness projector $\mathbb{B}$ and the gauge averaging $|\mathcal{G}|\mathbb{A}$ at the auxiliary puncture. The flatness projector leads to an additional delta function $\delta(g_4'',\mathbb{1})$. We use its solution in the second delta function factor on the r.h.s in (A.40). The gauge averaging leads in this gauge fixed setting to a summation over g_1'', that is we can solve e.g. the first delta function in (A.40) for g_1''. This results in

$$\begin{aligned}&|\mathcal{G}|\mathbb{A}\circ\mathbb{B}\circ\big(\mathcal{R}_1[G_1,H_1]\mathcal{R}_2[G_2,H_2]\mathcal{R}_3[G_3,H_3]\triangleright\psi_0^{3\to 4}\big)_{|\text{g.f.}}\\ &\quad=|\mathcal{G}|^{1/2}\delta(G_1^{-1}H_1G_1G_2^{-1}H_2G_2,H_3)\,\delta(g_4'',e)\;\delta(g_1'g_0,G_2G_3)\delta(g_4',H_2)\\ &\qquad\times\;\delta(g_1g_0,G_1G_3)\delta(g_4,H_1)\;.\end{aligned} \tag{A.41}$$

We have now projected away any charge contend at the auxiliary puncture, and can therefore use the equivalence relations in sec. 4.2.2, to express the state on a minimal graph for the thrice-punctured sphere. (The gauge fixing is the same as in (4.31)). We write this as

$$\begin{aligned}&\big((|\mathcal{G}|\mathbb{A}\circ\mathbb{B}\circ(\mathcal{R}_1[G_1,H_1]\mathcal{R}_2[G_2,H_2]\mathcal{R}_3[G_3,H_3]))\triangleright\psi_0^{\mathbb{Y}}\big)_{|\text{g.f.}}\\ &\quad=\delta(G_1^{-1}H_1G_1G_2^{-1}H_2G_2,H_3)\;\delta(g_1',G_2G_3)\delta(g_4',H_2)\delta(g_1,G_1G_3)\delta(g_4,H_1)\;.\end{aligned} \tag{A.42}$$

We now transform the three ribbons to charge ribbons and contract the appropriate N-indices with a Clebsch-Gordan coefficient. This gives

$$\begin{aligned}
&\left(\left(|\mathcal{G}|\mathbb{A}\circ\mathbb{B}\circ\sum_{N_1,N_2,M_3}\mathcal{C}^{\rho_1\rho_2\rho_3}_{N_1N_2M_3}\mathcal{R}_1[\rho_1,M_1N_1]\mathcal{R}_2[\rho_2,M_2N_2]\mathcal{R}_3[\rho_3,M_3N_3]\right)\triangleright\psi_0^{\mathbb{Y}}\right)_{|\text{g.f.}}\\
&\quad=\sum_{\substack{G_1,G_2,G_3,\\ H_1,H_2,H_3}}\sum_{N_1,N_2,M_3}\left(\prod_{\alpha=1}^{3}\frac{d_{\rho_\alpha}}{|\mathcal{G}|}D^{\rho_\alpha}_{M_\alpha N_\alpha}(G_\alpha\otimes\delta_{H_\alpha})\right)\mathcal{C}^{\rho_1\rho_2\rho_3}_{N_1N_2M_3}\\
&\qquad\times\delta(G_1^{-1}H_1G_1G_2^{-1}H_2G_2,H_3)\;\delta(g_1'g_0,G_2G_3)\delta(g_4',H_2)\delta(g_1g_0,G_1G_3)\delta(g_4,H_1)\\
&\quad=\sum_{\substack{G_1,G_2,G_3,\\ H_1,H_2}}\sum_{N_1,N_2,M_3}\frac{d_{\rho_1}d_{\rho_2}d_{\rho_3}}{|\mathcal{G}|^3}D^{\rho_1}_{M_1N_1}(G_1G_3^{-1}\otimes\delta_{H_1})\,D^{\rho_2}_{M_2N_2}(G_2G_3^{-1}\otimes\delta_{H_2})\,\mathcal{C}^{\rho_1\rho_2\rho_3}_{N_1N_2M_3}\\
&\qquad\times D^{\rho_3}_{M_3N_3}(G_3\otimes\delta_{G_3G_1^{-1}H_1G_1G_2^{-1}H_2G_2G_3^{-1}})\,\delta(g_1'g_0,G_2)\delta(g_4',H_2)\delta(g_1g_0,G_1)\delta(g_4,H_1)\;.
\end{aligned}\tag{A.43}$$

For the second equation we solved the delta function for H_3, and furthermore translated the summation variables $G_1\to G_1G_3^{-1}$ and $G_2\to G_2G_3^{-1}$. We proceed by using eq. (4.38)

$$\begin{aligned}
&\sum_{N_1,N_2,M_3}D^{\rho_1}_{M_1N_1}(G_1G_3^{-1}\otimes\delta_{H_1})D^{\rho_2}_{M_2N_2}(G_2G_3^{-1}\otimes\delta_{H_2})\,\mathcal{C}^{\rho_1\rho_2\rho_3}_{N_1N_2M_3}\,D^{\rho_3}_{M_3N_3}(G_3\otimes\delta_{G_3G_1^{-1}H_1G_1G_2^{-1}H_2G_2G_3^{-1}})\\
&\quad=\sum_{N_1,N_2}D^{\rho_1}_{M_1N_1}(G_1\otimes\delta_{H_1})D^{\rho_2}_{M_2N_2}(G_2\otimes\delta_{H_2})\,\mathcal{C}^{\rho_1\rho_2\rho_3}_{N_1N_2N_3}\;,
\end{aligned}\tag{A.44}$$

and performing the (now trivial) summation over G_3:

$$\begin{aligned}
&\left(\left(|\mathcal{G}|\mathbb{A}\circ\mathbb{B}\circ\sum_{N_1,N_2,M_3}\mathcal{C}^{\rho_1\rho_2\rho_3}_{N_1N_2M_3}\mathcal{R}_1[\rho_1,M_1N_1]\mathcal{R}_2[\rho_2,M_2N_2]\mathcal{R}_3[\rho_3,M_3N_3]\right)\triangleright\psi_0^{\mathbb{Y}}\right)_{|\text{g.f.}}\\
&\quad=\sum_{\substack{G_1,G_2\\ H_1,H_2}}\sum_{N_1,N_2,M_3}\frac{d_{\rho_1}d_{\rho_2}d_{\rho_3}}{|\mathcal{G}|^2}D^{\rho_1}_{M_1N_1}(G_1\otimes\delta_{H_1})\,D^{\rho_2}_{M_2N_2}(G_2\otimes\delta_{H_2})\,\mathcal{C}^{\rho_1\rho_2\rho_3}_{N_1N_2N_3}\\
&\qquad\times\delta(g_1'g_0,G_2)\delta(g_4',H_2)\delta(g_1g_0,G_1)\delta(g_4,H_1)\;.
\end{aligned}\tag{A.45}$$

The right hand side of this equation can be compared with the definition of the fusion basis state in (4.31) and (4.33). Note that $\psi^{\mathbb{Y}}_{G_1,H_1|G_2,H_2}=|\mathcal{G}|^3\delta(g_1'g_0,G_2)\delta(g_4',H_2)\delta(g_1g_0,G_1)\delta(g_4,H_1)$. We finally obtain

$$\begin{aligned}
&\left(\sum_{N_1,N_2,M_3}\left(\mathcal{R}_1[\rho_1,M_1N_1]\mathcal{R}_2[\rho_2,M_2N_2]\mathcal{C}^{\rho_1\rho_2\rho_3}_{N_1N_2M_3}\right)\star\mathcal{R}_3[\rho_3,M_3N_3]\right)\triangleright\psi_0^{\mathbb{Y}}\\
&\quad:=\left(|\mathcal{G}|\mathbb{A}\circ\mathbb{B}\circ\sum_{N_1,N_2,M_3}\mathcal{C}^{\rho_1\rho_2\rho_3}_{N_1N_2M_3}\mathcal{R}_1[\rho_1,M_1N_1]\mathcal{R}_2[\rho_2,M_2N_2]\mathcal{R}_3[\rho_3,M_3N_3]\right)\triangleright\psi_0^{\mathbb{Y}}\\
&\quad=\frac{\sqrt{d_{\rho_1}d_{\rho_2}}d_{\rho_3}}{|\mathcal{G}|^3}\;\psi^{\mathbb{Y}}_{\mathfrak{f}}\begin{bmatrix}\rho_1,M_1\\ \rho_2,M_2\\ \rho_3,N_3\end{bmatrix}\;.
\end{aligned}\tag{A.46}$$

A.5 The S-matrix

The S-matrix can be defined as [87, 170]

$$\mathbf{S}_{CR,C'R'}\;=\;\frac{1}{|\mathcal{G}|}\sum_{h_i\in C,h_j'\in C'}\delta(h_ih_j',\,h_j'h_i)\;\overline{\chi^R(q_i^{-1}h_j'q_i)}\,\overline{\chi^{R'}((q_j')^{-1}h_iq_j')}\;.\tag{A.47}$$

with $h_i := q_i c_1 q_i^{-1}$ and $h'_j := q_j c'_1 q_j^{-1}$ where $c_1 \in C$, $c'_1 \in C'$ and $q_i \in Q_C$, $q'_j \in Q_{C'}$. Since h'_j commutes with h_i, it has to be of the form

$$q'_j c'_1 (q'_j)^{-1} = h'_j = q_i z q_i^{-1} \quad \text{with} \quad z \in Z_C \,. \tag{A.48}$$

Here, z is given by

$$z = q_i^{-1} q_j c'_1 (q'_j)^{-1} q_i = q_{z,k}\, c'_1\, q_{z,k}^{-1} \,. \tag{A.49}$$

The second equation comes from (4.93) and defines $q_{z,k}$. Note that we use $c'_1 = c_{z,1}$. Thus $(q'_j)^{-1} h_i q'_j = q_{z,k}^{-1} c_1\, q_{z,k} \in D_{z,c_1}$. This shows that the summation over $h_i \in C$ is superfluous, and we can write

$$\begin{aligned} \mathbf{S}_{CR,C'R'} &= \frac{1}{|\mathcal{G}|} \sum_{h_i \in C} \sum_{z \in Z_C} \delta_{C',C_z}\, \overline{\chi^R(z)}\, \overline{\chi^{R'}(D_{z,c_1})} \\ &= \frac{1}{|Z_C|} \sum_{z \in Z_C} \delta_{C',C_z}\, \overline{\chi^R(z)}\, \overline{\chi^{R'}(D_{z,c_1})} \,. \end{aligned} \tag{A.50}$$

Appendix B

Fusion basis states for the computation of entanglement entropy

B.1 Alternative fusion basis states

In this appendix, we construct an alternative fusion basis for states defined on the four-punctured sphere. In sec. 4.4.3, the following basis states were introduced

$$\psi_{\mathfrak{f}}^{\Sigma_4^0}[\{\rho_i\}_{i=1}^5, \{M_k\}_{k=1}^3, N_4] = \tag{B.1}$$

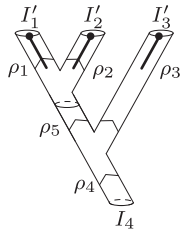

$$= \sum_{\{N\}} \psi_{\mathfrak{f}}^{\mathbb{I}}[\rho_1, M_1 N_1] \psi_{\mathfrak{f}}^{\mathbb{I}}[\rho_2, M_2 N_2] \psi_{\mathfrak{f}}^{\mathbb{I}}[\rho_3, M_3 N_3]\, \mathcal{C}_{N_1 N_2 N_5}^{\rho_1 \rho_2 \rho_5}\, \mathcal{C}_{N_5 N_3 N_4}^{\rho_5 \rho_3 \rho_4} \,. \tag{B.2}$$

These states form an orthonormal basis of the Hilbert space $\mathcal{H}_{p=4}$. An alternative basis is

$$\widehat{\psi}_{\mathfrak{f}}^{\Sigma_4^0}[\{\rho_i\}_{i=1}^5, \{M_k\}_{k=1}^2, \{N_k\}_{k=1}^2] = \mathcal{N} \tag{B.3}$$

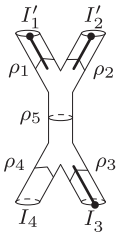

$$= \mathcal{N} \sum_{\{N\}} \psi_{\mathfrak{f}}^{\mathbb{I}}[\rho_1, M_1 N_1] \psi_{\mathfrak{f}}^{\mathbb{I}}[\rho_2, M_2 N_2] \psi_{\mathfrak{f}}^{\mathbb{I}}[\rho_3, M_3 N_3]\, \mathcal{C}_{N_1 N_2 N_5}^{\rho_1 \rho_2 \rho_5}\, \overline{\mathcal{C}_{N_4 M_3 N_5}^{\rho_4 \rho_3 \rho_5}} \,, \tag{B.4}$$

where the factor $\mathcal{N}$ remains to be determined. To do so we ask the states $\widehat{\psi}_{\mathfrak{f}}^{\Sigma_4^0}$ to be orthonormal. The orthonormality is defined with respect to the inner product (7.17) where the integral is over the holonomy variables implicitly represented by the bold edges. It follows from the orthonormality of the states $\psi_{\mathfrak{f}}^{\mathbb{I}}$ and the orthogonality of the Clebsch-Gordan coefficients that the normalization factor must satisfy the identity

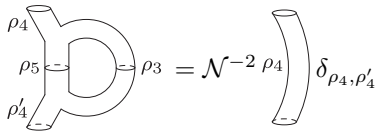

(B.5)

which after contracting both side with the identity $\delta_{N_4,M_4'}$ gives

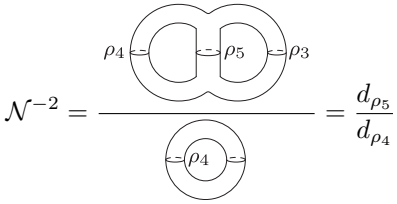

(B.6)

where we used the unitarity of the Clebsch-Gordan map. Explicitly, this can be rewritten

$$\sum_{N_3,N_5} \mathcal{C}^{\rho_4\rho_3\rho_5}_{N_4N_3N_5} \overline{\mathcal{C}^{\rho_4'\rho_3\rho_5}_{M_4N_3N_5}} = \frac{d_{\rho_5}}{d_{\rho_4}} \delta_{\rho_4\rho_4'} \delta_{N_4M_4} \,. \tag{B.7}$$

Putting everything together, the alternative fusion basis states read

$$\widehat{\psi}_{\mathfrak{f}}^{\Sigma_4^0}[\{\rho_i\}_{i=1}^5, \{M_k\}_{k=1}^2, \{N_k\}_{k=1}^2] \tag{B.8}$$

$$= \sqrt{\frac{d_{\rho_4}}{d_{\rho_5}}} \sum_{\{M,N\}} \psi_{\mathfrak{f}}^{\mathbb{I}}[\rho_1, M_1N_1] \psi_{\mathfrak{f}}^{\mathbb{I}}[\rho_2, M_2N_2] \psi_{\mathfrak{f}}^{\mathbb{I}}[\rho_3, N_3M_3] \, \mathcal{C}^{\rho_1\rho_2\rho_5}_{N_1N_2N_5} \overline{\mathcal{C}^{\rho_4\rho_3\rho_5}_{N_4M_3N_5}} \,. \tag{B.9}$$

The same procedure can be easily employed in order to define the alternative fusion basis states $\widehat{\psi}_{\mathfrak{f}}^{\Sigma_n^0}$ on the n-times-punctured sphere.

B.2 States from ribbon operators

In this appendix, we study the states which are generated from the BF vacuum by non-intersecting ribbon operators going from a region B to a region A. In particular, we are interested in the case of two ribbon operators $\mathcal{R}_1[\rho_1]$ and $\mathcal{R}_2[\rho_2]$ acting on the vacuum state defined on the four-punctured sphere as depicted in figure B.1.

The starting point is the vacuum on the four-times-punctured sphere which is expressed in its gauge fixed form as

$$\psi_0^{\Sigma_4^0}{}_{|\text{g.f.}} \;=\; \delta(g_4, \mathbb{1})\delta(g_4', \mathbb{1})\delta(g_4'', \mathbb{1}) \,. \tag{B.10}$$

We then apply two charge ribbon operators

$$\big(\mathcal{R}_1[\rho_1, M_1N_1]\mathcal{R}_2[\rho_2, M_2N_2] \triangleright \psi_0^{\Sigma_4^0}\big) \tag{B.11}$$

$$= \frac{1}{|\mathcal{G}|^2} \sum_{\substack{G_1,H_1\\G_2,H_2}} \sqrt{d_{\rho_1} d_{\rho_2}} D^{\rho_1}_{M_1N_1}(G_1 \otimes \delta_{H_1}) D^{\rho_2}_{M_2N_2}(G_2 \otimes \delta_{H_2}) \big(\mathcal{R}_1[G_1, H_1] \circ \mathcal{R}_2[G_2, H_2] \triangleright \psi_0^{\Sigma_4^0}\big) \,.$$

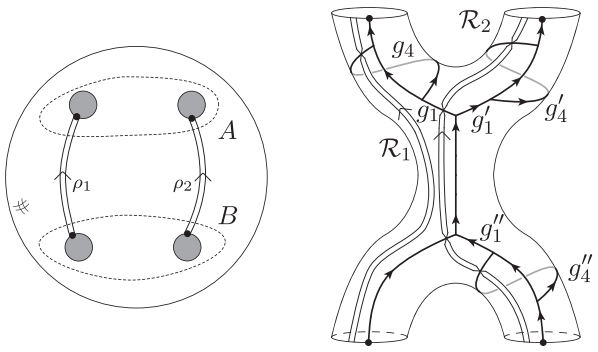

Figure B.1. The left panel depicts the situation where two non-intersecting ribbon operators go from a region B to a region A respectively defined as a set of two punctures on a four-punctured sphere. The right panel represents a topology equivalent to a four-punctured sphere. The solid lines represent the graph embedded on the surface while the double lines correspond to the ribbon operators acting on the links they cross. We can perform a gauge fixing by setting the group variables which are not labelled on the drawing to the identity.

Now, the action of the (holonomy) ribbon operators on the vacuum state gives

$$\big(\mathcal{R}_1[G_1,H_1]\mathcal{R}_2[G_2,H_2]\triangleright\psi_0^{\Sigma_4^0}\big)_{|\text{g.f.}}=\delta(G_1,g_1)\delta(H_1,g_4)\delta(H_2,g_4')\delta(G_2,g_1'g_1'')\delta(H_2,G_2g_4''G_2^{-1})\ , \quad \text{(B.12)}$$

which through the multiplication in $\mathcal{D}(\mathcal{G})$, $\widetilde{G}\otimes\delta_{\widetilde{H}}\star G\otimes\delta_H=\delta(\widetilde{H},\widetilde{G}H\widetilde{G}^{-1})\widetilde{G}G\otimes\delta_{\widetilde{H}}$, can be rewritten as

$$\big(\mathcal{R}_1[G_1,H_1]\mathcal{R}_2[G_2,H_2]\triangleright\psi_0^{\Sigma_4^0}\big)=\sum_{\substack{J_2^a\\ J_2^aJ_2^b=G_2}}\big(\mathcal{R}_1[G_1,H_1]\mathcal{R}_2^a[J_2^a,H_2]\star\mathcal{R}_2^b[J_2^b,(J_2^a)^{-1}H_2J_2^a]\triangleright\psi_0^{\Sigma_4^0}\big)\ . \quad \text{(B.13)}$$

Here, the ribbon operator $\mathcal{R}_2^a$ ($\mathcal{R}_2^b$) goes along the link l_1' (l_1'', respectively) and intersects the link l_4' (l_4'', respectively). Using the same factorization for the Drinfel'd double elements inside the representation matrices as for the ribbon operators, we can rewrite the action of the charge ribbons as

$$\big(\mathcal{R}_1[\rho_1,M_1N_1]\mathcal{R}_2[\rho_2,M_2N_2]\triangleright\psi_0^{\Sigma_4^0}\big) \quad \text{(B.14)}$$

$$=\frac{1}{|\mathcal{G}|^2}\sum_{\substack{G_1,H_1\\ G_2,H_2\\ J_2^a}}\sum_{O_2}\sqrt{d_{\rho_1}d_{\rho_2}}D^{\rho_1}_{M_1N_1}(G_1\otimes\delta_{H_1})D^{\rho_2}_{M_2O_2}(J_2^a\otimes\delta_{H_2})D^{\rho_2}_{O_2N_2}(J_2^b\otimes\delta_{(J_2^a)^{-1}H_2J_2^a})\delta(J_2^aJ_2^b,G_2)$$
$$\times\big(\mathcal{R}_1[G_1,H_1]\mathcal{R}_2^a[J_2^a,H_2]\star\mathcal{R}_2^b[J_2^b,(J_2^a)^{-1}H_2J_2^a]\triangleright\psi_0^{\Sigma_4^0}\big)\ . \quad \text{(B.15)}$$

At this point it is useful to invoke the following identity

$$\sum_{O_2}D^{\rho_2}_{M_2O_2}(J_2^a\otimes\delta_{H_2})D^{\rho_2}_{O_2N_2}(J_2^b\otimes\delta_{\widetilde{H}_2})=\sum_{O_2}D^{\rho_2}_{N_2O_2}(J_2^a\otimes\delta_{H_2})D^{\rho_2}_{O_2N_2}(J_2^b\otimes\delta_{\widetilde{H}_2})\delta(\widetilde{H}_2,(J_2^a)^{-1}H_2J_2^a)\ , \quad \text{(B.16)}$$

which shows that $\widetilde{H}_2=(J_2^a)^{-1}H_2J_2^a$ is automatically implemented by the contraction. This can be proven by inserting the resolution of the identity $\delta_{M,N}=\sum_{\widetilde{H}\in\mathcal{G}}\sum_O D^{\rho_2}_{MO}(\mathbb{1}\otimes\delta_{\widetilde{H}})D^{\rho_2}_{ON}(\mathbb{1}\otimes\delta_{\widetilde{H}})$ in the expression of the $\star$-multiplication in the Drinfel'd double representation ρ_2. Using this relation

together with an obvious change of summation variables, we finally obtain

$$\big(\mathcal{R}_1[\rho_1, M_1N_1]\mathcal{R}_2[\rho_2, I_2'I_2] \triangleright \psi_0^{\Sigma_4^0}\big) \tag{B.17}$$

$$= \frac{1}{\sqrt{d_{\rho_2}}}\frac{|\mathcal{G}|}{|\mathcal{G}|^3} \sum_{\substack{G_1,H_1\\ J_2^a,K_2^a\\ J_2^b,K_2^b}} \sum_{O_2} \sqrt{d_{\rho_1}} d_{\rho_2} D^{\rho_1}_{M_1N_1}(G_1 \otimes \delta_{H_1}) D^{\rho_2}_{M_2O_2}(J_2^a \otimes \delta_{K_2^a}) D^{\rho_2}_{O_2N_2}(J_2^b \otimes \delta_{K_2^b})$$

$$\times \big(\mathcal{R}_1[G_1, H_1]\mathcal{R}_2^a[J_2^a, K_2^a] \star \mathcal{R}_2^b[J_2^b, K_2^b] \triangleright \psi_0^{\Sigma_4^0}\big) \tag{B.18}$$

$$= \frac{|\mathcal{G}|}{\sqrt{d_{\rho_2}}} \sum_{O_2} \big(\mathcal{R}_1[\rho_1, M_1N_1]\mathcal{R}_2^a[\rho_2, M_2O_2] \star \mathcal{R}_2^b[\rho_2, O_2N_2] \triangleright \psi_0^{\Sigma_4^0}\big)\ . \tag{B.19}$$

Notice also that at this point the $\star$ multiplication between ribbons in the last term is completely redundant. Moreover, one could have guessed this result directly from the $\star$ multiplication rules for charge ribbons. We preferred, however, a more explicit approach which makes clear the underlying path and graph structures, and the role of the generalized Fourier transforms as well.

Finally, we insert the resolution of the identity provided by the Clebsch-Gordan coefficients between the path associated to the ribbon operators $\mathcal{R}_2^a$ and $\mathcal{R}_2^b$ in order to obtain

$$\big(\mathcal{R}_1[\rho_1, M_1N_1]\mathcal{R}_2[\rho_2, M_2N_2] \triangleright \psi_0^{\Sigma_4^0}\big) \tag{B.20}$$

$$= \frac{|\mathcal{G}|}{\sqrt{d_{\rho_2}}} \sum_{\rho_3} \sum_{\{N,O,P\}} \psi_{\mathfrak{f}}^{\mathbb{I}}[\rho_1, M_1O_1]\psi_{\mathfrak{f}}^{\mathbb{I}}[\rho_2, M_2O_2]\psi_{\mathfrak{f}}^{\mathbb{I}}[\rho_2, P_2N_2]\ \mathcal{C}^{\rho_1\rho_2\rho_3}_{O_1O_2N_3}\ \overline{\mathcal{C}^{\rho_1\rho_2\rho_3}_{N_1P_2N_3}} \tag{B.21}$$

$$= |\mathcal{G}| \sum_{\rho_3} N^{\rho_3}_{\rho_1\rho_2} \sqrt{\frac{d_{\rho_3}}{d_{\rho_1}d_{\rho_2}}}\, \widehat{\psi}_{\mathfrak{f}}^{\Sigma_4^0}[\rho_1, \rho_2, \rho_3, \rho_2, \rho_1; M_1, M_2, N_1, N_2]\ . \tag{B.22}$$

where the state $\widehat{\psi}_{\mathfrak{f}}^{\Sigma_4^0}$ was defined in app. B.1. Note that the states (B.22) are not not normalized and we therefore need to divide them by $|\mathcal{G}|$.

Appendix C

Irreducible representations of the quantum triple

C.1 Defining property of the representations

The irreducible representations of the quantum triple are homomorphisms and as such they preserve the algebraic structure. The following shows how the irreducible representations are compatible with the multiplication rule $\star$:

$$
\begin{aligned}
&\sum_{b,\beta,n} D^{\wp}_{a\alpha m,b\beta n}(g_1\otimes\delta_{h_1}\otimes\delta_{k_1})D^{\wp}_{b\beta n,c\gamma o}(g_2\otimes\delta_{h_2}\otimes\delta_{k_2})\\
&\quad=\sum_{b,\beta,n}\delta(k_1,c_a)\delta(c_a,g_1c_bg_1^{-1})\delta(h_1k_1,k_1h_1)\delta(d_\alpha,p_a^{-1}g_1p_bd_\beta p_b^{-1}g_1^{-1}p_a)\delta(p_a^{-1}h_1p_a,d_\alpha)\\
&\qquad\times\delta(k_2,c_b)\delta(c_b,g_2c_cg_2^{-1})\delta(h_2k_2,k_2h_2)\delta(d_\beta,p_b^{-1}g_2p_cd_\gamma p_c^{-1}g_2^{-1}p_b)\delta(p_b^{-1}h_2p_b,d_\beta)\\
&\qquad\times D^R_{mn}(q_\alpha^{-1}p_a^{-1}g_1p_bq_\beta)D^R_{no}(q_\beta^{-1}p_b^{-1}g_2p_cq_\gamma)\\
&\quad=\delta(k_1,c_a)\delta(c_a,g_1g_2c_cg_2^{-1}g_1^{-1})\delta(h_1k_1,k_1h_1)\delta(d_\alpha,p_a^{-1}g_1g_2p_cd_\gamma p_c^{-1}g_2^{-1}g_1^{-1}p_a)\delta(d_\alpha,p_a^{-1}h_1p_1)\\
&\qquad\times\underbrace{\delta(k_2,g_2c_cg_2^{-1})}_{\delta(k_2,g_1^{-1}k_1g_1)}\underbrace{\delta(h_2,g_2p_cd_\gamma p_c^{-1}g_2^{-1})}_{\delta(h_2,g_1^{-1}h_1g_1)}D^R_{mo}(q_\alpha^{-1}p_a^{-1}g_1g_2p_cq_\gamma)\\
&\quad=D^{\wp}_{a\alpha m,c\gamma o}((g_1\otimes\delta_{h_1}\otimes\delta_{k_1})\star(g_2\otimes\delta_{h_2}\otimes\delta_{k_2}))
\end{aligned}
\tag{C.1}
$$

where we used the fact that the irreducible representations of the stabilizer Z_D preserve the group multiplication rule.

C.2 Orthogonality of the irreducible representations

The space of functions on $\mathcal{T}(\mathcal{G})$ is equipped with an inner product defined by

$$
\langle\psi,\phi\rangle=\frac{1}{|\mathcal{G}|}\sum_{g,h,k\in\mathcal{G}}\overline{\psi(g\otimes\delta_h\otimes\delta_k)}\phi(g\otimes\delta_h\otimes\delta_k)\;. \tag{C.2}
$$

The matrix elements of the irreducible representations of the quantum triple form an orthogonal set with respect to this inner product, *i.e.*

$$\begin{aligned}
&\frac{1}{|\mathcal{G}|}\sum_{g,h,k\in\mathcal{G}}\overline{D^{\wp}_{a\alpha m,b\beta n}(g\otimes\delta_h\otimes\delta_k)}D^{\widetilde{\wp}}_{\widetilde{a}\widetilde{\alpha}\widetilde{m},\widetilde{b}\widetilde{\beta}\widetilde{n}}(g\otimes\delta_h\otimes\delta_k)\\
&\quad=\frac{1}{|\mathcal{G}|}\sum_{g,h,k\in\mathcal{G}}\delta(k,c_a)\delta(c_a,gc_bg^{-1})\delta(hk,kh)\delta(p_a^{-1}hp_a,d_\alpha)\delta(d_\alpha,p_a^{-1}gp_bd_\beta p_b^{-1}g^{-1}p_a)\\
&\qquad\qquad\times\delta(k,\widetilde{c}_{\widetilde{a}})\delta(\widetilde{c}_{\widetilde{a}},g\widetilde{c}_{\widetilde{b}}g^{-1})\delta(\widetilde{p}_{\widetilde{a}}^{-1}h\widetilde{p}_{\widetilde{a}},\widetilde{d}_{\widetilde{\alpha}})\delta(\widetilde{d}_{\widetilde{\alpha}},\widetilde{p}_{\widetilde{a}}^{-1}g\widetilde{p}_{\widetilde{b}}\widetilde{d}_{\widetilde{\beta}}\widetilde{p}_{\widetilde{b}}^{-1}g^{-1}\widetilde{p}_{\widetilde{a}})\\
&\qquad\qquad\times\overline{D^R_{mn}(q_\alpha^{-1}p_a^{-1}gp_bq_\beta)}D^{\widetilde{R}}_{\widetilde{m}\widetilde{n}}(\widetilde{q}_{\widetilde{\alpha}}^{-1}\widetilde{p}_{\widetilde{a}}^{-1}g\widetilde{p}_{\widetilde{b}}\widetilde{q}_{\widetilde{\beta}})\\
&\quad=\frac{1}{|C||D||Z_D|}\sum_{g\in\mathcal{G}}\delta_{C,\widetilde{C}}\delta_{a,\widetilde{a}}\delta_{b,\widetilde{b}}\delta_{D,\widetilde{D}}\delta_{\alpha,\widetilde{\alpha}}\delta_{\beta,\widetilde{\beta}}\delta(c_a,gc_bg^{-1})\delta(d_\alpha,p_a^{-1}gp_bd_\beta p_b^{-1}g^{-1}p_a)\\
&\qquad\qquad\times\overline{D^R_{mn}(q_\alpha^{-1}p_a^{-1}gp_bq_\beta)}D^{\widetilde{R}}_{\widetilde{m}\widetilde{n}}(q_\alpha^{-1}p_a^{-1}gp_bq_\beta)\\
&\quad=\frac{\delta_{C,\widetilde{C}}\delta_{D,\widetilde{D}}\delta_{R,\widetilde{R}}}{|C||D|d_R}\delta_{a,\widetilde{a}}\delta_{b,\widetilde{b}}\delta_{\alpha,\widetilde{\alpha}}\delta_{\beta,\widetilde{\beta}}\delta_{m,\widetilde{m}}\delta_{n,\widetilde{n}}=\frac{\delta_{\wp,\widetilde{\wp}}}{d_\wp}\delta_{M,\widetilde{M}}\delta_{N,\widetilde{N}}
\end{aligned}\tag{C.3}$$

where we used between the last two lines the orthogonality of the irreducible representations of the stabilizer Z_C and the fact that the cardinality of the group $\mathcal{G}$ decomposes as $|\mathcal{G}|=|C|\cdot|D|\cdot|Z_D|$.

C.3 Completeness of the set of irreducible representations

The irreducble representations form a complete set of representations, since they resolve the identity on $\mathcal{T}(\mathcal{G})$:

$$\begin{aligned}
&\sum_{\wp}\sum_{\substack{a,\alpha,m\\b,\beta,n}}d_\wp\overline{D^{\wp}_{a\alpha m,b\beta n}(g_1\otimes\delta_{h_1}\otimes\delta_{k_1})}D^{\wp}_{a\alpha m,b\beta n}(g_2\otimes\delta_{h_2}\otimes\delta_{k_2})\\
&\quad=\sum_{\wp}\sum_{\substack{a,\alpha,m\\b,\beta,n}}\delta(k_1,c_a)\delta(c_a,g_1c_bg_1^{-1})\delta(h_1k_1,k_1h_1)\delta(p_a^{-1}h_1p_a,d_\alpha)\delta(d_\alpha,p_a^{-1}g_1p_bd_\beta p_b^{-1}g_1^{-1}p_a)\\
&\qquad\qquad\times\delta(k_2,c_a)\delta(c_a,g_2c_bg_2^{-1})\delta(h_2k_2,k_2h_2)\delta(p_a^{-1}h_2p_a,d_\alpha)\delta(d_\alpha,p_a^{-1}g_2p_bd_\beta p_b^{-1}g_2^{-1}p_a)\\
&\qquad\qquad\times|C||D|d_R\overline{D^R_{mn}(q_\alpha^{-1}p_a^{-1}g_1p_bq_\beta)}D^R_{mn}(q_\alpha^{-1}p_a^{-1}g_2p_bq_\beta)\\
&\quad=|\mathcal{G}|\sum_{C,D}\sum_{\substack{a,\alpha\\b,\beta}}\delta(k_1,c_a)\delta(c_a,g_1c_bg_1^{-1})\delta(h_1k_1,k_1h_1)\delta(p_a^{-1}h_1p_a,d_\alpha)\delta(d_\alpha,p_a^{-1}g_1p_bd_\beta p_b^{-1}g_1^{-1}p_a)\\
&\qquad\qquad\times\delta(g_1,g_2)\delta(k_2,c_a)\delta(h_2k_2,k_2h_2)\delta(p_a^{-1}h_2p_a,d_\alpha)\\
&\quad=|\mathcal{G}|\delta_{g_1,g_2}\delta_{h_1,h_2}\delta_{k_1,k_2}\delta_{h_1k_1,k_1h_1}
\end{aligned}\tag{C.4}$$

where we used the completeness of the set of Wigner matrices.

C.4 Invariance property of the $3\wp M$–symbols

Let us focus on the case of the $3\wp M$–symbols defined with respect to the comultiplciation Δ_{I}. The defining equation for the Clebsch-Gordan coefficients ${}_{\mathrm{I}}\mathcal{C}$ of the quantum triple reads

$$D^{\wp_1}_{M_1N_1} \otimes_{\mathrm{I}} D^{\wp_2}_{M_2N_2}(\Delta_{\mathrm{I}}(g\otimes\delta_h\otimes\delta_k)) = \sum_{\wp_3}\sum_{M_3,N_3} {}_{\mathrm{I}}\mathcal{C}^{\wp_1\wp_2\wp_3}_{M_1M_2M_3}\, D^{\wp_3}_{M_3N_3}(g\otimes\delta_h\otimes\delta_k)\, \overline{{}_{\mathrm{I}}\mathcal{C}^{\wp_1\wp_2\wp_3}_{N_1N_2N_3}} \tag{C.5}$$

which, using the unitarity of the map ${}_{\mathrm{I}}\mathcal{C}^{\wp_1\wp_2}$, can be rewritten

$$\sum_{N_1,N_2} D^{\wp_1}_{M_1N_1} \otimes_{\mathrm{I}} D^{\wp_2}_{M_2N_2}(\Delta_{\mathrm{I}}(g\otimes\delta_h\otimes\delta_k))\, {}_{\mathrm{I}}\mathcal{C}^{\wp_1\wp_2\wp_3}_{N_1N_2N_3} = \sum_{M_3} {}_{\mathrm{I}}\mathcal{C}^{\wp_1\wp_2\wp_3}_{M_1M_2M_3}\, D^{\wp_3}_{M_3N_3}(g\otimes\delta_h\otimes\delta_k)\,. \tag{C.6}$$

We can now make use of the equation

$$\begin{aligned}&\sum_{N_3}\sum_{h,k\in\mathcal{G}} D^{\wp_3}_{M_3N_3}(g\otimes\delta_h\otimes\delta_k) D^{\wp_3}_{N_3O_3}(g^{-1}\otimes\delta_{g^{-1}hg}\otimes\delta_{g^{-1}kg})\\ &\quad= \sum_{h,k\in\mathcal{G}} D^{\wp_3}_{M_3O_3}(\mathbb{1}_{\mathcal{G}}\otimes\delta_h\otimes\delta_k) = D^{\wp_3}_{M_3O_3}(\mathbb{1}_{\mathcal{T}(\mathcal{G})}) = \delta_{M_3O_3}\end{aligned} \tag{C.7}$$

by multiplying (C.6) from the right with $D^{\wp_3}_{N_3O_3}(g^{-1}\otimes\delta_{g^{-1}hg}\otimes\delta_{g^{-1}kg})$ and summing over h,k. Resolving the comultiplication and remembering the definition (6.22) of the dual representation $\wp^{*_{\mathrm{I}}}$, we finally obtain the invariance property of the Clebsch-Gordan coefficients:

$${}_{\mathrm{I}}\mathcal{C}^{\wp_1\wp_2\wp_3}_{M_1M_2M_3} = \sum_{\substack{h_1,h_2\\k}} D^{\wp_1}_{M_1N_1}(g\otimes\delta_{h_1}\otimes\delta_k) D^{\wp_2}_{M_2N_2}(g\otimes\delta_{h_2}\otimes\delta_k) D^{\wp_3^{*_{\mathrm{I}}}}_{M_3N_3}(g\otimes\delta_{h_2^{-1}h_1^{-1}}\otimes\delta_k)\, {}_{\mathrm{I}}\mathcal{C}^{\wp_1\wp_2\wp_3}_{N_1N_2N_3} \tag{C.8}$$

from which, it is straightforward to deduce the invariance property of the $3\wp M$–symbols

$$\begin{pmatrix}\wp_1 & \wp_2 & \wp_3\\ M_1 & M_2 & M_3\end{pmatrix}_{\mathrm{I}} = \sum_{\substack{h_1,h_2\\k}} D^{\wp_1}_{M_1N_1}(g\otimes\delta_{h_1}\otimes\delta_k) D^{\wp_2}_{M_2N_2}(g\otimes\delta_{h_2}\otimes\delta_k) D^{\wp_3}_{M_3N_3}(g\otimes\delta_{h_2^{-1}h_1^{-1}}\otimes\delta_k) \begin{pmatrix}\wp_1 & \wp_2 & \wp_3\\ N_1 & N_2 & N_3\end{pmatrix}_{\mathrm{I}}\,. \tag{C.9}$$